SESSION VIII

RADIOIODINE REMOVAL

Wednesday, August 14, 1974
CHAIRMAN: Victor Deitz

DEVELOPMENT AND PERFORMANCE EVALUATION OF AN IMPROVED STANDBY GAS
TREATMENT SYSTEM FOR ENRICO FERMI - UNIT 2
H. Parish, L.E. Schuerman
D. Siegwarth

ELEMENTAL IODINE AND METHYL IODIDE ADSORPTION ON ACTIVATED CHARCOAL
AT LOW CONCENTRATIONS (WORK PERFORMED AT OHIO STATE UNIVERSITY)
R.R. Bellamy

THE BEHAVIOR OF HIGHLY RADIOACTIVE IODINE ON CHARCOAL
R.A. Lorenz, W.J. Martin
H. Nagao

IODINE FISSION PRODUCT MASS TRANSFER IN ADSORBENT MEDIA
J.L. Kovach, J.R. Hunt

EFFECT OF ALKALI METAL CONTENT OF CARBON ON RETENTION OF IODINE AT
HIGH TEMPERATURES   A.G. Evans

SOLID ADSORBENTS FOR COLLECTION AND STORAGE OF IODINE-129 FROM
REPROCESSING PLANTS   D.T. Pence, B.A. Staples

TESTING AND EVALUATION OF ABSORBERS FOR GASEOUS PENETRATIVE FORMS
OF RADIOIODINE   M.J. Kabat

PERFORMANCE OF NON-COCONUT BASE ADSORBERS IN REMOVAL OF IODINE AND
ORGANIC IODIDES   M. Pasha, E.E. Fowler,
R.D. Rivers, J.M. Goldsmith

ADSORPTION OF METHYL IODIDE ON IMPREGNATED ALUMINA
I.J. Gal, A. Muk, M. Todorovic,
J. Rajnvajn, D. Cvjeticanin,
L. Vujisic, J. Rajnvajn

IODINE SCRUBBING FROM OFF-GAS WITH CONCENTRATED NITRIC ACID
O.O. Yarbro, J.C. Mailen,
W.S. Groenier

THE CALCULATION OF CHARCOAL HEATING IN AIR FILTRATION SYSTEMS
E.A. Bernard, R.W. Zavadoski

DEVELOPMENT AND PERFORMANCE EVALUATION OF AN IMPROVED STANDBY GAS TREATMENT SYSTEM FOR ENRICO FERMI - UNIT 2

Harold C. Parish
CVI Corporation, Columbus, Ohio

Larry E. Schuerman
Detroit Edison Company, Detroit, Michigan

Dr. David P. Siegwarth
Nuclear Energy Division
General Electric Company, San Jose, California

Abstract

The Enrico Fermi Atomic Power Plant - Unit 2 utilizes two natural draft cooling towers. These large structures create the potential for entrainment of the stack effluent in a down wash from the leeward side of the cooling towers, thereby reducing the effectiveness of the stack. Thus, a stack of reasonable height would not be sufficient to secure compliance with 10 CFR 100 under design basis accident conditions.

Detroit Edison evaluated three methods for further reducing the potential doses and hence complying with 10 CFR 100. The solution chosen by Edison was to develop a Standby Gas Treatment System of advanced design which could justifiably be credited with an iodine removal efficiency of 95 percent or higher (90% maximum was the AEC standard prior to the issuance of Regulatory Guide 1.52). A Standby Gas Treatment System, manufactured by the CVI Corporation, was chosen for this application. The CVI system features an all welded, submerged inlet carbon adsorber design which assures high performance by eliminating all elastomer seals and thereby, the chance for bypassing of the charcoal.

In order to secure credit for higher iodine removal efficiency, system performance was demonstrated by testing a large scale system under simulated design basis accident conditions. The test program was conducted by the General Electric Co. at General Electric's Gas Technology Facility, Vallecitos Nuclear Center. The unit tested was a 400 cfm module supplied by the CVI Corporation which incorporated the same design features as the full scale unit.

I.   Introduction

One of the criteria imposed by the Atomic Energy Commission (AEC) upon an applicant who seeks to operate a light water cooled nuclear power reactor is that the applicant prove he can do so in accordance with Title 10, Code of Federal Regulations, Part 100 (10 CFR 100).

This regulation, in part, requires that any person (1) located at any point of the exclusion boundary for two hours, or (2) located at any point of the outer boundary of the low population zone (during the entire period of passage of released fission products), not receive a total radiation dose to the whole body in excess of 25 rem, or a total radiation dose in excess of 300 rem to the thyroid from iodine exposure. These limits are applied to potential reactor accidents which have an exceedingly low probability of occurrence.

The most radiologically significant potential reactor accident is the Loss of Coolant Accident (LOCA). The LOCA is defined as a circumferential reactor-coolant recirculation pipe line rupture. This potential accident has been analyzed for Enrico Fermi Unit 2 (EF-2) in accordance with extremely conservative assumptions of core melt and fission product release. (Detroit Edison is the Owner and Architect-Engineer for EF-2 which is under construction on the western shore of Lake Erie, approximately 30 miles southwest of the City of Detroit. The plant will have a nominal electrical capacity of 1150 megawatts and utilize a General Electric Company Boiling Water Reactor).

One of the Engineered Safety Systems used during a LOCA is the Standby Gas Treatment System (SGTS). The SGTS effluent was originally to be released from a 100 meter freestanding stack. The benefits of releasing the effluent from the tall stack were essentially negated with the advent of two natural draft cooling towers, each 122 meters high. The intermingling of the effluent plume with the potential downwash from the leeward side of the cooling tower is the principal reason. It is generally concluded[1] that the turbulence generated by large structures or buildings will not cause downwash from a stack, provided the stack is at least two and one-half times the height of any structure located within twenty (20) stack heights of the stack. This would then require that the freestanding stack, to be truly effective, would have to be 305 meters tall or located outside of the exclusion boundary. It is obvious that neither approach was realistic.

Prior to the Atomic Energy Commission issuance of Regulatory Guide 1.52, all SGTS designs had been limited by the AEC to an overall system efficiency of 90 percent (maximum) in the licensing of Boiling Water Reactors. Faced with the requirement to provide additional means to limit the potential doses from the postulated LOCA to below the requirements of 10 CFR 100, Edison considered 3 possible alternative solutions:

1.   Provide an engineered air-recirculation system in the Secondary Containment. A reduction by a factor of 2 in the fission products released from secondary containment should be achieved by using this system. This system was not pursued because the addition of this system alone was not capable of reducing the doses sufficiently.

2.   Increase distance to exclusion boundary and increase the distance to the outer boundary of the low population zone. Dose reductions provided by this alternative required doubling the distance to the site boundary (from 915

meters to approximately 1800 meters). Studies indicated this solution would be prohibitive in cost.

      3.   Prove that an appropriately designed SGTS could justifiably be credited with an iodine removal efficiency of 95 percent or higher.

      The last solution was considered to be the best single alternative for reducing the calculated potential dose. Edison, therefore, elected to seek or develop a SGTS which was an improvement over previous designs.

II.   Design of an Improved SGTS

A.   System Description

      The design of the entire SGTS, as supplied to Edison, will be described briefly with the aid of Figure 1.

      Air from the secondary containment is introduced into a demister/roughing filter section. Water droplets and particulate matter larger than 10 micron are removed in this section. From the roughing filter the air passes through a prefilter section where additional particulates are removed. The prefilter efficiency is 85% NBS atmospheric stain (dust spot) average. The air is then directed to an electric heater which raises the air temperature from 135 Degrees F (max.) to 150 Degrees F. That temperature increase assures that the relative humidity will not exceed approximately 70%.

      The very fine particulates are then removed in the high efficiency particulate absolute (HEPA) filters with a removal efficiency of approximately 99.97% for particles 0.3 micron in diameter or larger. From the HEPA filter, air is introduced into the carbon adsorber section where radioactive isotopes of iodine are removed through a mechanism of adsorption and isotopic exchange on KI_3 impregnated carbon. The carbon adsorber will be discussed more completely in later sections. Air from the carbon adsorber section is then directed to the downstream HEPA filters where any carbon dust which may have been carried over from the carbon is removed. The air is then discharged by an exhaust fan through a roof vent into the atmosphere.

B.   Carbon Adsorber Design Considerations

      The net system removal efficiency for gaseous phase, radioactive iodine and methyl iodide may be considered to be a function of both the performance of the adsorbent and a system "mechanical efficiency" term. The term mechanical efficiency is used here to represent all factors contributing to a potential reduction in system performance other than the limitations of the adsorbent operating under design conditions.
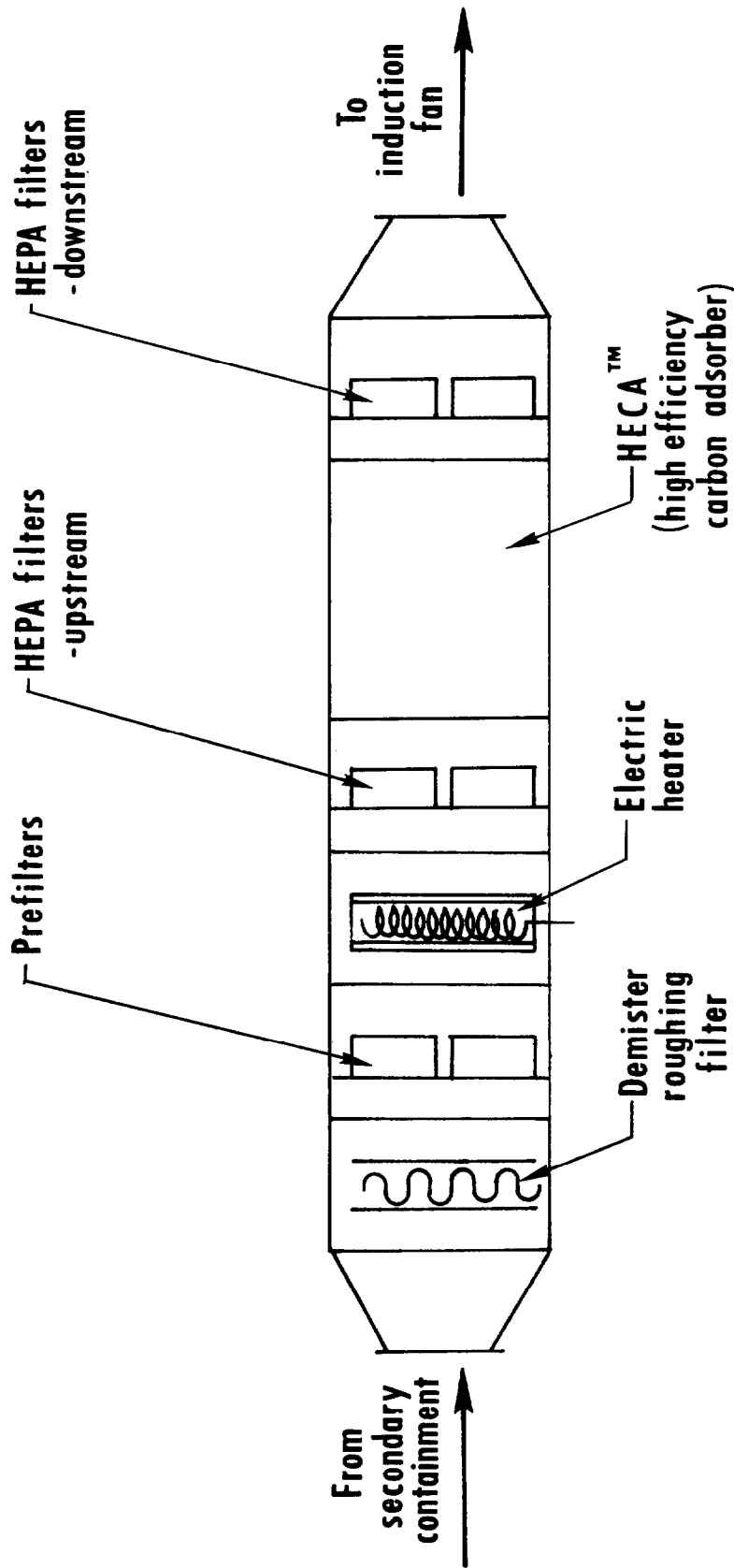
Figure 1. SGTS simplified flow schematic.

The performance of the adsorbent is affected by mass transport rates, the residence time of the methyl iodide in a physically adsorbed state (to be distinguished from gas residence time) and the kinetics of the isotopic exchange phenomena. The above parameters are affected by such design variables as particle size, relative humidity of the gas stream and system temperature. The above listing is not intended to be all inclusive but is presented for illustrative purposes.

Factors to be considered in the mechanical efficiency of the system include bypassing of the adsorbent and uniformity of flow through the adsorbent or flow channeling. Historically, the potential for bypass flow has been a factor in limiting the credit given for system performance. To this extent, the system efficiency would be governed by the mechanical efficiency of the system rather than by the performance of the adsorbent.

The system described herein incorporates the $HECA^{TM}$ (CVI trade name for High Efficiency Carbon Adsorber) which eliminates the potential for bypassing of the adsorbent. The mechanical efficiency is considered to approach 100% and the performance of the $HECA^{TM}$ in the removal of gaseous phase, radioactive elemental iodine and methyl iodide is expected to be limited principally by the performance of the adsorbent (carbon).

A summary of design features which are incorporated in the $HECA^{TM}$ unit supplied for the Detroit Edison Company are as follows:

1. The carbon filter is designed with a submerged inlet such that any flow path from inlet to outlet of the adsorber must be through charcoal of sufficient depth to remove any radioactive iodine or methyl iodide with an efficiency of greater than 99.99% under design conditions.

2. The system is designed such that any possible leakage through gasketed access doors, ports, etc., would be in-leakage into the filter housing.

3. The carbon beds are designed to ensure uniform flow of containment air across each of the bed face areas. Any permissible degree of non-uniformity must lie entirely within the range of proven bed adsorption capacity.

4. Provisions are made to empty the carbon when required and to refill without compromising the integrity of the seal weld.

C.   Carbon Adsorber Description

Attention is directed to Figure 2 which shows, in perspective, the carbon adsorber section of the SGTS. This section, shown with the outer housing removed, is comprised of six (6) carbon beds in parallel, each sharing the common inlet duct. The air flow is directed through the carbon as indicated by the flow arrows in Figures 2 and 3. The clean air is then contained by an outer housing (not shown in Figure 2), which acts as the common out-
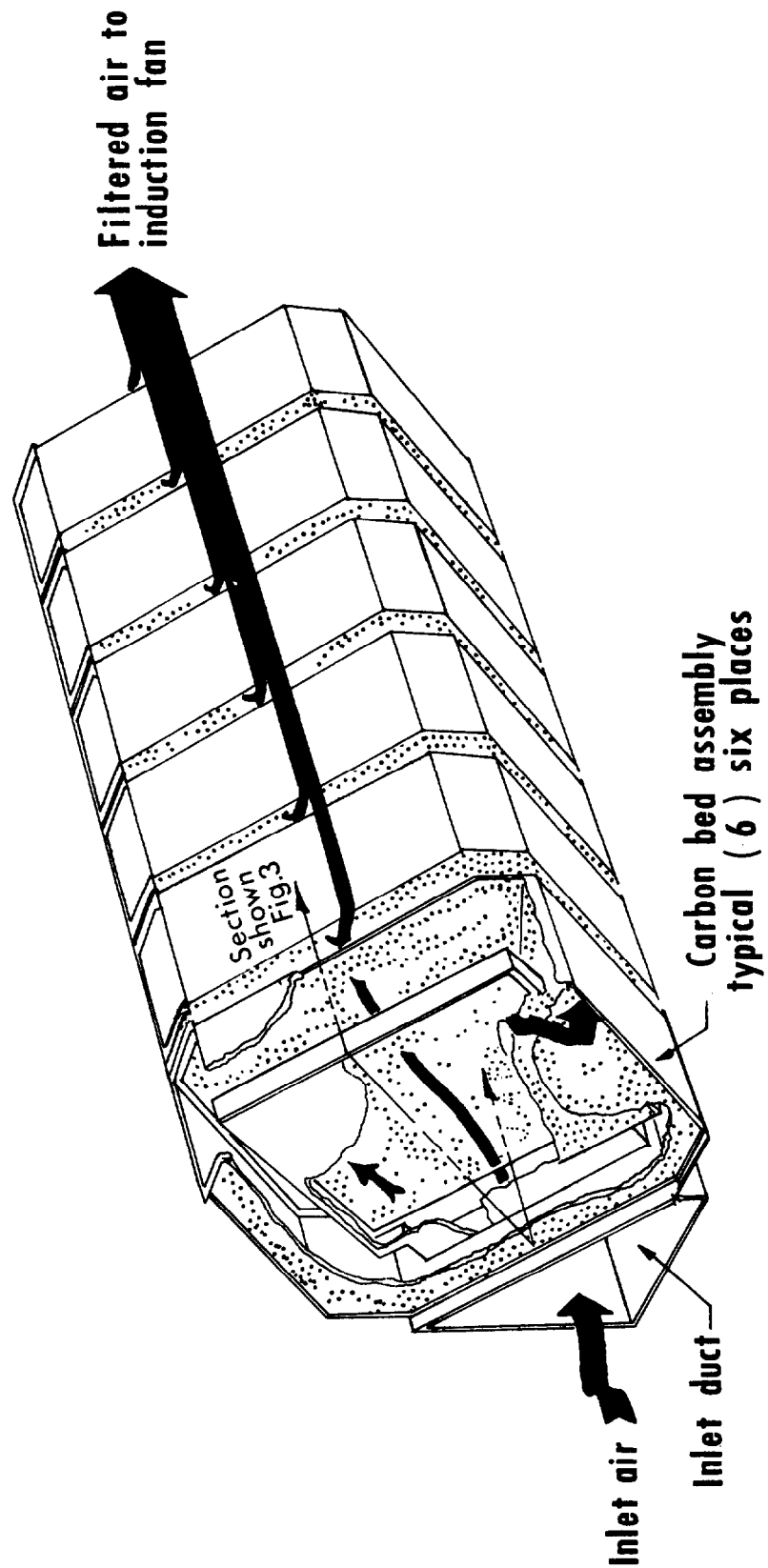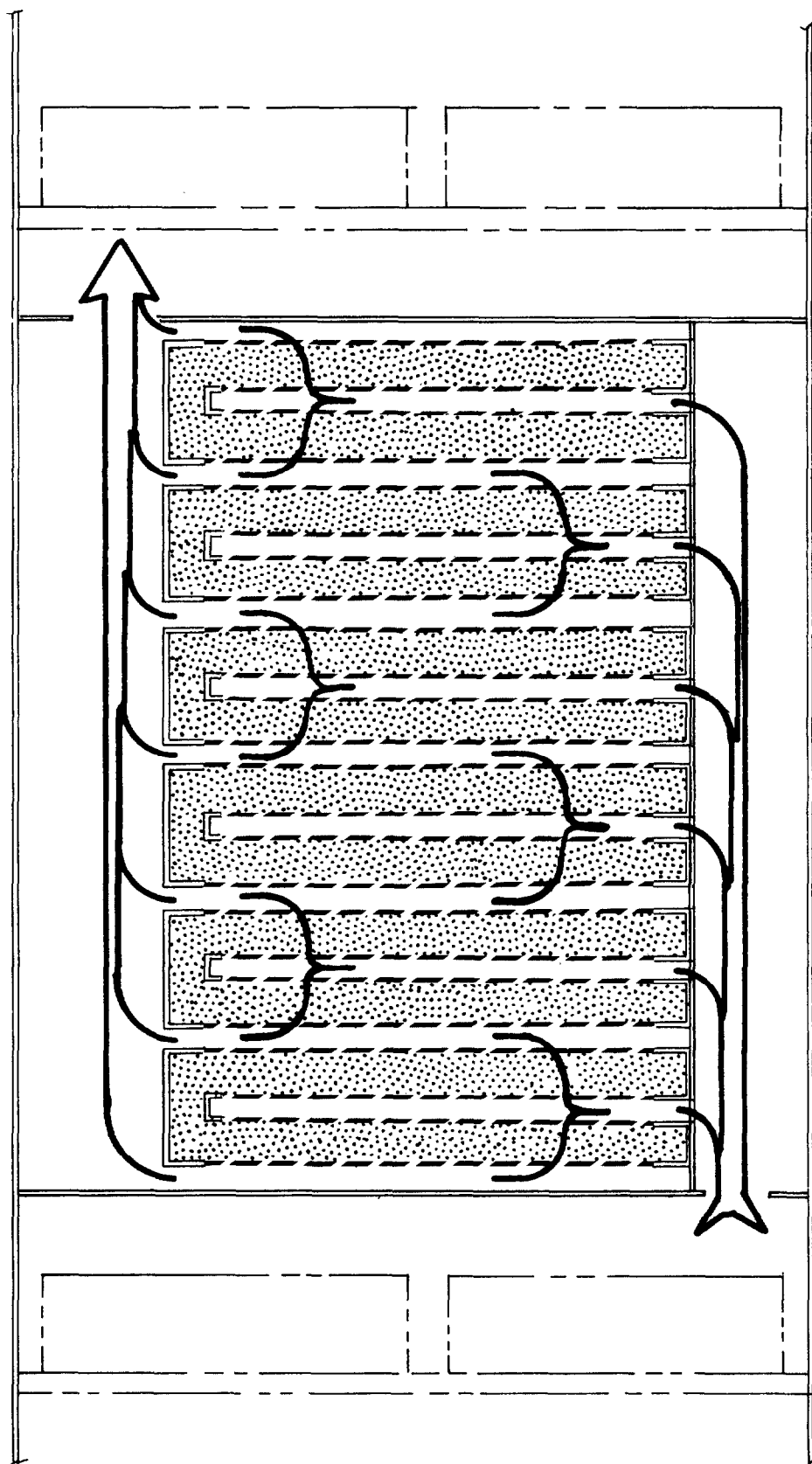
Figure 2. Beds & inlet duct assembly.

Figure 3. Cross section of carbon adsorber.

let duct for transmission to the downstream particulate filters and subsequent venting.

Figure 2 illustrates the submerged inlet concept wherein the inlet screen is submerged within a bed of carbon. Further, all seal welds, which isolate the inlet duct from the outlet duct, are located in the inlet duct and are accessible from one of two access plates for inspection, testing, and if necessary, repair. This design approach assures that any flow path from inlet to outlet of the adsorber is through carbon of sufficient depth to ensure attainment of the design efficiency.

Figure 3 is a schematic drawing of the carbon adsorber section, representing a cross sectional view through the beds.

As indicated in Figure 1, the fan is located downstream of the SGTS so that the SGTS operates slightly below atmospheric pressure and any air leakage through gasketed doors, etc., is into the SGTS.

The air passages, including the inlet duct, the inlet and outlet plenums (air volume between 6" adsorber elements) and the outlet duct are designed to obtain a balanced flow. That is, the system was designed to assure a minimum residence time for each of the adsorber elements. This was accomplished by maximizing the ratio of flow resistance in the carbon to flow resistance in the air spaces and by balancing flow resistance in the air spaces. These precautions minimize any tendency for flow channeling; flow channeling could cause less than minimum residence time for a portion of the flow. These engineered features were demonstrated and proven by flow tests conducted at the Ohio State University. The test results[2] showed that the pressure drop through the bed varied by no more than $\pm$ 3% across the face of the bed. Therefore, the face velocity would vary by no more than $\pm$ 2.3%, since the pressure drop was shown to vary as:

$$\Delta P = aV^{1.4} \qquad (a = constant).$$

For the purpose of draining used carbon, a specially designed change cart is utilized. Carbon loading and unloading is performed only at the time when a carbon change becomes necessary as determined by a sampling program. The remote change out equipment is described in Reference[3] and therefore, will not be discussed here. The important design consideration, in the context of this paper, is that the carbon can be replaced without compromising the integrity of the seal weld.

III.   Testing of the Improved SGTS Design

Based on the design rationale as described above, it was believed that

the system performance would approach the performance of the adsorbent. As a step in fulfilling a licensing commitment, Edison decided to support this concept by testing a large scale adsorber unit. The test filter module was furnished by CVI Corporation and Detroit Edison funded the test program which was conducted by General Electric Co., at it's Vallecitos Nuclear Center Gas Technology Facility.[4]

A.   Test Conditions

The test was conducted under simulated LOCA conditions. A comparison of the LOCA conditions[5] and the test conditions is tabulated in Table 1, along with design parameters for the system supplied to Edison and the test module.

Table 1

Comparison of Test Conditions and Test
Equipment With LOCA Conditions and Equipment Supplied to
Edison

Variable	LOCA Condition	Test Conditions
Temperature (Degrees F)	150	147-167
Relative Humidity (%)	70	0-83
Duration of Flow (days)	30	0.08-32
CH_3I Loading (mg/g carbon)	0.25	0.064-0.292
I_2 Loading (mg/g carbon)	2.25	0
Flow (CFM)	1000-4000	329-406
Adsorber Flow Area (ft^2)	100	10
Adsorbent Depth (in)	6	6
Superficial Gas Velocity (fpm)	10-40	32.9-40.6
No. of Beds	6	2

About 90% of the iodine released to the SGTS after a LOCA is in the elemental form and 10% is assumed to be in the organic form as methyl iodide. A mixture of nonradioactive methyl iodide traced with radioactive methyl iodide ($CH_3^{131}I$) was used in this test program to measure the ability of the carbon beds to immobilize radioactive methyl iodide. Previous data on KI_3 impregnated carbons have shown the removal efficiencies for elemental iodine are at least an order of magnitude greater than the methyl iodide removal efficiencies.[6-8] Therefore, if one assumes the removal efficiency for elemental iodine is at least equal to that measured with methyl iodide, a conservative estimate of the overall SGTS carbon bed performance is obtained.

B.   Experimental Equipment

The 400 cfm SGTS test facility shown schematically in Figure 4 is designed to simulate the above mentioned LOCA operating conditions. The facility consists of the following major components:

1.   Inlet air flow measurement section;

2.   Constant volume flow controller;

3.   Teflon coated prefilter;

4.   Electric duct heater;

5.   Electric boiler-steam humidifier system;

6.   CVI test filter section which consists of (a) Teflon-coated demister element, (b) (HEPA), (c) four 2.5-ft^2 by 6-in. deep carbon sections, and (d) a second HEPA;

7.   Backup filter section containing (a) electric duct heater, (b) tray type backup carbon filter, and (c) HEPA filter;

The operation of the test facility can be described as follows:

1.   The CH_3I and $CH_3{}^{131}I$ are added to the air stream at a fixed flow rate. In the first two tests, the methyl iodide labeled with $CH_3{}^{131}I$ and additional unlabeled CH_3I were added to a 5 gallon stainless steel storage cylinder and pressurized with nitrogen. The CH_3I-$CH_3{}^{131}I$ mixture was added to the system from the pressurized cylinder. Following the second test, the facility was modified so that liquid CH_3I could be metered into the air duct with a syringe pump and the cylinder was used for the $CH_3{}^{131}I$ gas mixture only.

2.   The air is heated with an internal duct heater (heater downstream of prefilter in Figure 4). It should be noted that the entire duct downstream of this heater is traced with electrical heaters and is fully insulated.

3.   The hot air is humidified with superheated steam. The humidity is normally manually controlled and monitored with several LiCl type dew point probes.

4.   Water droplets are removed from the air stream by a demister followed by removal of particulates by a HEPA filter.

5.   The $CH_3{}^{131}I$ is removed by the adsorbent in the CVI HECA^{TM} test module.

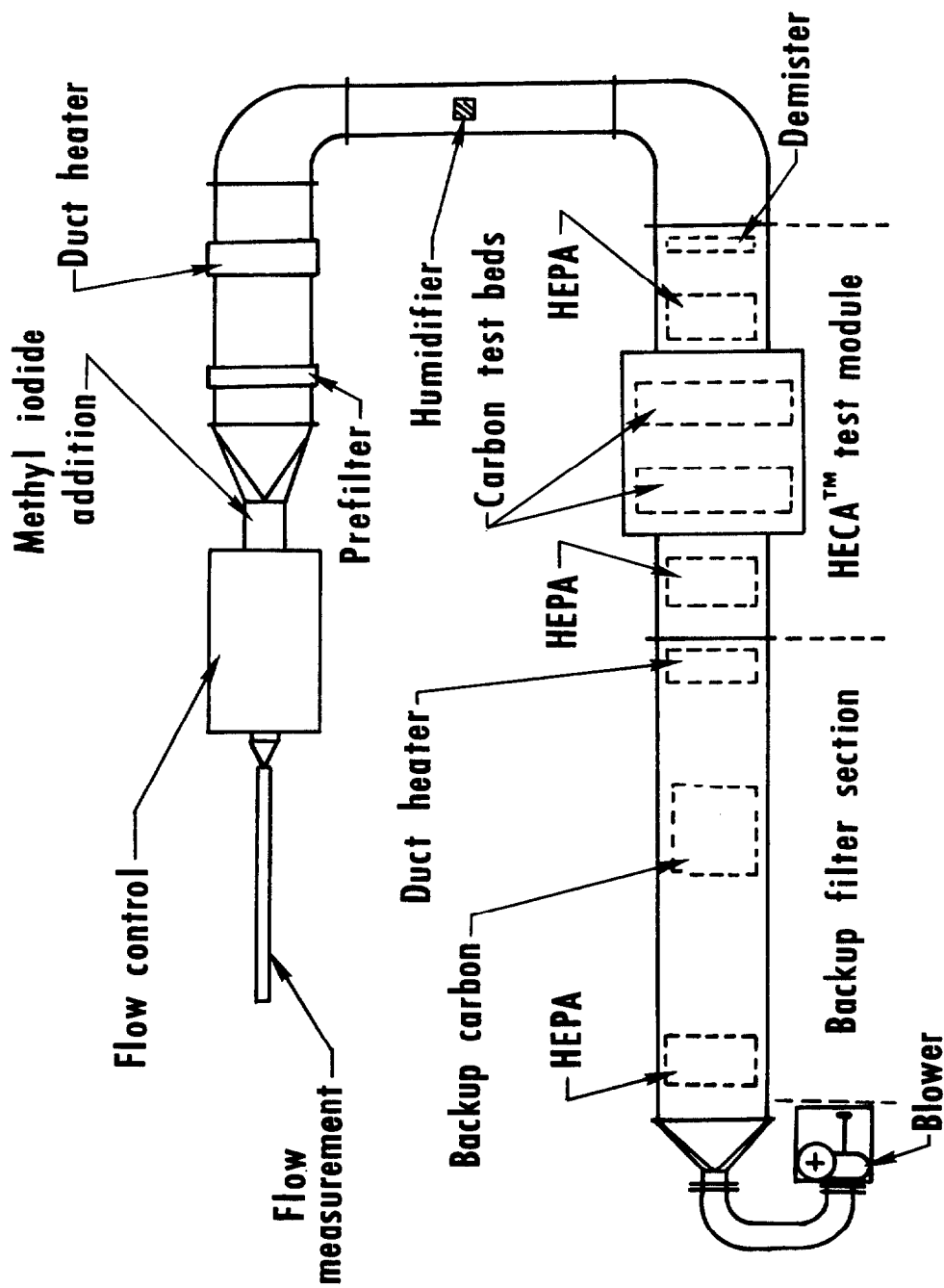6.   Particulates such as carbon dust are removed by a second HEPA filter.

Figure 4.   SGTS test facility, large scale.

7.   The gas stream is heated with an internal duct heater to approximately 185 Degrees F to reduce the relative humidity.

8.   The remaining $CH_3{}^{131}I$ is removed by the backup carbon bed.

9.   Dust in the gas stream is removed by a third HEPA filter.

10.   The gas is discharged to the building exhaust system by a high-head blower. The blower maintains the entire system at negative pressures (approximately 4 in. water gage at the methyl iodide injection point and 10 in. water gage at the blower suction).

Figure 5 is a picture of the test facility. The inlet is at the right side of the picture and the discharge is near the center at the top of the picture.

A continuous sample flow (approximately 4.4 liters/min.) is drawn from the duct immediately upstream of the carbon beds and transferred through a heated, insulated sample tube to a fume hood in the laboratory. The sample gas is passed through a hot water jacketed column containing two 3-in. deep carbon beds. The water is removed from the sample column effluent and the flow of dry air is measured with a rotameter. Upstream of the sample column, about 100 cc/min. of gas is diverted to an electron capture detector gas chromatograph for CH_3I analysis.

The test carbon bed inlet activity is determined by removing the carbon from the inlet sample column after the test, placing each of the two 3-in. layers of carbon in separate Petri dishes, and then transferring the samples to the radiochemical counting laboratory for Iodine-131 analysis. The quantity of CH_3I loaded on the carbon test bed is calculated from the results of the gas chromatographic analyses.

The test carbon bed outlet samples are taken downstream of the second HEPA to ensure that the sample will be representative of the bulk flow. The outlet sampling system is shown in Figure 6. Approximately 75 liters/min. are drawn through the sample system by the diaphragm vacuum pumps in the lower right hand corner of Figure 6 and then discharged to the duct again immediately upstream of the system discharge fan. The sample gas first passes through a water-cooled heat exchanger where the gas is cooled and the moisture condenses. The water from the heat exchanger is collected in a plastic bottle (lower left corner of Figure 6). The gas then passes through a mass flow meter which continuously indicates and totalizes the flow. From the flow meter, the gas stream goes to the oven where it is first preheated to 150 Degrees F and then flows through the outlet sampler carbon beds.

The close-up view of the outlet sampler is shown in Figure 7. The sampler was developed for this program to allow large sample flow rates, and therefore, increase the sensitivity for low levels of activity in the sample gas. The quantity of carbon in each 2.75 in. dia. by 3 in. long section
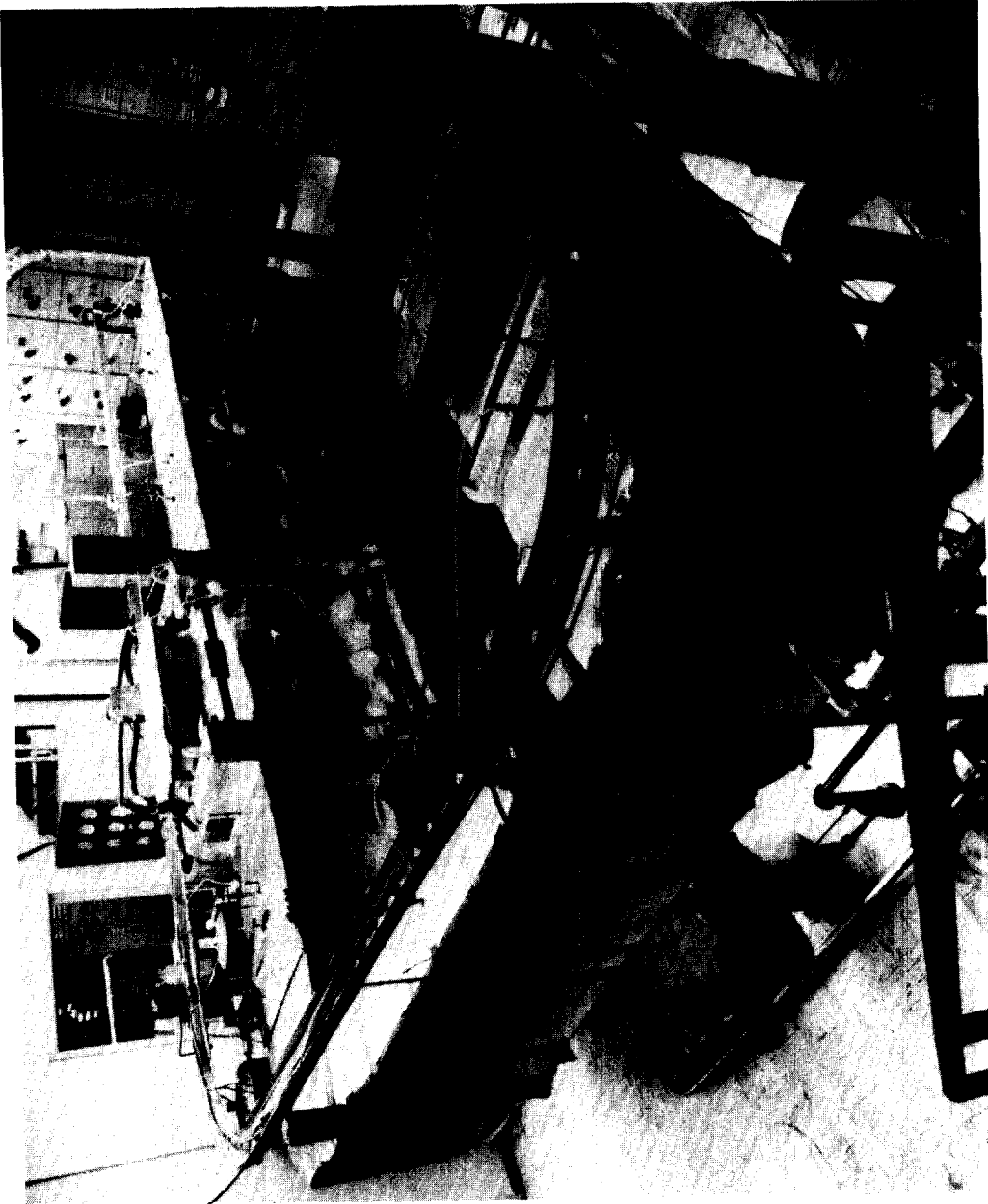
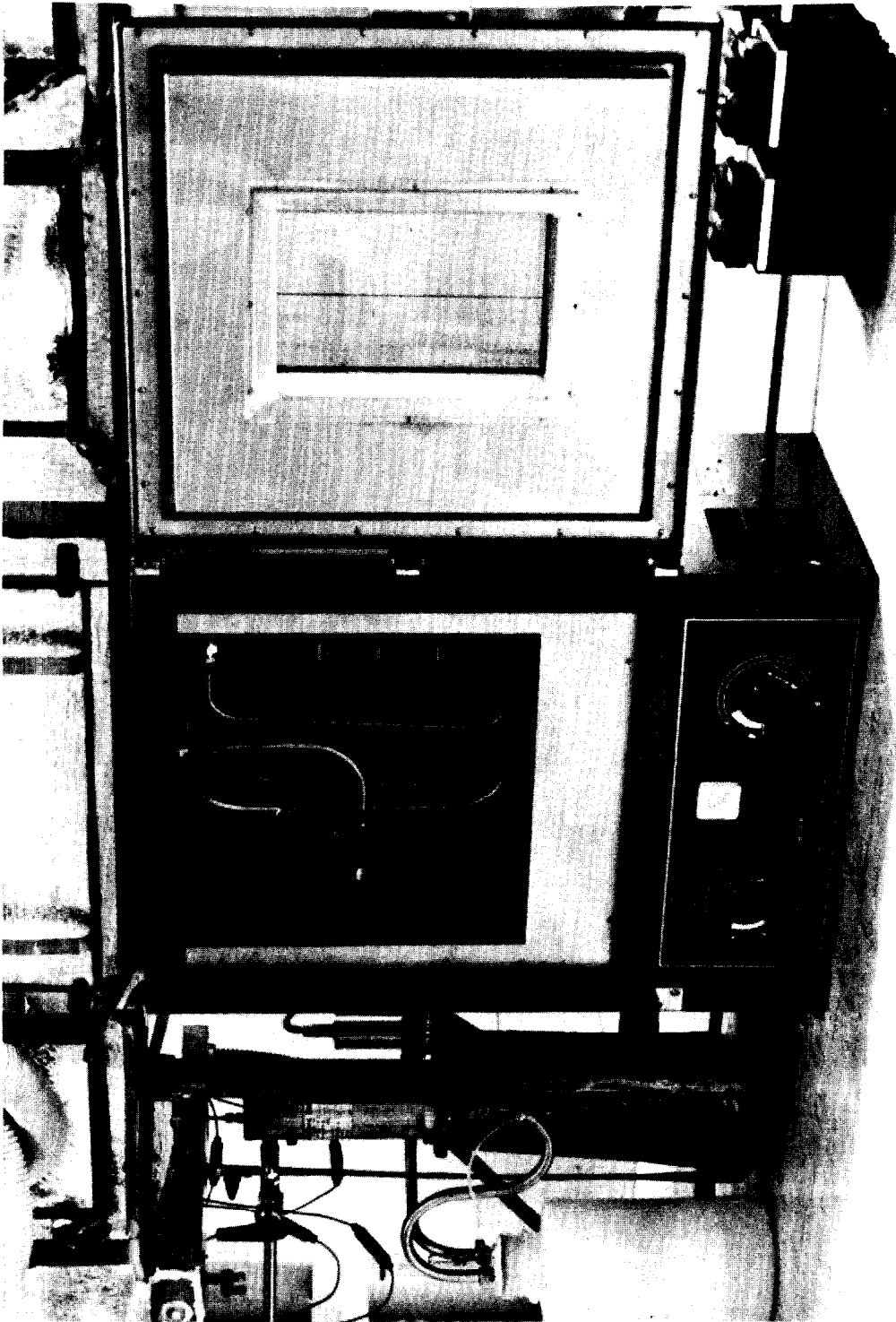Figure 5.   Large scale SGTS over-all view.

Figure 6. Large scale SGTS carbon bed outlet sample system.
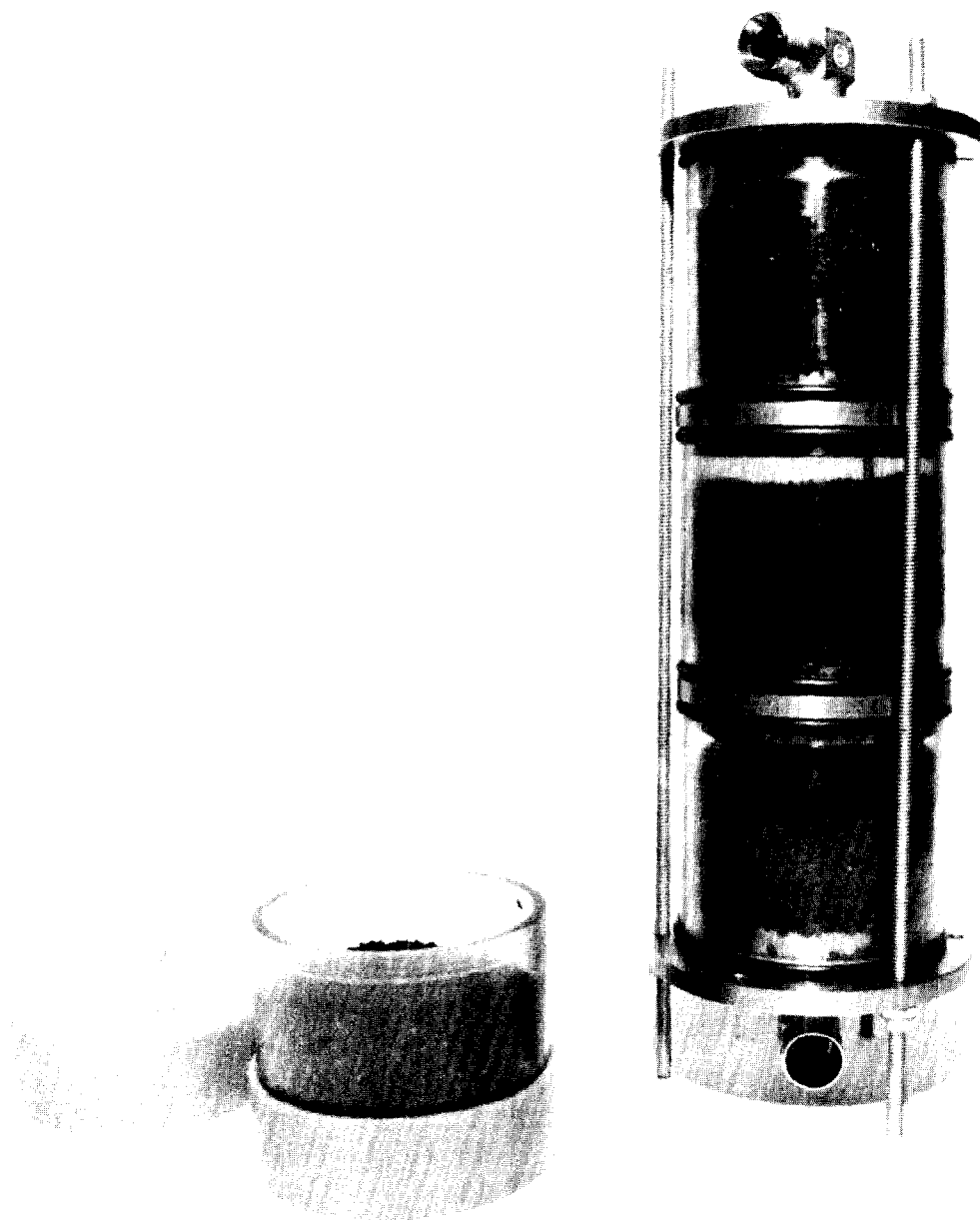
Figure 7.   Large scale SGTS sampler.

(approximately 90 g) is too large for the normal counting dishes, therefore, the sampler was designed to allow counting of the carbon in the same plastic containers as used in the individual sections. After the completion of a test, the sampler is taken to a fume hood, the tie bolts removed, the metal sections replaced by a plastic cap (Figure 7), the sampler sections shaken to mix up the carbon, and then the sections transferred to the radiochemical counting laboratory for analysis. Geometry factors were determined for the sampler sections to permit conversion of the count rate to microcuries. The carbon test bed removal efficiency is calculated with the following equation:

$$\text{Removal Efficiency (\%)} = 100 \left[1 - \frac{V_1 A_2}{V_2 A_1} \right]$$

where as shown in Figure 8:

$$V_1 = \text{inlet sampler flow, } \ell/\text{min,}$$

$$V_2 = \text{outlet sampler flow, } \ell/\text{min,}$$

$$A_1 = \text{inlet sampler activity, } \mu\text{Ci,}$$

$$A_2 = \text{outlet sampler activity, } \mu\text{Ci.}$$

The detection limits for each section of the inlet and outlet sampler beds are $5 \times 10^{-5} \mu\text{Ci}$ and $1 \times 10^{-4} \mu\text{Ci}$ respectively.

C.   Results And Discussion

A summary of the operating conditions and experimentally measured $CH_3^{131}I$ removal efficiencies for the individual tests is given in Table 2. The normal test procedure was to precondition the carbon test bed for 1 hour with hot, humid air; then load the bed with a $CH_3I\text{-}CH_3^{131}I$ mixture for 2 hours; followed by a 1 hour postconditioning period with hot, humid air; and finally, removal of the carbon from the samplers for counting. With the exception of Test 6, the test duration times given in Table 2 represent the methyl iodide loading period only. Test 6 was continued for 771 hours to simulate SGTS operation for the 30 day post-LOCA period, during which time the primary containment leakage is assumed to continue. The steam flow (70% relative humidity) was only maintained for the first 122 hours, since the primary containment pressures and temperatures are near ambient after 5 days. [9] To determine the effect of continuous operation on the carbon residual removal efficiency, the normal quantity of CH_3I was divided into three equal portions for Test 6 and loaded at three different times. The CH_3I loading and sampling schedule for Test 6 is given in Table 3.

HECA™ test module

400 cfm →

Flow = V_1

Flow = V_2

Nº 1 sample bed

Activity = A_1

Nº 2 sample bed

Activity = A_2

Removal efficiency (%) = $100 \left[1 - \dfrac{V_1 A_2}{V_2 A_1} \right]$
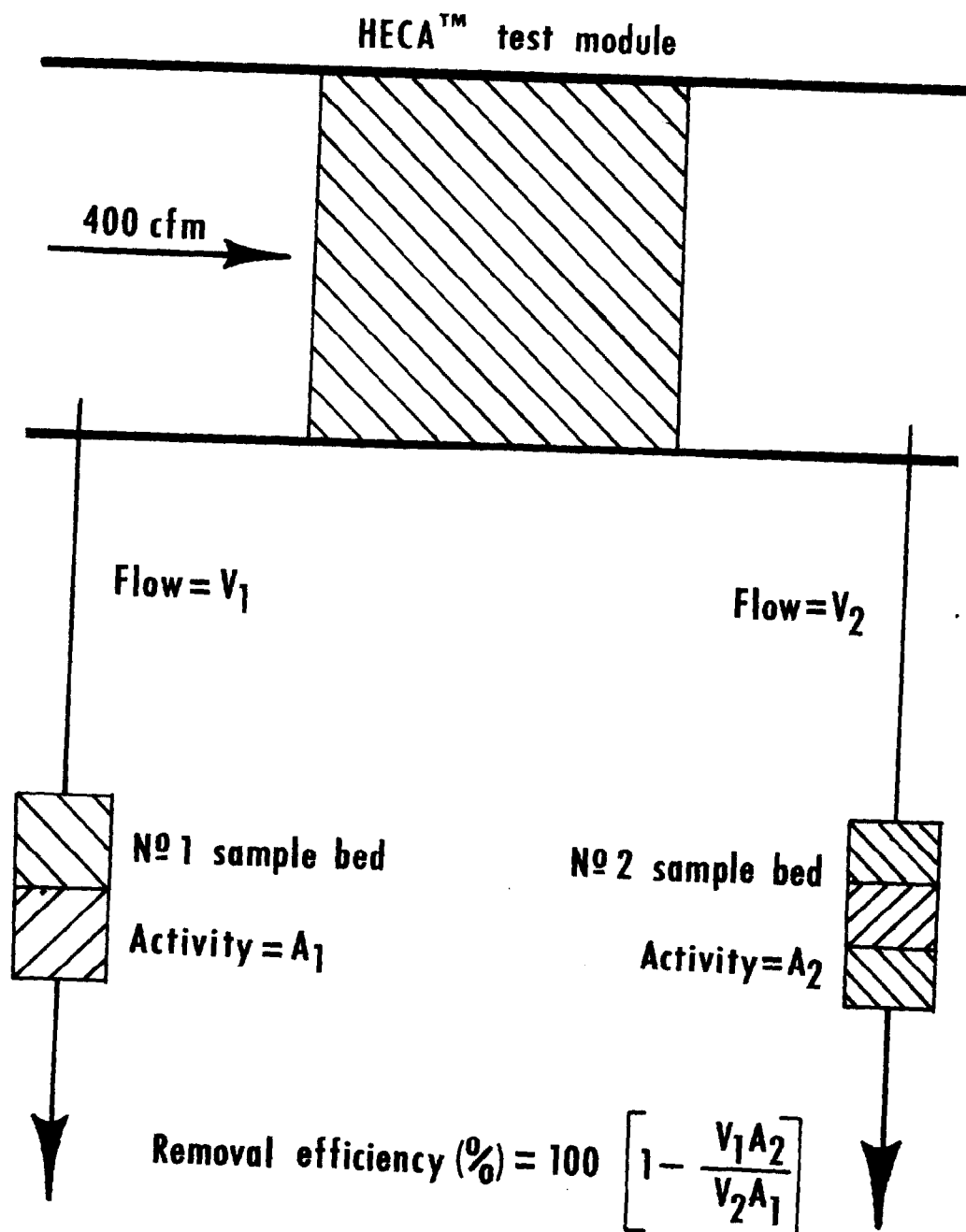
Figure 8. Large-scale standby gas treatment system samplers.

Table 2 Large-Scale System Test Summary

Carbon Type: BC-727
Carbon Lot No.: Mixture of M-1848, M-1850, and M-1856 for Test 1 and M-1874 for all others
Carbon Test Bed Area, ft²: 10
Carbon Test Bed Depth, in.: 6

Test	Test Duration, hours	Temperature, °F	RH %	Flow, cfm	Loading, mg CH_3I/gC	Activity Loading, μCi $CH_3{}^{131}I/gC$	Removal Efficiency, %
1	2	151	70	398	0.129	0.020	>99.998
2	2	151	72	395	0.292	0.014	>99.996
3	2	147-150	89-96	405	0.150	0.0084	98.8
4	2	167	70	405	0.183	0.0057	>99.993
5	2	153	83	406	0.179	0.014	>99.997
6A	4	152	70	402	0.067	0.031	>99.998
6B	122	150	72	402	0.064	0.047	>99.998
6C	771	158	0	329	0.067	0.041	>99.998
7	2	154	68	396	0.185	0.143	>99.999

Table 3   Test 6 Time Schedule

Time, hours	Comments
0	Operating temperature and humidity attained.
1	Start first addition of CH_3I-$CH_3^{131}I$ mixture.
3	Stop CH_3I-$CH_3^{131}I$ addition.
4	Remove carbon from carbon bed inlet and outlet samplers for counting.
24	Remove carbon from outlet sampler for counting.
48	Remove carbon from outlet sampler for counting.
72	Remove carbon from outlet sampler for counting.
96	Remove carbon from outlet sampler for counting.
119	Start second addition of CH_3I-$CH_3^{131}I$ mixture.
121	Stop CH_3I-$CH_3^{131}I$ addition.
122	Stop steam addition. Remove carbon from inlet and outlet samplers for counting.
168	Remove carbon from outlet sampler for counting.
336	Remove carbon from outlet sampler for counting.
528	Remove carbon from outlet sampler for counting.
672	Remove carbon from outlet sampler for counting.
768	Start third addition of CH_3I-$CH_3^{131}I$ mixture.
770	Stop CH_3I-$CH_3^{131}I$ addition.
771	Stop test and remove carbon from inlet and outlet samplers for counting.

The temperatures and relative humidities (RH) in Table 2 are the carbon test bed inlet conditions. The listed flow is the volumetric flow rate at the test bed inlet temperature and RH. The volume of carbon through which the gases flow is taken to be equal to the total screened area of the test bed (10 ft^2) times the bed thickness (0.5 ft). The carbon packing density is about 31 lb/ft^3 to give a usable carbon weight of 155 lb. although the test module total carbon inventory is approximately 400 lb. The CH$_3$I loadings and CH$_3{}^{131}$I activities reported in Table 2 are based on a carbon weight of 155 lb.

As previously mentioned, the methyl iodide for Tests 1 and 2 was metered into the test facility as a gas from a pressurized cylinder containing a mixture of CH$_3{}^{131}$I, CH$_3$I and nitrogen. However, modification of this procedure was necessary because, at the required high concentrations for these tests, the room temperature vapor pressure of CH$_3$I was exceeded in the pressurized cylinder and some liquid CH$_3$I remained in the cylinder. In Tests 3 through 7, this problem was overcome by using the pressurized cylinder for the radioactive CH$_3$I only and adding the nonradioactive CH$_3$I, as liquid, to the system with a syringe pump. The quantity of CH$_3$I actually injected in each test with the syringe pump was equivalent to 0.24 mg/g carbon.

The concentration of CH$_3$I in the test bed influent was measured with an electron capture detector gas chromatograph. The CH$_3$I loadings reported in Table 2 were based on the gas chromatographic analyses. Except for Test 3 (62%) the reported loadings are 75 to 85% of the quantity actually injected with the syringe pump, which is within the limits of accuracy of the data. As will be discussed later, condensation within the test system occurred in Test 3 and the CH$_3$I washed out by the condensate probably accounts for the observed lower bed inlet concentration.

Tests were performed without carbon in the test bed to determine whether the sample gas is representative of the bulk gas flow. The agreement between the test module inlet and outlet CH$_3$I concentrations was within 10% which is within the limits of accuracy of the gas chromatographic analyses. A test was also performed with CH$_3{}^{131}$I and the agreement between the inlet and outlet activity concentrations was within 16%. It should be noted that a $\pm$ 16% error in the measured activity would change the percent removal efficiencies reported in Table 2 by less than $\pm$ 0.001.

The CH$_3{}^{131}$I activity loadings (Table 2) are calculated from the total activity (A_1) measured on the inlet sampler. The CH$_3{}^{131}$I tracer supplied for the tests was not calibrated, therefore, it was not possible to determine an activity balance.

The removal efficiencies for Tests 1, 2 and 6A indicate the reproducibility of the data, since except for the CH$_3$I loadings the experimental conditions were essentially identical. The activity of each of the three sections of the downstream sampler was less than the detection limit ($1 \times 10^{-4} \mu$Ci) in

all tests except for Test 3. The removal efficiencies reported in Table 1 were calculated assuming the downstream sampler contained $3x10^{-4}$ μCi of $CH_3^{131}I$. Therefore, the indicated removal efficiencies are conservative and actually represent the detection limits of the experimental equipment rather than the limitation of the $HECA^{TM}$ test module.

The low removal efficiency observed in Test 3 was due to moisture on the carbon bed. As previously explained, the inlet air is heated before humidification, and the duct walls are traced with electric heaters and insulated to prevent condensation upstream of, or on, the test carbon bed. However, the wall heaters did not maintain the walls of the entire test module above the dew point of the gas (144° F in Test 3) and the subsequent condensation resulted in wetting of the test carbon bed. In addition to the wall temperature measurements, evidence of moisture on the carbon was observed when the carbon was removed from the bed.

The difficulty in maintaining the required wall temperatures was caused by the large mass of the test bed and the large heat losses through the support structure. After Test 3, the capability of the test system wall heaters was increased by modifying the heaters and operating procedures. No further problem with condensation within the test system was encountered in subsequent tests.

Test 5 was a repeat of Test 3, except it was conducted on the carbon that had been previously used in Test 4. The somewhat lower removal efficiency reported for Test 4 can be attributed to the low activity trapped on the inlet sampler. The activity distribution on the inlet sampler indicates the sampler temperature was probably below the sample gas dew point (151° F) and that some of the activity may have passed through the sampler carbon because of condensation on the carbon. The higher activity observed on the inlet sampler in Test 5 is a further indication of activity loss from the Test 4 inlet sampler because the same $CH_3^{131}I$ mixture and activity injection rates were used in both tests. Therefore, the actual removal efficiency for Test 4 was undoubtedly higher than the experimental results indicate.

The removal efficiency measured after 4 hours of operation in Test 6 was the same as the efficiencies measured after 122 hours of operation at 70% RH and after an additional 649 hours of operation with dry air. The activity on the test bed outlet sampler carbon was measured periodically throughout the test (see Table 3 for times). The activity on the test bed outlet sampler was less than the detection limit in all cases. The activity used in Test 7 was between 3 and 10 times higher than the activity used in the other tests, yet there was still no detectable activity on the carbon test bed outlet sampler.

IV.   Summary

The Standby Gas Treatment System supplied for the Enrico Fermi

Unit 2 plant had associated with it high performance requirements. Several design innovations were incorporated in the carbon adsorber to preclude any loss of efficiency due to mechanical reasons. That is, the adsorber was designed in such a way that the efficiency of the system would approach the efficiency of the adsorbent.

These concepts were tested on a 400 cfm module under design basis accident conditions. The results indicated removal efficiencies greater than 99.99% for methyl iodide under design conditions.

Acknowledgements

The authors wish to acknowledge the contributions of the following General Electric personnel to the test program; M. Siegler who made a major contribution toward the planning and execution of the program and T. L. Wong who supervised a portion of the experimental work. The authors also wish to acknowledge the contributions of T. Hickey and J. Tennyson of the CVI Corporation who were instrumental in the development of the HECA^{TM} design.

References

1. Meteorology and Atomic Energy, Prepared by United States Department of Commerce Weather Bureau for United States Atomic Energy Commission, Washington, D. C., July 1955, Pages 66 and 67.

2. Sepsy, Charles F., and Jones, Charles D., "Pressure Drop and Temperature Distribution in a Single Cell Charcoal Filter", March 14, 1972.

3. Hickey, T. N., and Edwards, J.,"Economic Comparison of an Improved Nuclear Filter System Considering Space, Operation, Testing and Maintenance Costs", 13th AEC Air Cleaning Conference.

4. Siegwarth, D. P., and Siegler, M.,"Detroit Edison Standby Gas Treatment System Gasketless Filter Test Series", General Electric Co., Report NEDC-12431, July 1973.

5. The Detroit Edison Company Specification 3071-56, "Standby Gas Treatment System Filter Units, Enrico Fermi Atomic Power Plant Turbine Generator Unit No. 2", August 12, 1971.

6. Cottrell, W. B., "ORNL Nuclear Safety Research and Development Program Bimonthly Report for July-August 1967", ORNL-TM-1986, September 21, 1967.

7. Cottrell, W. B., "ORNL Nuclear Safety Research and Development Program Bimonthly Report for January-February 1968", ORNL-TM-2164, March 26, 1968.

8. Cottrell, W. B., "ORNL Nuclear Safety Research and Development Program Bimonthly Report for January-February 1969", ORNL-TM-2533, May 1969.

9. The Detroit Edison Company, "Enrico Fermi Atomic Power Plant - Unit 2, Preliminary Safety Analysis Report, Exhibit C, Volume 2", April 29, 1969.

DISCUSSION

SHAPIRO: I'd like to know if the efficiencies you have tabulated include the HEPA filters apparently incorporated between the two sample points and if an activity balance was performed on the entire filter set to establish charcoal adsorber efficiency?

PARISH: No. The reported efficiencies were what you would consider, I guess, a system efficiency. Of course the arrangement of HEPA filters and carbon beds is the same as in the production unit.

SHAPIRO: There was no attempt made to identify the removal effects of the HEPA filters?

PARISH: No, there was not. There would be no reason to expect that the HEPA filters were a factor, since there was essentially no particulate activity present.

ELEMENTAL IODINE AND METHYL IODIDE ADSORPTION ON
ACTIVATED CHARCOAL AT LOW CONCENTRATIONS

By Ronald R. Bellamy*
Nuclear Engineering Department
The Ohio State University
Columbus, Ohio

Abstract

The capability of activated charcoal to adsorb elemental iodine and methyl iodide at low concentrations has been experimentally evaluated to observe the effect of the variation of certain operating parameters within specified limits. The operating parameters include inlet concentration, superficial velocity, relative humidity, type of charcoal and impregnant, charcoal mesh size, duration of test and bed depth. The data obtained in an intensive study of these parameters have been correlated assuming a two-step adsorption mechanism for radioiodine on activated charcoal. The correlation is presented to aid the nuclear industry in designing charcoal adsorber systems for radioiodine retention.

I. Introduction

Recent consideration to assign numerical guides as design objectives and limiting conditions for operation of light-water-cooled nuclear power reactors to keep radioactive material in effluents as low as practicable[1],[2] has placed additional responsibility on the designers of air filtration systems for nuclear facilities. Gaseous effluent streams may require treatment to remove radioiodine to levels where little operating or laboratory data are available to substantiate design and performance of individual components. There is a need for the adsorption properties of elemental radioiodine (^{131}I) and methyl iodide (CH$_3$^{131}I) on activated charcoal at low concentrations to be put on a definitive experimental engineering foundation.

Past efforts to obtain experimental data and provide a firm basis for design of iodine removal systems have been limited to either specific removal systems or well-controlled bench-scale studies. Primary emphasis has been directed at understanding specific reaction steps or the effect of a single service parameter on filter efficiency (humidity, charcoal mesh size, impregnant, weathering, aging, poisoning, flow rate or inlet concentration)[3]-[11]. With the exception of a few studies, [12],[13] no attempt has been made to obtain adsorber bed efficiencies based on a comprehensive program in which the important operating parameters enumerated above are controlled and systematically varied. This paper presents experimental data obtained on a bench-scale adsorption system with no uncontrolled parameters. These parameters were

---

*Present affiliation USAEC, Directorate of Licensing, Bethesda, Maryland.

systematically varied to observe the effect of each on the adsorption properties of radioiodine on activated charcoal.

Although the presentation of radioiodine adsorption data as discussed in this paper may aid the nuclear power industry in designing more efficient radioiodine removal systems, the application of correlation techniques to the data would be additionally instrumental in establishing this important aspect of nuclear safety on a firm engineering foundation. This approach has only been followed to a limited degree on the existing experimental data presented to date in the literature[13]-[16] and has met with little success. The results of the correlation presented in this paper provide a means to (1) present unambiguously the dependence of adsorber efficiencies on important system parameters, (2) provide greater insight into the adsorption mechanisms of radioiodine on activated charcoal, and (3) provide an engineering method of designing charcoal adsorption beds based on experimental data.

II. Radioiodine Adsorption Principles

The means of adsorption of radioiodine on activated charcoal depends on the form of the radioiodine (elemental or organic) and the type of impregnant (if any) associated with the charcoal. Elemental iodine is largely adsorbed physically on active carbon surfaces, irrespective of any impregnant. Organic iodides are chemisorbed on potassium iodide $K^{127}I$ impregnated activated charcoal by the isotopic exchange reaction[10]

$$CH_3{}^{131}I \text{ (air)} + K^{127}I \text{ (charcoal)} \rightarrow$$

$$CH_3{}^{127}I \text{ (air)} + K^{131}I \text{ (charcoal)}$$
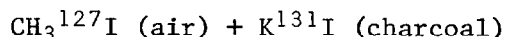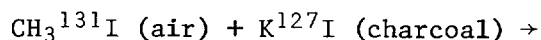
using $CH_3{}^{131}I$ as the typical organic iodide. Although it is only the ^{131}I constituent of the $CH_3{}^{131}I$ molecule that is trapped by the isotopic exchange mechanism, it is common practice to refer to the removal efficiency for the ^{131}I constituent as being that for $CH_3{}^{131}I$.

If the activated charcoal is impregnated with triethylenediamine (TEDA), a heterocyclic amine compound, a different mechanism exists for $CH_3{}^{131}I$ removal. As a group, amines are more receptive to methyl iodide molecules than to water molecules; therefore, superior operation at high humidities would be expected[12]. The initial reaction of the amine group with $CH_3{}^{131}I$ converts the radioiodine molecule to an ionic form which reacts more easily with the base charcoal, symbolized by

$$R_3N + CH_3{}^{131}I \rightarrow R_3N^+CH_3{}^{131}I^-.$$
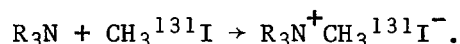
The quaternary iodide produced ($R_3N^+CH_3{}^{131}I^-$) is a stable nonvolatile compound that is adsorbed strongly on the charcoal. When TEDA is the amine, the quaternary iodide has a melting point of 390°C. Heterocyclic amines which contain a second amine group or other reactive group at the opposite end of the molecule show superior chemisorption properties for organic iodides

due to the ability to attach the amine firmly to the charcoal and yet retain a sufficiently reactive basic amine group to react with the organic iodide. TEDA is obviously of this group, as evidenced by Fig. 1.

III. Experimental Procedure

Figure 2 presents a schematic of the experimental system employed to acquire experimental information on the adsorption properties of radioiodine on charcoal beds. The open-loop system of 3-inch diameter glass pipe includes charcoal test beds, air rotameters, glass wool filters and thermocouples. "Pyrex" glass pipe was chosen for the facility in order to minimize plate-out of the radioiodine. The system was designed and operated to eliminate all unknown variables and to control and observe all pertinent operating parameters.

Air (atmospheric) was prefiltered before entering the system to remove foreign substances (particulates). Air flows were measured by a number of calibrated rotameters, each with a different range of flow. An iron-constantan thermocouple was used to determine the air temperature upstream of the test beds. Two thermometers were placed in the air stream to determine relative humidity from the dry-bulb and wet-bulb temperatures. To control the relative humidity, air was permitted to flow through a combination of 3 different gas dispersion tubes in series. This maintained the relative humidity of the air stream at a constant predetermined value for the duration of any one test.

During testing with ^{131}I as source material, crystals of the iodine were allowed to sublime in the filtered air flow upstream of any charcoal beds. To produce a methyl iodide source, liquid $CH_3^{131}I$ was evaporated from a planchet placed in the air stream. Before radioactivity was introduced into the flow system, the air was permitted to flow over the four charcoal beds in series for at least one hour to equilibrate the beds.

The design of the charcoal test canisters was critical, since bypass of the beds and leakage had to be eliminated. Pieces of carbon-steel pipe were cut to varying lengths (from 1/2 inch to 6 inches), then a 40-mesh screen was welded to each end to retain the charcoal in the beds. Standard ball-and-socket joints, affixed over the 40-mesh screen, allowed the beds to be inserted (with no leakage) into the glass pipe at approximately 12-inch intervals. A screw tap on the top of each canister allowed the beds to be filled with charcoal prior to a test and then emptied at the end of the experiment.

Charcoal efficiencies were determined by a sodium-iodide (NaI) well-type scintillation crystal and photomultiplier tube, high voltage supply, scaler, counter and timer. After an experimental run was completed, each bed was individually removed from the flow system and its activity counted. Efficiencies reported in this paper represent the ratio of the change in the inlet and outlet concentration (for any one charcoal bed) to the inlet concentration. Since the fourth bed in series was always a minimum of 3 inches deep and contained little or no activity, no radioiodine (elemental or organic) passed through all four beds without adsorption. Therefore, the total activity contained on all beds represents an inlet concentration, and this total activity was compared to a standard source of known activity of ^{131}I to calculate the inlet concentration.
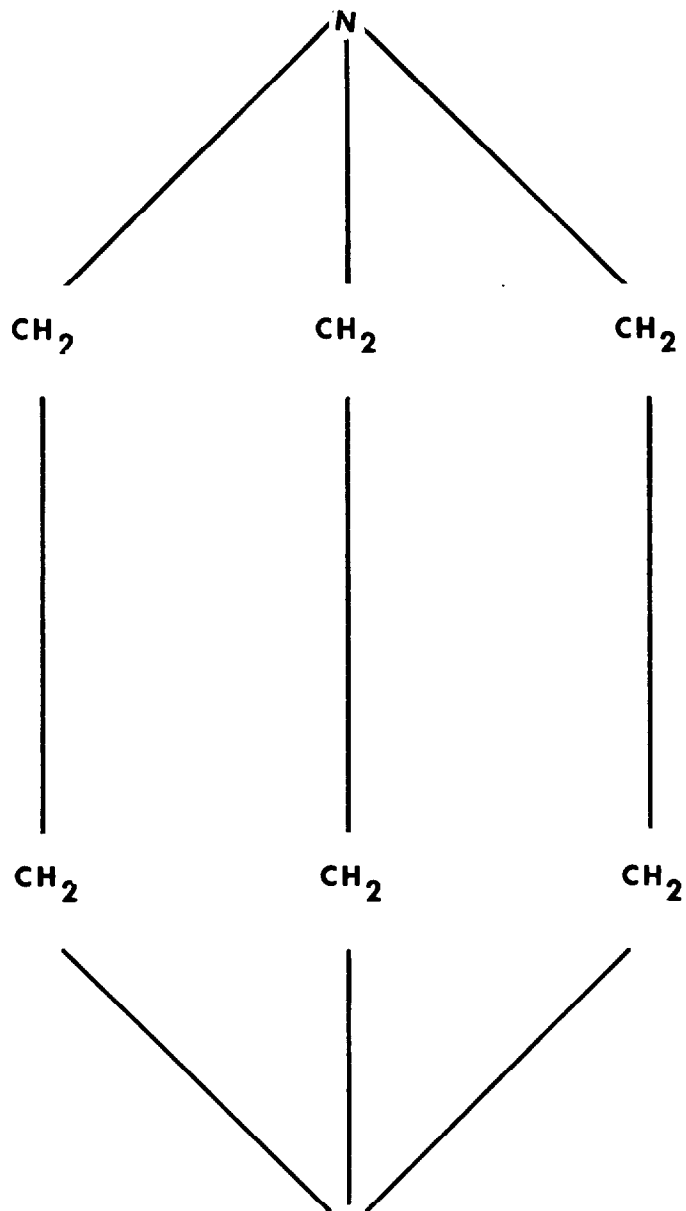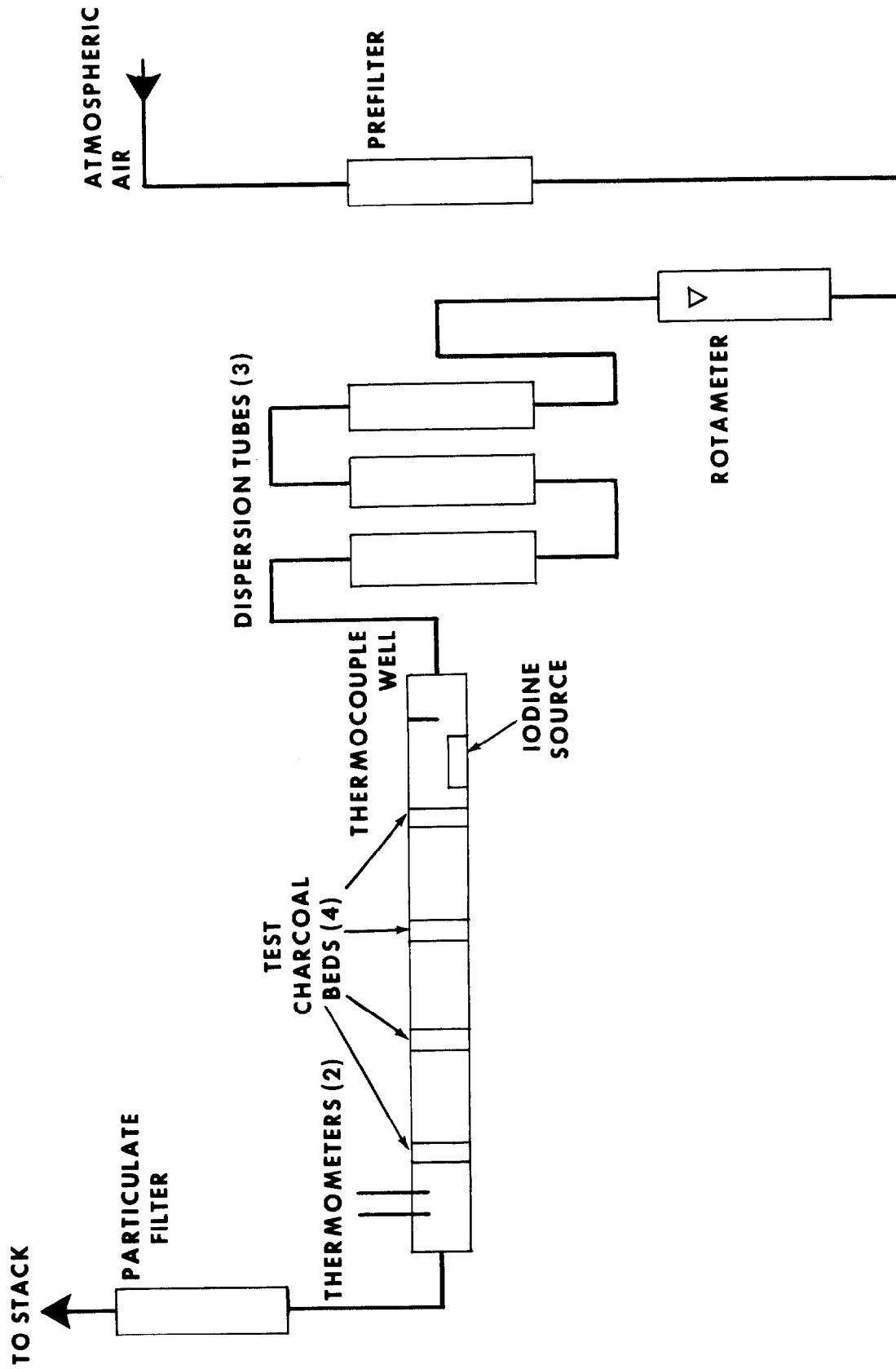
N

CH$_2$ CH$_2$ CH$_2$

CH$_2$ CH$_2$ CH$_2$

Fig. 1 A TEDA molecule.

Fig. 2 The experimental system.

IV. ^{131}I Adsorption Efficiencies

Removal of ^{131}I was studied using a minimum bed depth of 1 inch, and all experiments yielded a removal efficiency of 99.99$^+$%. This removal efficiency implies the limits of measurement have been reached with the available apparatus. None of the parameters studied (inlet concentration, superficial velocity, relative humidity, charcoal mesh size and charcoal manufacturer and impregnant) affected the observed removal efficiency. The ^{131}I adsorption efficiencies reported in this paper are all at a temperature of 25°C and a pressure of 1 atm. Reference 17 contains a detailed tabulation of the data.

Inlet Concentration

The inlet concentration was varied from 6.62×10^{-9} to 1.54×10^{-7} µCi/ml of ^{131}I by varying the amount of ^{131}I used as source material. A 1-inch bed of Barnebey-Cheney (BC) 727 charcoal was observed to adsorb 99.99$^+$% of the inlet activity for a 3-hr experiment, independent of the inlet concentration for the stipulated range. Other experimental conditions were a relative humidity of 25% and a superficial velocity of 40 feet per minute (fpm).

Superficial Velocity

A series of 3 calibrated rotameters was available to adjust the air flow rate as required. The superficial velocity was varied from 5 to 135 fpm. A bed depth of 1 inch of BC 727 charcoal was observed to adsorb 99.99$^+$% of the ^{131}I injected into the system for a 3-hr experiment, independent of the superficial velocity for the stipulated range. Other experimental conditions were a relative humidity of 25% and an ^{131}I inlet concentration of 5×10^{-8} µCi/ml.

Relative Humidity

Three gas dispersion tubes used in series in various combinations permitted the relative humidity to be varied from 22% to saturated air (100%). A relative humidity of 100% was accompanied by moisture droplets condensing on the charcoal test cartridges and on the glass pipe. A 1-inch bed of BC 727 charcoal was observed to adsorb 99.99$^+$% of the ^{131}I injected into the system for a 3-hr experiment, independent of the relative humidity for the stipulated range. Other experimental conditions were a superficial velocity of 40 fpm and an ^{131}I inlet concentration of 5×10^{-8} µCi/ml.

Charcoal Mesh Size

Charcoal supplied by a vendor is stipulated to be a certain mesh size; BC 727 (KI impregnated) is 8 x 14 mesh. Using a set of Tyler mesh sieves the charcoal was sorted based on mesh size, and the various specific meshes tested to determine any effect on iodine removal efficiencies. Of the mesh sizes tested, no mesh size combination was found to affect the removal efficiency of ^{131}I. A 1-inch bed of BC 727 charcoal removed 99.99$^+$% of the ^{131}I injected into the system for a 3-hr experiment. The mesh sizes tested were 2 x 4, 2 x 6, 6 x 8, 8 x 16, 16 x 18, 16 x 32, and 2 x 32. Other experimental conditions were a relative humidity of 25%, a superficial velocity of 40 fpm and an ^{131}I inlet concentration of 5×10^{-8} µCi/ml.

Type of Charcoal

Various types of charcoal with different impregnants were tested to ascertain if this parameter had any effect on iodine removal efficiencies. Of the charcoal types and impregnants tested, none had any effect on the adsorption efficiency of ^{131}I. A 1-inch bed removed 99.99+% of the ^{131}I injected into the system for a 3-hr experiment. The charcoals and impregnants tested were BC 416 (no impregnant), BC 727 (KI impregnant), Witco 42 (KI impregnant), North American Carbon NACAR G 210 (no impregnant), NACAR G 615 (KI & TEDA impregnant), Pittsburgh Activated Carbon PCB (no impregnant, coal based), Pittsburgh Activated Carbon FCA (metallic oxide impregnant, coal based), and Pittsburgh Activated Carbon BPL (no impregnant, cocoanut based). Other experimental conditions were a relative humidity of 30%, a superficial velocity of 40 fpm and an ^{131}I inlet concentration of 4 x 10^{-8} µCi/ml.

V. $CH_3^{131}I$ Adsorption Efficiencies

Removal of $CH_3^{131}I$ was found to be a function of inlet concentration, superficial velocity, relative humidity and bed depth. $CH_3^{131}I$ adsorption efficiencies were observed not to be a function of charcoal mesh size, type of charcoal or duration of experimental run. However, a 5-inch bed of charcoal adsorbed 99.99+% of the inlet $CH_3^{131}I$ activity, for any combination of parameters used in an experiment. The $CH_3^{131}I$ adsorption efficiencies reported in this paper are all at a temperature of 25°C and a pressure of 1 atm. Reference 17 contains a detailed tabulation of the data.

Inlet Concentration

The inlet concentration was varied from 2.26 x 10^{-9} to 1.58 x 10^{-4} µCi/ml of $CH_3^{131}I$ by varying the amount of $CH_3^{131}I$ used as liquid source material. Bed depths studied were 1/2 inch, 1 inch, 2 inches, and 5 inches. The variation of methyl iodide removal efficiency with inlet concentration and bed depth is presented in Fig. 3.

A number of conclusions can be immediately reached upon perusal of the experimental data. At inlet concentrations less than 10^{-6} µCi/ml, a 1/2-inch bed of BC 727 charcoal removes 99.99+% of the inlet activity for a 3-hr experiment. At inlet concentrations above 10^{-6} µCi/ml, the removal efficiency drops off drastically for a 1/2-inch bed of charcoal. As the bed depth is increased, a higher inlet activity will be removed, and a 5-inch bed of BC 727 charcoal will remove 99.99+% for the upper limit of 1.58 x 10^{-4} µCi/ml of $CH_3^{131}I$ injected for a 3-hr experiment. Other experimental conditions were a relative humidity of 25% and a superficial velocity of 40 fpm.

Although the removal efficiency decreases as the inlet concentration of $CH_3^{131}I$ is increased, the amount of $CH_3^{131}I$ adsorbed increases as the inlet concentration of $CH_3^{131}I$ is increased. This implies in part that the adsorption mechanism may be controlled by gas-phase diffusion of adsorbate to the adsorbent surface. Since more molecules of $CH_3^{131}I$ are present at
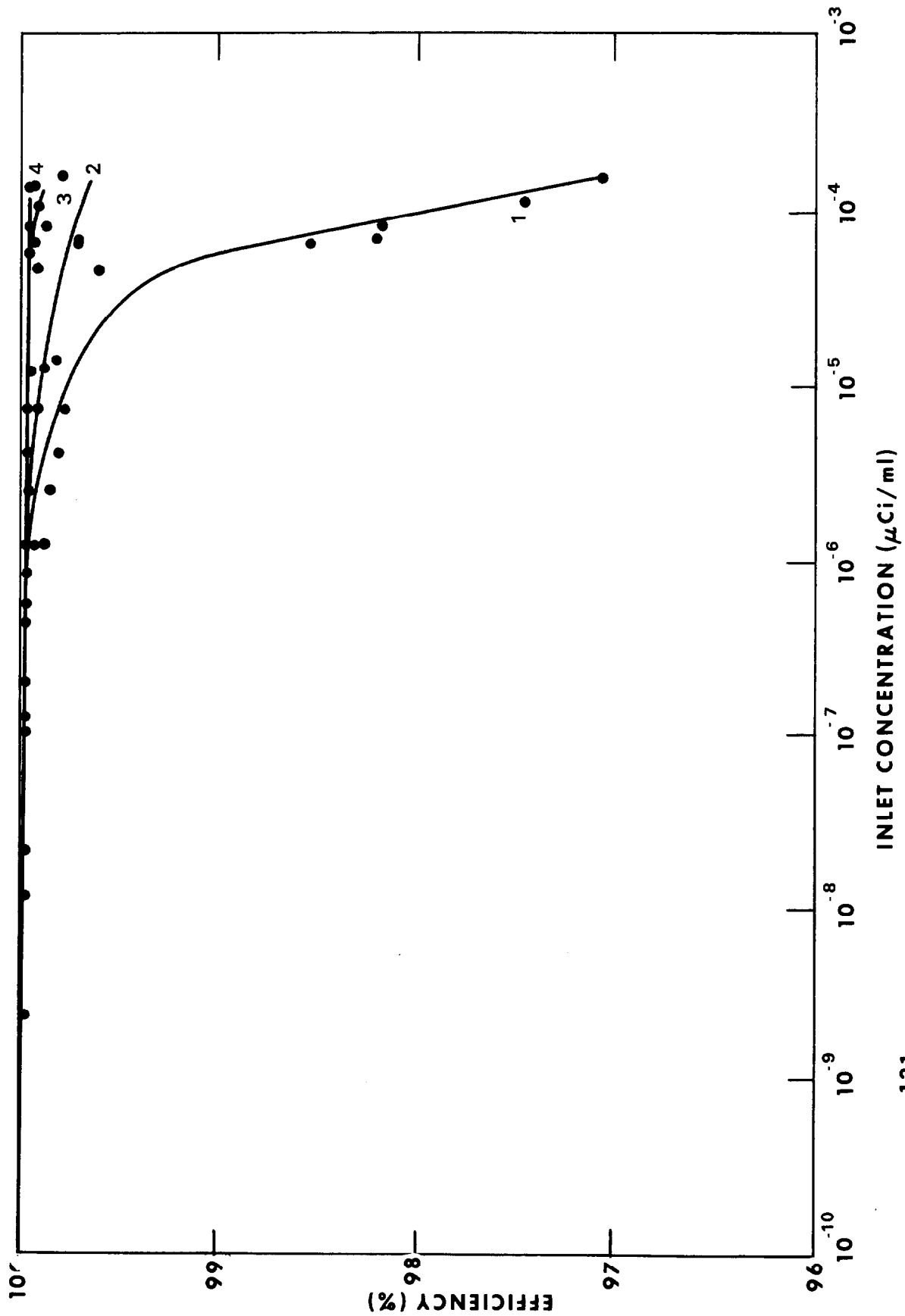
Fig. 3 CH$_3$ ^{131}I removal efficiency as a function of inlet concentration and bed depth. 1, 1/2-inch bed. 2, 1-inch bed. 3, 2-inch bed. 4, 5-inch bed.

higher concentrations and more are removed, it would appear the rate of adsorption of $CH_3^{131}I$ is dependent on the concentration gradient (driving force) of $CH_3^{131}I$ between the air stream and the charcoal surface.

Relative Humidity

Three gas dispersion tubes used in series in various combinations permitted the relative humidity to be varied from 30% to saturated air (100%). Saturated air conditions were confirmed by the condensation of water droplets on the inside of the glass pipe and on the test charcoal cartridges, and resulted in a drastic reduction in $CH_3^{131}I$ removal efficiencies. This type of behavior has been noted previously[4],[8],[12],[16],[18],[19]. The variation of methyl iodide removal efficiency with relative humidity and bed depth is presented in Fig. 4. For a 1/2-inch bed of BC 727 charcoal and a 3-hr experiment, the removal efficiency decreased from 99.77% at 30% relative humidity to 66.28% at 100% relative humidity. The reduction is much less severe for a 1-inch bed (from 99.97% at 30% relative humidity to 99.53% at 100% relative humidity), and for a 2-inch or deeper charcoal bed there is no noticeable effect on $CH_3^{131}I$ removal efficiencies by relative humidity for the conditions of these tests. Other experimental conditions were a superficial velocity of 40 fpm, a $CH_3^{131}I$ inlet concentration of 1.4 x 10^{-5} µCi/ml and a 3-hr experiment.

The severe reduction in $CH_3^{131}I$ removal efficiency at a relative humidity greater than 95% and the observation of water condensation on the charcoal suggests that there is a surface phenomenon that controls radioiodine adsorption to some unknown degree. It is postulated that the presence of water on the charcoal, whether or not the charcoal pores are clogged by the water, adds a resistance to the $CH_3^{131}I$ adsorption.

Superficial Velocity

The calibrated rotameters were employed to vary the superficial velocity from 20 to 200 fpm. Figure 5 shows that the $CH_3^{131}I$ removal efficiency decreases as the flow velocity is increased when the other variables were kept constant. The effect was not drastic. With increased bed depth, the dependence of removal efficiency on flow rate was less, and for 2-inch or deeper charcoal beds, 99.99 % of the inlet activity was removed during a 3-hr experiment, independent of the superficial velocity for the stipulated range. Other experimental conditions were a relative humidity of 25% and a $CH_3^{131}I$ inlet concentration of 1 x 10^{-5} µCi/ml. It is noted that a more severe reduction of removal efficiency with increasing superficial velocity has been reported elsewhere[12], but the results were obtained at a significantly different inlet concentration and relative humidity.

The removal efficiency of $CH_3^{131}I$ does drop as the molecules travel at a faster rate of speed through a charcoal bed when other variables are kept constant. This implies that some of the adsorption sites available at lower flow rates are not available at the higher flow rates. One possible explanation is that once a molecule is adsorbed on an adsorption site, the adsorbed molecule must travel into a capillary before the adsorption site is again available for further adsorption. During the time interval when diffusion
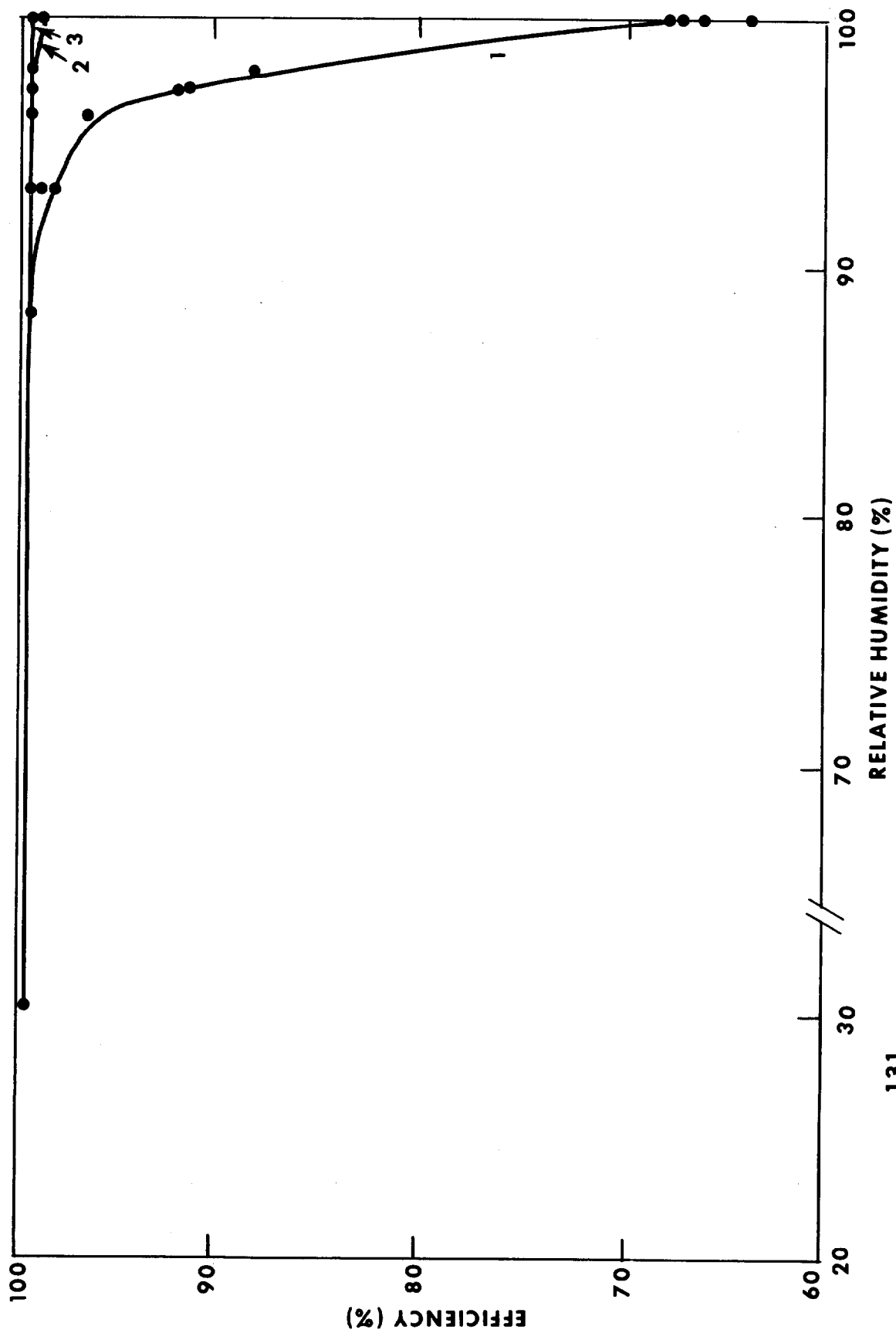
Fig. 4 CH$_3$ ^{131} I removal efficiency as a function of relative humidity and bed depth.
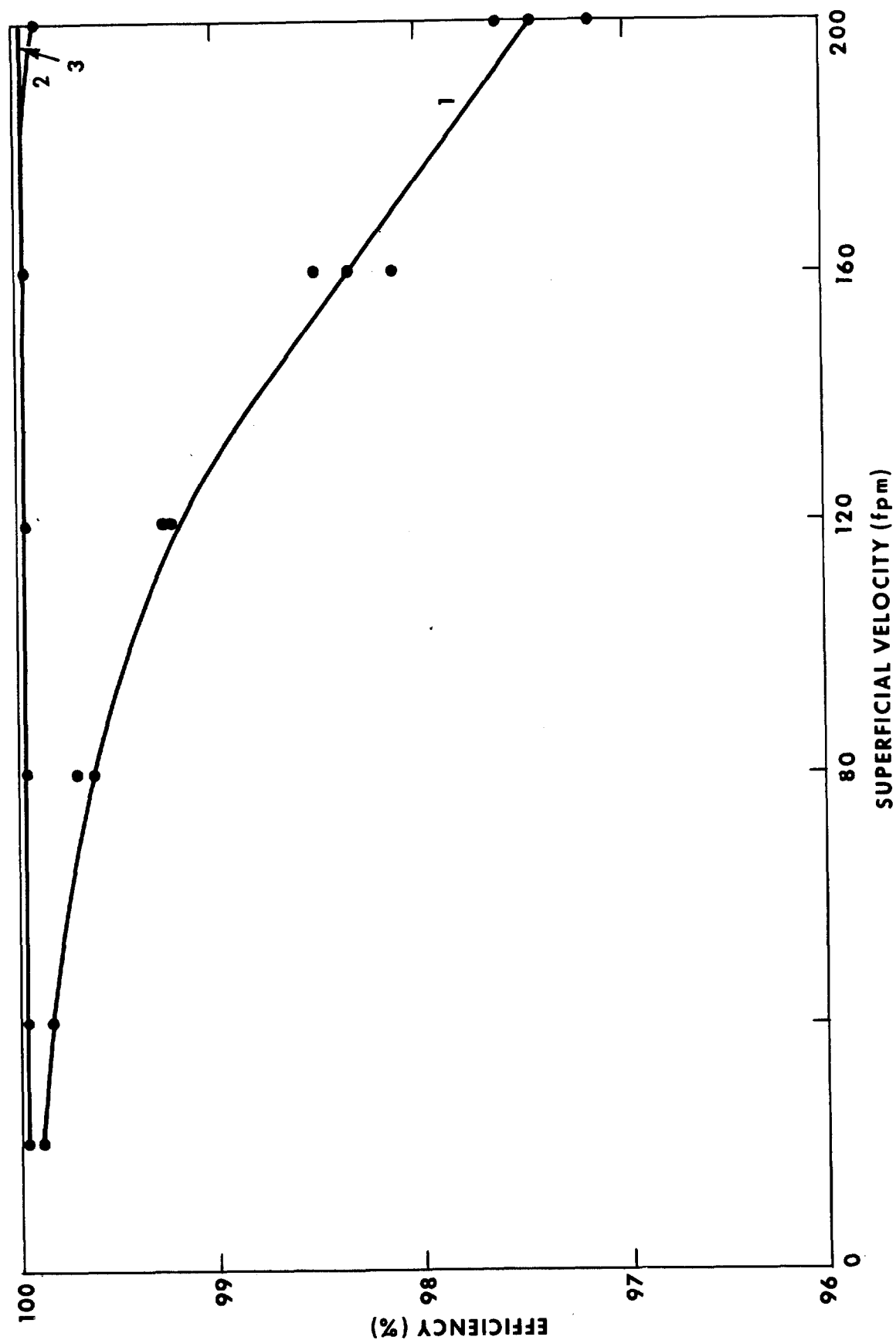1, 1/2-inch bed. 2, 1-inch bed. 3, 2-inch bed.

Fig. 5 CH$_3$ ^{131}I removal efficiency as a function of superficial velocity and bed depth. 1, 1/2-inch bed. 2, 1-inch bed. 3, 2-inch bed.

of the absorbed molecule into a capillary is occurring, the adsorption site is $\underline{not}$ available for adsorption, and a $CH_3{}^{131}I$ molecule striking the adsorption site cannot be adsorbed. Thus, the removal efficiency is lower as the superficial velocity is increased.

Charcoal Mesh Size

A set of Tyler mesh sieves was employed to sort BC 727 charcoal according to mesh size, or equivalently, average particle diameter. The charcoal is stipulated by the vendor to be 8 x 14 mesh, but a sizeable fraction (greater than 5%) is larger than 8 mesh, and mesh sizes smaller than 14 mesh may easily be obtained by pulverizing the charcoal. Varying the mesh size showed no effect on the adsorption efficiency of $CH_3{}^{131}I$. The mesh sizes considered for these tests were 2 x 8, 8 x 10, 10 x 12, 12 x 14, 14 x 20, and 20 x 28. At an inlet concentration of 1 x 10^{-5} µCi/ml, a relative humidity of 25% and a 40 fpm superficial velocity, a 1/2-inch bed of BC 727 charcoal removed 99.36% of the $CH_3{}^{131}I$ inlet activity, while a 1-inch bed removed 99.99+% of the $CH_3{}^{131}I$ inlet activity, for a 3-hr experiment, irrespective of the mesh size for the stipulated range. It is noted that a reduction of removal efficiency with smaller mesh sizes has been reported elsewhere[12], but the results were obtained at a significantly different inlet concentration and relative humidity.

Type of Charcoal

Various charcoals were tested to determine if the charcoal of one vendor or the type of impregnant would have any effect on the removal efficiency of $CH_3{}^{131}I$. Five types of charcoal were tested: BC 727 (KI impregnant), BC 416 (no impregnant), NACAR G 615 (KI & TEDA impregnant), Witco 42 (KI impregnant) and Pittsburgh Activated Carbon FCA (metallic oxide impregnant, coal based). Of these charcoals, none had any effect on $CH_3{}^{131}I$ adsorption efficiency, and a 1/2-inch bed of charcoal was observed to adsorb 99.99+% of the inlet $CH_3{}^{131}I$ activity for a 3-hr experiment. Other experimental conditions for these results were a relative humidity of 25%, a superficial velocity of 40 fpm and a $CH_3{}^{131}I$ inlet concentration of 1 x 10^{-7} µCi/ml.

Duration of Experimental Run

The effect of the duration of an experimental run on $CH_3{}^{131}I$ removal efficiency was studied by performing a series of tests that varied the duration of the experiment. In all cases, no effect on $CH_3{}^{131}I$ removal efficiency was noted for the conditions reported herein. Runs were performed for 3, 6, and 12 hours at an inlet concentration of 2.5 x 10^{-7} µCi/ml. A 1/2-inch bed of BC 727 charcoal was observed to adsorb 99.99+% of the $CH_3{}^{131}I$ inlet activity, irrespective of the duration of the experiment for the stipulated range. Similarly, at an inlet concentration of 3 x 10^{-6} µCi/ml a 1/2-inch bed of BC 727 charcoal produced a removal efficiency of 99.82% for a 3-hr run, and 99.83% for a 12-hr run. For a 1-inch bed of BC 727 charcoal, an inlet concentration of 3 x 10^{-6} µCi/ml was completely adsorbed (99.99+%) during both a 3-hr experiment and a 12-hr experiment. Other experimental conditions were a relative humidity of 25% and a superficial velocity of 40 fpm.

It was not surprising that the duration of the experimental run had no effect on $CH_3{}^{131}I$ removal efficiency for these tests, since the adsorption capacity

of BC 727 charcoal is reported as 10 mg/gm of charcoal[20], and the conditions of the experiments reported herein deposit a maximum of 10^{-8} mg/gm. Therefore, the adsorption capacity of the charcoal for $CH_3^{131}I$ is not in any way being approached.

Additionally, these results predict that no aging of the charcoal will occur during 12 hours of operation, nor are there sufficient poisons in normal atmospheric air to accumulate on the charcoal in 12 hours that would interfere with the adsorption process.

VI. The Surface Rejuvenation Adsorption Mechanism

Figures 3 through 5 show experimental data that support the conclusion that the removal efficiency of $CH_3^{131}I$ on activated charcoal is a function of the inlet stream properties, notably inlet concentration, relative humidity and superficial velocity (other experimental conditions are as discussed above). Conversely, the charcoal properties, including mesh size, charcoal manufacturer and type of impregnant (if any) appear to have no effect on the $CH_3^{131}I$ removal efficiencies, for ambient conditions of temperature, pressure, relative humidity and a superficial velocity of 40 fpm.

More specifically, $CH_3^{131}I$ removal efficiencies decrease with increasing relative humidity and superficial velocity, with a more drastic reduction for the humidity increase. The inlet concentration shows a similar effect. Removal efficiencies decrease as the inlet concentration approaches 10^{-4} µCi/ml. Gas-phase diffusion should be one resistance to adsorption (more molecules are adsorbed when there are more to diffuse to the adsorbent surface), but this does not fully explain the large decrease in removal efficiencies at high humidities. Thus, a second resistance is theorized as a resistance to surface diffusion. Once a molecule reaches an adsorptive site by gas-phase diffusion, it undergoes surface diffusion through a capillary to a site inside a pore. This leaves the original adsorption site free for further adsorption (the site is rejuvenated). At high humidities, water clogs the pores and increases the resistance to surface diffusion, decreasing removal efficiencies. At high flow rates, the adsorbate molecules reach adsorption sites too quickly in succession to allow surface diffusion to regenerate the adsorption site.

The proposed $CH_3^{131}I$ adsorption mechanism on activated charcoal is therefore composed of two steps. First, the adsorbate molecule must reach an active adsorption site by gas-phase diffusion. Second, the adsorbate molecule must leave the now-inactive adsorption site by surface diffusion, diffuse through a capillary to a site inside a charcoal pore and create an active adsorption site where an inactive adsorption site once resided. This proposed type of radio-iodine adsorption will be termed the surface rejuvenation adsorption mechanism.

The Surface Diffusion Phenomenon

Once a molecule is adsorbed on a charcoal surface, the molecule is presumed not to be stationary but to travel by surface diffusion to other adsorption sites on the charcoal. The phenomenon of surface diffusion is concerned with the behavior of the adsorbed molecule during the time it is traveling from one adsorption site to another on the charcoal surface. The surface diffusion phenomenon will only be introduced here; detailed information on the subject is available in Refs. 21 through 31.

This phenomenon can be pictured as a molecule hopping from site to site on an adsorbent surface, and will take place only if the adsorbate molecule acquires sufficient energy from fluctuations of whatever source to overcome the heat of adsorption. Three possible sources of energy can be postulated: a molecule striking the adsorbent surface at an angle with a momentum component in a direction parallel to the surface, temperature-induced movement of the atoms of the surface, and fluctuation of the adsorption energy on the surface due to the structural arrangement (including defects) of the surface atoms.

Qualitative Treatment

The proposed mechanism for the adsorption of iodine on activated charcoal consists of two steps. First, the adsorbate molecule diffuses through the gas film and finds an active (unoccupied) adsorption site and is adsorbed. The site is immediately rendered inactive, and is incapable of further adsorption until it is reactivated. The rejuvenation (or reactivation) process proposes surface diffusion of the adsorbate molecule through a pore to a secondary active site located somewhere in the capillary. Once the adsorbate molecule leaves the surface adsorption site, the site is rejuvenated for further adsorption. However, during the time the adsorbate molecule is situated on this primary adsorption site, the site is inactive and cannot be used for adsorption. This time of adsorption will be considered constant for a given set of experimental conditions, or at least it is proposed that some characteristic average adsorption time τ_m exists.

If a second adsorbate molecule strikes a primary adsorption site that is still occupied, adsorption will not occur. Therefore, adsorption efficiencies will be influenced by the rejuvenation process for the primary adsorption site, presumed to be surface diffusion. Factors that hinder surface diffusion should hinder the adsorption process, such as the relative humidity. Moisture on the charcoal (as evidenced experimentally) retards surface diffusion and should lower the adsorption efficiency of the charcoal. This effect was observed experimentally and illustrated in Fig. 4. Similarly, any experimental parameter that causes adsorbate molecules to reach a primary adsorption site already containing an adsorbed molecule should lower adsorption efficiencies. This will occur whenever the adsorbed molecule has not resided on the site for the time τ_m and therefore the site has not had sufficient time to rejuvenate itself by surface diffusion. Thus, as the superficial velocity is increased, the removal efficiencies for iodine on activated charcoal would be expected to be lower, due to the molecules moving too fast to occupied primary adsorption sites. This effect was observed experimentally and illustrated in Fig. 5. An increase in adsorbate concentration should also lower removal efficiencies since too many molecules are present in the gas stream to allow an occupied primary adsorption site sufficient time for rejuvenation by surface diffusion. This effect was observed experimentally and illustrated in Fig. 3.

Quantitative Treatment

A mathematical treatment of the surface rejuvenation adsorption model is possible by assuming that the mean time for regeneration, i.e., the time interval commencing when an adsorbate molecule attaches to an unoccupied site and ending when that same site is ready for further adsorption, is a constant for specified operating conditions. The following parameters may also be defined:

$V(z)$ = number of vacant adsorption sites per unit adsorbent length;

V_m = total number of adsorption sites per unit adsorbent length;

$V_m - V(z)$ = number of occupied adsorption sites per unit adsorbent length;

A_t = area available for transfer from fluid to solid;

A_f = area available for fluid flow;

τ_m = mean time for regeneration;

k = overall mass transfer coefficient from fluid to solid; and

$C(z)$ = concentration of adsorbate in fluid stream at the bed depth z.

With the aid of these parameters, the following terms may be defined:

$kC(z)\dfrac{V(z)}{V_m} A_t dz$ = transfer rate of adsorbate from fluid to adsorbent vacancies, assuming the concentration of adsorbate at the fluid-solid interphase is negligible compared to the concentration of adsorbate in the fluid stream for any z;

$\dfrac{V_m - V(z)}{\tau_m} dz$ = rate of regeneration of occupied adsorbent sites; and

$A_f v dC(z)$ = rate of change of adsorbate concentration in fluid flow.

If a steady-state condition on $V(z)$ is assumed, the transfer rate of adsorbate to adsorbent vacancies equals the rate of regeneration of occupied adsorbent sites, and therefore

$$kC(z)\frac{V(z)}{V_m} A_t dz = \frac{V_m - V(z)}{\tau_m} dz.$$

Additionally, a mass balance on adsorbate molecules within dz yields

$$A_f v \frac{dC(z)}{dz} + kC(z) \frac{V(z)}{V_m} A_t dz = 0$$

These two expressions may be combined to eliminate $V(z)/V_m$, then solved to yield:

$$\ln \frac{C(z)}{C(0)} + \frac{C(z) - C(0)}{C_o} = -\lambda z$$

where λ and C_o, constant for a given set of experimental conditions, are defined below:

$$C_o = \frac{V_m}{\tau_m kA_t} \qquad\qquad \lambda = \frac{kA_t}{A_f v} \qquad .$$

The experimental results presented have indicated that activated charcoal is an efficient adsorber of radioiodine, and therefore $C(z)$ is expected to be much less than $C(0)$. Thus,

$$\ln \frac{C(z)}{C(0)} = \frac{C(0)}{C_o} - \lambda z.$$

Defining ε as the efficiency represented as a fraction (the efficiency divided by 100), this yields

$$\ln(1-\varepsilon) = \frac{C(0)}{C_o} - \lambda z .$$

This suggests that if the surface rejuvenation model is applicable, a plot of $\ln(1-\varepsilon)$ versus $C(0)$ should be linear with slope $1/C_o$ for a given bed depth z. It would be expected that a series of straight lines all with slope $1/C_o$ should result for varying bed depths z. The lines should each be displaced by λz.

A plot of $\ln(1-\varepsilon)$ versus $C(0)$ was attempted for bed depths of 1/2 inch, 1 inch and 2 inches. The result is illustrated in Fig. 6. Although lines of approximately constant slope result for each bed depth, the lines are not displaced by the expected λz increment. This indicates that although the surface rejuvenation adsorption model is approximately correct, it does not accurately represent the entire picture of radioiodine adsorption on activated charcoal. Therefore, an empirical attempt to correlate experimental adsorption data, based on the surface rejuvenation model is presented.
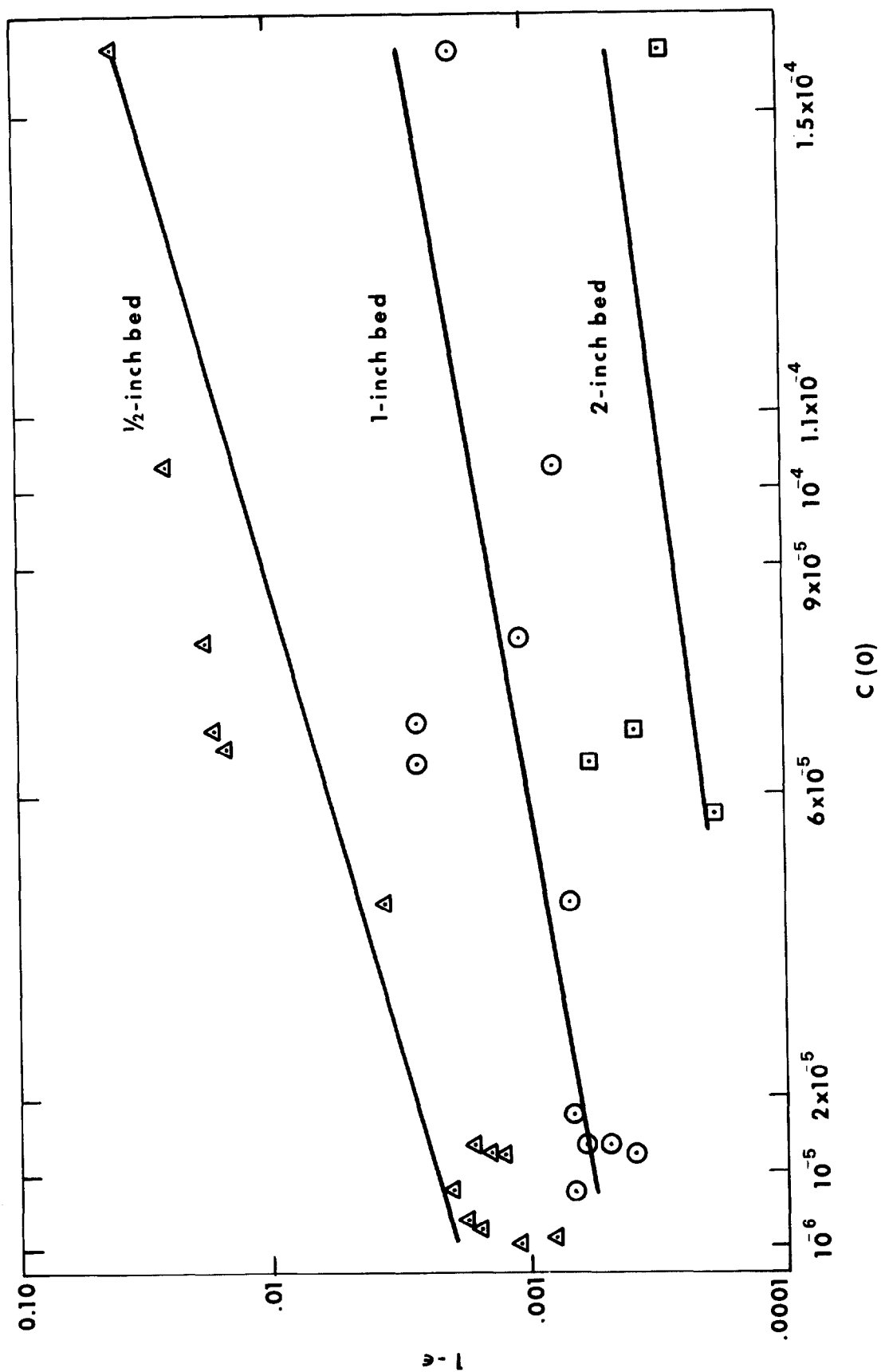
Fig. 6 The surface rejuvenation correlation.

It is worthwhile first to discuss qualitatively the results of the surface rejuvenation adsorption model. The results above express the efficiency of the charcoal bed as a function of those parameters expected to influence the efficiency. The experimental data of this investigation have shown that the efficiency of a charcoal bed decreases with increasing inlet concentration $C(0)$ with all other experimental parameters constant. This is the predicted trend since as $C(0)$ is increased, $\ln(1-\varepsilon)$ and $(1-\varepsilon)$ increases, or ε decreases.

A similar analysis applies to the superficial velocity variable (v). If k is assumed to be a mass transfer coefficient, k is proportional to $v^{0.49}$. This is based on the Gamson-Hougen empirical correlation of gas-phase mass transfer coefficients[32],[33]. Therefore, C_0 is proportional to $v^{-0.49}$ and as the velocity is increased, C_0 decreases. This increases $\ln(1-\varepsilon)$ and $(1-\varepsilon)$ and decreases the expected adsorption efficiency. Similarly, λ is proportional to $v^{-0.51}$ and as v is increased, λ is decreased. This increases $\ln(1-\varepsilon)$ and $(1-\varepsilon)$ and decreases the expected adsorption efficiency. These two effects indicate the surface rejuvenation adsorption model predicts decreasing adsorption efficiencies with increasing superficial velocity (all other parameters constant). This prediction is in agreement with the experimental trends illustrated.

The relative humidity variable can be postulated to affect the C_0 term through

$$\frac{V_m}{\tau_m}$$

Two effects may be considered. First, as the relative humidity is increased the resistance to surface diffusion increases and τ_m would be expected to increase. Second, as the relative humidity is increased V_m can be considered to decrease as water condensation effectively removes some unknown number of adsorption sites. Both of these effects tend to decrease C_0 as the relative humidity is increased, and as C_0 is decreased, the predicted efficiency drops. This prediction is in agreement with the experimental trends illustrated.

VII. The Empirical Surface Rejuvenation Correlation

Figure 6 illustrates three approximately straight lines for the three bed depths, with similar slopes. From the three lines, an average $1/C_0$ (obtained from the slope) and an average λ (obtained from the y-intercept) may be calculated and employed to predict adsorber bed efficiencies. However, since the lines for varying bed depths are not displaced by λz as expected, this approach needs to be modified. After calculation of C_0 and λ, an empirical approach to a correlation of the experimental data is presented. This empirical correlation is still based on the proposed surface rejuvenation adsorption model.

The average value of the term C_0 obtained from the three slopes in Fig. 6 is 8.51×10^{-5} μCi/ml. The average value of λ obtained from the three intercepts in Fig. 6 is 3.21 cm^{-1}. Inserting these values yields

$$\ln(1-\varepsilon) = \frac{C(0)}{8.51 \times 10^{-5}} - 3.21z.$$

To improve the correlation, two empirical corrections will be included. The first is to raise the term 3.21z to the 1/2 power. The second is to multiply the term

$$\frac{C(0)}{8.51 \times 10^{-5}}$$

by $E^{0.5}$, where E is represented by

$$E = \frac{M_{(R.H.)}}{M_{(25\%)}}$$

In this term, $M_{(R.H.)}$ represents the equilibrium moisture content of the charcoal in the test bed at the relative humidity of the test, and $M(25\%)$ represents the equilibrium moisture content of the charcoal in the test bed at a standard relative humidity of 25%.

With these corrections, a graph according to

$$\ln(1-\varepsilon) = E^{0.5} \frac{C(0)}{C_o} - (\lambda z)^{0.5}$$

is constructed. The results are indicated in Fig. 7, and the calculated points follow a smooth curve reasonably well.

This correlation is useful in predicting the expected removal efficiency of a charcoal bed for $CH_3{}^{131}I$ under any given set of experimental conditions. Data are necessary to obtain C_0 and λ, but once these parameters are available, Fig. 7 is applicable to predict the expected removal efficiency of a charcoal bed for radioiodine under any given set of experimental conditions.

VIII. CONCLUSIONS

The proposed surface rejuvenation adsorption mechanism and empirical correlation appear extremely useful in explaining the iodine-charcoal adsorption system and in predicting adsorber bed efficiencies under a given set of operating conditions with a minimum of experimental data. Further data, either bench-scale or operating, should yield beneficial comparisons and additional information. Data at extremely low inlet concentrations (approaching 10^{-13} μCi/ml) would prove especially valuable.

The illustrated experimental data provide evidence for the high efficiencies expected when activated charcoal adsorbs radioiodine. A deep charcoal
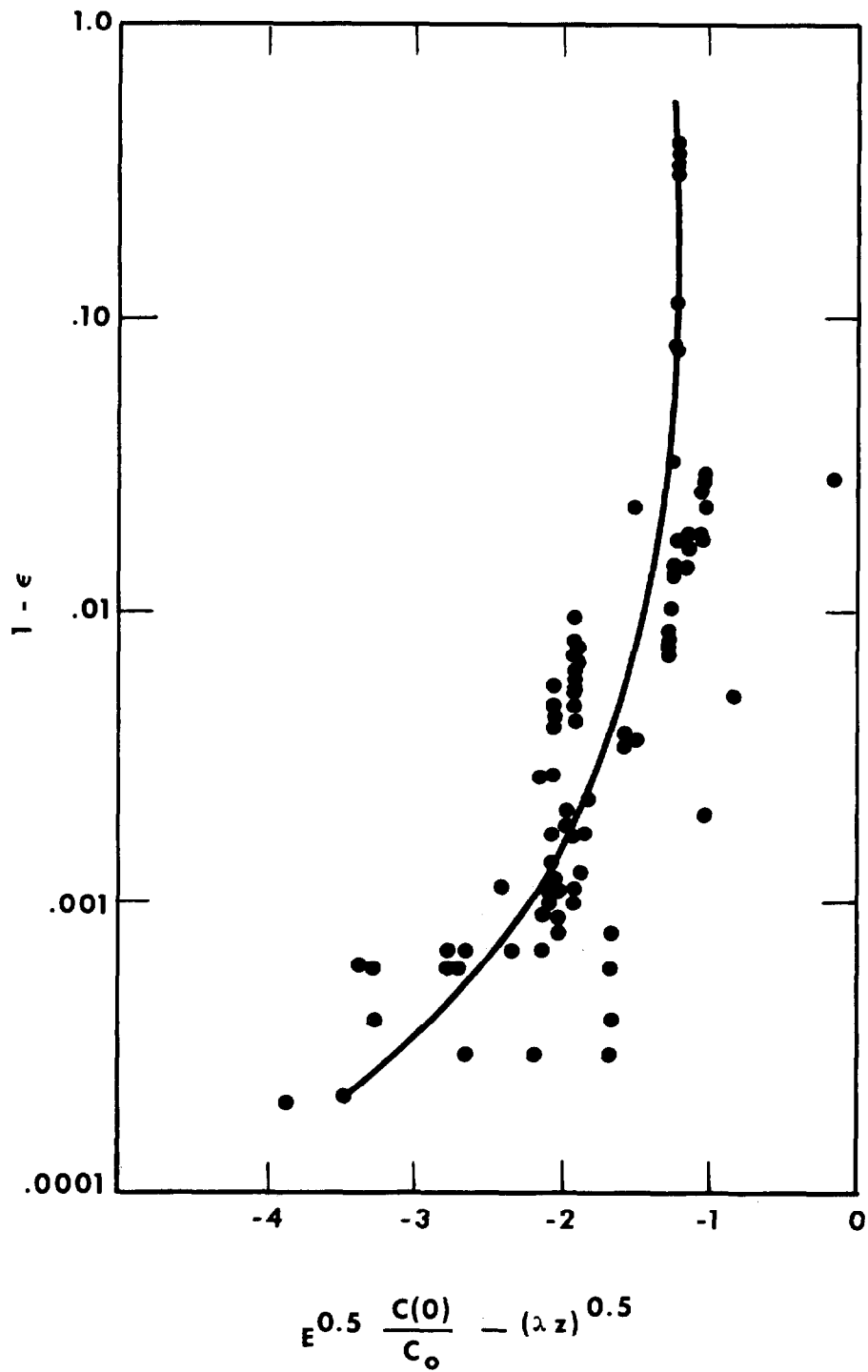
$$\varepsilon^{0.5} \ \frac{C(0)}{C_o} \ - \ (\lambda z)^{0.5}$$

Fig. 7 The empirical surface rejuvenation correlation.

bed (5 inches) is shown to be highly efficient for adsorbing both ^{131}I and CH_3^{131}I under all the reported experimental parameters, but for beds not as deep, certain combinations of parameters will cause severe reductions in removal efficiencies.

<u>References</u>

1. "Radioiodine Discharge Limits," <u>Nucl. Ind.</u>, 18(6): 17 (June 1971).

2. "Final Environmental Statement Concerning Proposed Rule Making Action: Numerical Guides for Design Objectives and Limiting Conditions for Operation to Meet the Criterion 'As Low As Practicable' for Radioactive Material in Light-Water-Cooled Nuclear Power Reactor Effluents," USAEC Report WASH-1258, July 1973.

3. American Air Filter, Inc., "Impregnated Activated Carbon for Removal of Radioiodine Compounds from Reactor Containment Atmospheres," Report AAF TR-7102, September 1972 (Revised January 1973).

4. R. D. Ackley and R. E. Adams, "Removal of Radioactive Methyl Iodide from Steam-Air Systems (Test Series II)," USAEC Report ORNL-4180, Oak Ridge National Laboratories, October 1967.

5. R. C. Milham and L. R. Jones, "Iodine Retention Studies, Progress Report: January - June, 1969," Report DP-1213, E.I. duPont de Nemours and Company, November 1969.

6. R. C. Milham and L. R. Jones, "Iodine Retention Studies, Progress Report: July-December, 1969," Report DP-1234, E. I. duPont de Nemours and Company, April 1970.

7. J. A. Buckham, "Iodine Adsorbent Program," Report BUC-331-72, Allied Chemical Corporation, November 1972.

8. R. E. Adams, R. D. Ackley and Z. Combs, "Trapping of Radioactive Iodine and Methyl Iodide by Iodized Charcoal," USAEC Report ORNL-4228, Oak Ridge National Laboratories, April 1968.

9. H. Schuttelkopf and J. Wilhelm, "Iodine Filter Program," Karlsruhe Nuclear Research Society, March 1970.

10. R. E. Adams, R. D. Ackley and R. P. Shields, "Application of Impregnated Charcoals for Removing Radioiodine from Flowing Air at High Humidity," in <u>Treatment of Airborne Radioactive Wastes</u>, Symposium Proceedings, New York, Aug. 26-30, 1968, pp. 387-402, International Atomic Energy Agency, Vienna, 1968 (STI/PUB/195).

11. R. J. Davis and R. D. Ackley, "Long-term Effects of Radioiodine Trapping by Charcoal," in <u>Proceedings of the Twelfth AEC Air Cleaning Conference,</u> Oak Ridge, Tennessee, Aug. 28-31, 1972, USAEC Report CONF-720823, Vol. 1, pp. 469-483, 1972.

12. D. A. Collins, L. R. Taylor and R. Taylor, "The Development of Impregnated Charcoals for Trapping Methyl Iodide at High Humidity," UKAEA Report TRG 1300(W), 1967.

13. G. H. Prigge, "Application of Activated Carbon in Reactor Containment," Report DP-778, E. I. duPont de Nemours and Company, 1962.

14. H. C. Parish, "Methyl Iodide Adsorber Efficiency as Affected by Air Velocity, Particle Size and Bed Depth," Report No. 26, CVI Corporation, Nov. 9, 1972.

15. R. D. Rivers, M. Pasha and W. H. Buckler, "Correlation of Radioiodine Efficiencies Resulting from a Standardized Test Program for Activated Carbons," in Proceedings of the Twelfth AEC Air Cleaning Conference, Oak Ridge, Tennessee, Aug. 28-31, 1972, USAEC Report CONF-780823, Vol. 1, pp. 445-468, 1972.

16. R. D. Ackley et al., "Retention of Methyl Iodide by Charcoal Under Accident Conditions," USAEC Report ORNL-3915, Oak Ridge National Laboratories, March 1966.

17. R. R. Bellamy, "The Adsorption of Elemental Iodine and Methyl Iodide on Activated Charcoal from Flowing Air Streams at Low Inlet Concentrations," Ph.D. Thesis, The Ohio State University, 1973.

18. R. D. Ackley and R. E. Adams, "Effect of Containment Spray Solutions on Trapping of Radioactive Methyl Iodide from Flowing Steam-Air by Iodized Charcoal: Westinghouse Test Series," USAEC Report ORNL-TM-2805, Oak Ridge National Laboratories, January 1970.

19. R. E. Adams, R. D. Ackley and Z. Combs, "Trapping of Radioactive Iodine and Methyl Iodide by Impregnated Charcoals," USAEC Report ORNL-4374, Oak Ridge National Laboratories, June 1969.

20. R. E. Adams, R. D. Ackley and W. E. Browning, Jr., "Removal of Radioactive Methyl Iodide from Steam-Air Systems," USAEC Report ORNL-4040, Oak Ridge National Laboratories, January 1967.

21. J. H. deBoer, The Dynamical Character of Adsorption, pp. 90-122, Oxford at the Clarendon Press, Great Britain, 1968.

22. R. Ash, R. M. Barrer and C. G. Pope, "Flow of Adsorbable Gases and Vapours in a Microporous Medium," Proc. Roy. Soc. (London), Sec. A, 271:19 (1963).

23. R. M. Barrer and J. A. Barrie, "Sorption and Surface Diffusion in Porous Glass," Proc. Roy. Soc. (London), Sec. A, 213:250 (1952).

24. R. M. Barrer and T. Gabor, "Sorption and Diffusion of Simple Paraffins in Silica - Alumina Cracking Catalyst," Proc. Roy. Soc. (London), Sec. A, 256:267 (1960).

25. P. C. Carman and P. Le. R. Malherbe, "Diffusion and Flow of Gases and Vapors through Micropores," Proc. Roy. Soc. (London), Sec. A., 203:165 (1950).

26. T. W. Ross and R. J. Good, "Activated Adsorption of Oxygen on Glass," J. Phys. Chem., 60:1167 (1956).

27. R. M. Barrer and T. Gabor, "A Comparative Structural Study of Cracking Catalyst, Porous Glass, and Carbon Plugs by Surface and Volume Flow of Gases," Proc. Roy. Soc. (London), Sec. A, 251:353 (1959).

28. D. M. Grove and R. Ash, "Low Pressure Gas Flow in Consolidated Porous Media," Trans. Faraday Soc., 56:1357 (1960).

29. E. R. Gilliland, R. F. Baddour and J. L. Russell, "Rates of Flow through Microporous Media," Am. Inst. Chem. Engrs. J., 4:90 (1958).

30. J. D. Babbitt, "On the Diffusion of Adsorbed Gases through Solids," Can. J. Phys., 29:437 (1951).

31. E. A. Flood, R. H. Tomlinson and A. E. Leger, "The Flow of Fluids Through Activated Charcoal Beds," Can. J. Chem., 30:348 (1952).

32. B. W. Gamson, G. Thodos, and O. A. Hougen, "Heat, Mass and Momentum Transfer in the Flow of Gases through Granular Solids," Trans. Am. Inst. Chem. Engrs., 39:1 (1943).

33. C. R. Wilke and O. A. Hougen, "Mass Transfer in the Flow of Gases through Granular Solids Extended to Low Modified Reynolds Numbers," Trans. Am. Inst. Chem. Engrs., 47:445 (1945).

DISCUSSION

KOVACH: Can you tell me what is the expected counting error at the extremely low concentration?

BELLAMY: The counting error in the inlet concentration is as much as 150%.

JONAS: I would like to comment that one cannot justify using the concept of mass transfer as a rate controlling step in the overall process before confirming that it is indeed the controlling step. I might add that Masamune & Smith, Schneider & Smith, and others conceive of gas adsorption taking place in three sequential steps, (1) mass transfer or external diffusion from the air stream to the carbon granule surface, (2) internal diffusion (some authors break this up into surface diffusion followed by pore diffusion) of the gas into the micropores of the carbon, and (3) adsorption of the gas molecule by the active site. Schneider & Smith and Jonas & Rehrmann have shown that adsorption processes by sorbent granules in the velocity range of 2 to 50 cm/sec are characterized by internal diffusion as the rate controlling step. Schneider & Smith show the detailed method of analyzing experimental data upon which this conclusion is based.

THE BEHAVIOR OF HIGHLY RADIOACTIVE IODINE ON CHARCOAL[*,**]

R. A. Lorenz, W. J. Martin, and H. Nagao[***]

Oak Ridge National Laboratory
Oak Ridge, Tennessee

Abstract

The behavior of highly radioactive iodine adsorbed on charcoal has been investigated in a series of seven experiments which used amounts of radioactive I-130 ranging from 0.2 to 1100 Ci on well-insulated adsorber beds containing 28 cm³ of impregnated charcoal. Desorption of several forms of iodine into flowing dry air were observed at moderate temperatures (80 to 125°C). When the air velocity was reduced from 28.5 fpm (25°C)to 3.8 fpm (25°C), the charcoal temperature rose quickly during experiments which contained 500 Ci or more because of reduced air cooling.

Ignition of the charcoal occurred during four of the experiments. Heat released from the slow oxidation of charcoal below its ignition temperature was measured and was found to contribute significantly to the attainment of ignition. CHART, a computer program for calculating charcoal adsorber bed temperatures, accurately duplicated the experimentally observed temperature behavior, including ignition, after the program had been modified to include the heat released by oxidation of the charcoal.

A penetrating form of iodine, probably methyl iodide, was released continuously at low rates which were compatible with previously proposed radiation-induced mechanisms. The distribution and movement of elemental iodine in the test bed were followed by means of a movable collimated gamma scanner. Linear adsorption isotherm coefficients were calculated, but some correction appeared to be appropriate at high iodine concentrations. Retention of iodine was better at high temperature when the total atomic concentration of potassium was greater than that of iodine.

Introduction

The charcoal adsorber systems of some nuclear power reactors contain several tons of charcoal loaded in 2-in.-deep trays stacked rather compactly so that the only cooling mechanism of consequence is forced air circulation. If normal air flow can be obtained when needed, there is little question that the heat from deposited radioiodine can be removed. However, if 25% of the reactor iodine inventory should be released to the containment shell as assumed with some design basis accidents, and if this amount of radioactive iodine should be collected by the charcoal cleanup system within several hours of reactor shutdown, calculations show that the ignition temperature might be reached in cases where the air flow is severely reduced (1).

We are presently carrying out a series of experiments to determine whether the ignition of charcoal can occur from the decay heat of highly radioactive iodine before the iodine desorbs, thereby precluding ignition. The second objective of our program is to provide supportive data for the calculation of charcoal bed temperatures. The third objective is to study the movement of iodine within charcoal beds and the desorption of iodine from these beds during exposure to intense radiation fields and elevated temperatures so that this information can be included in the temperature calculation and in the estimation of radioactivity release.

We have used four types of charcoal in our experiments, as described in Table I. All of them are coconut-based charcoals except for WITCO Grade 42, which is petroleum-based. Each batch has performed satisfactorily in other iodine or methyl iodide adsorption tests. Other batches of charcoal were included in a series of 13 preliminary laboratory experiments in which a small electric heater was used in the bed inlet region to simulate decay heat (2). Because some large differences in iodine desorption and oxidation rates or ignition temperatures have been observed from batch to batch of a given manufacturer's type number, we caution that the experimental results presented here apply only to the particular batches tested.

Our experimental charcoal bed is shown in Fig. 1. The charcoal is contained to a depth of 2-1/8-in. (5.4 cm) in a quartz Dewar flask with an inside diameter of 1.03 in. (2.62 cm). A heater on the outside of the flask follows the temperature of the center of the bed in order to further reduce the chance for heat loss through the side in simulation of an essentially semi-infinite reactor adsorber system. Except for a small heat loss via conduction and heat radiation, the only cooling mechanism is the forced flow of air upward through the bed. Thermocouples measure the temperature distribution in the charcoal. Except for runs 1 and 2, the inlet temperature was controlled at either 100°C or 70°C in simulation of an accident ambient temperature, while the charcoal reached a higher temperature depending on the amount of radioactive iodine present and the air flow rate.

Experimental Procedure

The radioactive I-130 was obtained by irradiating a mixture of 86% I-129--14% I-127 in the chemical form PdI_2 packed as powder in quartz ampoules and seal-welded in an aluminum capsule. We irradiated this material for 30 hr in the High Flux Isotopes Reactor (HFIR) at a thermal flux of 2.5×10^{15} n/cm$^2 \cdot$sec,

which resulted in specific activities of 5.7 Ci I-130/mg I and 1.4 x 10^{-3} Ci I-131/mg I at the time of removal from the reactor.

After irradiation the capsule was transported to the hot cell and sealed into the recirculating loop system shown in Fig. 2. The tips of the capsule and ampoules were then sheared off, thus allowing the ampoules to fall into a quartz-lined furnace where the PdI_2 was thermally decomposed to palladium metal and I_2 at 600 to 700°C. Air circulating at the normal flow rate carried the radioactive iodine through two layers of Cambridge 1G HEPA filter media into the test charcoal bed. Decay time between withdrawal from the reactor and start of decomposition ranged from 1.3 to 2.3 hr. Time for decomposition ranged from 1.7 to 2.3 hr.

A collimated radiation detector was moved in 1/8-in. increments to follow the distribution of iodine in the bed as the experiments progressed. The collimator contained a slit that was 1/16 in. wide and 8 in. long.

Iodine that penetrated or was desorbed from the test bed was collected in sequentially operated traps. Silver-plated honeycombs (3) were used to collect elemental iodine, HEPA filters (Cambridge 1G) to collect particular matter, and charcoal and silver-exchanged zeolite to collect the more penetrating organic forms of iodine. The charcoal cartridges of one trap were located and shielded remotely to permit continuous monitoring of organic iodides. In cases where the traps did not contain silver-plated honeycombs, we examined the distribution of iodine among the cartridges to determine the relative amounts of elemental and organic iodine.

The experimental procedure can be described as follows. The installed collection traps and heated loop were purged with dried and filtered air, using a once-through mode and a flow rate of 4.9 liters/min for 2.5 hr to dry the loop and remove volatile contaminants. A 28-cm^3 volume of the test charcoal in the as-received moisture condition was then poured into the insulated bed through the outlet tube. (The presence of many thermocouples and the restricted fall resulted in a packing density somewhat less than that measured by the method of ASTM-D-2854-70. Assuming a void fraction of 0.43 for normal packing, we estimate 0.45 for the test bed void fraction.) Subsequently, the loop heaters were turned on, the irradiation capsule installed, air circulation started, and the capsule sheared when the desired bed temperature was reached.

The air inlet temperature to the bed was controlled at either 100°C (runs 1-5) or 70°C (runs 6 and 7), and the charcoal bed was heated by the decay heat to some higher temperature, depending upon the level of radioactivity and air flow rate, as shown in Tables II-VI. The period of operation at normal air flow rate at the beginning of each experiment enabled observation of the iodine movement and desorption at nearly constant-temperature conditions. The air flow rate was then reduced in simulation of an accident situation, allowing the temperature to rise because of reduced air cooling.

The temperature behavior during run 4 is shown in Fig. 3. The heat from slow oxidation of the charcoal resulted in an acceleration in the temperature rise above 215°C. The heat from oxidation increased with temperature and was equal to the decay heat when the bed midpoint temperature reached 271°C, 30.5 min after air flow reduction. Combustion was stopped in each ignition experiment by dis-continuing the circulation of the air. The temperature behavior in run 5 was nearly identical to that of run 4. The rate of temperature rise during runs 6 and 7 was much lower because of a lower radioactivity level and, in run 6, a lower

rate of oxidation. Tables II-VI summarize the radioactivity level, air flow rate, and temperature behavior.

The distribution of iodine in the test beds, as determined by the collimated scanner, indicated that the original loadings contained on the order of 10% of a penetrating form of iodine, probably methyl iodide. During earlier decomposition tests in the loop apparatus, we collected the iodine directly in charcoal cartridges, and this indicated a penetrating iodine content of 1 to 3%. Based on the available literature, the distribution corresponds to that for methyl iodide collected on dry charcoal. Although the mass of iodine was large and the heated loop had been cleaned by air purging, we believe that sufficient organic material was available to allow the formation of 10% methyl iodide in the high-temperature high-radiation environment during decomposition of the PdI_2. In the remainder of this paper we will refer to similar penetrating forms as methyl iodide, even though no positive identification of the species was made.

Oxidation of Charcoal

The rate of heat release from the oxidation of charcoal during the experiments was calculated by using a heat balance for the bed:

Heat from oxidation = (Heat absorbed by charcoal)

+ (Heat absorbed by quartz container and thermocouples)

+ (Heat removed by flowing air)

+ (Heat lost from quartz container) - (Heat from iodine decay).

The heat balance was programmed for a computer, and the container heat absorption and loss rate were determined during laboratory runs in which alumina bubbles were used in place of the charcoal and decay heat was simulated by a small electric heater at the bed entrance. A typical example of the heat balance is given below for run 4 32.4 min after reduction of the air flow when the center of the bed reached 300°C, the average temperature of the bed was 286°C, and the rate of temperature rise was 20°C/min at the center and 15°C/min avg:

Heat in: iodine decay heat rate = 37 cal/min

oxidation heat release rate = 100 cal/min

Heat out: rate of heat absorption by charcoal = 45 cal/min

rate of heat absorption by container = 60 cal/min

rate of heat removal by air = 28 cal/min

rate of heat loss from container = 4 cal/min.

The results for the four hot-cell ignition experiments and one laboratory experiment in which an electric heater was used are shown in Fig. 4. In each experiment the heat release from oxidation increased continuously with temperature until a maximum value, which depended upon the air flow rate was

attained. For experiments 4, 5, and 7, the air flow rate was 622 cm^3/min (25°C) so that the maximum heat release rate would be 512 cal/min if all of the oxygen reacted to form CO_2 with a heat of reaction of 96,000 cal/mole. This is equivalent to 46 cal/min·g charcoal for run 4 and 35 cal/min·g for run 7. The maximum would be 8.9 cal/min·g charcoal for the low air flow rate (0.71 fpm, 25°C) in run 6. The oxidation reaction was strongly inhibited in this run until the velocity was increased (1.9 fpm, 25°C) during the final 2 min. The total amount of charcoal oxidized was usually of the order of 150 to 200 mg per experiment.

The heat release data for uninhibited oxidation was correlated for each experiment using the Arrhenius-type equation

$$H = H_o e^{-A/RT},$$

where

H_o = a constant (cal/min·g charcoal),

A = an activation energy (cal/mole),

R = 1.987 cal/mole·°K,

H = the rate of heat release by oxidation (cal/min·g charcoal).

The values of H_o and A are given in Table VII for the four hot-cell ignition experiments and for several laboratory experiments in which the miniature electric heater was used.

The above heat release data are most accurate in the heat release range between 0.5 and 20 cal/min·g charcoal; the accuracy of extrapolations below these rates is uncertain. Considerable interest has been expressed recently in oxidation rates at 150°C and lower temperatures since, even though the heat release rates might be very low, the trend toward deeper charcoal beds increases the mass of charcoal available for oxidation and decreases the rate of heat loss. One ource of lower-temperature oxidation data is the work of Bratzler (4). His data tend to indicate little difference in oxidation rate between dry air and moisture-saturated (at room temperature) air, although the results were obtained with charcoal types which are different from those pr ently used in nuclear reactors. The equations for runs 4 and 5 extrapolate to oxidation rates in the vicinity of those found by Bratzler at temperatures in the vicinity of 80°C (2.1 to 6.0 x 10^{-4} cal/min·g charcoal); however, valid experimental data with the modern, high-surface-area, impregnated charcoals would be essential for the evaluation of temperature rise in critical situations.

An example of higher heat release rates at low temperature occurs with charcoals containing TEDA, such as the GX-176 used in run 7. Charcoals containing more than 1% TEDA have ignited at temperatures near 190°C due to combustion of the TEDA (5-7). The heat of combustion of TEDA (solid, at 25°C) is 970,800 cal/mole (8). Under the conditions of run 7 the oxidation of the TEDA (possibly affected by the proprietary flame retardant) did not result in early ignition of the charcoal.

Our experimental experience has been limited to unused charcoals in low-humidity atmospheres with fairly short-term oxidation. Continued exposure to flowing air ordinarily results in the accumulation of organic material (9)

and some NO_2, as well as the loss of chemically reactive sites, all of which can affect the oxidation rate. Milham found that the ignition temperature of BC-416, an unimpregnated charcoal, increased with service time (10) but also experienced some unusual low-temperature ignitions (11). He did not measure heat release rate as a function of temperature. Woods and Johnson (12) found that coconut charcoal exposed to submarine atmospheres accumulated organic material and observed that this usually resulted in a lowered SIT (spontaneous ignition temperature). The SIT is an ignition temperature measured with no air flowing so that heat loss from the charcoal sample is small.

Our oxidation rate data are insufficient to determine the effect of radiation. At low temperatures, where the rates are slow, one would expect some enhancement. Kosiba and Dienes (13) observed an increase by a factor of 2.6 in the very slow rate of oxidation of graphite in oxygen at 300°C on exposure to a gamma radiation field of 0.61×10^7 rads/hr.

Calculation of Charcoal Bed Temperatures

The CHART computer program is a modification of a general-purpose heat-transfer program, which is capable of solving three-dimensional problems, to the more specific conditions encountered with radiation decay heat in the charcoal adsorber beds of reactor air cleaning systems (1, 14) Initial development of the computer program did not include secondary heat sources, such as the oxidation of charcoal and the heat of absorption/desorption of water on charcoal (15), nor did it include provision for movement of the radio-active iodine heat source within the bed and desorption of iodine from the bed.

We modified CHART to include heat from the oxidation of charcoal and used the parameters for hot-cell run 4 as input. The comparison of calculated and experimental temperatures is shown in Fig. 3. The modified CHART-calculated axial temperature distribution from inlet to outlet agreed very well with the thermocouple readings, ignition being indicated near the 1-in. depth in both cases.

We have also recalculated, with oxidation heat, some of the sample problems presented in ORNL-4602 (14) and found that ignition would occur in many of the examples. For instance, the very severe accident situation described in example 4, Fig. 11 of ORNL-4602, would result in ignition even with the slow oxidation rates that we measured for lot No. 62469 of WITCO Grade 42 charcoal.

The main conclusion from Bratzler's study may be helpful in the design, analysis, and operation of large (especially deep) reactor charcoal adsorber systems. He concluded that there are certain conditions for charcoal adsorber beds (usually large beds) at moderate temperatures under which continued air flow (usually quite low) would allow the heat from slow oxidation to build up until ignition was reached. To prevent such occurrences, one must (1) stop the air flow completely or limit it so that the total oxidation heat release rate is less than the total heat loss rate, (2) cool the bed to a temperature where the oxidation heat release rate is below the total heat loss rate, or (3) increase the air flow sufficiently to provide adequate "air" cooling. Caution should be exercised in the third case since, at temperatures approaching ignition, particularly with a deep bed, the increased air flow may cause ignition to be reached before the entire bed length begins to be cooled.

Release and Desorption of Iodine

As mentioned previously, we used sequentially operated traps composed of silver-plated honeycombs, high-efficiency filters, and charcoal cartridges to identify the iodine forms released during the course of the experiments. The results are summarized in Tables II-VI. Identification of the form of the collected iodine was uncertain in some cases. For example, when the particulate iodine concentration was high, the deposition of particles on the honeycombs obscured the elemental iodine. Particulate iodine release occurred early in each run, and the lowest releases were noted during runs 1, 2, and 3, the low-activity runs.

Release of Methyl Iodide

Evans (16) has shown that methyl iodide is formed and released continuously from elemental iodine loaded on charcoals, in flowing moist air, as the result of a gamma radiation field. For good-quality impregnated charcoals, he reports a fractional release rate of radioactive iodine of approximately 50×10^{-6}/hr when the gamma dose rate is 1.5×10^{7} rads/hr, the temperature is 80°C, the velocity 55 fpm (80°C reference), the relative humidity is $\sim 75\%$ (~ 265 torr water vapor), and the bed depth is 1 in. The release rate increases with radiation and with moisture content of the air.

Our experiments are similar to those of Evans with regard to charcoal types, except that we use a lower air velocity (33.8 fpm at 80°C and 38.1 fpm at 125°C), the bed depth is 2 in., the radiation source is iodine decay (mainly beta), and the moisture content is much lower. Our methyl iodide release rates, summarized in Table VIII, are compatible with Evans' data and proposed radiation reaction mechanisms when these differences are taken into account.

The decreasing rate of release of CH_3I with an increase in radiation intensity, which was observed in the first three experiments, suggested radiation decomposition of methyl iodide. On the other hand, the release rates during the first two experiments were not monitored long enough to give a realistic picture of the release behavior. Jones (17) showed that a gamma radiation field decreased the rate of release of methyl iodide when radioactive methyl iodide was loaded along with nonradioactive elemental iodine on unimpregnated charcoal in continuously flowing moist air.

In our experiments the rate of release of methyl iodide decreased when the flow rate was reduced, increased again if the radioactivity was sufficient to increase the temperature to the 200°C range at the low flow rate, and then approached zero at higher temperatures, probably because of oxidation or thermal decomposition of the methyl iodide. The amount released at low flow and high temperature varied greatly with charcoal type, as seen in Tables III-VI.

The distribution of iodine collected in the charcoal cartridges during operation at normal air velocity generally corresponded to distributions for methyl iodide published in the literature when mass transfer differences were taken into account. The iodine that was collected in the charcoal cartridges of run 3 was somewhat more penetrating than in other runs. In runs 6 and 7 the first trap was located close to the main test bed and showed a skewed distribution that might have resulted from poisoning of the first few cartridges. The traps used with low air velocity indicated differing degrees of penetration.

Many of these traps were in use for only a short period of time so that the collected radioactive iodine was probably a mixture of adsorbed radioactive methyl iodide and isotopically exchanged iodine. For short-term operation, the temporarily adsorbed radioactive methyl iodide would have a steeper distribution than that which had undergone isotopic exchange.

Methyl iodide behavior has frequently been correlated with the moisture and organic material content of the test atmosphere. We determined the moisture content of the air in the closed 20-liter test loop following runs 5 and 6 and measured water vapor partial pressures of 9 and 3 torr, respectively. Most of the moisture put into the loop with the test charcoal was held in the charcoal of the collection beds and cleanup bed (Fig. 2).

Air remaining in the closed loop was analyzed by gas chromatographic techniques for methane following runs 5, 6, and 7; concentrations of 30, 100, and 20 ppm were found for the respective runs. No other low-molecular-weight hydrocarbons were found.

Desorption of Elemental Iodine

In order to describe the rate of desorption of elemental iodine quantitatively, we made use of the data collected by the collimated gamma scanner which was used to monitor the movement of iodine within the bed. Gamma scan data are shown in Figs. 5 and 6 and in Table IX. A computer program was written to calculate the partial pressure of iodine in equilibrium with the charcoal according to the observed rate of movement within the bed. The rate of mass transfer for elemental iodine is very rapid, so that there is an essentially continuous equilibrium between the charcoal and the vapor phase. Therefore, the movement of iodine should be directly proportional to the air velocity within the bed. The gamma scanner monitored 17 increments or slabs along the length of the bed. We assumed that iodine which desorbed from the first (inlet) slab was readsorbed on the second slab, etc. We assumed a linear adsorption isotherm; thus the partial pressure of iodine is directly proportional to the mass concentration on the charcoal, $P = x/k$, where P i the partial pressure of iodine (atm), x is the total concentration of iodine on the charcoal, including impregnant (0.03 to 0.1 g of iodine per gram of charcoal), and k is the adsorption coefficient.

The calculation is most accurate for the first 1/2-in. of bed depth; hence we correlated experimental k values for this region with the temperature obtained from a thermocouple located in that region of the bed. Results are shown in Fig. 7. For each type of charcoal we can express the value of k satisfactorily with the equation $k = k_o e^{-A/RT}$, where A is the activation energy (cal/mole), R is the gas constant, T is the absolute temperature ($^\circ$K), and k_o is a constant for each type of charcoal (g I/g charcoal·atm I). For MSA 85851 charcoal, A = -19,000 cal/mole and k_o = 3.3 x 10^{-6} g/g·atm. No radiation effect on k was detected in the range 100 to 1100 Ci of I-130.

The WITCO Grade 42 and GX-176 charcoals from runs 6 and 7 have lower values of k at low temperatures (i.e., higher partial pressures of iodine). The BC-727 charcoal k-values from run 5 are intermediate to the above.

In order to check the validity of the desorption model described above, we developed a second computer program, DESORB, in which very thin slabs were assumed and the mass transfer correlation of Chu (18) was used to describe the rate of mass transfer between gas phase and charcoal grain surface. This,

in effect, allows some of the iodine vapor to bypass the following slab, depending principally on the velocity, gas-phase diffusion coefficient, and charcoal particle size. For calculation of the diffusion coefficient, we used the equations assembled by Knudsen (19). Agreement with the observed iodine distribution was satisfactory.

In order to compare our desorption rates with those measured in the absence of a high radiation field, we calculated k-values for the desorption of impregnant tagged with radioactive methyl iodide, mixed to distribute the activity, and exposed for 4 hr each at succeeding temperatures of 150, 200, 250, and 300°C with low-relative-humidity air (15 torr water vapor) flowing at a face velocity of 40 fpm (25°C reference)(20). The averages of the results are shown in Fig. 7.

The large difference in k-values should not be attributed to a radiation effect since the experiments are very dissimilar with respect to the charcoals and experimental methods employed. One significant difference is the greater mass of iodine used in our experiments. In the laboratory tests in which a small electric heater was used to simulate radioactive decay heat, it was observed that the fractional desorption of iodine (including impregnant iodine) was greater when the charcoal was heavily loaded with iodine (2). We also observed that a charcoal with unusually high potassium content lost very little iodine during the ignition cycle even when heavily loaded.

An empirical correlation devised to relate the above observations was successful in reducing some of the scatter in the impregnant desorption tests. The empirical correlation specified a standard charcoal containing potassium and iodine in equal atomic amounts, including natural and impregnant potassium as well as impregnant and loaded iodine. The k-value for the standard was 3×10^4 at 200°C, changed with temperature according to an activation energy of 17,000 cal/mole, and decreased (or increased) by a factor of 10 for an increase (or decrease) of 65 $\pm$ 35 mgI/g charcoal. The excesses of iodine (mgI/g charcoal) over KI for the first 1/2-in. depth of bed were: run 3, 1; run 4, 44; run 5, 40; 4un 6, 53; and run 7, 15. These are, generally speaking, compatible with the above empirical correlation and observed low k-values.

Trial runs with DESORB covering the entire duration of runs 4 and 6 using the bed inlet region temperature variation with time reproduced the activity distribution in the first 1/2-in. bed depth reasonably well when k was assumed to vary a factor of 10 for every 100 mgI/g charcoal change in concentration. When k was assumed to vary a factor of 10 with every 50 mgI/g charcoal change, the activity distribution peaks tended to be flatter than observed experimentally. Since k varies rapidly with temperature, more accurate modeling will require inclusion of the complete axial temperature profile.

The effect of potassium concentration at very high temperatures was explored by Lingjaerde and Podo (21). They performed experiments at 450°C and higher in helium atmosphere and found that coconut charcoals naturally containing potassium retained iodine well at these temperatures but that the iodine retention was poor when the potassium was removed by acid washing. When KOH was added in increasing amounts, iodine retention was improved. They also found that compounds containing sulfur destroyed the ability of charcoals to retain iodine at high temperatures.

715

Summary

The information obtained from the series of experiments performed to date applies to low-moisture atmospheres; similar experiments to be performed during the next year will be conducted with water vapor partial pressures of 250 torr.

No large deleterious effects of the high radiation intensity were observed, other than those associated with the temperature increase resulting from decay heat.

Below the ignition temperature, the greatest difference in behavior at a given radiation intensity occurred as a result of differences in the rate of heat release from oxidation. For comparable radiation intensities, ignition was attained in run 7 70 min after air flow reduction to 3.8 fpm (25°C), but in run 6 a maximum temperature of approximately 220°C was approached at the same velocity. Longer operation at high temperature during run 6 allowed a much greater total movement of elemental iodine before the experiments were terminated.

The CHART computer program was shown to be capable of calculating the temperature behavior within the charcoal beds for the conditions of our high-activity ignition experiments. Temperature calculations must include ambient temperature increases and heat from oxidation and from moisture adsorption.

The linear adsorption isotherm appears adequate for expressing the equilibrium between iodine vapor and adsorbed iodine when the concentration of total iodine does not vary greatly, but some adjustment appears to be required for large variations in concentration.

The formation and release of penetrating forms of iodine (probably mostly methyl iodide) were low but compatible with previously proposed mechanisms (16).

It is possible to adjust the impregnant concentrations, particularly total potassium and iodine, in order to obtain charcoals especially suited to certain conditions. If ignition should be of particular concern, lower potassium content and higher iodine content would generally result in higher ignition temperatures (low oxidation rates). For especially good retention of iodine at high temperatures, along with a greater risk of reaching ignition, high total potassium and low iodine concentrations should give favorable results. In any case, especially for critical applications, the charcoal must be carefully tested.

References

1. R. P. Shields, "Ignition of charcoal adsorbers by fission product decay heat," Proceedings of the 11th AEC Air Cleaning Conference, Hanford, Washington, Aug. 31-Sept. 3, 1970, CONF-700816.

2. R. A. Lorenz and W. J. Martin, ORNL Nuclear Safety Research and Development Program Bimonthly Report for May-June 1972, USAEC Report ORNL-TM-3900 (September 1972), pp. 122-25.

3. R. L. Bennett and R. E. Adams, "Development of a sampling device for distinguishing the forms of iodine in a humid atmosphere," Proceedings of the 10th AEC Air Cleaning Conference, New York, New York, August 28, 1968, USAEC Report CONF-680821, pp. 235-61.

4. K. Bratzler, "Die Selbstentzundung des Kohlenstoffs als verfahrenstechnisches Problem," Chemie-Ing.-Tech., 28(8/9): 569-576 (1956); Translation: The Spontaneous Ignition of Carbon as a Process Problem, USAEC Report ORNL-tr-2568.

5. R. E. Adams, R. D. Ackley, and R. P. Shields, "Application of impregnated charcoals for removing radioiodine from flowing air at high relative humidity," Treatment of Airborne Radioactive Wastes, Proceedings of a Symposium, New York, 26-30 August 1968, IAEA, Vienna, 1968, p. 398.

6. A. G. Evans, Confinement of Airborne Radioactivity, Progress Report: July-December 1972, USAEC Report DP-1329 (June 1973), pp. 10-16.

7. A. G. Evans, Confinement of Airborne Radioactivity, Progress Report: January-June 1973, USAEC Report DP-1340 (October 1973), pp. 9-11.

8. E. S. Domalski, "Selected values of heats of combustion and heats of formation of organic compounds containing the elements C, H, N, O, P, and S," J. Phys. Chem. Ref. Data, 1 (No. 2), 253 (1972).

9. E. C. Bennett and D. E. Strege, Evaluation of Weathered Impregnated Charcoals for Retention of Iodine and Methyl Iodide, USAEC Report UNI-39 (July 1973).

10. R. C. Milham, High Temperature Adsorbents for Iodine, Progress Report: January 1965-September 1966, DP-1075 (Dec. 1966), pp. 8, 16.

11. R. C. Milham and L. R. Jones, Iodine Retention Studies, Progress Report: January-June 1969, DP-1213 (November 1969), p. 24.

12. F. J. Woods and J. E. Johnson, The Ignition and Combustion Properties of Activated Carbon Containing Adsorbed Hydrocarbons, Naval Research Laboratory Report NRL-6090 (March 1964).

13. W. L. Kosiba and G. J. Dienes, "The effect of displaced atoms and ionizing radiation on the oxidation of graphite," Advances in Catalysis, 9, 398-405 (1957).

14. R. P. Shields and M. Siman-Tov, The Effect of Iodine Decay Heat on Charcoal Adsorbers, USAEC Report ORNL-4602 (April 1971).

717

15. R. D. Ackley and R. E. Adams, _Trapping of Radioactive Methyl Iodide from Flowing Steam-Air: Westinghouse Test Series_, USAEC Report ORNL-TM-2728 (December 1969).

16. A. G. Evans, "Effect of intense gamma radiation on radioiodine retention by activated carbon," _Proceedings of the 12th AEC Air Cleaning Conference, Oak Ridge, Tennessee, 28-31 August 1972_, CONF-720823, pp. 401-15.

17. L. R. Jones, "Effect of gamma radiation on adsorption of iodine and methyl iodide on activated carbon," _Proceedings of the 11th AEC Air Cleaning Conference, Richland, Washington, 31 August-3 September 1970_, CONF-700816, pp. 526-37.

18. J. C. Chu, J. Kalil, and W. A. Wetteroth, "Mass transfer in a fluidized bed," _Chem. Eng. Progr._, 49 (No. 3), 141-49 (1953).

19. J. G. Knudsen, _Properties of Air-Steam Mixtures Containing Small Amounts of Iodine_, USAEC Report BNWL-1326 (April 1970).

20. R. E. Adams, R. D. Ackley, and R. P. Shields, "Application of impregnated charcoals for removing radioiodine from flowing air at high relative humidity," _Treatment of Airborne Radioactive Wastes, Proceedings of a Symposium, New York, 26-30 August 1958_, International Atomic Energy Agency (1968), pp. 396-97.

21. R. O. Lingjaerde and L. Podo, _A Study on the Trapping of Iodine at High Temperatures on Activated Charcoal_, Dragon Project Report DP-Report-213 (September 1963).

TABLE I

CHARACTERISTICS OF CHARCOALS INVESTIGATED

Charcoal Type	ORNL Lot No.	Experiment No.	Dry Mass in Each Exp. (g)	Apparent Density[a] (g/cm3)	Mean Particle Size[b] (cm)	Surface Moisture Content[c] (%)	K[c] (%)	I[c] (%)
MSA 85851[d]	51969	1, 2, 3, 4	11.2	0.45	0.161	6.73	2.85	4.41
BC-727[e]	1683	5	13.1	0.562	0.169	17.9	1.87	3.79
WITCO Grade 42[f]	62469	6	10.9	0.398	0.171	3.49	0.90	3.07
GX-176[g]	SR-7	7	14.7	0.563	0.151	7.0	1.26	1.30

[a] Apparent density of the moist charcoal according to the method of ASTM D-2854-70.

[b] Particles collected on 8-mesh or passing 16-mesh (U.S.) screens eliminated.

[c] Weight percent of moist (as-received) charcoal. Moisture content varied because of different storage conditions.

[d] Product of Mine Safety Appliances Company, Pittsburgh, Pa.

[e] Product of Barnebey-Cheney, Columbus, Ohio. Charcoal obtained from A. G. Evans, Savannah River Laboratory.

[f] Product of Witco Chemical Corporation, New York, N.Y.

[g] Product of North American Carbon, Inc., Columbus, Ohio. This charcoal also contains 1% TEDA (triethylenediamine) and a proprietary flame retardant. Charcoal and chemical analyses obtained from A. G. Evans, Savannah River Laboratory.

TABLE II

SUMMARY OF OPERATING CONDITIONS AND RADIOIODINE RELEASE, RUN 3, MSA 85851 CHARCOAL

Time interval (min)	$0-620^a$	620-1790
Main bed activity (Ci $^{130}I)^b$	94	31
Bed midpoint temp. range (°C)	$100-103^c$	100-101
Flow velocity^d (fpm at 25°C)	28.5^c	28.5

Iodine Form	Fraction of Radioactive Iodine Released (10^{-6})	
Elemental	~ 0.2	~ 0.06
Particulate	1.0	0.0010
Penetrating	0.76	1.01
Total^e	1.97	1.07

^{a}Loading of 139 mg of radioactive iodine took place between 0 and 120 min.

^{b}Activity at end of time interval. Peak activity was 150 Ci at 120 min.

^{c}Flow velocity reduced to 3.8 fpm (25°C) between 516 and 576 min. Bed midpoint temperature rose to 115°C.

^{d}Air at 0.98 atm; water vapor partial pressure estimated at 4 torr.

^{e}Grand total fractional release of radioactive iodine was 3.04×10^{-6}.

TABLE III

SUMMARY OF OPERATING CONDITIONS AND RADIOIODINE RELEASE, RUN 4, MSA 85851 CHARCOAL

Time interval (min)	-245 to 0[a]	0 to 28	28 to 36
Main bed activity (Ci ^{130}I)[b]	1000	980	970
Bed midpoint temperature range (°C)	100-135	124-252	252-485[c]
Flow velocity[d] (fpm at 25°C)	28.5	3.8	3.8

Iodine Form	Fraction of Radioactive Iodine Released (10^{-6})		
Elemental	0.5 $\pm$ 0.5	0.40	0.38
Particulate	17.3 $\pm$ 0.5	0.0003	0.014
Penetrating	3.3	0.14	0.04
Total[e]	21.2	0.54	0.43

[a]Loading of 259 mg of radioactive iodine took place between -245 and -135 min.
[b]Air velocity reduced to 3.8 fpm (25°C reference) at 0 min in runs 4-7. Activity at end of time interval.
[c]Ignition temperature of 300°C reached at 32.5 min at approximately 0.8-in. bed depth.
[d]Air at 0.98 atm; water vapor partial pressure estimated at 4 torr. All velocities are face or superficial, not interstitial. In metric units the velocities are 14.5 and 1.93 cm/sec at 25°C.
[e]Grand total fractional release was 22.2 x 10^{-6}.

TABLE IV

SUMMARY OF OPERATING CONDITIONS AND RADIOIODINE RELEASE, RUN 5, BC-727 CHARCOAL

Time interval (min)	-240 to 0[a]	0 to 29	29 to 39
Main bed activity (Ci ^{130}I)[b]	990	960	940
Bed midpoint temperature range (°C)	100-130	130-252	252-473[c]
Flow velocity[d]	28.5	3.8	3.8

Iodine Form	Fraction of Radioactive Iodine Released (10^{-6})		
Elemental	< 0.5	0.78	4.7
Particulate	1.9	0.001	0.06
Penetrating	6.7	2.07	0.19
Total[e]	8.6	2.85	4.9

[a]Loading of 231 mg of radioactive iodine took place between -240 and -135 min.

[b]Activity at end of time interval. The half-life of I-130 is 12.3 hr.

[c]Ignition temperature of 315°C reached at 35.5 min at approximately 0.8-in. bed depth.

[d]Air at 0.98 atm, 25°C reference temperature; water vapor partial pressure, estimated at 9 torr. The velocities are 14.5 and 1.93 cm/sec at 25°C.

[e]Grand total fractional release was 16.4 x 10^{-6}.

TABLE V

SUMMARY OF OPERATING CONDITIONS AND RADIOIODINE RELEASE, RUN 6, WITCO GRADE 42
CHARCOAL

Time interval (min)	-252 to -150[a]	-150 to 0	0 to 120	120 to 248
Main bed activity (Ci ^{130}I)[b]	650	570	510	450
Bed midpoint temp. range (°C)	70-91	83-91	83-210	210-507[c]
Flow velocity[d] (fpm at 25°C)	28.5	28.5	3.8	e

Iodine Form	Fraction of Radioactive Iodine Released (10^{-6})			
Elemental	3.2	0.09	0.56	∿ 10,000
Particulate	10.6	0.38	0.0008	4.4
Penetrating	0.78	1.84	3.47	0.34
Total[f]	14.6	2.31	4.03	∿ 10,000

[a]Loading of 144 mg of radioactive iodine took place during this period.

[b]Activity at end of time interval. The half-life of I-130 is 12.3 hr.

[c]Ignition temperature of 368°C reached at 229 min at approximately 0.8-in. bed depth.

[d]Air at 0.98 atm; water vapor partial pressure estimated at 3 torr.

[e]Velocity was reduced to 1.43 fpm at 120 min (210°C), reduced to 0.71 fpm at 163 min (236°C), and increased to 1.9 fpm at 246 min (429°C).

[f]Grand total fractional release of radioactive iodine ∿ 0.01.

TABLE VI

SUMMARY OF OPERATING CONDITIONS AND RADIOIODINE RELEASE, RUN 7, GX-176 CHARCOAL

Time internal (min)	-390^a to -226	-266 to 0	0 to 75
Main bed activity[b] (Ci ^{130}I)	810	630	590
Bed midpoint temp. range (°C)	70-98	84-93	84-445[c]
Flow velocity[d] (fpm at 25°C)	28.5	28.5	3.8

Iodine Form	Fraction of Radioactive Iodine Released (10^{-6})		
Elemental	1.8	0.16	1.4
Particulate	10.1	0.04	0.08
Penetrating	0.9	2.6	2.1
Total[e]	12.8	2.8	3.6

[a]Loading of 193 mg of radioactive iodine took place between -390 and -330 min.

[b]Activity at end of time period.

[c]Ignition temperature of 292°C reached at 70 min at approx. 1.3-in. bed depth.

[d]Air at 0.98 atm; water vapor partial pressure estimated at 4 torr.

[e]Grand total fractional release was 19.2×10^{-6}.

TABLE VII

CHARCOAL OXIDATION CHARACTERISTICS

Charcoal Type	Run No.	Air Velocity (fpm at 25°C)	Heat Input (watts)	Oxidation Rate Parameters		Ignition Temp. (°C)	
				H_o (cal/min·g)	A (cal/mole)	By Rate of Rise	By H = 15 cal/g·min
MSA 85851 Lot No. 51969	4	3.8	2.7,decay	6.35×10^8	20,000	300	300
	Lab 7, 10, 13	3.9	1.94,elec.	2.54×10^9	22,000	310-312	311
BC-727 Lot No. 1683	5	3.8	2.6,decay	1.65×10^8	19,000	315	317
WITCO Grade 42 Lot No. 62469	6	0.71	1.4,decay	a	a	a	a
	Lab 11, 12	3.9	2.31,elec.	6.35×10^9	25,000	365-372	360
GX-176 Lot No. SRL-7	7	3.8	1.6,decay	5.9×10^6	14,500	292	293

[a]The heat release data were insufficient to determine these parameters.

TABLE VIII

RATE OF RELEASE OF METHYL IODIDE AT 28.5 fpm (25°C)

Run No.	Peak Activity[a] Ci 130I	10^7 rads/hr	Time from Start of Loading (min)	Average Temp. (°C)	Release Rate (fraction/hr)	Water Partial Pressure (torr)
1	0.2	0.01	0-385	110	10×10^{-6}	4
2	8	0.4	0-346	110	1.0×10^{-6}	4
3	150	7.2	100-800	100	0.075×10^{-6}	4
3	78	3.7	800-1800	100	0.054×10^{-6}	4
4	1040	50	150-245	125	0.45×10^{-6}	4
5	1040	50	150-240	125	1.58×10^{-6}	9
6	650	31	102-252	85	0.75×10^{-6}	3
7	760	36	125-390	85	0.70×10^{-6}	4
SRL[b]	0	1.5	60-300	80	$\sim 50 \times 10^{-6}$	265

[a]Radiation intensity in the first 1/8-in. depth of bed.
[b]Results for a typical good-quality impregnated carbon in 1-in. deep bed, air flowing at 46.4 fpm (25°C reference, ~75% relative humidity in gamma radiation field at Savannah River Laboratory.

TABLE IX

DISTRIBUTION OF RADIOACTIVE IODINE

Slab No.[a]	Percent of Total Radioactivity in Each Slab									
	Run 3			Run 5			Run 7			
	Time from Start of Loading (min)			Time from Flow Reduction (min)			Time from Flow Reduction (min)			
	130	950	1790	-113	-6	38	-327	-14	60	75
0	10.6	6.09	4.64	7.98	6.57	3.70	14.2	9.43	6.85	4.35
1	61.6	51.8	47.9	45.2	40.4	21.1	60.6	58.6	52.4	34.7
2	18.5	25.9	27.5	23.0	24.1	18.0	15.8	20.1	25.6	29.3
3	4.75	8.6	10.9	11.9	13.5	14.4	4.53	6.05	8.23	14.8
4	1.77	3.13	3.67	5.85	7.31	11.0	1.86	2.47	3.23	7.17
5	0.94	1.51	1.76	2.87	3.74	8.37	0.92	1.14	1.35	3.99
6	0.54	0.89	1.06	1.39	1.93	6.57	0.59	0.68	0.76	2.32
7	0.38	0.55	0.64	0.71	1.02	5.10	0.41	0.44	0.46	1.30
8	0.27	0.36	0.41	0.42	0.55	3.94	0.28	0.30	0.31	0.76
9	0.19	0.29	0.33	0.27	0.34	2.74	0.19	0.20	0.22	0.46
10	0.13	0.21	0.24	0.18	0.22	1.96	0.14	0.14	0.15	0.25
11	0.07	0.15	0.19	0.12	0.14	1.36	0.09	0.09	0.10	0.15
12	0.04	0.12	0.15	0.07	0.09	0.85	0.05	0.06	0.07	0.10
13	0.03	0.10	0.11	0.05	0.05	0.45	0.03	0.03	0.04	0.07
14	-	-	-	-	-	0.21	-	-	0.03	0.05
15	-	-	-	-	-	0.12	-	-	-	-
16	-	-	-	-	-	0.08	-	-	-	-
17	-	-	-	-	-	-	-	-	-	-
Background 1.28	1.28	1.28	1.28	0.43	0.43	0.43	0.41	0.41	0.41	0.41
Bed mid-point Temp.(°C)	103	102	101	138	130	473	95	85	210	444

[a]Each slab is determined by collimator movement of 0.125 in.
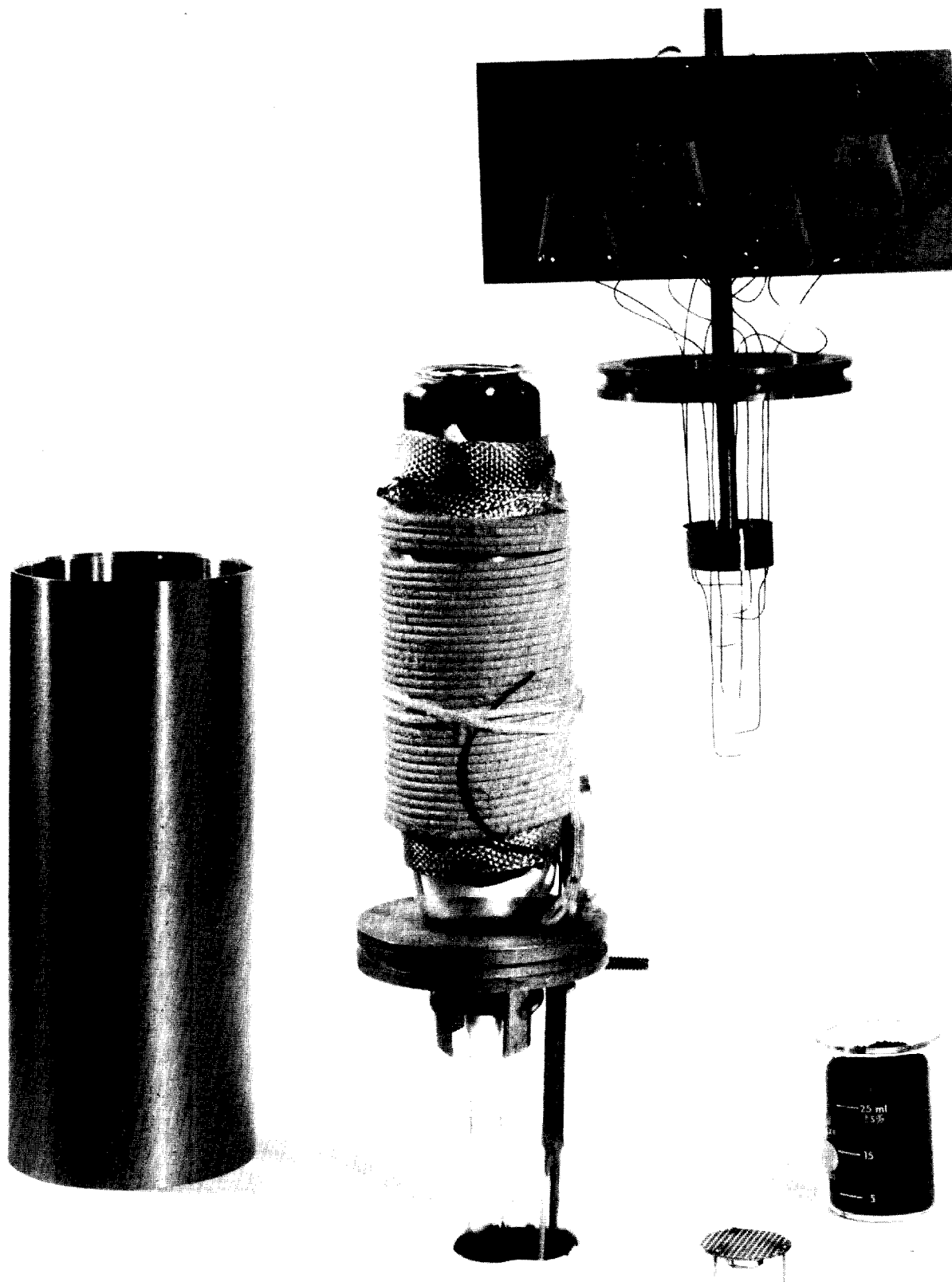
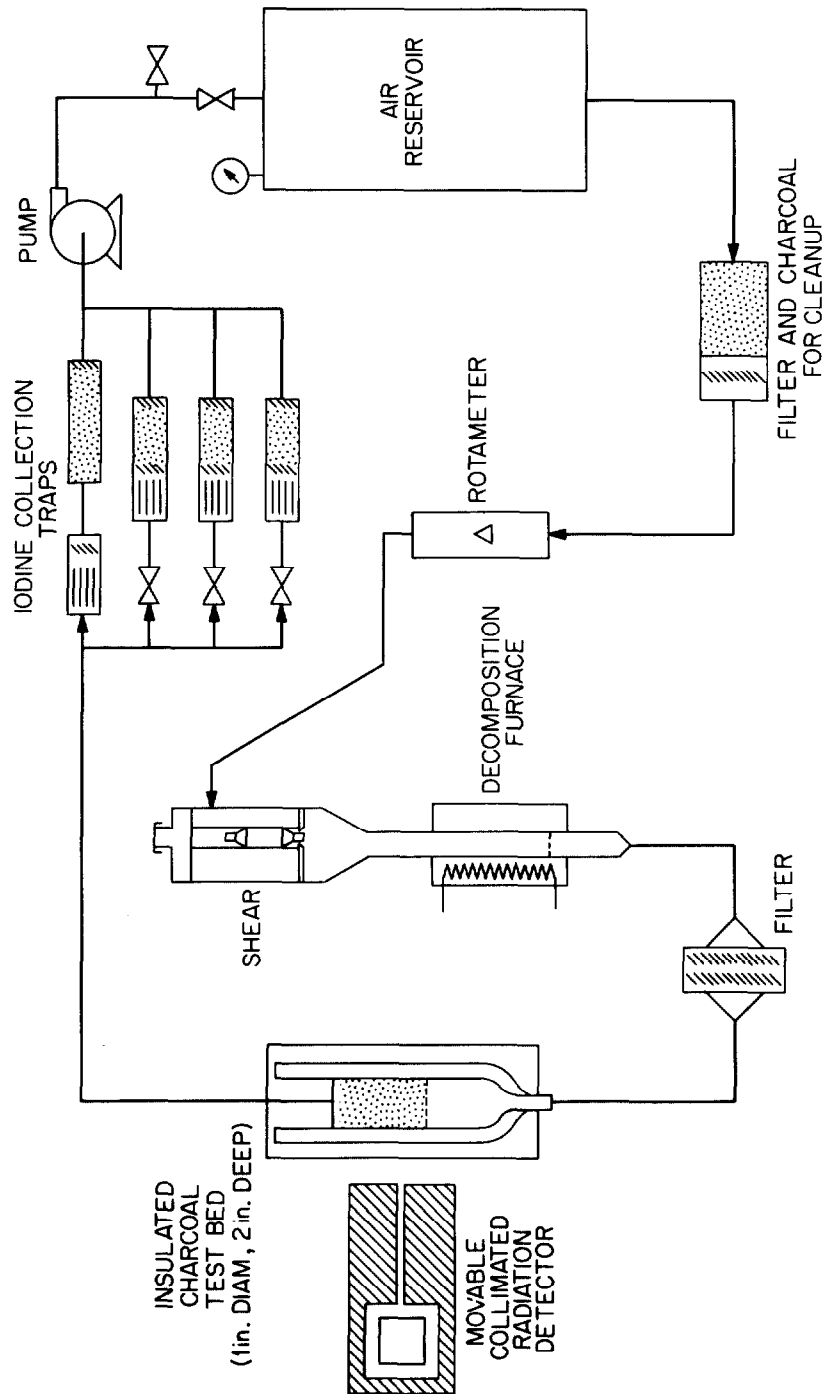FIGURE 1.   INSULATED TEST BED COMPONENTS.

ORNL-DWG 73 - 7318

FIGURE 2.   CHARCOAL IGNITION EXPERIMENT.
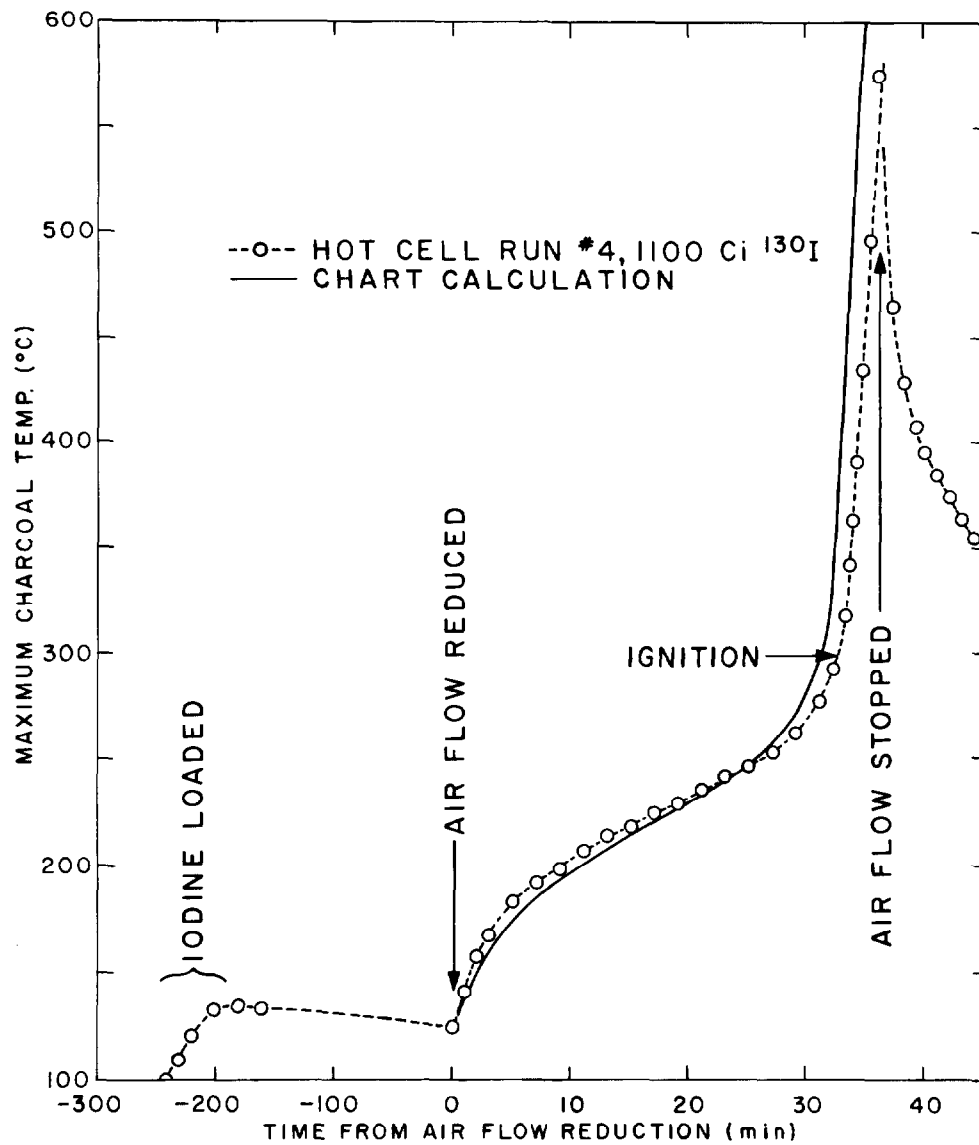
ORNL DWG 73-7696

FIGURE 3.   COMPARISON OF CHART CALCULATION AND RUN 4.
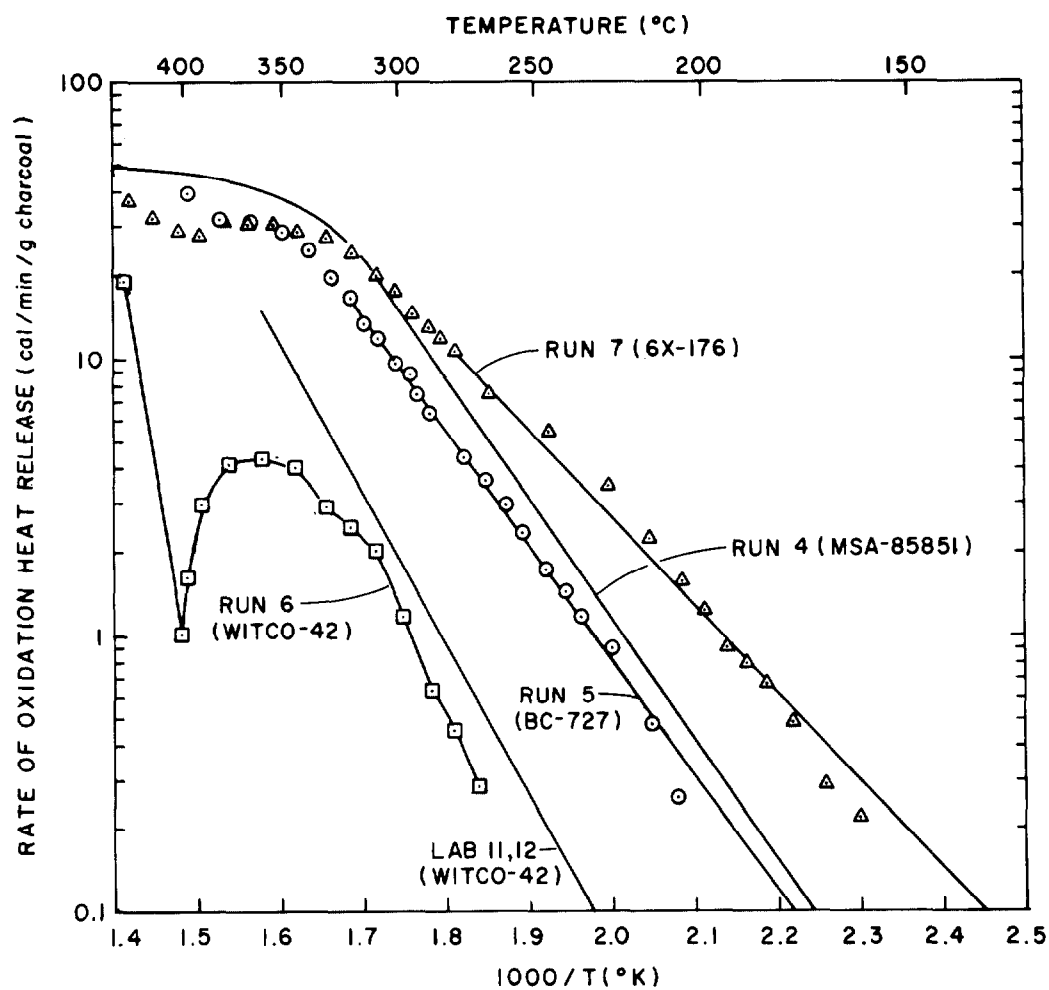
ORNL DWG 74-7398

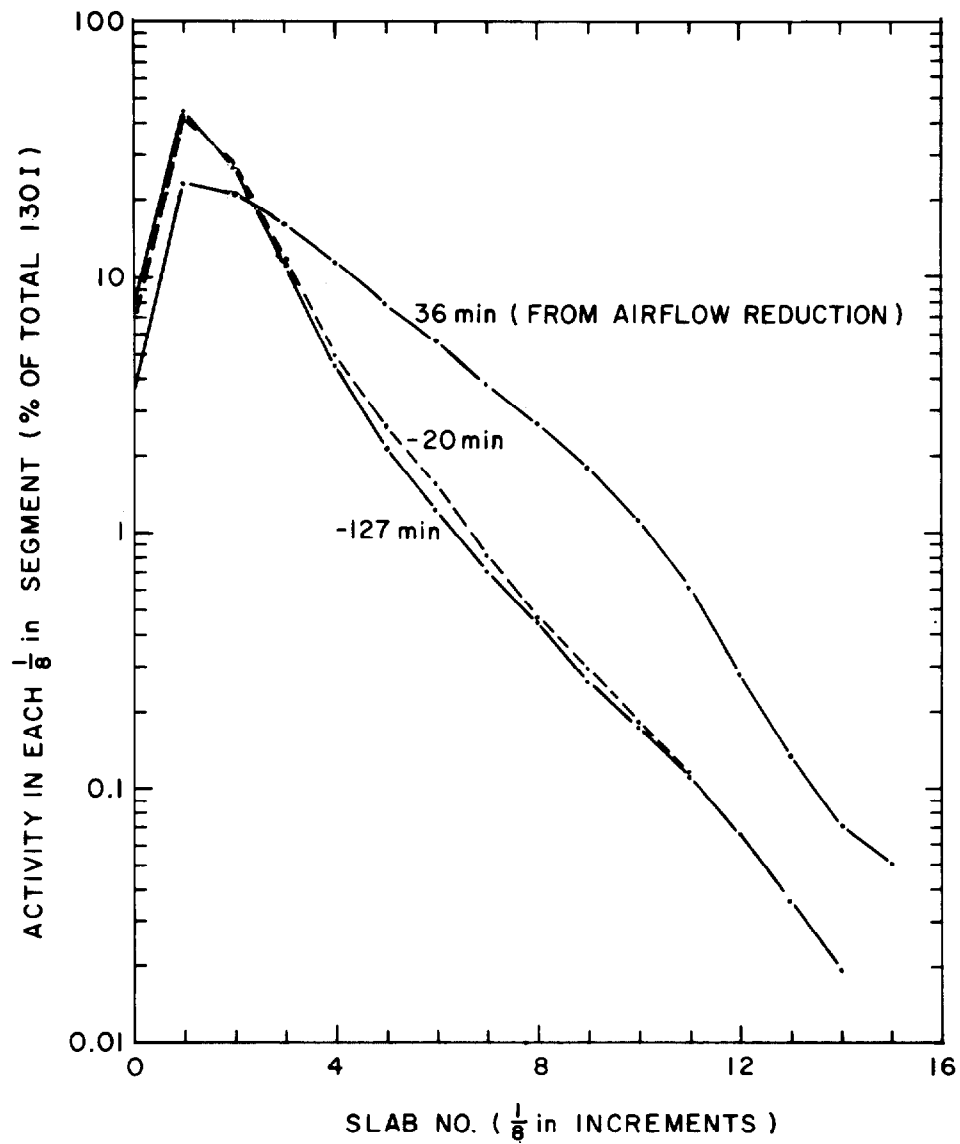FIGURE 4. RATE OF OXIDATION HEAT RELEASE.

ORNL DWG 74-7400

FIGURE 5. DISTRIBUTION OF RADIOIODINE DURING RUN 4.
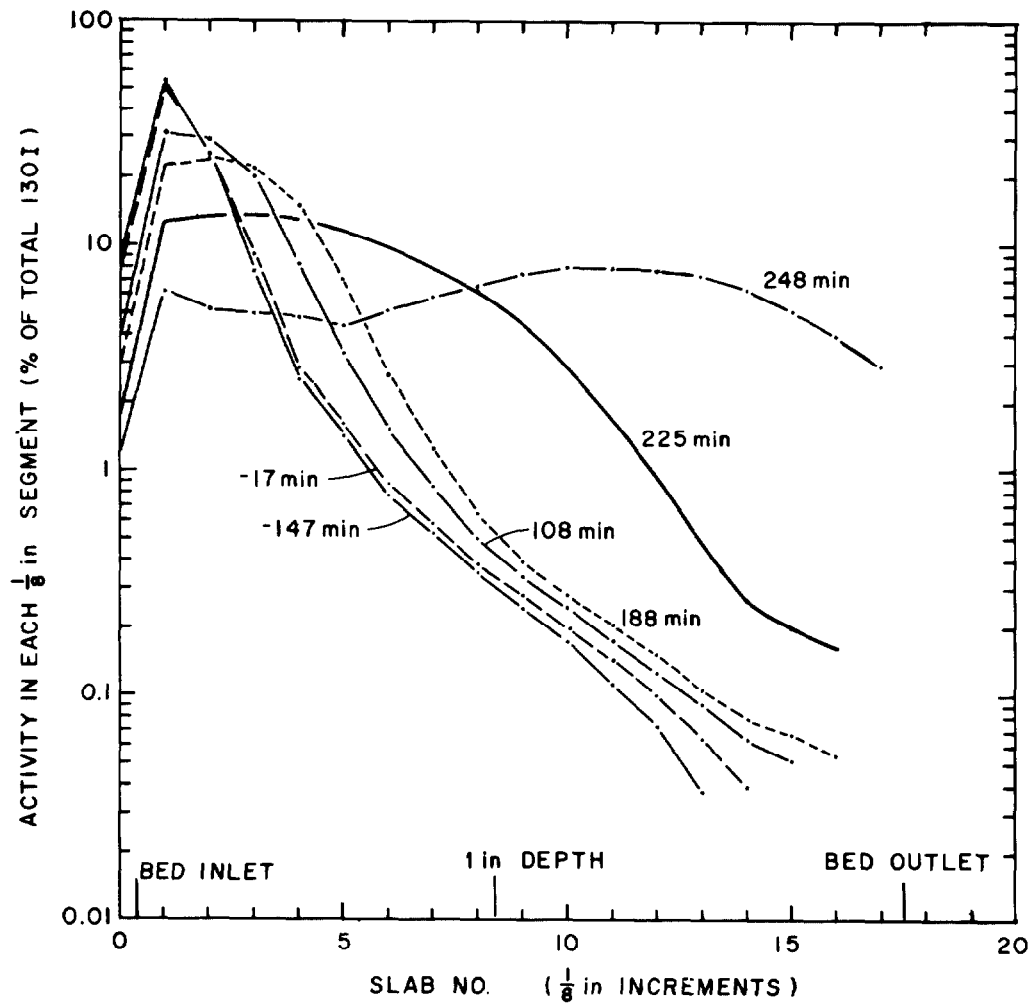
ORNL DWG. 74-7397
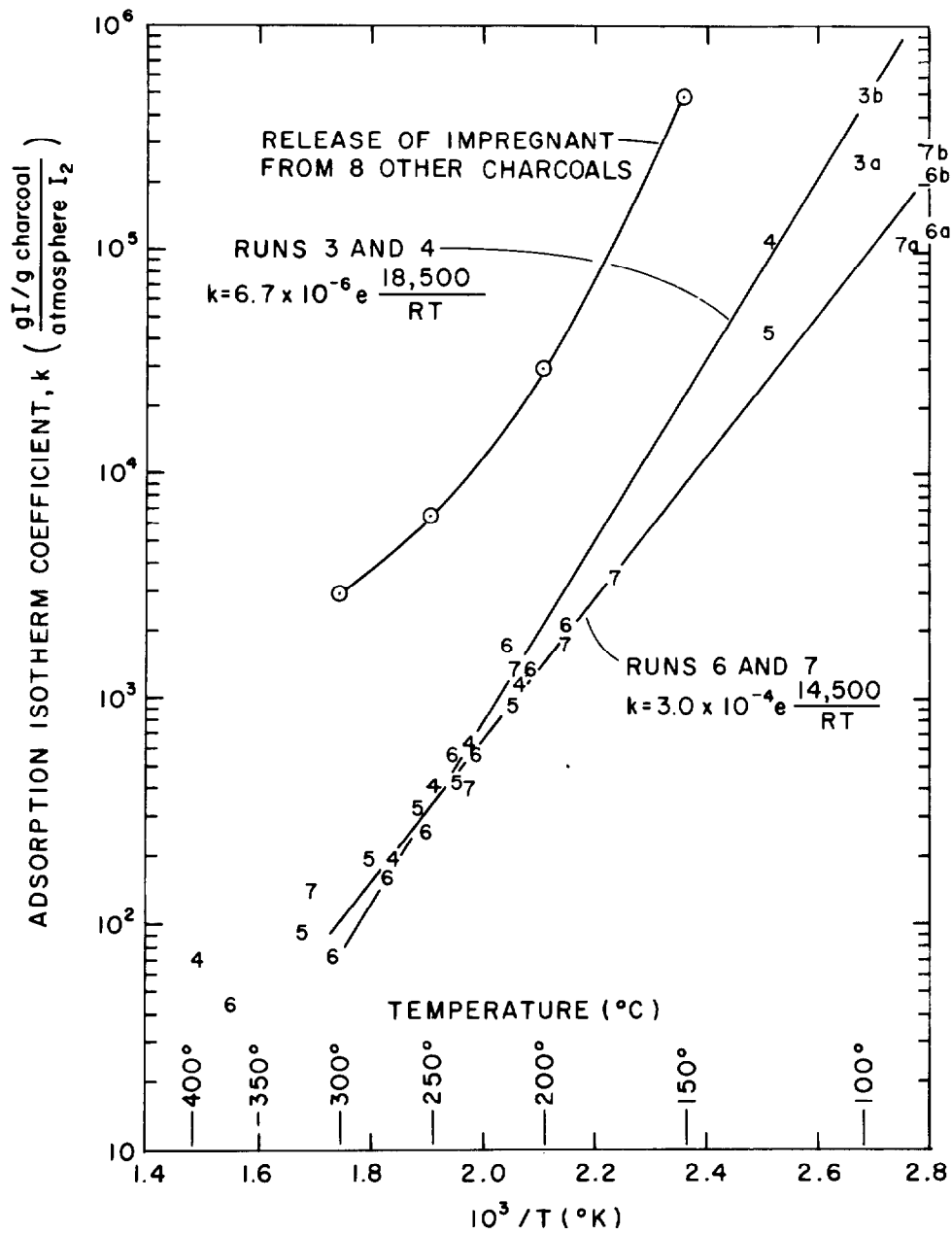

FIGURE 6.   DISTRIBUTION OF RADIOIODINE DURING RUN 6.

ORNL DWG 74-7399 RI

FIGURE 7. ADSORPTION ISOTHERM COEFFICIENTS.

DISCUSSION

JONAS: How can you differentiate between the heat caused by physical adsorption of the gas by the carbon and the heat of reaction caused by the subsequent chemical reaction between the adsorbed methyl iodide (or iodine) and the carbon impregnants when you only report the overall heat from the combination?

LORENZ: Since the iodine does not leave the bed, any desorption at one location is equalized by adsorption at another location.

JONAS: I would like to make the following comment. One can consider as a simple model the overall heat measured as an additive sum of both the physical adsorption and the subsequent chemical reaction. It is now necessary to obtain the active carbon before impregnation and, under the same conditions of concentration, flowrate, and humidity, determine the heat due to physical adsorption. The heat due to chemical reaction can be obtained by subtraction of the physical adsorption heat from the overall heat.

VELEZ*: At what specific level (curies/gram) did the test specimen achieve ignition?

LORENZ: There is no simple answer to this question as it depends on other charcoal exposure conditions, such as oxidation rate, as well. The total number of curies and weight of charcoal for each experiment are given in the several tables, so it is possible to calculate the curies per gram. However, it does not mean that that was the critical value causing ignition. Usually, there was about 500 curies in about 10 grams of charcoal, or about 50 curies per gram. In more recent experiments, we have decreased the radioactivity to about 25 curies per gram. Since preparing the paper, we have run a sample of used charcoal taken from one of the ORNL systems and found it ignites at a lower temperature than clean charcoal, all else being the same. We believe this results from heat released from the oxidation of the adsorbed materials added to decay heat plus charcoal oxidation heat.

*Question submitted in writing after conclusion of Conference.

IODINE FISSION PRODUCT MASS TRANSFER IN ADSORBENT MEDIA

J.L. Kovach and J.R. Hunt
Nuclear Consulting Services Inc.
Columbus, Ohio

Abstract

The iodine and methyl iodide removal efficiency of new and exposed adsorbent media was evaluated using tracer techniques. Particular attention was paid to keep the inlet iodine concentration near the atmospheric iodine concentration of 10^{-3} $\mu g/m^3$. The zone depth of activity was measured at 5.08 - 81.28 cm/sec (10 - 160 fpm) in a segmented adsorber system. The obtained results are useful for both the design of air cleaning systems and iodine fission product sampling cartridges.

I Introduction

Recently a very significant emphasis is placed on the removal efficiency of adsorbents for continuously released iodine fission products. Generally these iodine FP concentrations are defined in units of microgram/m^3 at 10^{-8} to 10^{-12} values. Although these concentrations can validly be postulated for 131I quantity, they do not represent the total iodine concentration. Typical atmospheric iodine content is in the range of 10^{-2} to 10^{-3} $\mu g/m^3$, [1, 2, 3, 4], therefor it is difficult to postulate that an adsorbent system would be exposed to lower total iodine concentration than these values.

In this series of experiments the iodine removal efficiency of adsorbents was determined as a function of superficial space velocity, bed depth, time and within limits adsorbent exposure to typical reactor atmosphere.

Most of the experiments were performed using methyl iodide as the chemical species of the fission product iodine, because the elemental iodine removal efficiency is generally order or orders of magnitude higher than the methyl iodide removal efficiency. Both 131I and 3H were used as tags to permit the development of mass transfer information.

II Materials, Equipment, and Procedures

Methyl ^{3}H iodide at 2.5C/mM specific activity and methyl ^{131}I iodide at 20 - 25C/mgI specific activity was used for the experiments. Elemental iodine was tagged to the 20 - 25C/mgI level for the experimental series.

The experiments were conducted in a dual water/air environmental chamber system. The compressed air used for the experiments was dried to -50°C dew point, passed through a 1m^3 carbon adsorbent bed to remove the atmospheric iodine and filtered through a series of four particulate filters to remove all particles with at least a 99.97% efficiency. The air was prehumidified in the water filled environmental chamber, where dew points within 0.2°C were maintained. The air was passed to the air thermostated environmental chamber which is also equipped with both heater and refrigeration systems and internal blowers to maintain the temperature within 0.3°C set point. In both chambers the air is passed through a series of copper coils to permit temperature equilibration. The control of humidity by setting the two systems at different

temperatures permits very close control of relative humidity. The actual temperature settings are based on the air temperature and calibration is performed against an NBS calibrated thermometer.

The methyl iodide is injected in liquid form with a syringe into the refrigerated valve of a 1000ml stainless steel cylinder and pressurized with high purity nitrogen. The thus diluted methyl iodide is metered through a calibrated rotameter into the main carrier gas stream. The methyl iodide nitrogen flow is in the range of 0.01 to 0.2 of the total carrier gas flow, therefore its effect on the relative humidity of the test loop is insignificant.

The adsorbent media for these experiments was placed in the standard NUCON environmental sampling cartridges. These cartridges have an internal diameter of 40mm, the filled height is 52.3mm resulting in a cross sectional area of 1,256.6mm^2 and a filled volume of 65,720.2mm^3. Each cartridge has a 5mm non-perforated blank margin at both faces to prevent high velocity bypass along the walls. One or more of these cartridges was used in series to result in the desired bed depth. The total flow was measured by a rotameter after the test beds and by a Rockwell totalizing gas meter. Guard beds were used where required.

Counting of the sample cartridges was done in a Harshaw 10cm NaI well crystal. The entire cartridge fits into the well avoiding the mixing or rearrangement of the adsorbent during successive test runs and measurements. A Canberra preamplifier, amplifier, discriminator, and scales system was used to obtain counts at the 0.3645 McV photopeak. Counting efficiency was approximately 46%.

The cartridges when used in series were counted and reassembled for the additional time runs in the same geometry order as used in the previous runs. Each of the cartridges was also counted after prequilibration with humid air for background correction of the counts.

The breakthrough and transit characteristics of the tritiated methyl iodide were measured using an Overhoff and Associates Betatec which has a sensitivity of 1.0 μC/m^3. Data for the counts and ion chamber displays was printed out using a Hewlett-Packard digital printer.

The inlet total iodine concentration was maintained at 0.9 - 1.2 X 10^{-3} μg/m^3 which corresponds to the lowest atmospheric iodine concentration in the United States. The ^{131}I concentration corresponded to 0.8 - 1.1 X 10^{-5} μg/m^3.

The main adsorbent evaluated was NUSORB 101621 which is a coconut shell based KI and TEDA coimpregnated adsorbent. Additional adsorbents evaluated were Barnebey-Cheney 727 and Sutcliffe-Speakman KI$_3$ impregnated carbon. Both of these were 8 X 16 (U.S. Sieve) mesh, approximately 1400m^2/g surface area coconut shell carbons. Several samples of used BC 727 (from 18 to 36 months exposure) were also obtained from nuclear reactor air cleaning systems.

III   Presentation of the Results

Methyl 131 Iodide Series

All of these experiments were performed at 25°C and 95% RH. The bed was segmented into six 52.3mm beds. Tests on new NUSORB 101621 adsorbent were run

at 5.08, 20.32, 40.64, and 81.28 cm/sec (10, 40, 80, and 160 fpm) superficial air velocities. Used carbons and other adsorbents were tested only at 20.32 cm/sec. Most tests were performed at 1, 2, 4, 8, and 16 hours loading time on the same cartridges. In several cases a 16 hour post sweep using air under the test conditions was also performed. The results of these experiments are shown on Tables 1, 2, 3, 4, and 5.

Table 1

Loading	Efficiency %					
Bed Depth cm	5	10	15	20	25	30
Res. Time sec	1.03	2.06	3.09	4.12	5.15	6.18
1 Hr	99.72	99.79	99.84	99.88	99.96	99.99
2 Hr	99.90	99.91	99.94	99.96	99.99	99.99+
4 Hr	99.94	99.95	99.97	99.98	99.99	99.99+
8 Hr	99.95	99.96	99.97	99.98	99.99+	99.99+
16 Hr	99.97	99.98	99.99	99.99+	99.99+	99.99+
16 Hr Post Sweep	99.95	99.97	99.98	99.99+	99.99+	99.99+

Conditions: 25°C, 95%RH, 5.08 cm/sec (10 fpm)

Table 2

Loading	Efficiency %					
Bed Depth cm	5	10	15	20	25	30
Res. Time sec	.26	.52	.78	1.04	1.30	1.56
1 Hr	99.25	99.68	99.80	99.89	99.95	99.99
2 Hr	99.45	99.82	99.88	99.93	99.96	99.99
4 Hr	99.44	99.89	99.98	99.99	99.99+	99.99+
8 Hr	99.35	99.87	99.94	99.96	99.98	99.99+
16 Hr	99.29	99.97	99.99	99.99+	99.99+	99.99+
16 Hr Post Sweep	99.03	99.97	99.99	99.99+	99.99+	99.99+

Conditions: 25°C, 95%RH, 20.32 cm/sec (40 fpm)

Table 3

Loading	Efficiency %						
Bed Depth cm		5	10	15	20	25	30
Res. Time sec		.13	.26	.39	.52	.65	.78
1 Hr		95.72	99.78	99.89	99.99	99.99+	99.99+
2 Hr		96.62	99.89	99.95	99.99	99.99+	99.99+
4 Hr		95.85	99.84	99.94	99.99	99.99+	99.99+
8 Hr		94.61	99.73	99.90	99.99	99.99+	99.99+
16 Hr		91.39	99.76	99.90	99.99	99.99+	99.99+
16 Hr Post Sweep		91.38	99.75	99.90	99.99	99.99+	99.99+

Conditions: 25°C, 95%RH, 40.64 cm/sec (80 fpm)

Table 4

Loading	Efficiency %						
Bed Depth cm		5	10	15	20	25	30
Res. Time sec		.065	.13	.20	.26	.33	.39
1 Hr		93.31	99.95	99.99	99.99+	99.99+	99.99+
2 Hr		91.81	99.84	99.99	99.99+	99.99+	99.99+

Conditions: 25°C, 95%RH, 81.28 cm/sec (160 fpm)

Table 5

Carbon	Efficiency %						
Bed Depth cm		5	10	15	20	25	30
Res. Time sec		.26	.52	.78	1.04	1.30	1.56
BC 727 new		98.25	99.08	99.70	99.88	99.95	99.99+
SS KI new		93.55	98.93	99.70	99.90	99.95	99.99+
BC 727 used*		74.62	96.46	99.55	99.81	99.95	99.99
BC 727 used**		35.20	66.11	83.87	93.13	97.63	99.05

Conditions: 1 Hour Loading, 25°C, 95%RH, 20.32 cm/sec (40 fpm)

* Continuously exposed in a power reactor environment for 1 year
** Continuously exposed in a power reactor environment for 2 years

In the standard RDT condition methyl iodide tests, both of the used carbons showed less than 10% efficiency for a 5cm (2 inch) bed depth at the same 95% relative humidity.

Methyl 3H Iodide Series

All of these experiments were performed at 25°C, 95%RH, and 20.32 cm/sec (40 fpm) air velocity on sample cartridges. After temperature and humidity equilibriums were achieved CH_2TI was injected to result in a 10,000 $\mu C/m^3$ inlet spike. The outlet activities were continuously monitored. Total iodine content was maintained at the $0.9 - 1.2 \times 10^{-3}$ $\mu g/m^3$ level.

The time after injection and maximum reading data is shown in Table 6.

Table 6

Carbon Type	Max Outlet $\mu C/m^3$	Peak Appearance Time min
NUSORB 101621	10	105
BC 727	50	40
BC 727 used*	220	7.5
BC 727 used**	860	7.5

Conditions: 25°C, 95%RH, 20.32 cm/sec, (40 fpm)

*   Continuously exposed in a power reactor environment for 1 year
** Continuously exposed in a power reactor environment for 2 years

Table 7

Velocity		Efficiency %		
cm/sec	Res. Time sec	1.03	.78	.26
5.08		99.72	---	---
20.32		99.89	99.80	99.25
40.64		---	99.99	99.78
81.28		---	---	99.99

All data shown 1 Hour loading.

IV Evaluation of the Results

The ^{131}I tagged methyl iodide series indicate several significant facts.

The first one of these is that methyl iodide removal efficiency at this atmospheric iodine concentration is not lower than for the high (mg/m^3 range) concentrations.

The mass transfer zone of the methyl iodide removal, particularly at the low velocity operation appears to be longer after short loading times, however this may be an effect of the lower counting precision, because at longer loading times and higher subsequent cpm/cartridge levels the observed efficiency improved.

The methyl iodide removal efficiency can not be correlated on the basis of residence time. As an example, Table 7 shows equal residence time efficiencies at different carrier gas velocities. In all cases at higher velocities and equal residence times the efficiency increased.

Actual activity wave (mass transfer zone) progression was observed only at and above 40.64 cm/sec (80 fpm) velocities.

Below 40.64 cm/sec velocity there appears to be a leading edge resulting in a mass transfer zone of approximately 15cm which should correspond to minimum bed depth design for continuously operated adsorbent beds.

The rate of movement of the methyl iodide decontamination front can be approximated only from the obtained results; for accurate design measurements, adsorption runs with an order of magnitude longer loading times are required. However, as an example the results indicate that even at 40.64 cm/sec (80 fpm) velocity the rate of zone movement is much less than 5cm/16 hours (or 0.32 cm/hours). From standard adsorption equations the zone rate of movement has the following relationship:

$$u_D = v \frac{C_o}{N_o} \qquad (1)$$

where u_o: rate of zone movement
       v : carrier gas velocity
       C_o: inlet concentration
       N_o: adsorption capacity

The adsorption isotherms (capacity versus concentration curves) for methyl iodide at no point indicate even a near order of magnitude drop in N_o when C_o decreases by an order of magnitude. Therefore, u will be significantly slower as the inlet concentration decreases. (5)

Additionally because the observed mass transfer zone is for the radioactive component only Equation (1) has to be modified to:

$$u = u_o \exp (-\mathcal{f} t) \qquad (2)$$

This equation indicates that the movement of $CH_3^{131}I$ will practically cease after the zone traveled for $3/\mathcal{f}$ time through the adsorbent bed. This zone movement is based on the one half inlet concentration movement which appears to

be of 0.05 cm/hour. This value would indicate that decay beds can be designed for iodine; a safe typical bed depth is indicated at the order of 30 cm or less. An order of magnitude drop in inlet concentration would result in an approximate 50% less bed depth.

The penetration of tritiated methyl iodide through new and exposed adsorbents appears to have a promise for aging evaluation. Regardless of the means of removal, the methyl iodide has to be present on the surface of the adsorbent to permit isotope exchange or reaction. If due to loss of reactant or coadsorption of poisoning agents the methyl iodide transport through the adsorbent bed is of insufficient duration the removal efficiency will decrease. Additional studies are required to present a conclusive case for this type of aging evaluation.

The low concentration methyl iodide removal efficiency of used adsorbents does not decrease as fast as their high concentration removal efficiency.

References

1. McFarland, R.C. et al. "Determination of Atmospheric Concentrations of Stable Iodine." Eng. Exp. Station, Georgia Inst. Tech. (1973)

2. Duce, R.A. and Winchester, J.W. "Determination of Iodine, Bromine, and Chlorine in Atmospheric Samples by Neutron Activation Analysis." Radiochem. Acta 4, 100, (1965)

3. Duce, R.A. et al. "Atmospheric Iodine, Bromine and Chlorine." J. Geophys Res. 68, 3943, (1963)

4. Kovach, J.L. "Evaluation of Currently Available Data for Low Concentration Iodine Fission Product Removal." NUCON Report 078 (1974)

5. Kovach, J.L. "Sizing of Iodine Adsorbent Beds." NUCON Report 005 (1972)

DISCUSSION

DEITZ: When a removal efficiency is reported to be in the range above 99%, one is essentially dealing with differences between large numbers. It would be more significant, statistically speaking, to report the actual penetration and improve the detection to make the leakage observable.

KOVACH: Probably the best method would be to report decontamination factors. I don't think there is an established nomenclature at this time.

EFFECT OF ALKALI METAL CONTENT OF CARBON ON RETENTION OF IODINE AT HIGH TEMPERATURES

A. G. Evans
Savannah River Laboratory
E. I. du Pont de Nemours and Company
Aiken, South Carolina 29801

Abstract

Activated carbon for filters in reactor confinement systems is intentionally impregnated with iodine salts to enhance the removal of radioiodine from air streams containing organic iodides. When a variety of commercial impregnated carbons were evaluated for iodine retention at elevated temperatures (4 hours at 180°C), wide variations in iodine penetration were observed. The alkali metal and iodine content of carbon samples was determined by neutron activation analysis, and a strong correlation was shown between the atom ratio of iodine to alkali metals in the carbons and the high-temperature retention performance. Carbons containing excess alkali (especially potassium) have iodine penetration values 10 to 100 times lower than carbons containing excess iodine. Both low I/K ratios and high pH values were shown essential to high efficiency iodine retention; therefore, conversion of elemental iodine to ionic iodine is the basic reaction mechanism.

The natural high K^+ content and high pH coconut carbons make coconut the preferred natural base material for nuclear air cleaning applications. Studies show, however, that treatment of low potassium carbons with a mixture of KOH and I_2 may produce a product equal to or better than I_2-impregnated coconut carbons at a lower cost.

Introduction

The airborne activity confinement systems for the Savannah River production reactors are designed to collect halogens and particulates that might be released in the highly unlikely event of a reactor accident[1]. A continuing program is in progress at the Savannah River Laboratory to evaluate the performance of the confinement systems (each reactor has an identical system) for removing airborne radioactivity under accident conditions and to develop techniques to enhance the reliability and efficiency of the systems.

Previous studies at Savannah River showed that the unimpregnated type 416* carbon used for many years in the system retained iodine less effectively than many types of impregnated carbons when exposed to an intense radiation field such as that which would result from the accumulation of radioiodine following a major reactor accident[2,3]. The results of a series of screening tests conducted to aid in the selection of a suitable replacement carbon were reported at the Twelfth Air Cleaning Conference[4]. In these tests, coconut-shell carbons impregnated with triethylenediamine (TEDA) or a combination of TEDA and KI were shown to be the most effective for iodine retention in the Savannah River confinement systems.

Subsequent testing at Savannah River[5] confirmed the earlier observations of Adams, *et al.*[6] that carbons with high TEDA content exhibit significantly reduced ignition temperatures as the result of the fairly low ($\sim$190°C) flash point of TEDA. Savannah River studies showed, however, that carbons with reduced TEDA content could be manufactured which exhibit satisfactory ignition temperature and iodine retention properties[7]. A 1% TEDA - 2% KI product (designated GX-176**) is currently being installed in the Savannah River confinement system.

With the selection of a suitable replacement carbon for the confinement system[7], research efforts were directed toward explaining the anomalous thermal desorption behavior of iodine from various commercial iodized carbons. In the earlies screening tests[2,3], similar iodized carbons (nominally 5% KI-I_2 on 1500-m^2/g coconut carbon) exhibit highly variable results when tested for thermal desorption at 180°C (penetration values ranging from 0.023% to 12.8%

---

* Product of Barnebey-Cheney Company, Columbus, Ohio.

** Product of North American Carbon Company, Columbus, Ohio.

in a four-hour test). The extremes in penetration values were obtained from two different lots of carbon from the same vendor. Investigation revealed that the principal factors in retention behavior were the iodine and potassium content of the carbon (especially the atom ratio I/K) and the pH of the carbon[8].

Discussion

High-Temperature Desorption Tests

The high-temperature desorption test was initially designed as a screening test to aid in selecting potential replacement carbon types for the Savannah River confinement system[2]. The test conditions (10-minute loading of elemental iodine at ambient temperature and humidity followed by 4 hours desorption at 180°C and <1% relative humidity) were selected to prevent damage to the "Teflon"*-coated test apparatus and "Neoprene"* "O"-rings used as seals in the apparatus. The 180°C temperature is also near the upper limit of usefulness for nuclear carbons because thermal desorption of iodine becomes significant in this temperature range. HEPA filter blinding data presented in an earlier paper in this conference[9] show that this elevated temperature could be attained in a hypothetical accident. Moreover, because of the sensitivity of some commercial carbons to high temperatures, the high-temperature desorption test has been proposed for inclusion in the ASTM Standards for carbon testing.

In the original screening test series[3], 13 of the 21 candidate adsorbers were subjected to the high-temperature test and had penetration values ranging from 0.003% (5% TEDA on coconut carbon) to 12.8% (KI-I_2 on coconut carbon)[3,4]. The data fall into three broad penetration categories:

(1) very low (<0.010%): coconut base carbons either unimpregnated or impregnated with TEDA or TEDA and KI;

(2) intermediate (0.01 to 0.10%): coconut base carbon impregnated with I_2, KI-I_2, or PbI_2; and

(3) very high (>1.0%): coconut base carbons impregnated with KI-I_2, and petroleum base carbons impregnated with KI or TEDA.

The anomaly in the data is that four of the products originally tested were nominally identical ($\sim$5% KI-I_2 on 1500-m^2/g coconut carbon), yet the high-temperature penetration values ranged from 0.028% to 12.8%. Subsequent testing of a different manufacturing lot of the carbon showing 12.8% penetration had a penetration of only 0.023%.

Preliminary investigation of the cause of the variability indicated that different methods of impregnation may have been used by the four vendors[3]; however, confirmation of the techniques could not be obtained because of the proprietary nature of the processes. Because the two principal methods which

---

*Registered tradenames of E. I. du Pont de Nemours and Company.

could be employed* could result in different degrees of alteration of the chemical content of the carbon, samples of the five carbons were analyzed for K, Na, and I content by neutron activation analysis and for residual alkalinity by measuring the pH of a water extract of the carbons. The results of these analyses indicated a strong correlation between the atom ratio of iodine to potassium (I/K ratio) and the high-temperature iodine penetration test results. The sodium content of the carbons was consistently <0.2% (by weight) and was not related to penetration.

Chemical Analysis of Carbons

Results of neutron activation analyses of several commercial I_2-impregnated carbons are shown in Table I along with the pH and iodine penetration data. The comparison between I/K ratios and high-temperature penetration data for coconut carbons is presented graphically in Figure 1.

To rule out the possibility of variations in the natural K^+ content of the base carbon (three of the four vendors use the same base carbon), representative samples of base carbon from lots manufactured over a 5-year period were also analyzed for K^+ and Na^+ content. The data show very little change from lot to lot as indicated in Table II.

Table I   Chemical analysis of commercial iodized coconut carbons.

Carbon Vendor	Potassium, wt %	Iodine, wt %	Atom Ratio I/K	pH^a	Iodine Penetration, $\%^b$
A^c	0.958	4.01	1.29	7.05	12.82
B	1.14	4.42	1.19	9.56	2.41
C	1.75	3.78	0.664	9.36	0.052
$D-1^d$	1.55	3.01	0.600	9.62	0.028
A^c	2.23	4.23	0.586	9.02	0.023
D-2	1.04	1.31	0.387	9.86	0.006
D-3	1.26	1.30	0.318	10.06	0.003

a. 5 g carbon in 20 ml distilled water. pH of water measured after 20 minutes soaking.

b. High-temperature desorption, see text for test description.

c. One of two manufacturing lots of the same type carbons.

d. 1, 2, and 3 represent 3 different carbon types from the same vendor.

---

* The "dip" method could possibly result in a water leached carbon; and the "spray" method could result in an unleached carbon, if the liquid addition is controlled below the saturation level of the carbon.
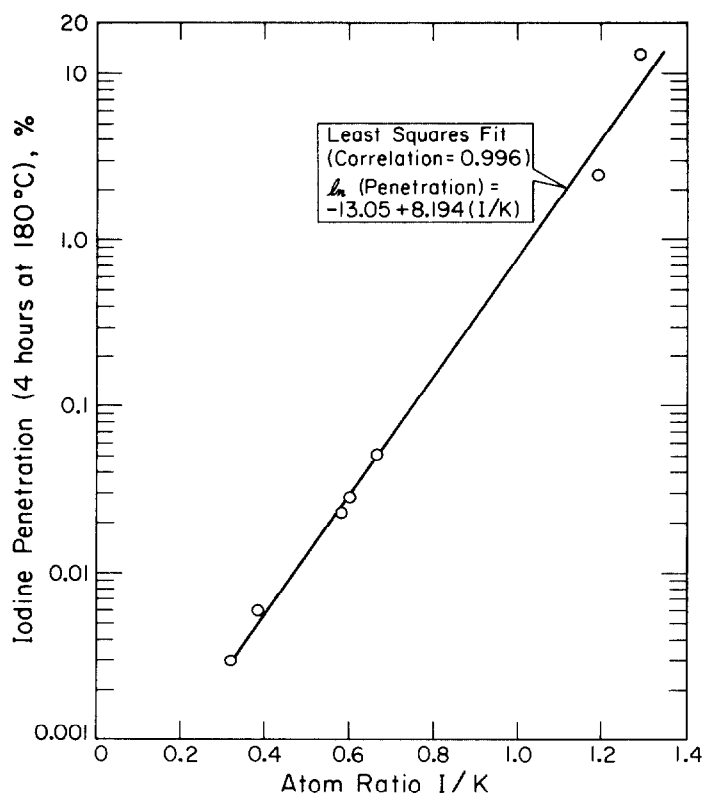
Figure 1   Penetration vs. I/K Ratio for
Commercial I$_2$-Impregnated Carbons

Table II   Chemical content of 1500 m^2/g coconut base carbons.

Manufacture Date	pHα	K$^+$, wt %	Na$^+$, wt %
3/69	9.9	1.18	0.11
6/70	10.0	1.17	0.07
2/71	9.9	1.19	0.08
3/72	9.9	1.30	0.09
10/73	10.3	1.27	0.06

a.   See Table I for test description.

The data suggest a basic reaction mechanism for high efficiency elemental iodine retention by activated carbon as shown in idealized form in Equation (1).

$$I_2 + 2K^+ + 2(OH)^- \rightarrow 2K^+ + 2I^- + H_2O + \tfrac{1}{2}O_2 \tag{1}$$
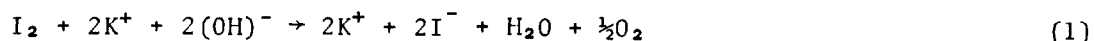
In a strongly basic environment (pH >9.0), one could postulate the formation of the iodate, hypoiodite, or periodate ions as well, but the simplified view of conversion of I_2 to I^- is adequate to illustrate the point. The potassium salts of iodine show high inherent stability and indicate that the combination of excess K^+ and a basic environment best promote stabilized ionic iodine formation. Thus coconut carbon, because of its high natural basicity and high natural K^+ content, is the best natural iodine adsorber.

Laboratory Impregnated Carbons

In an effort to define specific reaction mechanisms, three series of experiments were undertaken: (1) vapor-phase I_2 impregnation of natural-K^+ carbon (constant K^+, varying I_2 concentration); (2) vapor-phase I_2 impregnation of a K^+-free carbon, followed by KOH impregnation (constant I_2, varying K^+ concentration; and finally (3) liquid KOH-I_2 impregnation of a K^+-free carbon.

To minimize the effect of a variable base carbon (base carbons have inherently different iodine capacities), a 5-gallon drum of ∿1500-m^2/g coconut carbon was obtained from a carbon vendor. After preliminary analysis, a portion of the carbon was vapor-phase impregnated with I_2 at three different concentrations (nominally 2%, 4%, and 6% by weight). To test the Savannah River impregnation techniques, a commercial vendor also supplied samples of the same base carbon impregnated with the same concentrations of I_2.

Analyses of potassium and iodine contents of the I_2-impregnated, natural potassium carbons are shown in Table III with high temperature iodine penetration data. The I/K ratio vs. the logarithm of penetration is also plotted in Figure 2 along with the data from commercial carbons. A slightly better least squares correlation (0.963 vs. 0.952) was obtained when the function (I/K)/pH was plotted against the logarithm of penetration instead of I/K. This correlation indicates some dependancy on pH as shown in Figure 3.

The second phase of the study involved removal of soluble potassium from the base carbon, vapor-phase impregnation with a constant I_2 content (∿4%), and addition of potassium (as KOH) at various concentrations. In these experiments, two methods of K^+ removal were used: (1) repeated distilled water washes (in a soxhlet extractor); and (2) dilute H_3PO_4 leaching followed by repeated distilled water washes. In all cases, the reconstituted potassium samples showed a marked deviation from a straight logarithmic increase in penetration with increasing I/K ratios (or (I/K)/pH ratios). Samples washed with distilled water and impregnated with KOH showed consistently lower iodine penetration than commercial carbons or I_2-impregnated carbons at all (I/K)/pH ratios. The H_3PO_4-treated samples were about equivalent to natural K^+ samples at I/K ratios <1 [(I/K)/pH <0.1] and similar to water-washed samples at I/K ratios >1 [(I/K)/pH >0.1] (Figure 4). These experiments indicate that added potassium (as KOH) is more readily available for reaction than the natural potassium present in coconut carbon. The data also suggest a method for improving the high-temperature performance characteristics of noncoconut base carbons.

Table III   Chemical analysis of I_2-impregnated, natural-potassium carbons.

Carbon[a]	Potassium, wt %	Iodine, wt %	I/K	pH	$\frac{(I/K)}{pH}$	Penetration, %[b]
SRL-24V	1.57	2.59	0.507	10.28	0.049	0.018
SRL-25V	1.55	3.63	0.720	9.69	0.074	0.115
SRL-26V	1.40	5.45	1.203	9.50	0.127	0.339
SRL-24	1.64	1.53	0.287	9.68	0.030	0.015
SRL-25	1.52	2.67	0.541	9.30	0.058	0.057
SRL-26	1.44	5.52	1.181	8.05	0.147	0.755

a.   Arbitrary numbers: those followed by V's were vendor impregnated; the remainder were impregnated at Savannah River.

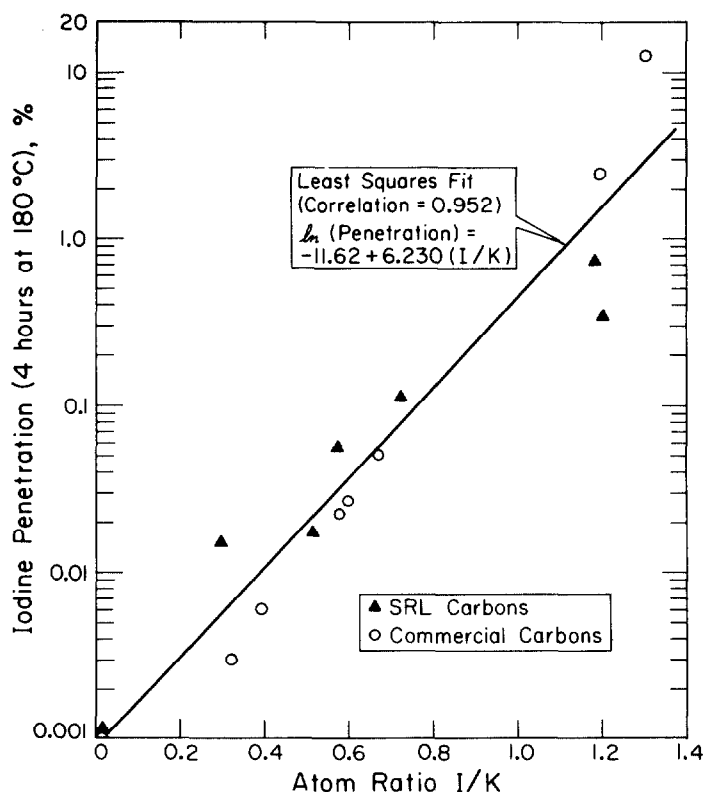b.   High-temperature desorption; see text for conditions.

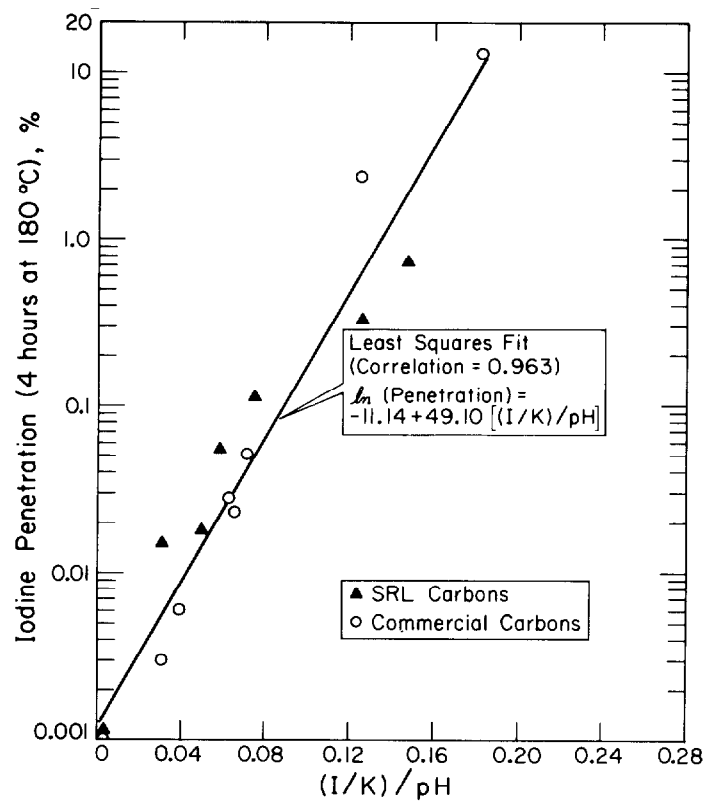Figure 2   I/K vs. Penetration for I_2-Impregnated Carbons with Natural Potassium

Figure 3   (I/K)/pH vs. Penetration for I_2-Impregnated
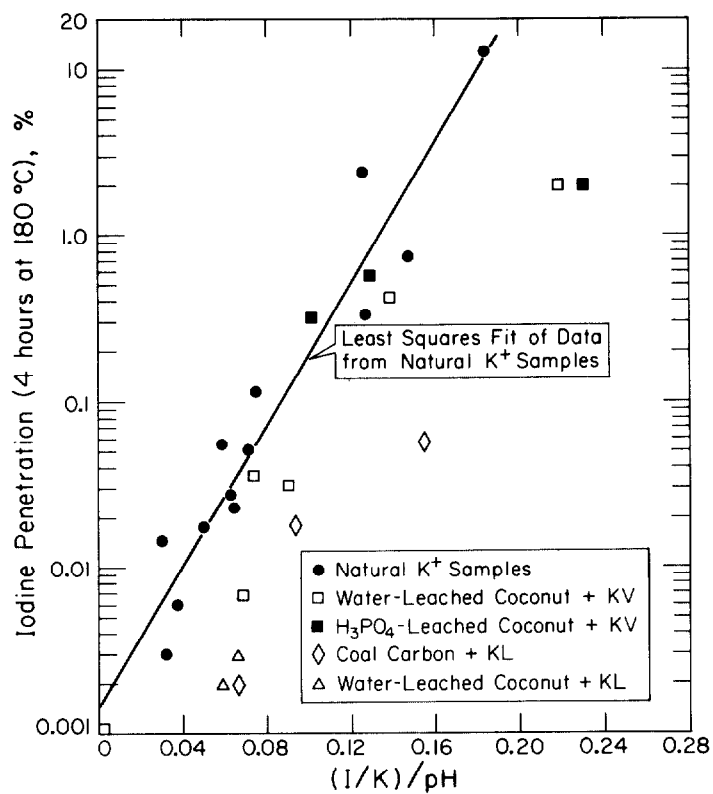   Carbons with Natural Potassium

Figure 4   (I/K)/pH vs. Penetration for All Carbons

The third set of experiments involved co-impregnation of K^+-free carbons (coconut and noncoconut) with K^+ and I^- using a KOH-I_2 solution. Two samples were also prepared using NaOH rather than KOH to determine whether K^+ is the preferred impregnant. In the first experiments, several batches of water-washed coconut carbon were combined (our soxhlet extractor has about a 200-g capacity for coconut carbon) and were blended, and the blend was divided into two portions. The first portion was vapor-phase impregnated with I_2 ($\sim$3.0%). One half of the iodine-impregnated carbon was then impregnated with $\sim$1.5% K^+ (as KOH) and designated KV for KOH + I_2 vapor. The other half was impregnated with $\sim$1.5% Na^+ (as NaOH) and designated NaV for NaOH + I_2 vapor. The second portion of the original blended sample was also divided into two samples. The first was impregnated with a solution of KOH-I_2 and designated KL for KOH + I_2 liquid. The second was impregnated with a solution of NaOH-I_2 and designated NaL for NaOH + I_2 liquid. The iodine/alkali metal ratio was chosen to approximately duplicate the (I/K)/pH ratio of one of the better commercial I_2-impregnated carbons. The (I/A) pH (where A = alkali metal) ratios are compared with high-temperature iodine penetration values in Table IV. The commercial carbon is also shown for comparison.

The data show that KOH-I_2 liquid impregnation produces a superior product (sample KL) when evaluated by the high-temperature desorption test.

To investigate the applicability of the impregnation technique to other carbon types, a sample of a commercial coal base carbon was obtained. This carbon had been screened to an 8 x 16 particle size distribution (the same

Table IV Iodine penetrations of selected coconut carbons.

Carbon	(I/K)/pH	(I/Na)/pH	Iodine Penetration, %[a]
KV[b]	0.069	--	0.007
NaV[b]	--	0.040	0.014
KL[b]	0.059	--	0.002
NaL[b]	--	0.052	0.041
Commercial	0.062	--	0.028

a. High-temperature desorption; see text for conditions.

b. See text for sample description.

particle size distribution as the coconut-base carbon). Both vapor-phase iodine impregnation followed by KOH impregnation and KOH-I_2 coimpregnation were used. The test data show that noncoconut carbons can be made into effective iodine adsorbers. Analytical and test data are shown in Table V; coconut carbon sample KL is shown for comparison.

Table V   KOH impregnated coal base carbon samples.

Sample	(I/K)/pH	Iodine Penetration, %[a]
Coal KV[b]	0.093	0.018
Coal KL-1[c]	0.066	0.003
Coal KL-2[d]	0.066	0.002
Coconut KL[e]	0.059	0.002

a. High-temperature desorption test; see text for conditions.

b. Vapor-phase iodine (~4%) + ~1.2% K (as KOH).

c. KOH-I_2 coimpregnation (2.8% I_2, 1.2% K by weight).

d. KOH-I_2 coimpregnation (4.4% I_2, 1.9% K by weight).

e. KOH-I_2 coimpregnation (2.2% I_2, 1.1% K by weight).

Other Tests of KOH-Impregnated Carbons

Impregnation of activated carbon with potassium salts lowers the ignition temperature of the carbon[10,11]. Thus, use of the KOH-I_2 impregnation technique involves balancing the iodine retention characteristics against the ignition characteristics of the carbon. Other factors to consider are the availability and cost of the base carbon and the physical properties of the base carbon that may limit its usefulness for air cleaning applications (specifically the hardness and resistance to attrition by a flowing air stream). Coconut carbon has long been used for air cleaning applications because its physical properties and iodine retention properties were satisfactory at a reasonable cost. Increasing worldwide demand for coconut carbon has caused significant price increases and accentuates the need to find alternative base materials suitable for nuclear applications.

Use of the KOH-I_2 impregnation technique may provide a means of improving the iodine retention properties of alternative base carbons to the extent that they perform as well as or better than coconut carbon. To this end, the coal base samples listed in Table V were tested for ignition temperature, and the better sample (Coal KL-1) was tested for iodine retention in an intense radiation field (the radiolytic desorption test[3]). Data are shown in Table VI along with comparable data for one of the better commercial coconut carbons.

Table VI Comparison of coconut and coal carbons.

Sample	(I/K)/pH	Ignition Temp., °C[a]	Thermal Iodine Desorption, %[b]	Radiolytic Iodine Desorption, %[c]
Coal (as received)	<.006	475	0.006	~0.3
Coal KL-1	0.066	330	0.003	0.020
Coal KL-2	0.066	310	0.002	--
Commercial Coconut Carbons	0.062	340[+]	0.028	0.016

a. As measured in a "standard" quartz apparatus at a heating rate of 5°C/min
and a superficial dry air velocity of 17 m/min (at 200°C).

b. Elemental iodine desorption in 4 hours at 180°C and <1% relative humidity.

c. Elemental iodine desorption in 5 hours at 180°C and ~95% relative humidity
and an adsorbed dose rate of 3×10^7 rad/hr.

The data show that the coal-base carbon has promise. Samples of this carbon
have been sent to other laboratories for CH_3I retention tests. Other base carbons
(wood, coal, and petroleum) have been requested from carbon vendors to further
evaluate the effectiveness of the impregnation technique.

Conclusions

Combining the thermal desorption test for elemental iodine retention by
activated carbon with neutron activation analysis of iodized carbons has led
to a better understanding of one of the basic reaction mechanisms for iodine
retention. Two essential components for high efficiency iodine retention
are excess potassium ion (atom ratio I/K <1.0) and a high pH for conversion
of I_2 to ionic iodine. Coconut-shell carbon, with its high natural K^+ content
and high pH, is the best natural base carbon for nuclear applications.

Preliminary test data show that impregnation of other base carbons with
a $KOH-I_2$ mixture can improve the high-temperature performance characteristics
of these carbons to the point that they are equal to or better than natural
coconut carbons impregnated with KI or $KI-I_2$. Additional studies, including
service-related effects, may lead to the development of domestic carbons which
perform better and cost less than imported coconut carbons.

References

1. W. S. Durant, R. C. Milham, D. R. Muhlbaier, and A. H. Peters. Activity Confinement System of the Savannah River Plant Reactors. USAEC Report DP-1071, E. I. du Pont de Nemours and Company, Savannah River Laboratory, Aiken, South Carolina (1966).

2. A. G. Evans and L. R. Jones. Confinement of Airborne Radioactivity - Progress Report: January 1971-June 1971. USAEC Report DP-1280, E. I. du Pont de Nemours and Company, Savannah River Laboratory, Aiken, South Carolina (1971).

3. A. G. Evans and L. R. Jones. Confinement of Airborne Radioactivity - Progress Report: July 1971-December 1971. USAEC Report DP-1298, E. I. du Pont de Nemours and Company, Savannah River Laboratory, Aiken, South Carolina (1972).

4. A. G. Evans, "Effect of Intense Gamma Radiation on Radioiodine Retention by Activated Carbon," Proceedings of the Twelfth Air Cleaning Conference, Oak Ridge, Tenn., August 28-31, 1972, CONF-720823, p. 401-414 (1973).

5. A. G. Evans. Confinement of Airborne Radioactivity - Progress Report: July 1972-December 1972. USAEC Report DP-1329, E. I. du Pont de Nemours and Company, Savannah River Laboratory, Aiken, South Carolina (1973).

6. R. E. Adams, R. D. Ackley, and R. P. Shields. "Application of Impregnated Charcoals for Removing Radioiodine from Flowing Air at High Relative Humidity." Treatment of Airborne Radioactive Wastes, Proceedings of a Symposium, New York, August 26-30, 1968, IAEA, Vienna (1968), p 398.

7. A. G. Evans. Confinement of Airborne Radioactivity - Progress Report January 1973-June 1973. USAEC Report DP-1340, E. I. du Pont de Nemours and Company, Savannah River Laboratory, Aiken, South Carolina (1973).

8. A. G. Evans and L. R. Jones. Confinement of Airborne Radioactivity - Progress Report: July 1973-December 1973. USAEC Report DP-1355, E. I. du Pont de Nemours and Company, Savannah River Laboratory, Aiken, South Carolina (1974).

9. L. R. Jones. "High Efficiency Particulate Air (HEPA) Filter Performance Following Service and Radiation Exposure." Paper presented at the Thirteenth Air Cleaning Conference, San Francisco, Calif. August 12-15, 1974 (1974).

10. J. Taylor and F. Pollok. "Effect of Various Chemicals, More Especially Sodium Bicarbonate, on the Ignition of Allulose, Coal Dust and Activated Charcoal." Fuel XXVIII, pp 77-87, Butterworths, London (1949).

11. J. L. Kovach and J. E. Green. "Evaluation of the Ignition Temperature of Activated Charcoals in Dry Air." Nucl. Safety 8, (1966).

DISCUSSION

DEITZ: To supplement the chemical analysis data in
Table 1 of Evans' paper, reference can be made to results in the
forthcoming report "Survey of Domestic Charcoals for Iodine Reten-
tion" by Deitz and Burchsted. The following table*summarizes anal-
ytical results for K and pH in four categories of charcoals. In
addition, when the absolute value of K is large, the ratio K/Na
> 1; when K is small, the same ratio < 1.

WILHELM: Did you measure the iodine removal efficiency
in air of higher relative humidity after impregnation with potass-
ium hydroxide? It may be that the charcoal will adsorb more water
because of the presence of a hygroscopic compound.

EVANS: The thermal desorption test used in most of
these experiments is run at low relative humidity (1%). We did,
however, test some of the KOH-impregnated carbons for radiolytic
desorption at high humidity (>95%) without any indication of
excessive moisture pickup by the carbon.

WILHELM: Did you measure the iodine removal efficiency
in air of higher relative humidity after impregnation with potass-
ium hydroxide? It may be that charcoal will adsorb more water
because of the presence of a hygroscopic compound.

EVANS: The principal test mentioned in this paper is
the thermal desorption test which is run at less than 1% relative
humidity. We have, however, run radiolytic desorption tests
(at >90% relative humidity) on some of the KOH impregnated carbons,
and found no moisture pickup problems. That is, no bed flooding
occurred which would indicate excessive moisture pickup. The amount
of KOH added to the low potassium carbons does not exceed the
natural potassium content of coconut carbons, so I wouldn't expect
any dramatic effects due to potassium addition.

DEITZ: Mr. Burchsted and I are making a survey of a
number of charcoals having different base materials, and here is
a summary of what is available. The coconut charcoals run about
1 percent potassium. The petroleum based charcoals are quite low.
Coal based charcoals can be anywhere from 1 to 1000 parts per
million, and some wood based charcoals are quite low. Where
potassium is high, the potassium - sodium ratio is very large;
where the potassium is small, the potassium - sodium ratio is very
small. These, and other results will be included in a survey report
that will be issued shortly.

*Table on p. 75·

Potassium and pH of Charcoals

Coal Base

	K ppm	pH
4008	790	8.4
4009	64	7.1
4012	900	8.3
4013	860	8.2

Wood Base

	K ppm	pH
4018	70	2.7
4019	110	2.8

Coconut Base

	K ppm	pH
4010	12900	9.6
4011	10800	9.7
4024	10700	9.6
4027	11400	9.8

Petroleum Base

	K ppm	pH
4006	15	9.0
4007	50	9.3

SOLID ADSORBENTS FOR COLLECTION AND STORAGE OF IODINE-129 FROM REPROCESSING PLANTS[*]

D. T. Pence and B. A. Staples
Allied Chemical Corporation
Idaho Chemical Programs - Operations Office
National Reactor Testing Station
Idaho Falls, Idaho 83401

Abstract

Because of the long half-life and relatively large quantities produced during fission of nuclear fuels, ^{129}I will have to be recovered and stored indefinitely to prevent undue radiation exposure to the local population around nuclear fuel reprocessing facilities. Although release limits have not been specified for reprocessing plants, an interim design objective of at least a 10^6 reduction is suggested. Methods proposed for collection of ^{129}I from reprocessing plant effluents include wet scrubbing and the use of solid adsorbents. The relative merits for the use of solid adsorbents for collection and long-term storage of iodine are discussed.

I. Introduction

Iodine-129 is produced by both natural and man-made sources. Natural production of ^{129}I is principally from spontaneous fission of uranium and cosmic-ray interaction with atmospheric xenon. Although the annual world-wide generation rate is quite low, ~10 mg/yr, the estimated pre-1940 inventory was about 2×10^5 g because of its long half-life, 1.6×10^7 yr.[1] The comparable global inventory of total iodine is estimated to be about 8×10^{16} g, giving a ratio of natural ^{129}I to total iodine of about 2×10^{-12}.

Recently in a USAEC Regulatory Guide[2], the design objective for the maximum annual dose or dose commitment to the thyroid of an individual in an unrestricted area from all pathways of exposure, as determined for ^{131}I from light water-cooled nuclear power reactors, was established to be 15 mrem. Using a procedure described by Russell and Hahn[3], the calculated quantity of ^{129}I required to yield a human thyroid dose of 15 mrem/yr was determined to be about 2 µg. Because the biological half-life of iodine in a human thyroid is about 100 days, an additional amount of ^{129}I has to be replaced to maintain a constant dose rate in the thyroid. The ratio of ^{129}I to total iodine, R_t (using the notation of Russell and Hahn[3]), to maintain the 15 mrem/yr dose for a normal human thyroid was calculated to be about 2.5×10^{-4}, or 0.025 percent ^{129}I of the total iodine.

Magno et al reported observing an average R_t of 6×10^{-4} in the environment near the perimeter of a commercial nuclear fuel reprocessing plant.[4] Brauer et al measured R_t quantities as high as 9.3×10^{-4} in grass samples collected near a nuclear fuel reprocessing plant.[5] Airborne gaseous and particulate materials showed R_t values of about 5×10^{-5} in the environment in the vicinity of the reprocessing facility. Fortunately, these values do not represent those in the thyroids of individuals working at or near these facilities. Brauer et al have calculated the maximum thyroid radiation doses received by residents near the processing facility to be about 0.4 mrem/yr and about 0.2 mrem/yr to the average adult.

The average ^{129}I unabated output of a single 5-tonne/d nuclear fuel reprocessing plant is estimated to be about 3.8×10^5 g/yr, more than the estimated pre-1940 global inventory of this isotope. Estimated requirements for the number of 5-tonne/d reprocessing plants in the United States are 4 in 1985, 7 by 1990, 18 by 2000, and 53 by 2020.[6] Considering these projections, the observed build-up of ^{129}I near nuclear fuel reprocessing plants, and the extremely long half-life of ^{129}I, it is clear why the collection and long-term storage of ^{129}I is a major concern of the Atomic Energy Commission.

The purpose of this paper is to briefly compare proposed methods for collection and containment of ^{129}I and to describe a recently funded program by the Atomic Energy Commission for Allied Chemical Corporation to evaluate solid adsorbents for the collection and long-term storage of ^{129}I.

II. Requirements

The overall iodine removal requirements for a nuclear fuel reprocessing plant depend to a large extent on the length of time between the discharge of the spent fuel from the reactor to reprocessing. Decontamination factors (DFs) of 10^8 to 10^{10} will probably be required for anticipated processing of 30-d cooled LMFBR fuel. For contemporary fuels, DFs of about 10^3 to 10^4 will probably be sufficient to reduce airborne levels low enough to attain the design objectives for ^{131}I exposure for 150-day and longer cooled fuels.

The long half-life of ^{129}I puts special requirements on the collection and long-term storage of this isotope. An acceptable DF for ^{129}I at a particular reprocessing plant is very difficult to establish because there are so many variables involved. In order to establish a practical target value until the problem is better understood, the following simplistic approach has been taken. Based on an average airborne gaseous concentration of total iodine measured by Brauer et al[5] of about 1×10^{-8} g/m^3 (corrected for the estimated 50 percent collection efficiency) and the calculated R_t value of 2.5×10^{-4}, the maximum allowable airborne concentration of ^{129}I should not exceed 2.5×10^{-12} g/m^3 (for the general population) to attain the design objectives suggested for radioiodine from power reactors. Assuming all of the fission product ^{129}I processed in a hypothetical 5-tonne/d reprocessing plant is released as gaseous iodine (250 g ^{129}I/tonne) and a 3000 m^3/min (106,000 ft^3/min) stack flow, the airborne concentration of ^{129}I at stack discharge would be about 3×10^{-4} g/m^3. Allowing a conservative diffusion factor of 10^5 to a point at the site boundary along the direction of the prevailing winds, the airborne concentration of ^{129}I would be 3×10^{-9} g/m^3. Therefore, a DF on the order of 10^3 would be required to meet the design objectives for the instantaneous concentration of ^{129}I.

Because this hypothetical plant discharges 4×10^6 m^3/d (1.4×10^8 ft^3/d) and will probably do so for approximately 40 years, considerable buildup of ^{129}I will occur; therefore, a plant DF much greater than 10^3 is required. On the other hand, there is a very large reservoir of stable iodine in the biosphere that will dilute the discharged ^{129}I, reducing its potential radiological effects on the human thyroid. Nevertheless, because of the irreversibility of the situation, a design objective of a DF in the range of 10^6 to 10^7 for ^{129}I discharged from a typical 5 tonne/d nuclear fuel reprocessing plant would seem prudent, at least until the problem can be better defined.

III. Wet Scrubbing Methods

Recently, there have been a number of reviews on the treatment of reprocessing plant effluents which included discussions on iodine removal systems.[6,7,8,9,10] Iodine removal requirements have, generally, been classified into primary, secondary, and final cleanup systems. The primary iodine removal systems are designed to remove the iodine from the dissolver off-gases. The secondary systems are generally designed to provide additional iodine removal from the dissolver off-gas and iodine removal from the vessel off-gas and other equipment vents. The final cleanup system provides additional removal after the primary and secondary systems.

Several wet scrubbing processes have been proposed for the primary removal system in which the major portion of the 300 g/tonne of spent fuel, about 20 percent of which is stable iodine, will be removed.[11] These processes employ either a mercuric nitrate-nitric acid or a highly concentrated nitric acid, ~ 20 $\underline{M}$, scrubbing solution. The mercuric nitrate-nitric acid method is the most attractive at the present because its development is further along. Elemental and alkyl iodides are readily complexed by the mercury, but the aromatic iodides are more elusive.[10] The scrubbing solution is periodically taken to a concentrator-evaporator where the iodine is precipitated as $Hg(IO_3)_2$. The supernatant liquid is removed prior to permanent storage of the $Hg(IO_3)_2$.

The highly concentrated nitric acid wet scrubbing technique, known as the Iodox process[12], is receiving considerable development effort at ORNL in connection with the LMFBR fuels reprocessing development program. The process uses packed and/or bubble-cap columns with a counter-current flow of 18 to 20 $\underline{M}$ nitric acid. The process appears to be satisfactory for the removal of all organic iodides, as well as elemental iodine. The present design[12] calls for the removal of iodine from the scrub solution in an evaporator where the iodine precipitates from the nitric acid as HIO_3, which can be converted further to a more anhydrous form for long-term storage.

As was noted by Yarbro et al, there is little incentive for designing primary iodine removal system with DFs greater than about 10^3 for "closed-cycle" processing plants designed for processing short-cooled fuels because of the high by-pass rates of ^{131}I.[9] Even for 30-day cooled fuels, the mass of ^{131}I only represents about 0.3 percent of the total iodine; therefore, from a waste management point of view, a DF greater than 10^3 would be desirable to remove as much ^{129}I as is practicable. However, large-scale systems may be impracticable due to increased design complexities required for the reduced flow rates of wet scrubbing methods that may be necessary to attain DFs greater than about 10^3. Based on laboratory tests, both the mercuric nitrate-nitric acid and the Iodox process appear to have the capability of attaining DFs of about 10^4.

Both wet scrubbing techniques and solid adsorbents have been proposed for secondary iodine removal systems. Alkaline solutions have been shown to contain some of the iodine but tend to promote the formation of species of iodine that are more difficult to remove. The mercuric nitrate-nitric acid wet scrubbing method has also been proposed for secondary iodine removal systems. The airborne concentration of iodine in the dissolver off-gas could be as high as about 50 mg/m^3, so a primary system DF of 10^3 would give a secondary iodine removal system input of ~ 50 µg/m^3. DFs of greater than 10^3 were shown in an 8-stage simulated bubble-cap laboratory apparatus using the mercuric nitrate-nitric acid wet scrub method and an initial airborne elemental iodine concentration of ~ 500 µg/m^3.[13] Data on alkaline scrubbing methods at low iodine concentrations were not found.

Most proposed final cleanup system designs employ solid adsorbents.

IV. Solid Adsorbents

A number of inorganic adsorbents have been proposed for use in radioiodine removal systems for nuclear fuel reprocessing plants. Some of the materials proposed include: silver and other metal-exchanged zeolites[14,15]; silver impregnated, amorphous silicic acid[16,17]; and silver and other metal cation impregnated alumina, and aluminum and silicon oxides[15]. Generally, impregnated carbons are not considered for treatment of reprocessing plant effluents because of the possible violent reaction of the activated carbon with NO_2 present in the off gas.

Solid, inorganic adsorbents offer several major advantages compared with the proposed wet scrubbing methods; solid adsorbents (1) allow a simpler design, (2) are comparatively noncorrosive, and (3) are in a form that does not require further treatment prior to long-term storage. In addition, the use of solid adsorbents allows relatively compact installations that are readily adaptable for remote operation. Because there could be few moving parts in the design, long reliable maintenance-free operation would be expected.

For primary removal systems, assuming a 5-tonne/d plant, the estimated characteristics and costs are shown in Table I. To obtain 15% utilization of the adsorbent, heating of the inlet off-gas stream and a special adsorbent bed design may be needed. Such a design would cause the second 5 cm (2 in.) of the adsorbent bed to be the first 5 cm (2 in.) of a new bed, when the original first 5 cm (2 in.) of the bed become loaded with iodine. This efficient use of the adsorbent material would also be desirable with regard to waste management of ^{129}I. Less than 0.02 m^3 (0.7 ft^3) per day of ^{129}I-containing adsorbent would be accumulated if 15% utilization of the adsorbent could be obtained.

Table I   Estimated characteristics for solid adsorbent iodine removal systems.

	Primary	Secondary[a]
Flow Rate - acmm (acfm)	18.4 (650)	142 (5,000)
Surface Area of Bed - m^2(ft^2)	1.2 (13)	9.3 (100)
Bed Depth - cm(in.)	10 (4)	5 (2)
DF	10^3	10^3
Estimated Lifetime Before Changeout (d)	6.5	300 - 600
Estimated Efficiency for Adsorbent Utilization Before Breakthrough (%)	15	10
Cost per day for Adsorbent ($)	300	36
Annual Adsorbent Cost ($)	90,000	10,800

[a] Costs are based on 300-d changeout.

Also presented in Table I are the characteristics and estimated costs for a secondary iodine removal system. The anticipated lifetime of the secondary bed is not well defined at this point. Unlike the primary system, the loss of efficiency due to poisoning from contaminant gases in the off-gas stream is expected years before the bed would become overloaded with iodine. The lifetime of the solid adsorbents in a secondary system should be at least one to two years before an

appreciable loss in efficiency occurs. The design and operation of a final cleanup system would be similar to the secondary system except the adsorbent lifetime would probably be longer.

Processing of the iodine-laden adsorbent from the primary system to obtain a more concentrated form would not appear to be necessary or desirable. The anticipated annual yearly accumulated adsorbent inventory from the primary system is about 5.7 m^3 (200 ft^3). This value will increase when fuels of greater burnup are processed and more fission product iodine is produced. The product should be ideally suited for long-term storage, provided excess NO_2 and moisture are purged from the adsorbent prior to packaging. Because the decay energy of ^{129}I is so low, a negligible amount of decay heat will be generated.

Because of the long-term storage requirements and the relatively small quantities of ^{129}I collected by an adsorbent bed before changeout in the secondary removal system, processing and reconcentration of the ^{129}I would be appropriate. The process will depend on the type of adsorbent and impregnants used. If silver were used as the active cation, its high cost would probably dictate recovery for reuse. The cost of processing the adsorbent will depend largely on the degree of contamination of other fission products that may collect on the adsorbent beds.

V. Conclusions

The cost of chemicals to remove iodine in a primary iodine removal system in a nuclear fuel reprocessing plant off-gas stream appear to be three to five times less for the mercuric nitrate-nitric acid method than for solid adsorbents. No information was available to attempt a cost comparison with the Iodox process. When the equipment installation, day-to-day operational and maintenance, and storage preparation costs are included, it is likely that use of solid adsorbents will be less than the mercuric nitrate-nitric acid method, because the chemicals will probably represent a minor fraction of the overall costs. At this point, however, any definite statements claiming large savings possible by the use of one method over another is premature. Neither the operational costs nor the absolute removal efficiencies of a pilot-plant-scale model of any of the methods using simulated reprocessing plant off-gas streams have been accurately determined.

For a secondary iodine removal system, the increased flow requirements would appear to make the use of solid adsorbents more attractive because of the increased size and complexity of the wet scrubbing methods. As with the proposed primary removal systems, high efficiency, long-term removal of all airborne species from anticipated contaminant gases in vessel off-gas streams has not been demonstrated with any of the methods.

Because there is little doubt concerning the need for highly efficient iodine removal systems in nuclear fuel reprocessing plants, the most economical and efficient designs should be identified and operational characteristics determined so they can be incorporated in present and future plants. The Atomic Energy Commission is supporting several programs to accomplish this. As part of this program, the work at the Idaho Chemical Processing Plant will be to develop iodine solid adsorbents, to evaluate others that are available, and to demonstrate the applicability of the most promising materials in the reprocessing facility.

VI. References

1. R. R. Edwards and P. Rey, <u>Terrestrial Occurrence and Distribution of Iodine-129</u>, NYO-3624-3 (1969).

2. U. S. Atomic Energy Commission, <u>Interim Licensing Policy on As Low As Practicable for Gaseous Radioiodine Releases from Light-Water-Cooled Nuclear Power Reactors</u>, Regulatory Guide 1.42, Revision 1 (March 1974).

3. J. L. Russell and P. B. Hahn, Radiol. Health and Data Rpt. <u>12</u>, 189 (April 1971).

4. P. J. Magno, T. C. Reavey, and J. C. Apidianakis, U. S. Environmental Protection Agency, <u>Iodine-129 in the Environment Around a Nuclear Fuel Reprocessing Plant</u> (October 1972).

5. F. P. Brauer, J. K. Soldat, H. Tenny, and R. S. Strebin, Jr., <u>Natural Iodine and Iodine-129 in Mammalian Thyroids and Environmental Samples Taken from Locations in the United States</u>, BNWL-SA-4694 (August 1973).

6. U. S. Environmental Protection Agency, <u>Environmental Analysis of the Uranium Fuel Cycle, Part III-Nuclear Fuel Reprocessing</u> (October 1973).

7. J. L. Russell and F. L. Galpin, "A Review of Measured and Estimated Offsite Doses at Fuel Reprocessing Plants", IAEA Symposium on the Management of Radioactive Wastes from Fuel Reprocessing Plants, Paris, France (27 November-1 December 1972).

8. E. D. North and R. L. Booth, <u>Fission Product Gas Retention Study Final Report</u>, ORNL-TM-4409 (August 1973).

9. O. O. Yarbro, F. E. Harrington, and D. S. Joy, <u>Effluent Control in Fuel Reprocessing Plants</u>, ORNL-TM-3899 (March 1974).

10. E. W. Murback, W. H. Carr, and J. H. Gray III, <u>Fission Product Gas Retention Process and Equipment Design Study</u>, ORNL-TM-4560 (May 1974).

11. D. J. Crouse and J. M. Schmitt, Trans. Amer. Nucl. Soc., <u>17</u>, 319 (1973).

12. W. E. Unger, J. C. Mailen, A. R. Irvine, and C. D. Watson, <u>Aqueous Fuel Reprocessing Quarterly Report for Period Ending September 30, 1973</u>, ORNL-TM-4394 (February 1974).

13. W. E. Unger, D. E. Blanco, D. J. Crouse, A. R. Irvine, and C. D. Watson, <u>Aqueous Fuel Reprocessing Quarterly Report for Period Ending June 30, 1973</u>, ORNL-TM-4301 (August 1973).

14. D. T. Pence, F. D. Duce, W. J. Maeck, <u>Metal Zeolites Iodine Adsorption Studies (Project Report January 1 - December 31, 1970)</u>, IN-1455 (June 1971).

15. R. D. Ackley and Z. Combs, <u>Applicability of Inorganic Sorbents for Trapping Radioiodine from LMFBR Fuel Reprocessing Off-Gas</u>, ORNL-TM-4227 (May 1973).

16. J. G. Wilhelm and H. Schuettelkopf, <u>Proceedings of the 11th AEC Air Cleaning Conference</u>, CONF 700816, p 568 (December 1970).

17. J. G. Wilhelm, <u>Commission of the European Communities Seminar on Iodine Filter Testing</u>, p 1, Karlsruhe, W. Germany (December 4-6, 1973).

DISCUSSION

<u>DEMPSEY</u>:   Just a comment; I infer from what you said that, from a waste management point of view it seems like these liquid scrubbing techniques just defer the problem because the material is releasable again in other steps in the reprocessing plant.

<u>PENCE</u>:   There is an additional statistic I could include: for a 5 ton/d reprocessing plant in which 15 percent efficiency is obtained for the adsorbent, the waste storage requirements would be about 0.7 cubic feet a day for the primary iodine removal system. That's not very much. It's in a fairly concentrated form that is ready for long-term storage.

<u>DEITZ</u>:   If 131-iodine emission greatly exceeds 129-iodine, is it possible that there is an isotopic exchange on the adsorber, and one does not realize the 129 iodine removal that is hoped for?

<u>PENCE</u>:   For short-cooled fuels, the I-131 will present a removal problem because of the large number of curies involved. For 30-day cooled fuels, the quantity of iodine 131 is quite small, on the order of less than 3 hundredths %, I believe. The primary clean-up systems should provide large enough DF's for the I-131 from the longer cooled fuels. But, as Yarbro pointed out, the primary system will not be as effective for iodine 131 from shorter cooled fuels. There is enough bypass around the primary system that the secondary and final clean-up systems are needed to clean up iodine 131. Therefore, the small quantities of iodine remaining should not present any problems in the secondary or final cleanup systems with regard to isotope exchange.

TESTING AND EVALUATION OF ABSORBERS
FOR GASEOUS PENETRATIVE FORMS OF RADIOIODINE

M.J. Kabat
Ontario Hydro
Central Health Physics Services
Pickering Generating Station
Box 175
Pickering, Ontario, Canada

Abstract

A significant fraction of airborne radioiodine, encountered at times in operational areas of Ontario Hydro nuclear power generating stations, was found to be penetrative inorganic and organic species.

Theoretical evaluation of iodine chemistry is presented in this paper based on analysis of operational iodine concentrations in station systems, areas and effluents under actual operating conditions. The theoretical evaluation and the operational experiments show that hypoiodous acid and organic iodides are the basic forms of airborne iodine which occur in the field and in station effluents.

A method was developed for laboratory generation of HOI and its identity confirmed by use of specific absorbers.

Six of the commercially available (and recently developed) absorbers were tested for HOI removal efficiency in the laboratory under conditions similar to those found in the field. Experimental equipment, methods used for the absorber testing and experimental conditions are described. It is evident from results of these measurements that charcoals have generally better initial absorption efficiency for hypoiodous acid than silver impregnated inorganic absorbers.

Both technical and economical aspects of the operational use of the tested absorbers are discussed in this paper.

1.0 Introduction

"On-power refuelling", which is performed on a routine basis, is one of the characteristic features of the CANDU system. Fuel performance is generally excellent but occasional fuel failures occur and volatile fission products are released from the fuel. These may escape from the heat transport or spent fuel handling system and migrate through ventilated areas into station gaseous effluents.

Investigations have been carried out in Ontario Hydro to improve control of airborne radioiodines under such circumstances. Theoretical analysis and experiments were made to evaluate operational concentrations and chemical forms of iodine in the station systems, areas and effluents. As a result of these investigations it was determined that iodine is present in ventilated areas in very low concentrations ($<<1\mu g/m^3$ of air) as HOI and organic iodides.

Two methods are employed to reduce the airborne iodine concentrations:

1. Control of iodine volatility and
2. Airborne iodine removal from the station gaseous effluents.

The main concern of this work was to evaluate the removal efficiency of existing absorbers for airborne radioiodine under real operating conditions.

Many reports are available quoting absorption efficiencies based on testing with CH_3I within a wide range of experimental conditions but no conclusive tests on HOI absorption were published.

Our theoretical and experimental investigation on iodine chemistry and testing of absorbers for HOI absorption efficiency are described. The results in this paper are related to the practical use of the absorbers.

2.0 Operational Concentrations of Fission Product Iodine

The origin of the various radioiodines and their subsequent migration from fuel → heat transport system → spent fuel transfer system → spent fuel storage → gaseous effluents was described in reference [1].

A brief review is presented in the next sections and the latest information included.

2.1 Iodine Isotopes in CANDU Reactor Fuel

Seven iodine isotopes ($T_{1/2} > 1$ min.) are generated in the fuel, mostly as products of Te decay. Only three of them (isotopes 131, 133 and 135) are radio-biologically significant and another two (127 and 129) are accumulated in higher concentrations than ^{131}I in fuel which has been at power for several months.

For the purposes of the following calculations, it is assumed that:

- Iodine isotopes are considered as direct products of ^{235}U fission.
- ^{129}I is considered as a stable isotope.
- No further neutron activation of the iodine isotopes takes place in the reactor.
- No release of iodines from the fuel occurs during its irradiation.
- The fuel bundle is located in the maximum neutron flux zone throughout all of its irradiation period.

The iodine generation rate - R(g x hr^{-1} x kg^{-1} uo_2) is calculated from:

$$R = \frac{C \times Y \times P \times M \times 3600}{Av \times 100}$$

(Eq. 1)

G, the equilibrium amount of iodine isotope in g x $kg^{-1}uo_2$, is derived from:

$$G = \frac{R}{\lambda}$$

(Eq. 2)

Where: C = 3.1 x 10^{10} (fissions x sec^{-1} x $Watt^{-1}$)
Y = fission yield of iodine isotope (%)
M = mass number of iodine isotope
λ = decay constant (hr^{-1})
P = specific power (= 30 kW/kg uo_2)
Av = Avogadro's number

The amount of the various iodines generated in Pickering G.S. fuel is shown in Table 1.

TABLE 1
Amounts of Iodine Isotopes in Candu Fuel

Isotope	^{127}I	^{129}I	^{131}I	^{133}I
Generation Rate R (g x hr^{-1} x kg$^{-1}_{UO_2}$)	9.7×10^{-7}	7.2×10^{-6}	2.1×10^{-5}	4.9×10^{-5}
Amount of I accumulated in the fuel after:				
1 week	1.6×10^{-4}	1.2×10^{-3}	2.6×10^{-3}	1.5×10^{-3}
1 month	6.4×10^{-4}	4.8×10^{-3}	5.8×10^{-3}	1.5×10^{-3}
6 months	3.9×10^{-3}	2.9×10^{-2}	5.9×10^{-3}	1.5×10^{-3}
12 months	7.8×10^{-3}	5.8×10^{-2}	5.9×10^{-3}	1.5×10^{-3}
(g x kg$^{-1}_{UO_2}$)				

2.2 Escape of Iodines from the Fuel into the Primary Heat Transport System

To determine the equilibrium concentrations of radioiodines in the heat transport system, it is assumed pessimistically that there are 100 fuel bundles present in the core, each of which contains 2 seriously defected elements continuously releasing 10% of their generated iodines.

The total weight of UO_2 in 200 elements = 169.2 kg. If we assume that the decay half-life of ^{131}I is longer than its diffusion time through the element then the release rates of iodines are proportional to their generation rates given in Table 1 under continuous release conditions. Their equilibrium concentrations in the heat transport D_2O are as given in Table 2.

Table 2 also shows that in the case of continuous iodine release from defective fuel elements the equilibrium concentration of $^{127}I + ^{129}I$ in the HT-D_2O is lower than the ^{131}I concentration. However if the fuel defect occurs after 12 months of full power operation, the initial ratio $(^{127}I + ^{129}I)/^{131}I$ can be derived from Table 1 to be as high as 10.

TABLE 2
Amounts of Iodine Isotopes in the Heat Transport D_2O

Isotope	^{131}I	^{129}I	^{127}I
Escape Rate (g x hr^{-1})	3.6×10^{-4}	1.2×10^{-4}	1.6×10^{-5}
Equilibrium Mass (g) $^{(+)}$	1.3×10^{-3}	4.4×10^{-4}	5.9×10^{-5}
Concentration in D_2O $^{(+)}$ (g x ℓ^{-1})	7.4×10^{-9}	2.5×10^{-9}	3.4×10^{-10}
Concentration in D_2O $^{(+)}$ (Molar)	6×10^{-11}	2×10^{-11}	3×10^{-12}

(+) Heat transport purification half-life = 2.5 hours, total amount of D_2O in the HT system = 175 Mg.

2.3 Release of Iodines into the Spent Fuel Transfer System

Fuel bundles discharged from the reactor pass through fuelling machines into spent fuel magazines and from these into an elevator mechanism in the spent fuel transfer room. They are exposed to an air atmosphere at this stage but pass quickly into water and are transferred by a shuttle mechanism into the spent fuel bay. Defective fuel elements may release a significant amount of volatile fission products when exposed to air in the elevator mechanism.

Iodine concentrations in the spent fuel transfer room were calculated using the following conservative assumptions:

- 8 seriously defected elements are discharged in 1 day
- 2% of the total iodine inventory is released from the element during this period
- The fuel transfer elevator chamber releases its inventory of iodines into the fuel transfer room, which is partially ventilated.

Under these conditions a total of 100 Ci of ^{131}I released in the spent fuel transfer room (= 30 mCi/m^3 = 3 x 10^6 MPCa) represents 3 μg of iodines/m^3 of air.

2.4 Iodine Concentration in Spent Fuel Bay Water

One hundred (100) μCi/ℓ was the highest ever identified concentration of ^{131}I in the spent fuel bay water. If the concentration of stable iodines was 10 times the ^{131}I concentration, the total iodine concentration in the bay water was = 8 x 10^{-9} g/ℓ = 3 x 10^{-11} M. About 100 times lower iodine concentrations are present in the bay water after discharging of a single defective fuel element.

2.5 Iodine Concentration in Stack Effluent

Iodine concentrations in the stack effluent were calculated from the gaseous release restrictions for Pickering G.S. under the following conditions:

- Station maximum permissible release limit for ^{131}I = 400 mCi/week/5 vent. units.

- The lowest ventilation flow rate = 185 m^3/min/unit.

- Iodine removal efficiency in the ventilation filters = 99%

- Concentration of (^{127}I + ^{129}I): ^{131}I = 10:1.

  The resulting airborne iodine concentrations:

- in the stack effluent <4 x 10^{-12} g/m^3

- at the ventilation filters inlet <4 x 10^{-10} g/m^3.

3.0 Chemistry of Iodine in Operational Systems

The chemistry of very low iodine concentrations, occurring in the systems under high temperature and/or high radiation conditions, is not a problem which can be solved entirely by way of operational research in the field. Nevertheless, some fundamental investigations were made by the Health Physics Department of Ontario Hydro in order to assure satisfactory control of airborne radioiodines in station areas and in gaseous effluents.

A discussion of results of the theoretical considerations and experimental studies follows.

3.1 Iodines in the Primary Heat Transport System

It is possible that small amounts of an organic binder are left in the UO_2 from the fuel manufacturing process. However there is little probability of organic iodines being present in the fuel during irradiation considering that operating temperature in the fuel elements reaches 2000°C. Therefore we would expect that the major portion of iodines released from the defective fuel into heat transport D_2O is in the gaseous, elemental form.

The operational parameters of the heat transport D_2O are as follows:

temperature   — 250-295°C
pressure   — 8.8 x 10^3 kPa
pH   — 10.3 (LiOH)
D_2 concentration — 15 ml/kg D_2O (average)

The reaction of gaseous iodine with D_2 is just exothermic [2] but its equilibrium is affected by the alkaline conditions. This reaction can be still more complicated by radiolytic products in the heat transport D_2O. In the final stage a major portion of dissolved iodine will be present as LiI. Besides a significant retention of iodine on internal surfaces and corrosion products is assumed in the primary heat transport system. If there is organic iodine released from defective fuel into the HT-D_2O it reacts with hydroxide ions by a nucleophilic displacement mechanism.

R.I + LiOH → R.OH + LiI
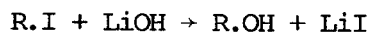
The rate constants for this reaction are [3] .

6.4 x 10^{-5} (ℓ x mol^{-1} x sec^{-1}) at 25°C, or
0.55   (ℓ x mol^{-1} x sec^{-1}) at 120°C

which show this reaction is very fast under heat transport operational conditions.

Escape of D_2O in liquid form from the heat transport system does not cause a significant airborne hazard because there is a minimum transfer of iodine from alkaline solutions of iodide into gaseous forms. This was proven experimentally when significant amounts of noble gas isotopes were escaping into the reactor building atmosphere from the primary heat transport system through a defective gasket in the bleed condenser. A negligible amount of radioiodine was detected in air samples, taken at this time in the reactor building.

If D_2O is leaking as steam, LiI appears in the airborne particulate form, which presents the same hazard as elemental radioiodine when inhaled.

3.2 Iodines in the Fuel Transfer System

High levels of radioiodines have been experienced in the spent fuel transfer elevator chamber, as calculated in part 2.3 of this paper. The airborne iodine migrates from the elevator chamber into the transfer room where it changes almost completely to organic iodides within a few days. There are two mechanisms involved in this reaction:

1. ### Reaction of I_2 with Airborne Methane

   Several authors have studied the reaction of I_2 with methane. A reaction with velocity constant of the order of 10^{-1} sec^{-1} at normal temperature has been reported [4]. According to some of the reports, the yield of CH_3I depends on the $CH_4:I_2$ ratio and radiation intensity. Up to 50% conversion was attained in a high radiation field with a $CH_4:I_2$ ratio of 500 [5].

   Under the assumptions that 1 PPM of CH_4 and 3 μg I_2/m^3 are present in the transfer room air (see 2.3), the volumetric ratio of $CH_4:I_2$ is 2000. The gamma radiation field in the transfer room is in the order of $10^4- 10^5$ R/hr during a refuelling process. It is likely, therefore, that significant amounts of CH_3I is formed by the reaction of iodine with CH_4 in the spent fuel transfer room air.

2. ### Reaction of I_2 with Organic Paints

   Bennet et.al. [6] concluded that methyl iodide and other organic species of iodine are formed when elemental iodine is exposed to paints and other organic films on vessel surfaces. Most surfaces in the transfer rooms are protected by organic paints and high sorption of radioiodine at the surfaces has been identified on several occasions. With the catalytic effect of the high radiation field an efficient transfer of the sorbed iodine into volatile organic species can be expected in this area.

Hypoiodous acid (HOI) is another chemical form of radioiodine which can be released from H_2O at the bottom of the elevator chamber during the process of defective fuel discharging. The mechanism of HOI generation and its properties will be discussed in Section 4.

On several occasions more than 90% of the airborne iodine was identified in its non-elemental form within 3-5 days after refuelling of defective fuel bundles in the fuel transfer room at the Douglas Point and Pickering nuclear power stations.

3.3 Iodines in the Spent Fuel Bay Water

When defective fuel is being discharged from the reactor into the receiving bay, the iodine leak rate is still high and relative humidity can approach the saturation point in the spent fuel bay room. Up to 500 Ci of ^{131}I was released into the spent fuel bay water within a few hours after discharging several defective fuel bundles (see 2.4).

It was mentioned in 3.1 that small quantities of organic iodides could be generated in the fuel elements. Organic iodides can also be formed by the reaction of I_2 released from the defective fuel with traces of organic compound extracted from the epoxy lining of the spent fuel bay, possibly from IX resin in the bay purification system and grease released from tools and mechanical equipment

in the bay. The presence of small amounts of organic iodides in the bay water was confirmed experimentally. The major portion of airborne radioiodine is released from the bay water as hypoiodous acid within a few hours after discharge of defective fuel elements.

The above conditions initially presented some difficulties with removal of airborne radioiodines from the bay room atmosphere and reduction of iodine releases in gaseous effluents.

The "HOI problem" is discussed in more detail in Section 5.

3.4 Summary

1. The calculated iodine concentration and the chemical forms in which it is occurring in Pickering systems and gaseous effluents are summarized in the following table:

TABLE 3

System	Concentration		Chem. Forms
	^{131}I	$^{127}I + ^{129}I$	
Fuel elements after 12 months of full power operation; $(g \times kg^{-1}_{UO_2})$	5.9×10^{-3}	6.6×10^{-2}	I_2 (org. iodides)
Heat transport D_2O $(g \times \ell^{-1}$ of $D_2O)$	7.4×10^{-9}	2.8×10^{-9}	I^-
D_2O (M)	6×10^{-11}	2.3×10^{-11}	
Spent fuel bay water $(g \times \ell^{-1}$ of $H_2O)$	8×10^{-10}	8×10^{-9}	HOI
Bay water (M)	3×10^{-12}	3×10^{-11}	$(I_2;$ org. iodides)
Spent fuel transfer room $(g \times m^{-3}$ of air)	3×10^{-7}	3×10^{-6}	HOI $(I_2;$ org. iodides)
Ventilation filters inlet $(g \times m^{-3}$ of air)	4×10^{-11}	4×10^{-10}	HOI, org. iodides, (I_2)

2. This shows that the operational iodine concentrations in all systems are extremely low even when the radioiodine activity is close to the maximum permissible operational limits.

3. Liquid D_2O leaking from the heat transport system is not a major source of gaseous iodine. Particulate LiI is the form of iodine which can be released from the heat transport system with D_2O steam.

4. The ratio of iodine species in the spent fuel transfer room varies with time. I_2 and HOI are the forms released into the room atmosphere. Organic iodides are formed by reaction of I_2 with airborne CH_4 and organic materials. They are the prevailing iodine form in the room within a few days after refuelling of defective element.

5. Very small amounts of organic iodide are released from the spent fuel bay water. A major fraction of the airborne radioiodines which is released from the bay water during the first 24 hours is hypoiodous acid.

<div align="center">

4.0   Formation and Control of the Inorganic
Penetrative Form of Iodine

</div>

4.1 Published Data on "Penetrative Iodines"

An exhaustive review of the chemistry and removal of methyl iodine was prepared by C.F. Parsly [7]. In his summary he discusses his doubts about quantitative assessment of CH_3I in samples which were analyzed by using May Pack sampler only. He refers to several experiments in which the methyl iodide concentration was measured both by May Packs and by gas chromatography, and the amount of CH_3I measured by May Pack was overestimated by factors up to 20 (average of 6). Other conclusions, made in this review, will be later compared with results of our investigations.

Graig [8] and Wilhelm [9] reported a concentration dependence of the charcoal absorption efficiency for elemental iodine at low concentrations (<1 $\mu g/m^3$). No such effect was observed when CH_3I was absorbed at normal conditions.

D. Pence [10] reported similar concentration dependency of CH_3I absorption efficiency on charcoals and Ag-X13 at 90°C and 90% RH.

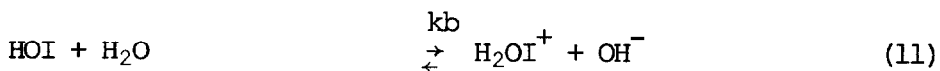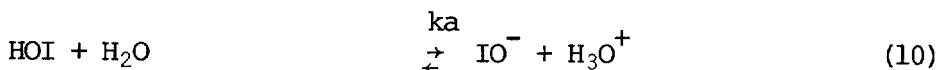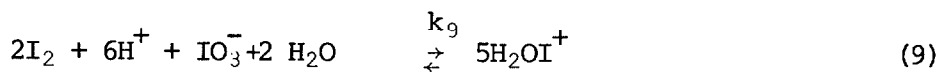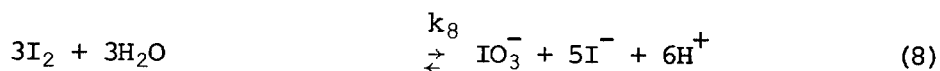It follows from chemical considerations that the more penetrative form of airborne iodine, occurring only at low concentrations, could be similar to the airborne iodine which is formed in the spent fuel bay water for a short time period after receiving a fresh defective fuel bundle and which we preliminarily identified as hypoiodous acid [1].

4.2 Published Data on Chemistry of Hypoiodous Acid

Hypoiodous acid (HOI) formation and its chemical behaviour has been discussed in many publications. Its existence was proven theoretically but because it can exist only in very diluted solutions and its stability is low, no direct experimental evidence has been submitted.

The following reactions are involved in formation of HOI and its dissociation in aqueous solutions:

$$I_2 + H_2O \underset{\leftarrow}{\overset{k_1}{\rightarrow}} HOI + H^+ + I^- \tag{1}$$

$$I_2 + H_2O \underset{\leftarrow}{\overset{k_2}{\rightarrow}} H_2OI^+ + I^- \tag{2}$$

$$H_2OI^+ + H_2O \underset{\leftarrow}{\overset{k_3}{\rightarrow}} HOI + H_3O^+ \tag{3}$$

$$I_2 + I^- \underset{\leftarrow}{\overset{k_4}{\rightarrow}} I_3^- \tag{4}$$

$$HOI + I^- \underset{\leftarrow}{\overset{k_5}{\rightarrow}} HOI_2^- \tag{5}$$

$$I_2 + OH^- \underset{\leftarrow}{\overset{k_6}{\rightarrow}} HOI_2^- \tag{6}$$

$$IO^- + I^- + H_2O \underset{\leftarrow}{\overset{k_7}{\rightarrow}} HOI_2^- + OH^- \tag{7}$$

$$3I_2 + 3H_2O \underset{\leftarrow}{\overset{k_8}{\rightarrow}} IO_3^- + 5I^- + 6H^+ \tag{8}$$

$$2I_2 + 6H^+ + IO_3^- + 2 H_2O \underset{\leftarrow}{\overset{k_9}{\rightarrow}} 5H_2OI^+ \tag{9}$$

$$HOI + H_2O \underset{\leftarrow}{\overset{ka}{\rightarrow}} IO^- + H_3O^+ \tag{10}$$

$$HOI + H_2O \underset{\leftarrow}{\overset{kb}{\rightarrow}} H_2OI^+ + OH^- \tag{11}$$
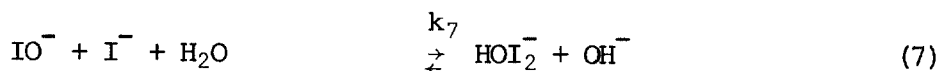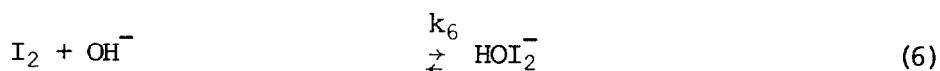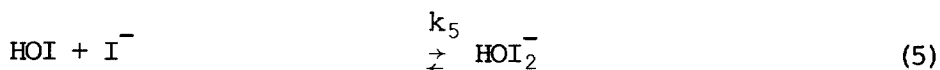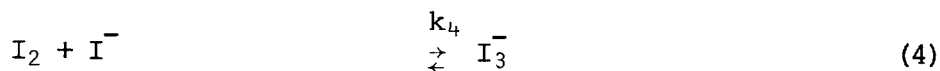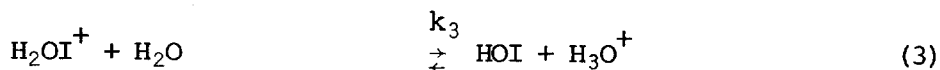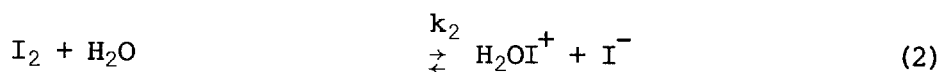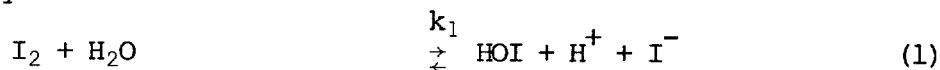
T. Allen and R. Keefer [11] studied the formation of hypoiodous acid and hydrated iodine cation (reactions 1,2) by spectrometric analysis of aqueous solutions of iodine. They determine the following equilibrium constants:

$$k_1 = 5.4 \times 10^{-13} \text{ at } 25°C$$
$$= 0.49 \times 10^{-13} \text{ at } 1.6°C$$

They set an upper limit of k_2 to 1×10^{-10} at 25°C and used 1.2×10^{-11} as the most probable value in their calculations.

The dissociation constant k_3 is given by the ratio of $k_1/k_2 = 4.5 \times 10^{-2}$ at 25°C.

If no impurities are present in an iodine solution then hydrolysis given by reactions (1) and (2) is the only source of iodide ion which can enter further into reactions (4), (5) and (7).

The equilibrium constant $k_4 = 768$ at 25°C as reported in [12] .

M. Eigen and K. Krestin [13] proposed a mechanism for iodine hydrolysis via an intermediate "ternary" compound HOI_2^- which from the reported equilibrium constants has relatively high stability:

$k_5 = 3 \times 10^2$

$k_6 = 1.5 \times 10^4$

Eggleton [14] refers to a value of $k_7 = 0.13$ and concludes that HOI_2^- exceeds only 20% of other iodine species present at pH > 8 and iodine concentrations of > 10^{-3} M.

The reaction (8) is relatively slow at low pH as reported by Bell and Geller [5]. It is suggested in publication [17] that its equilibrium constant $k_8 = 4 \times 10^{-48}$ cannot be used for solutions of iodine at low concentrations and pH > 7.

Allen and Keefer [11] reported a value of $k_9 = 6 \times 10^{-8}$. In their experiments most of the IO_3^- was reduced to H_2OI^+ in solutions of $I_2 + IO_3^- + H^+$ at low concentrations.

The HOI dissociation constants are very small. The most probable values are given in publication [2].

$ka = 4.5 \times 10^{-13}$

$kb = 3.2 \times 10^{-10}$

The above constants show that HOI has an amphiprotic character. Its reaction depends strongly on pH.

4.3 Theoretical Considerations

The relative contribution of the above chemical reactions to HOI formation within the range of pH (6-10) and Iodine concentrations ($10^{-8} - 10^{-12}$ M) were theoretically evaluated from the above chemical equations and their equilibrium constants.

Reaction (1)

It is obvious from Graph 1 that a high yield of HOI is obtained from this reaction within the above limits.

Reaction (2)

Graph 2 indicates that the hydrolytic yield of H_2OI^+ is far below HOI yield under the same conditions.

Reaction (3)

It is illustrated in Graphs 3 and 8 that H_2OI^+ is almost completely hydrolysed to HOI in neutral and alkaline solutions. Therefore, H_2OI^+ can be considered only as a transient hydrolytic product which is formed in negligible amounts under the conditions of pH and I_2 concentration met in practice.

Reaction (4)

It follows from Graph 4 that a significant amount of I_2 can be absorbed

from its solution by I^- only if I^- exists in relatively high concentrations ($> 10^{-6}$ M).

Reaction (5)

The intermediate "ternary" product formation in I_2 solutions is demonstrated on Graph 5. The $[HOI]/[HOI_2^-]$ ratio depends on pH and I_2 concentration. This graph shows that a negligible amount of HOI_2^- is present in I_2 solutions under the considered conditions.

Reaction (6)

According to Graph 6 significant amounts of HOI_2^- can be generated in alkaline solutions by hydrolysis of iodine. This intermediate product disintegrates to $HOI + I^-$ (see Graph 5) so that the final $[HOI]/[HOI_2^-]$ ratio is controlled by reaction (5).

Reaction (7)

Beside the disintegration of HOI_2^- through reaction (5) it has a high tendency to hydrolyse in alkaline solutions to $IO^- + I^-$ (see Graph 7).

Reactions (8) and (9)

Reaction (8) is slow [5]. Therefore, the effect of IO_3^- concentration on H_2OI^+ yield from reaction (9) was calculated and related to reaction (8).

Under the assumption that reaction (9) is faster than reaction (8) Graph 8 indicates a high transfer rate of IO_3^- to H_2OI^+ in neutral and slightly alkaline solutions of I_2.

Most of H_2OI^+ is immediately transferred to HOI according to the reaction (11).

The above considerations indicate that insignificant amounts of IO_3^- are formed in iodine-in-water solutions under the specified conditions of pH and Iodine concentration.

Reactions (10) and (11)

Dissociation of HOI to its anion and cation depends strongly on the pH of the solution. Graph 9 shows that less than 10% of the HOI is dissociated to H_2OI^+ at pH > 5.5 and a pH > 11.3 is necessary to obtain $> 10\%$ of its anion OI^-.

It follows from this graph that hypoiodous acid has an alkaline rather than acidic character and that more than 90% of the HOI is present in solution in its non-dissociated form within the pH range of $5.5 - 11.3$.

4.4 Volatility of Inorganic Iodine Species

Most of the iodine species considered above have a high partition coefficient. Eggleton [14] obtained partition coefficient value of:

1.4 x 10^{33} for I^-, and

3   x 10^{71} for H_2OI^+

and estimated that the partition coefficient of OI^- will lie between that of I^- and H_2OI^+. The partition coefficient of elemental iodine is in the region of $10^4 - 10^5$ and for HOI was calculated from approximate thermodynamic data to be in the range of 77 - 4300.

Keller et al [16] obtained a partition coefficient of about 300 for HOI from results of their experiments.

4.5 Summary

The above theoretical evaluation can be summarized as follows:

(1) The concentration of transient products such as H_2OI^+, HOI_2^-, IO_3^-, IO^- and I_3^- is low in iodine solutions under the considered conditions.

(2) Practically all I_2 is hydrolysed to HOI and I^- in this situation.

(3) The volatility of H_2OI^+, IO_3^-, IO^- and I^- from their aqueous solutions is very low.

(4) Besides elemental iodine, which is slightly volatile, HOI is the only inorganic iodine compound, formed in water solutions under the specified conditions, which is considered to be highly volatile.

5.0 Experimental Studies on HOI Formation

5.1 Identification of HOI in the Spent Fuel Bay Water at Pickering G.S.

As it was explained in part 2.4 of this report, the highest ever measured ^{131}I activity in the Pickering G.S. spent fuel bay water corresponds to total Iodine concentration of $<3 \times 10^{-11}$ M. It was derived theoretically that practically all the iodine can be hydrolysed in water at this concentration.

Measurements taken in the Pickering G.S. spent fuel bay in 1971-1972 were described in publication [1]. Ion exchangers were used to measure the concentration of both ^{131}I and ^{133}I in the bay water and also the ratio in which they were absorbed in cationic and anionic resins. It can be seen from Graph 10 that the ratio of ^{131}I absorbed on cationic to that on anionic resins increased rapidly during the first hour after discharging a defective bundle but then the relative amount of the "cationic iodine" decreased as the iodine concentration in bay water increases. This can be explained by the increased I^- and H^+ concentration in the bay water due to reaction (1).

Airborne concentration of the penetrative form of iodine in the bay room followed a similar pattern as the "cationic to anionic iodine" ratio in the bay water with the exception of slower decrease (see Graph 10).

This behaviour of the penetrative form of iodine gave good reason to believe that it was identical to the iodine form which dissociates in water to the cation. Hypoiodous acid is the only presently known form behaving this way in water solution,therefore it is the likely form present in bay water under such conditions.

There is a similarity between our observations and the cases reviewed in Parsly's annotation[7], as follows from his Summary: "In well over half the experiments in which the amount of charcoal seeking iodine was reported as a

function of time, the amount was highest immediately after iodine release and decreased with time. We cannot state with certainty that this was or was not methyliodide." It is also concluded in the Summary that: "It does seem fairly clear that when the release occurs into water less than 0.1% of the iodine will be converted to organic form."

5.2 Operational Control of Iodine Volatility

A method for iodine volatility control from the bay water was developed in Ontario Hydro. This employs hydrazine in about 50 PPM concentration in the bay water. Iodine is reduced to hydroiodic acid:

$$2I_2 + N_2H_4 \rightleftharpoons 4\ HI + N_2. \qquad (12)$$

Kolthoff [17] studied the effect of pH on the iodine-hydrazine reaction. He concludes that the optimum conditions for quantitative reduction of I_2 to HI are at pH 7-7.5. This is the pH range normally maintained in the bay water.

K.K. SenGupta and K.S. SenGupta [18] studied the kinetics of this reaction and found that increasing concentrations of H^+ and I^- leads to an overall decrease in the reaction rate. They suggest that HOI or H_2OI^+ is the reacting component.

Hydroiodic acid resulting from this reaction is not very volatile. It is continuously removed from the bay water by the bay purification system. On several occasions the airborne ^{131}I concentration in the bay room was reduced by a factor > 10 in a short period of time by adding hydrazine to the bay water after discharging defective fuel into the spent fuel bay at Pickering G.S.

5.3 Generation of the Non-elemental Iodine Species in the Laboratory

To provide for more accurate experimental investigations of HOI properties, a laboratory method was developed for the generation of HOI containing a minimum amount of both organic iodides and elemental iodine.

A solution of "carrier-free" iodide (as Na ^{131}I) was used for the above preparations. It was specified by the supplier that this solution contains a maximum of 4 x higher concentration of stable iodine than concentration of ^{131}I at the time of its delivery. This solution was used for a maximum of 2 weeks so that the iodine concentration from which HOI was generated in the laboratory was similar to its concentration under field conditions as analyzed in part 2 of this report.

5.3.1 Generation of HOI and CH_3I

1. A method which was used in the previous HOI investigations [16] and [21]:

    Elemental iodine was generated by the oxidation (using H_2O_2, $K_2Cr_2O_7$ or KIO_3) of "carrier-free" Na ^{131}I in acidic solutions using reaction (8). I_2 was stripped from this solution with a high purity Helium (1ℓpm) into a weak alkaline solution (pH = 10-11) where it was hydrolysed to HOI.

2. A method developed in our laboratory is based on the following chemical reactions:

$$2 \text{ NaI} + \text{Br}_2 \overset{\rightarrow}{\leftarrow} 2 \text{ NaBr} + \text{I}_2 \qquad\qquad (13)$$

$$\text{I}_2 + \text{NaOH} \overset{\rightarrow}{\leftarrow} \text{NaI} + \text{HOI} \qquad\qquad (14)$$

Elemental bromine is added to Na ^{131}I alkaline solution in slightly higher concentration than iodine. The above reactions are occurring in parallel with hydrolysis which eliminates the bromine excess from the solution, transferring it to a non-volatile bromide and hypo-bromide:

$$\text{Br}_2 + \text{NaOH} \overset{\rightarrow}{\leftarrow} \text{NaBr} + \text{NaBrO} + \text{H}_2\text{O} \qquad\qquad (15)$$
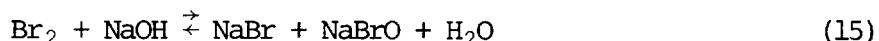
Fifty (50) ml of "carrier-free" ^{131}I (5 μCi/ml) in 5×10^{-2}N NaOH was used in the "Iodine Generator" which corresponds to $\sim 3 \times 10^{-9}$ M iodide if the ratio of stable $\text{I}/^{131}\text{I}$ is 10 in this solution.

1 μg of Br_2 which was added to this solution (giving concentration of 10^{-7} M Br_2) generated > 0.1 μCi of gaseous HOI.

3. In order to compare HOI and CH_3I properties, gaseous CH_3I was generated by purging He through a solution of a carrier-free $^{131}\text{I}^- + (\text{CH}_3)_2 \text{ SO}_4$, as described in publication [19].

5.3.2 Description of Apparatus

The apparatus, which is illustrated on Figure 1 was used for all of the methods described above.

The gaseous species of iodine were stripped from an alkaline solution AS and carried with He stream through a glass fibre filter F1, Cu screens (etched with HI) and bubblers B1-B4, which were filled with distilled water, for removal of the remaining I_2. The non-elemental iodine species, released from the last bubbler, were absorbed in 2 sampling cartridges in series (2 in. dia. x 1 in. depth) filled with 5% TEDA impregnated charcoal. The gas reaching the first cartridge was maintained at room temperature and 100% RH (it was saturated with H_2O in the preceding bubblers). A heater H was installed after the first cartridge to reduce the relative humidity of the gas sample before its entry to the second ("back-up") cartridge A2.

Total absorption of iodine in the second cartridge A2 was confirmed experimentally on several occasions, when another fresh cartridge (filled with impregnated charcoal or silver zeolite), installed after the cartridge A2,did not contain any measurable amount of iodine. The existence of an iodine species which could completely penetrate the third absorber under these conditions can be excluded from our considerations.

5.3.3 Evaluation of Properties of the Non-elemental Iodine Species

HOI Generation - Method 1

KIO_3 gave the best results of the tested oxidizing agents for HOI generation.

More than 70% of the iodine released from the generator G was retained in the alkaline solution AS. More than 90% of the gaseous iodine released from the alkaline solution (AS) was present in its non-elemental form.

The Partition Coefficient measurement indicated (see Table 6) that it was

difficult to generate HOI with low content of organic iodides when this method was applied.

HOI Generation - Method 2

The most advantageous feature of this method is that elemental iodine can be generated by reaction (13) directly in an alkaline solution where it hydrolyses immediately through reaction (14). The second product of the hydrolysis, NaI, is returned to the displacement reaction (13). A high yield of HOI can be obtained and much less of organic iodide is formed in parallel with these rapid reactions.

Results of our measurements are in agreement with the above theoretical considerations of Section 4.3.

1. The ratio of I_2/HOI in the He stream from the generator can be controlled by pH of the Na^{131}I solution in G as shown in Table 4.

TABLE 4

pH	% of I_2	% of HOI
2	75	25
12	<10	>90

2. The rate of hydrolysis was significantly reduced after the I^- concentration was increased. After adding HI to the basic solution in G the ratio of I_2/HOI increased as indicated in Table 5.

TABLE 5

I^- Concentration in G	Gaseous Iodine Purged with Helium from the Generator G	
	% of I_2	% of HOI
10^{-9} M	<10	>90
10^{-2} M	65	35

3. From the ^{131}I ratio in the four distilled water bubblers it was determined that > 85% of elemental iodine, released from the generator with HOI, was absorbed in bubbler 1. A fraction of this I_2 was hydrolysed there, giving a higher yield of HOI from the system.

4. Because of the high HOI yield from the generator, the apparatus was simplified by removing bubbler AS and the Cu screens and the final arrangement of the apparatus is given on Figure 2.

CH$_3$I Generation

No difficulties were experienced in the generation of CH$_3$I. Methyl-iodide was purged out of solution of Na ^{131}I + (CH$_3$)$_2$ SO$_4$ with He (1ℓpm). The CH$_3$I release rate was steady through the experimental periods and only

less than 1% of the ^{131}I was absorbed as I_2 on the Cu screens.

5.4 Absorption of HOI and CH_3I in Liquids

As explained above, a series of bubblers filled with distilled water (50 ml) was used to separate all soluble components from the gaseous non-elemental iodine, generated from the solutions of Na ^{131}I under conditions described in Section 5.3. A maximum of 4 bubblers could be installed in series because of their high flow resistance. It was found that 3 bubblers were sufficient for Partition Coefficient measurements because the distribution of dissolved iodine in these bubblers was reproducible under normal experimental conditions.

1. Measurement of the Water/Air Partition Coefficients

The water/gas partition of the investigated iodine form was calculated from the ratio of ^{131}I measured in the last bubbler to the total ^{131}I in the solid absorbers.

The partition coefficient (PC) is defined as:

$$PC = \frac{\text{Volumetric concentration in water}}{\text{Volumetric concentration in air}}$$

The typical ranges of PC measured at room temperature (22°C + 1) and at atmospheric pressure in the experimental conditions described are summarized in Table 6.

TABLE 6

Experimental Conditions	Chemical Forms of Iodine	Measured PC
HOI generated by Method 1. No He purge before absorption Use of demineralized H_2O in iodide solution and bubblers.	Org. iodides (HOI)	5 - 15
HOI generated by Method 1 after $^{131}I^-$ solution purged with He. Use of demineralized H_2O	Org. iodides + HOI	20 - 60
HOI generated by Method 2, He - purge, demineralized H_2O.	HOI (Org. iodides)	70 -120
HOI generated by Method 2, He - purge distilled H_2O	HOI	140 -200
CH_3I generated by the method described in publication [19]	CH_3I	1.5 - 2

The PC values in Table 6 suggest that:

(a) HOI generated by the Method 1 contains higher amounts of organic iodides

than HOI obtained from Method 2 under the same conditions.

(b) There were still some organic iodides present if HOI was generated by Method 2 when demineralized water was used to prepare the I^- solution in the generator and to fill the bubblers. This was probably due to the presence of organic traces eluted from the IX resin.

(c) Partition Coefficient of HOI generated from solutions of NaI + NaOH in distilled water was found to be in the range of 140-200 in more than 30 experiments. A PC = 180 can be recommended as the mean value for HOI from these experiments.

2. Scrubbing of the Non-elemental Gaseous Forms of Iodine

The scrubbing efficiency of several solutions for CH_3I and HOI was measured using three bubblers in series. Bubblers 1 and 3 were filled with distilled water and bubbler 2 contained 50 ml of the investigated solution.

Table 7 shows the typical ratio of ^{131}I absorbed in each bubbler respectively.

TABLE 7

Experiment Number	Chemical Form	Scrubbing Solution in the Bubbler 2	Distribution of ^{131}I Absorbed in 3 Bubblers		
			B1	B2	B3
1	HOI	Distilled water	70	17	13
2	HOI	5% $AgNO_3$	60	25	15
3	HOI	2.5% Phenol in 0.5 N NaOH	35	50	15
4	HOI	Cation exchange resin ARC351 in H_2O	42	40	18
5	HOI	ARC351 in 0.1 M H_2SO_4	35	48	17
6	CH_3I	Distilled water	38	31	31
7	CH_3I	5% $AgNO_3$	3	96.7	0.3
8	CH_3I	2.5% Phenol in 0.5 N NaOH	37	27	36
9	CH_3I	ARC351 in 0.1 M H_2SO_4	36	37	27

Results of the experiment 2 indicates a low affinity of HOI to $AgNO_3$ while CH_3I can be absorbed very efficiently in this solution as indicated by experiment 7.

The result of experiment 3 is in agreement with data published by V. Cofman [20]. He concluded from his experiments that HOI is solely responsible for the iodination of phenols (refer to the following reaction):

$$3 \text{ HOI} + 3 \text{ } C_6H_5OH = 3 \text{ } C_6H_4I.OH + 3H_2O \qquad (16)$$
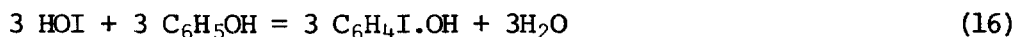
Dissociation of the generated HOI to the cations H_2OI^+ (see reaction 11) was confirmed by results of experiments No. 4 and 5.

Negligible CH_3I absorption was measured in the phenol solution and in the cation exchange resin under the same conditions.

5.5 Summary

1. In the first few hours after a defective spent fuel bundle is received in the spent fuel bay a highly volatile iodine species is formed in the bay water. Our investigations show that this is HOI.

2. Operational control of iodine volatility in the spent fuel bay is provided by the addition of hydrazine to the bay water in Ontario Hydro nuclear power stations.

3. A laboratory method has been developed for generation of HOI which appears to produce HOI reproducibly and with a minimum amount of organic iodides.

4. The experimentally determined mean value of the water/air Partition Coefficient of the generated HOI is 180 (for $CH_3I = 1.8$).

5. The experimentally determined pH and I_2 concentration effects on the HOI yield are in agreement with theoretically derived reactions (see 4.3).

6. The scrubbing efficiencies of various solutions have been determined for CH_3I and HOI. These differ markedly for the two species.

7. Reactions of the generated HOI with an alkaline phenol solution and a cation exchange resin are considered good proof of its identity.

8. The low absorption rate of gaseous HOI in the above solutions indicates that it has a low chemical reactivity.

6.0 Testing of Solid Absorbers

There is little information available on the ability of some of the common commercially available solid absorbers to remove HOI from an air stream. Six of these were tested for HOI removal capability. The technical specifications of these are given in Table 8. In addition two other potentially useful iodine absorbers (Nos. 7 and 8) and a sample of Barnaby and Cheney 727 charcoal which had been in use for two years continuously in the spent fuel bay at Pickering G.S. were tested. Apart from this sample (No. 4) all other samples were fresh, unused, and had been carefully stored in sealed glass containers. The three types of Barnaby and Cheney charcoal (177, 727 and CU) had all been prepared from the same batch of charcoal base.

TABLE 8

Absorber Number	Manufacturer	Absorber Designation	Base		Impregnant	
			Material	Size	Material	Weight
1	Barnaby and Cheney	B & Ch 177	Coconut Charcoal	8 x 16 mesh	0	0
2	Barnaby and Cheney	B & Ch 727	Coconut Charcoal	8 x 16 mesh	KI_3	5%
3	Barnaby and Cheney	B & Ch CU	Coconut Charcoal	8 x 16 mesh	TEDA	5%
4	Barnaby and Cheney	B & Ch 727	Coconut Charcoal	8 x 16 mesh	KI_3	5%
5	Davidson Chemical	Ag-X13	Molecular Sieve X 13	10 x 16 mesh	Ag	60%
6	Nuclear Consulting Services	NUSORB 1514782	Aluminum Silica	4 x 6 mesh	Ag NO_3	N.A.
7	A sample from Mr. J. Wilhelm Karlsruhe	Ag-SA	Amorph. Silicic Acid	1 - 2 mm	Ag NO_3	10%
8	Sample from Mr. J. Keller Idaho Falls	4-Ip	Alumina	30/60 mesh	4-iodo-phenol	5%

6.1 Testing System and Procedure

1. Testing Apparatus

The apparatus used for absorber testing is illustrated in Figure 2 and Figure 3. HOI was generated by Method 2, as described in 5.3.

He + HOI (at 1 ℓpm) from bubbler 3 was mixed with 19 ℓpm of air and passed through a column A1 filled with the absorber being tested. A glass filter F3 removed particles released from this absorber and the air sample was then heated in H1 to 50°C in order to obtain the total absorption of iodine in the "back-up" absorber A2.

2. Air Supply

The laboratory air was supplied through the valve V1 (V2 closed) when the absorbers were tested at room humidity (50%).

Air for the high humidity tests was supplied from the humidifier (with V1

closed) as described below:

- Laboratory air was heated at the evaporator E inlet in order to get the required evaporation rate;

- The excess water was condensed in a cascade of condensers $C_1 - C_6$ which were maintained at room temperature;

- Air, saturated to 100% RH from C_6 outlet, was mixed with the He + HOI stream and carried to the column A1.

3. The Arrangement of the Absorbers in the Testing Column A1

A column of 9 aluminum rings (Figure 4) with stainless screens at their bottom was filled with the tested absorber. Depth of the rings in the columns, used for our experiments, was as follows:

    3 x 3.3 mm
    4 x 6.5 mm
    2 x 12.5 mm

Diameter of the rings = 44 mm.

The flow rate of 20 ℓpm corresponds to a face velocity of 22 cm/sec through the tested absorber.

4. The Testing Procedure

(a) Conditioning of all the absorbers being tested was done for 15 hours before absorption of HOI, in order to equilibriate the absorber moisture to the relative humidity at which it was tested.

(b) Bromine solution was added to the $^{131}I^-$ solution in the generator at 10 minute intervals for a total of 1 hour, in order to smooth the HOI concentration in the gaseous sample.

(c) ^{131}I was measured separately in each component of the column, the filter F3 and the cartridge A2.

(d) The above components were assembled again and only air was passed through the system.

(e) The desorption rate of ^{131}I from the tested absorber was measured under the same experimental conditions as the HOI absorption was made.

The following experimental conditions were applied during the absorber testing:

Relative Humidity:- 55% RH ± 5%

- 100% RH, no condensation of H_2O in the tested absorber

- >100% RH, with an intentional slight condensation of H_2O in the tested absorber

HOI Concentration:

- 10^{-1} μCi of $^{131}I/m^3$ of air (± 30%) with the exception of a few experiments, discussed later.

784

Time of HOI absorption - 1 hour

Time of HOI desorption - 2 - 65 hours

6.2 Discussion of Results

The measured absorption efficiency and the approximate desorption rate values for three different moisture levels in the absorbers are summarized in Tables 9, 10, 11 and Graphs 11, 12 and 13.

1. Efficiency for HOI Absorption

Graphs 11, 12 and 13 illustrate that all three types of charcoal have a superior absorption efficiency for HOI as compared with the other types of absorber under all of the applied humidity conditions. Two factors affect their efficiency:

(a) Increased humidity, which reduces the HOI removal efficiency;

(b) Increased airborne HOI concentration significantly improves the HOI absorption. This is illustrated by Graph 17 which will be discussed in detail.

TABLE 9 (50% RH)

Absorber		Desorpt. Time (hours)	Absorpt. % in 0-10 mm	Absorpt. % in 10-30 mm	Absorpt. % in 30-60 mm	Penetrn. % Through 60 mm	Rate of Desorpt. % Per Hour
No.	Type						
1	B&Ch 177	0 55	93.5 93.0	4.4 4.5	2.0 1.3	0.1 1.2	0.02
2	B&Ch 727	0 63	98.8 92.6	0.9 3.4	0.3 1.3	0 2.7	0.04
3	B&Ch CU	0 55	98.9 96.0	1.1 2.1	0 0.9	0 1.0	0.018
5	Ag-X13	0 25	94.1 94.0	4.7 4.4	0.9 0.7	0.3 0.9	0.024
6	NUSORB	0 25	57.0 55.3	20.5 22.2	13.8 13.7	8.7 8.8	0.004
7	Ag-SA	0 25	75.6 75.2	12.5 12.2	7.5 7.2	4.4 5.4	0.04
8	4-Ip	0	37.0	27.5	22.8	12.7	

A concentration of 0.1 μCi/m^3 of HO^{131}I was used for all measurements shown in Graphs 11 and 12 with the exception of absorber 2 in Graph 12 and all absorbers in Graph 13 for which 0.5 μCi/m^3 was used. This results in Graph 12 showing a higher efficiency for absorber 2 than absorber 3. Graph 13 also indicated a higher efficiency of the charcoals to HOI when they are wetted (with condensed H$_2$O), compared with the efficiency of identical absorbers which were equilibrated to 100% RH

but tested with lower concentration of HOI.

Absorber 5 (Ag-X13) absorbs HOI efficiently at 50% RH but its efficiency is drastically reduced under high humidity conditions.

Absorber 8 (4-Iodophenol) which was tested for purposes of HOI sampling will be discussed with reference to Graph 18.

TABLE 10 (100% RH)

Absorber No.	Desorpt. Time (hours)	Absorpt. % in 0-10 mm	Absorpt. % in 10-30 mm	Absorpt. % in 30-60 mm	Penetrn. % Through 60 mm	Rate of Desorpt. % Per hour
1	0	83.4	6.3	7.2	3.1	0.06
	60	72.0	13.5	7.9	6.7	
2	0	93.1	5.4	1.0	0.5	0.043
	60	81.5	13.1	2.3	3.1	
3	0	91.2	4.6	3.5	0.6	0.05
	57	81.8	6.7	7.8	3.7	
5	0	51.0	28.5	13.9	6.6	0.04
	15	49.8	29.3	13.7	7.2	
6	0	25.6	16.4	19.0	39.0	0.025
	40	24.6	14.9	20.5	40.0	
7	0	78.7	10.0	6.3	5.0	0.14
	65	51.2	20.4	14.1	14.3	

TABLE 11 (Condensation)

Absorber No.	Desorpt. Time (hours)	Absorpt. % in 0-10 mm	Absorpt. % in 10-30 mm	Absorpt. % in 30-60 mm	Penetrn. % Through 60 mm	Rate of Desorpt. % Per Hour
1	0	96.6	2.2	1.2	0	0.1
	17	90.0	5.7	2.6	1.7	
2	0	93.0	5.1	1.6	0.3	0.03
	17	91.8	6.0	1.4	0.8	
3	0	98.0	1.8	0.2	0	0.02
	17	93.2	6.1	0.4	0.3	
	90	82.7	15.5	1.4	0.4	
5	0	35.1	12.7	9.0	43.2	0.012
	17	32.7	13.8	10.1	43.4	
6	0	39.3	5.2	5.8	49.7	0.4
	17	29.5	7.3	6.5	56.7	
7	0	54.8	10.1	8.0	27.1	0.25
	17	52.9	8.9	6.8	31.4	

2. **HOI Desorption with Air at Room Temperature**

Desorption rates of ^{131}I were measured from the tested absorbers. The same desorption time could not be applied for all measurements, therefore the ^{131}I which penetrated a 60 mm depth of absorber was expressed in Tables 9, 10 and 11 as "% desorption/hour". These approximate desorption rate values show that desorption of iodine from charcoals and Ag-X13 increases slightly with a humidity of the passing air. Iodine

desorption from absorbers 6 and 7, which are impregnated with Ag NO_3, is significantly increased under high humidity conditions (see Graphs 15 and 16). It was determined from measurements of the filter F3 that there was no significant release of iodine in particulate form from the tested absorber during the desorption time.

3. Absorption Efficiency of Used KI_3 Charcoal

A sample of Barnaby and Cheney type 727 charcoal was taken from the spent fuel bay ventilation filter for comparison of its HOI removal efficiency with fresh charcoal of the same type. The used charcoal had been installed in a 2 inch deep bed which operated continuously for 2 years under variable room temperatures and humidity conditions with an air face velocity of 45 cm/sec. Graph 14 shows that this charcoal is much less efficient than the fresh charcoal for HOI removal at 50% RH. It is also obvious from this graph that this charcoal is not satisfactory under high humidity conditions.

4. Dependence of Absorption Efficiency on HOI Concentration

As was discussed above, a distinct change of the absorption efficiency with HOI concentration was observed (see Graphs 12 and 13). Therefore a specific test was made with Barnaby and Cheney type CU and 727 charcoals at 60% RH. Graph 17 confirms a strong concentration dependence as expected. This effect requires more detailed investigation.

5. Selective Absorption of HOI

Absorbers 7 and 8 were tested for CH_3I and HOI removal efficiency at 60% RH. Results of these tests are given in Graph 18 and were as expected:

(a) Absorber 7 (Ag NO_3 impregnated silicic acid) is a very good absorber for CH_3I but it has much lower efficiency for HOI absorption.

(b) The adsorption efficiency of the absorber 8 (4-Iodophenol on Alumina) for HOI is relatively low under the applied experimental conditions but it does not absorb any CH_3I. This experiment demonstrated the suitability of this absorber for use in selective HOI sampling (as reported in publication [21]). This absorber was also used to confirm the identity of HOI generated for our experiments.

6.3 Summary on the Absorption Experiments

The results of the absorption measurements can be summarized as follows:

1. The efficiency of fresh charcoals for HOI absorption is good at 50% RH with low desorption rates.

2. These charcoals have retained an acceptable absorption efficiency for HOI at 100% RH with slightly increased desorption rates.

3. Of the tested charcoals the TEDA impregnated type was the best. Efficiency of the KI_3 impregnated charcoal was slightly lower under the applied experimental conditions.

4. Absorption efficiency of KI_3 impregnated charcoal, removed from a filter which had been in use for 2 years was found to be at unacceptable level under conditions of 100% RH.

5. The non-charcoal absorbers 5,6 and 7 are not as efficient for HOI removal as charcoals, particularly at high humidity.

6. 4-Iodophenol was shown to be a good selective absorber for HOI sampling at low sampling flow rate.

7. The experiments show that the absorption efficiency of the tested charcoals depends on the airborne HOI concentration. This is in agreement with the proposal (discussed in the Introductory part of this paper) that iodine concentrations and chemical forms used for filter testing should be similar to the concentrations and chemical forms occurring at filter inlet.

7.0 Discussion of Mechanism of HOI Absorption

Three processes are postulated to be involved in HOI absorption:

1. Physical adsorption
2. Chemisorption
3. Decomposition of HOI.

Physical adsorption is logically the primary process which significantly increases the effective residential time of HOI in the charcoal and gives a sufficient time to HOI to react chemically with an impregnant or to decompose itself. The results presented are not conclusive in terms of chemisorption and HOI decomposition. The results suggest that silver impregnated zeolite is more efficient than $Ag\,NO_3$ impregnated inorganic adsorbers and TEDA is a slightly more efficient impregnant than KI_3 for HOI chemisorption. The absorption characteristics of 4-Iodophenol indicate a purely chemisorption process by a relatively slow reaction (this is similar to the reaction of HOI with an alkaline Phenol solution).

HOI decomposition in charcoals is probably the basic process which is involved in its retention in charcoals. Decomposition is probably accelerated by:

1. catalytic effect of the charcoal surface
2. drying effect of the charcoal
3. alkaline products in charcoal

One of the decomposition products - (I^-) can be oxidized by air. This could cause a chromatographic movement of iodine similar to a physical desorption.

The suggested mechanism is only one of many other possible processes which can be involved in HOI absorption. Only a thorough theoretical and experimental study of this problem can lead to realistic conclusions.

8.0 Practical Application in Ontario Hydro

The foregoing studies on HOI generation and absorption have resulted in a technical evaluation of commercially available absorbers for airborne HOI. It is evident from the results that silver impregnated absorbers which have a high efficiency for CH_3I are much less efficient for HOI removal.

It is known that absorption efficiency of impregnated charcoal for CH_3I is good and we have shown that HOI retention is good at 50% RH for long term use.

The price of silver impregnated absorbers is such that their use is limited to those cases where specific operating conditions demand the characteristics displayed by the silver impregnated absorbers. The obvious absorber choice for

our station use is therefore an impregnated charcoal.

The results obtained will influence the design of filter systems for CANDU power stations. It is recommended that the filter systems contain a facility for preheating of the effluent air before it enters the charcoal filters. A temperature rise from ~ 20°C to 35°C will ensure that the relative humidity will not exceed 50% at the filter inlet.

The information obtained on absorbers and the capability of generating HOI reproducibly will assist in the establishment of a realistic and rational test program for ventilation filters used for iodine removal.

Acknowledgement

References:

1. M.J. Kabat
   Experience with Gaseous Fission Products and Radioiodines at Ontario Hydro
   Paper presented at the 17th Health Physics Society Meeting, June 1972,
   Las Vegas

2. N.V. Sidgwick
   The Chemical Elements and their Compounds
   Volume 2
   Oxford Univ. Press 1951

3. L.C. Schwendiman et. al.
   The Washout of Methyliodide by Hydrazine Sprays
   BNWL 935; November 1968

4. D.M. Golden, R. Walsh, S.W. Benson
   The Thermochemistry of the Gas Phase Equilibrium $I_2 + CH_4 \rightleftharpoons CH_3I + HI$ and the
   Heat of Formation of the Methyl Radical.
   JACS $\underline{87}$, 4053 (1965)

5. J.F. Kircher, R.H. Barnes
   Methyliodide Formation Under Postulated Nuclear Reactor Accident Conditions
   Symposium on Treatment of Airborne Radioactive Waste
   New York, 1968, 137-162

6. R.L. Bennett, R. Slusher and R.E. Adams
   Reaction of Iodine Vapour with Organic paint coatings.
   ORNL-TM-2760; April 1970.

7. L.F. Parsly
   Chemical and Physical Properties of Methyliodide and its Occurrence under
   Reactor Accident Conditions.
   ORNL-NSIC-82; December 1971.

8. D.K. Craig
   Effect of Iodine Concentration on the Efficiency of Activated Charcoal
   Adsorbers.
   H.P. $\underline{19}$, 437 (1970)

9. J.G. Wilhelm et.al.
   "Filter Program"
   KFK 1818 (1972)

10. D. Pence
    The Removal of Low Level Radioiodines from Reactor Off-gas Effluents.
    Paper presented at the 12th AEC Air Cleaning Conference; 1972

11. T.L. Allen and R.M. Keefer
    The Formation of Hypoiodous Acid and Hydrated Iodine Cation by the
    Hydrolysis of Iodine
    JACS $\underline{77}$; 2957-60, (1955)

12. M. Davies, E. Gwynne
    The Iodine-iodide Interation
    JACS 74; 2748, (1952)

13. M. Eigen, K. Krestin
    The Kinetics of Halogen Hydrolysis
    JACS 84; 1355-1361; April 1962

14. A.E.J. Eggleton
    A Theoretical Examination of Iodine-Water Partition Coefficients
    AERE-R-4887, (1967)

15. R.P. Bell and E. Gelles
    The Halogen Cations in Aqueous Solutions
    J.C.S.; 2734-40, (1951)

16. J.M. Keller; F.A. Duce; D.T. Pence; W.J. Maeck
    Hypoiodous Acid: An Airborne Inorganic Iodine Species in Steam-air
    Mixtures.
    A paper presented at the 11th USAEC Air Cleaning Conference
    September 1970.

17. Kolthoff;
    J.A.C.S. 46; 2009-16, (1924)

18. K.K. Sen Gupta and S.K. Sen Gupta
    Kinetics of Reaction between Hydrazine and Iodine Solutions
    Z. Phys. Chem. 45, 378-382, (1965)

19. J.J. Hillary
    Iodine Sorption Plant Testing Procedures in the United Kingdom.
    Presentation on Seminar on Iodine Filter Testing; Karlsruhe,
    Germany December 1973

20. V. Cofman
    The Active Substance in the Iodination of Phenols.
    J.C.S. 115, 1040-49 (1919)

21. J.H. Keller et.al.
    Air Evaluation of Materials and Techniques used for Monitoring
    Airborne Radioiodine Species.
    Paper presented at the 12th AEC Air Cleaning Conference; 1972.

FIGURE 1

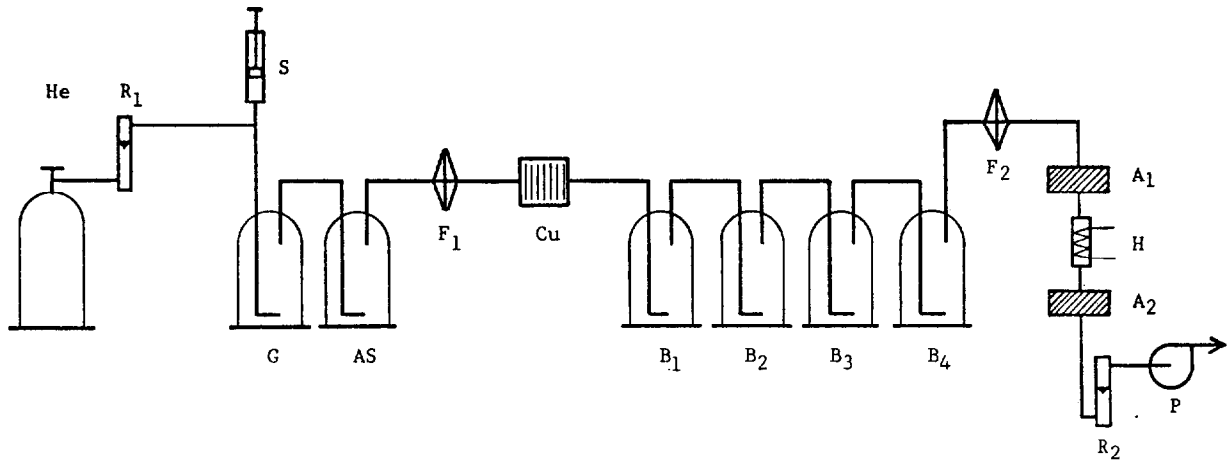|			
He	–	Helium	
R_1-R_2	–	Flow Rate Meters	
S	–	Syringe	
G	–	Iodine Generator	
AS	–	Alkaline Solution	
F_1-F_2	–	Glass Fibre Filters	

Cu	–	10 x Copper Screen (mesh 100)
B_1-B_4	–	Bubblers
A_1-A_2	–	Charcoal Cartridges
H	–	Heater
P	–	Air Pump
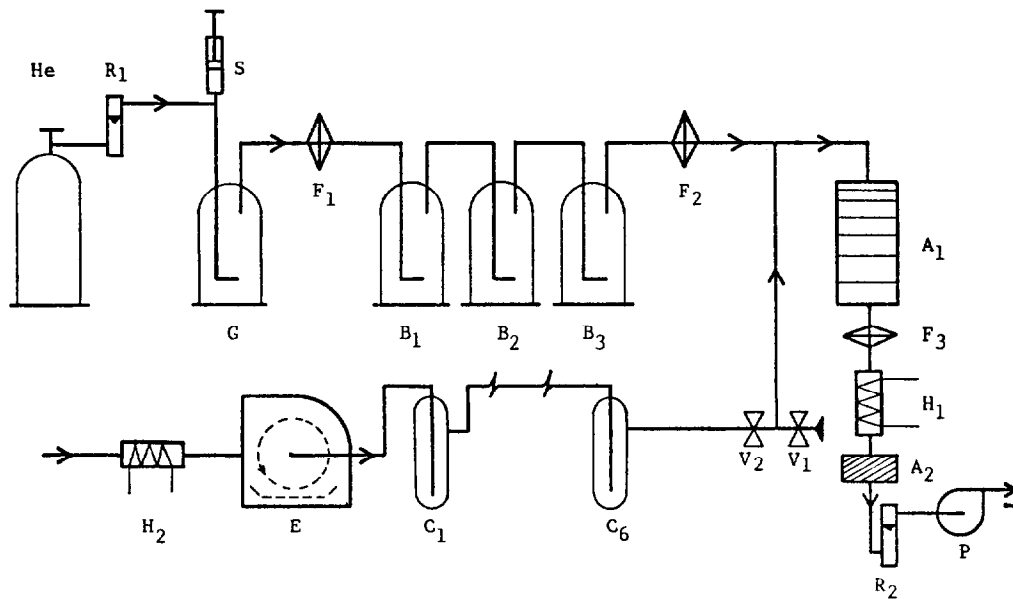
FIGURE 2

E – Evaporator

C_1 – C_6 – Condensers

V_1 – V_2 – Valves
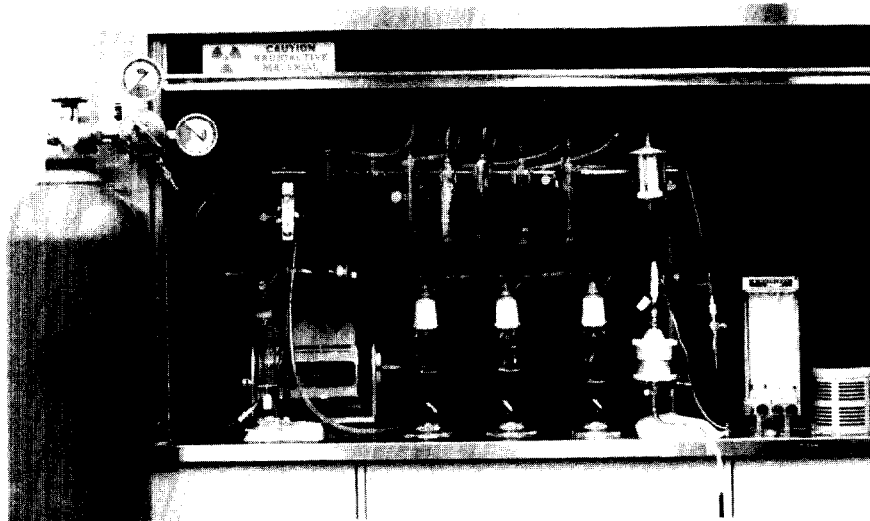
Figure 3
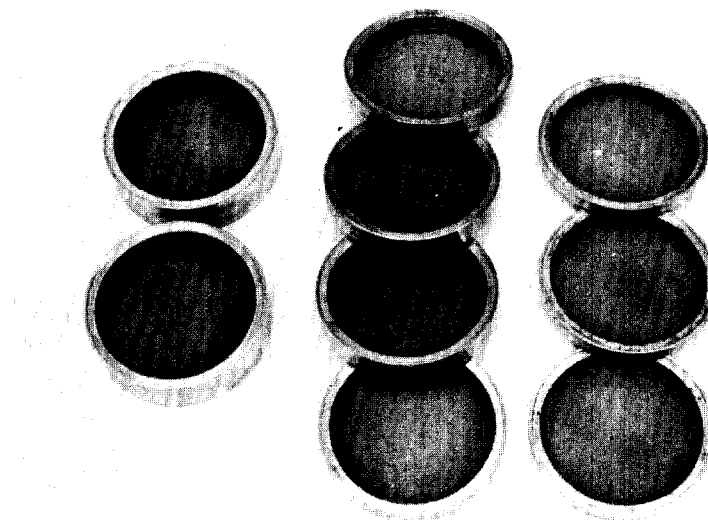
Figure 4
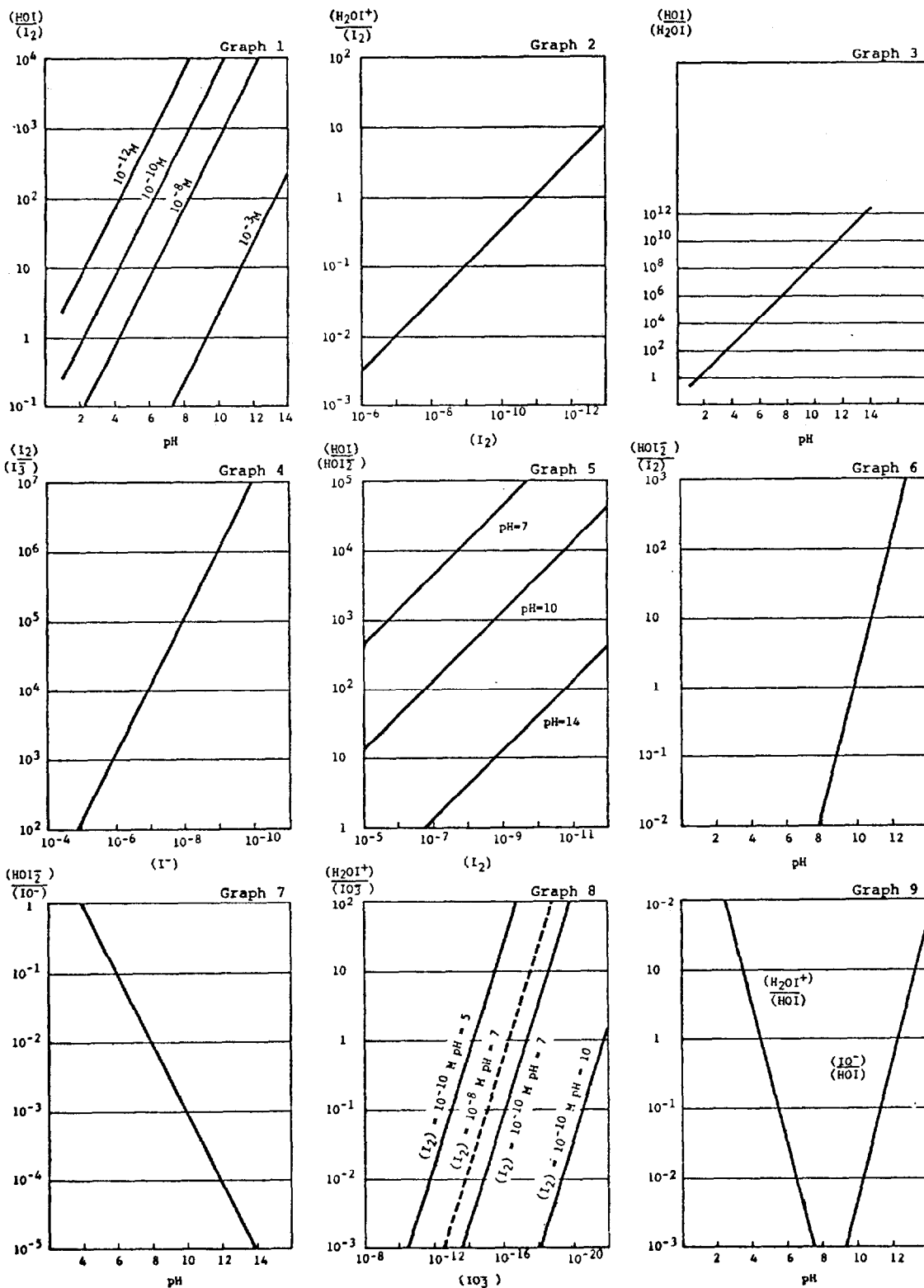
Graphs 1-9:   Equilibrium ratios of iodine species in aqueous solutions
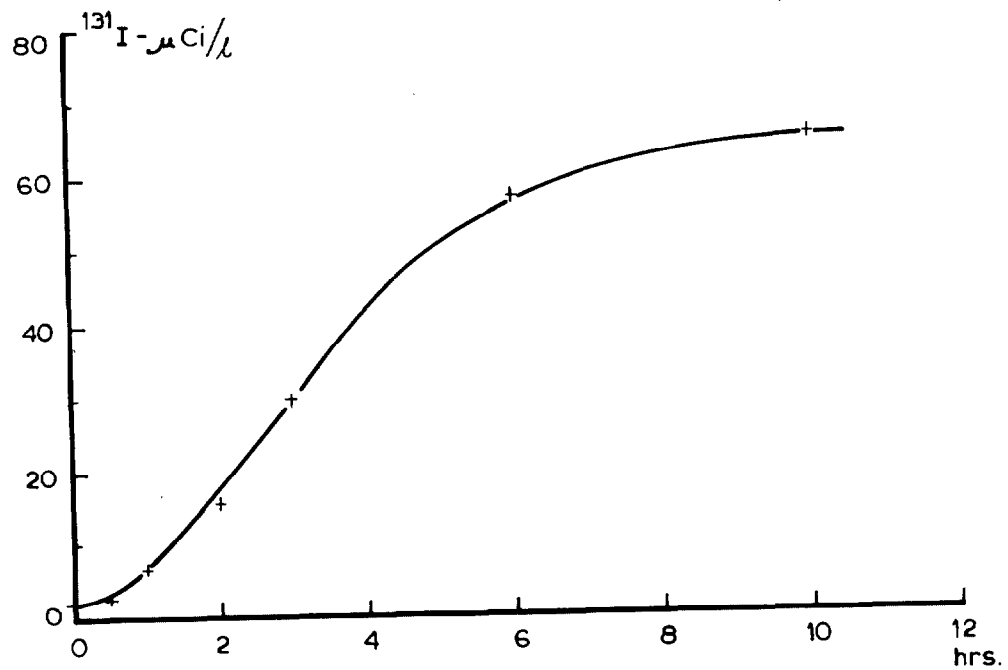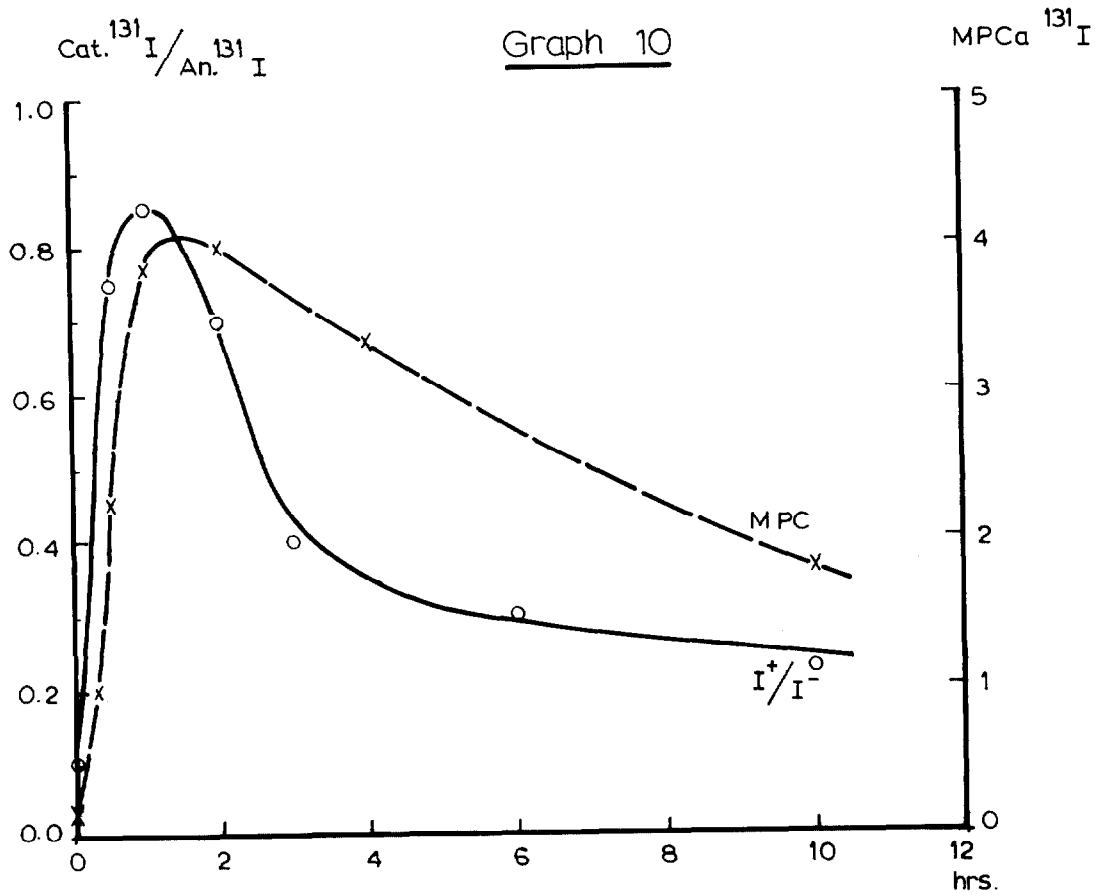
Graph 10

Graph 10:   Time dependence of iodine species in spent fuel bay

Graph 12
100% RH

Graph 11
50% RH

Graph 14

Aging effect

% HOI penetration

100% RH

4 (used)

50% RH

4 (used)

50% RH
2 (fresh)

bed depth — mm

Graph 13

H₂O condens.

6
5
7

% HOI penetration

2

1

3

bed depth — mm

Graph 16

HOI Desorption
100 % RH

% HOI penetration

bed depth

Graph 15

HOI Desorption
50 % RH

% HOI penetration

bed depth

Graph 18
60 % RH
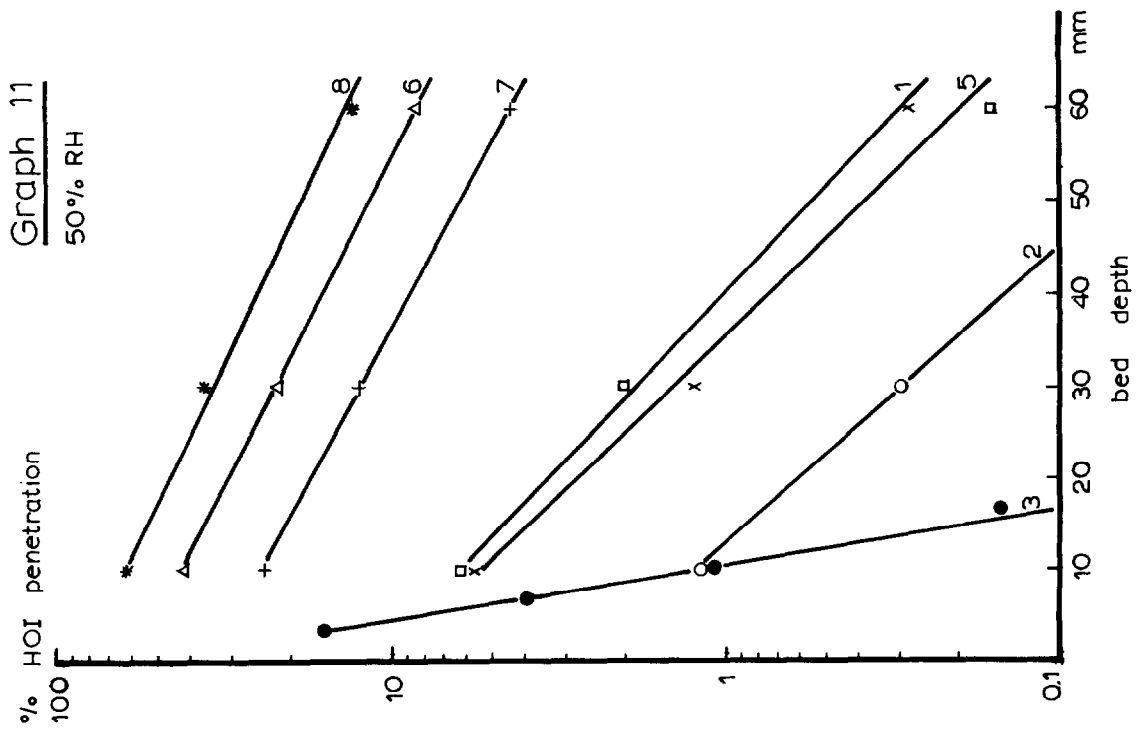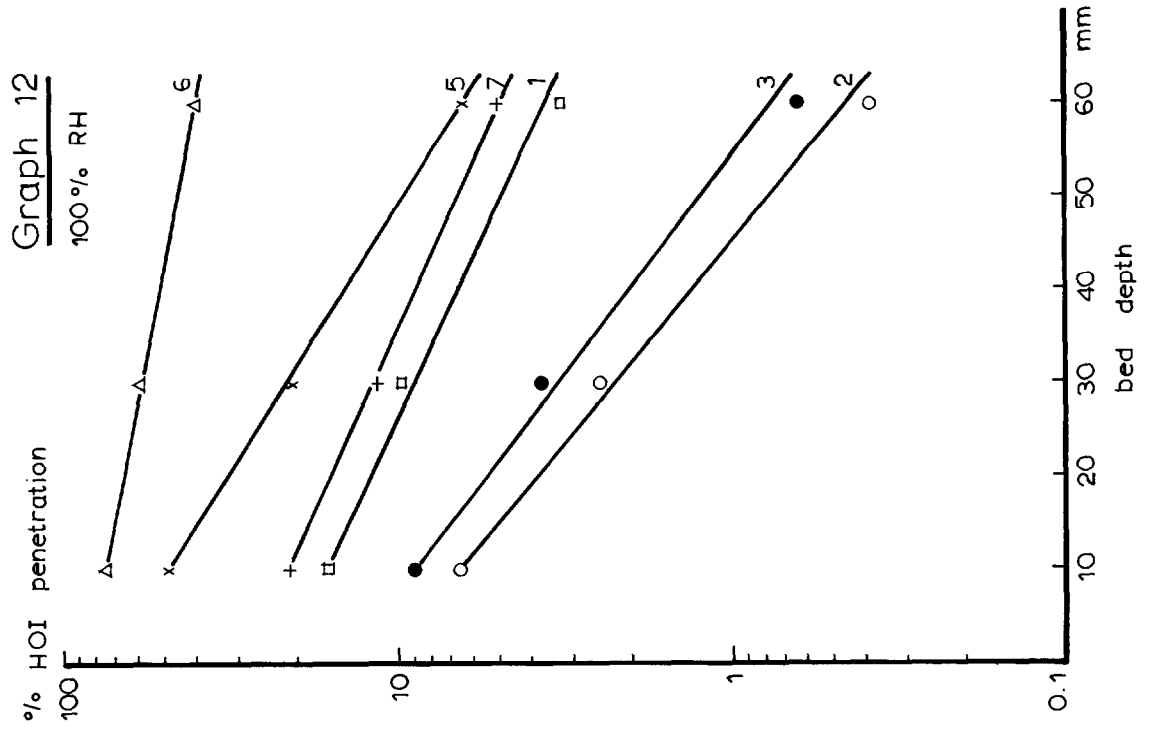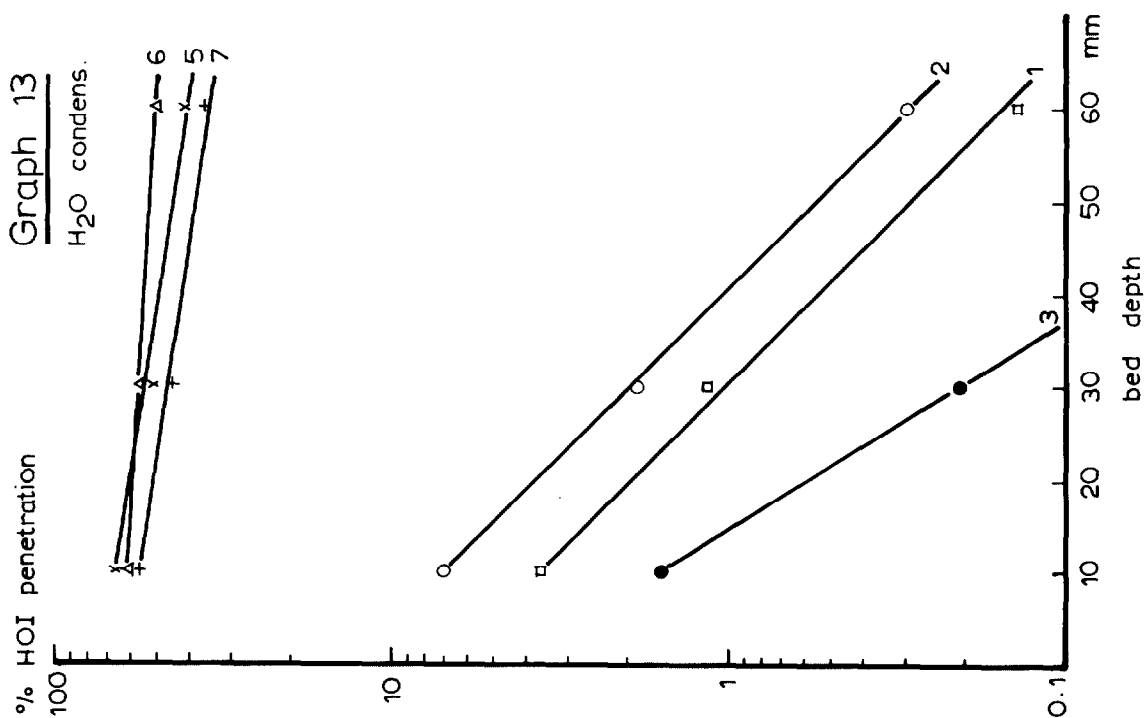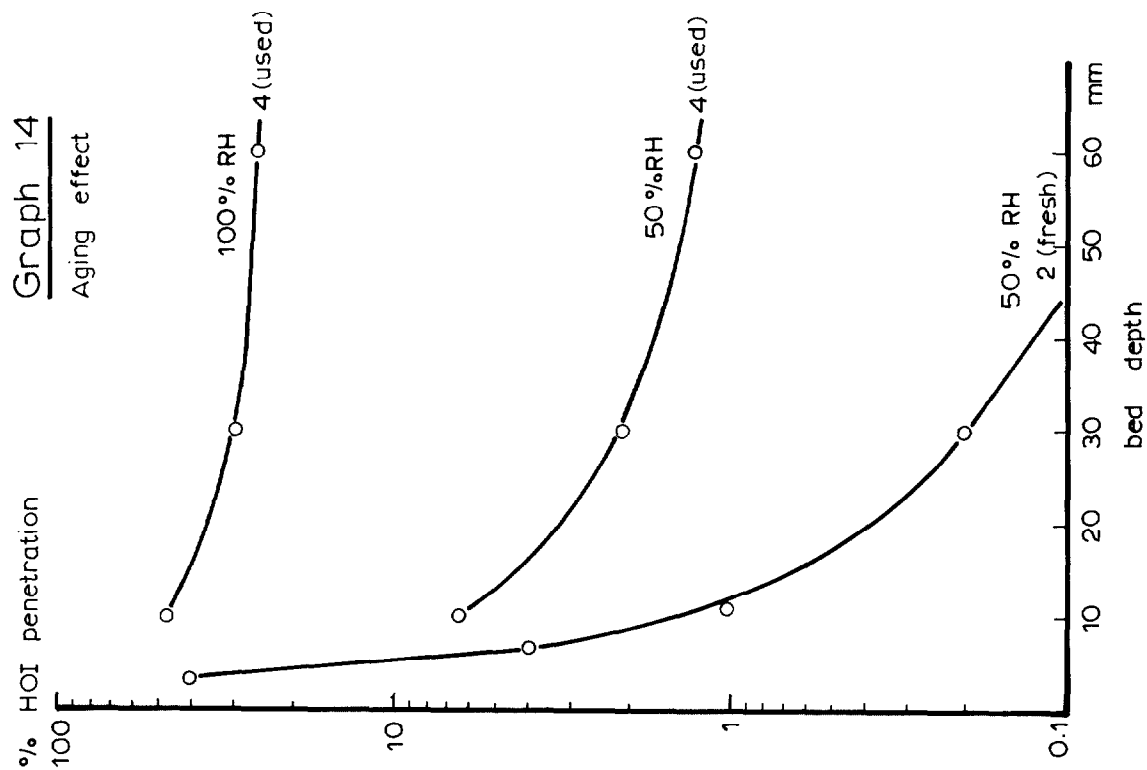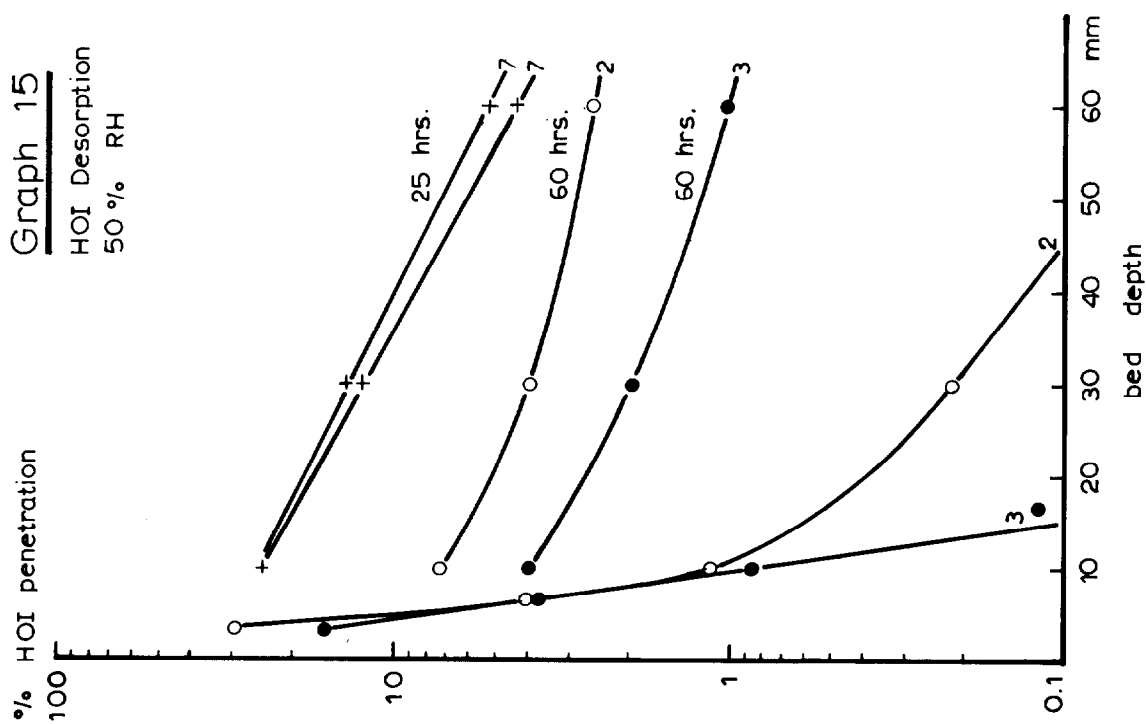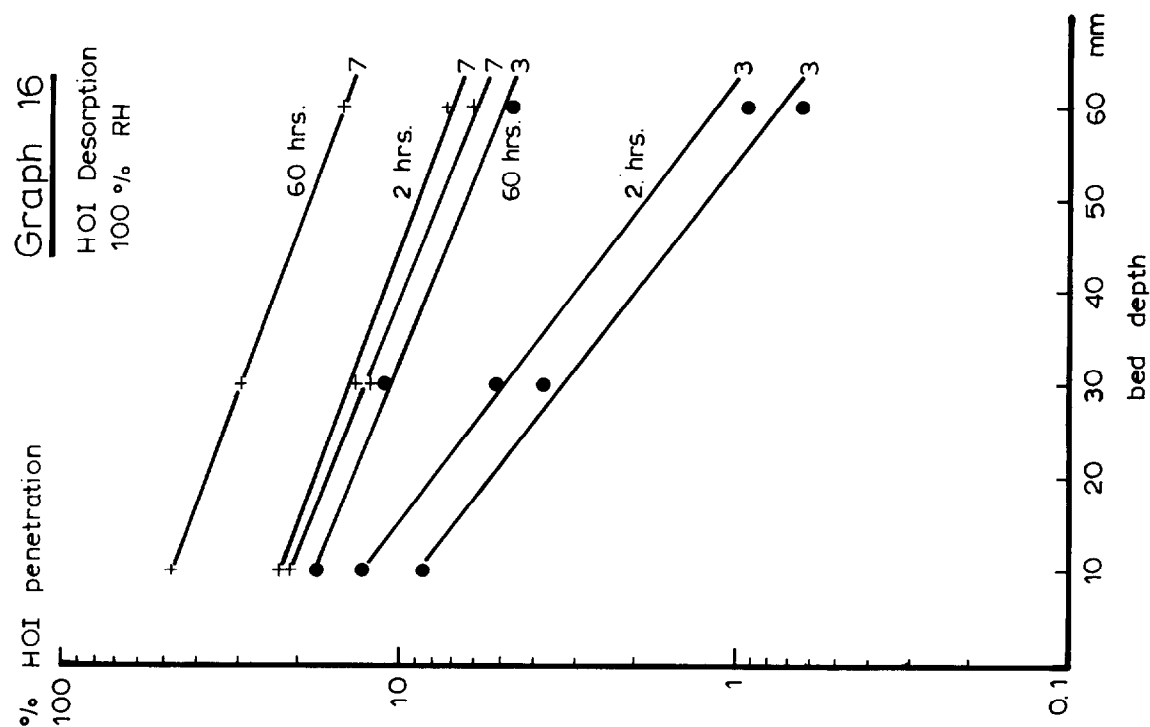
Graph 17
Concentration dependence
60 % RH
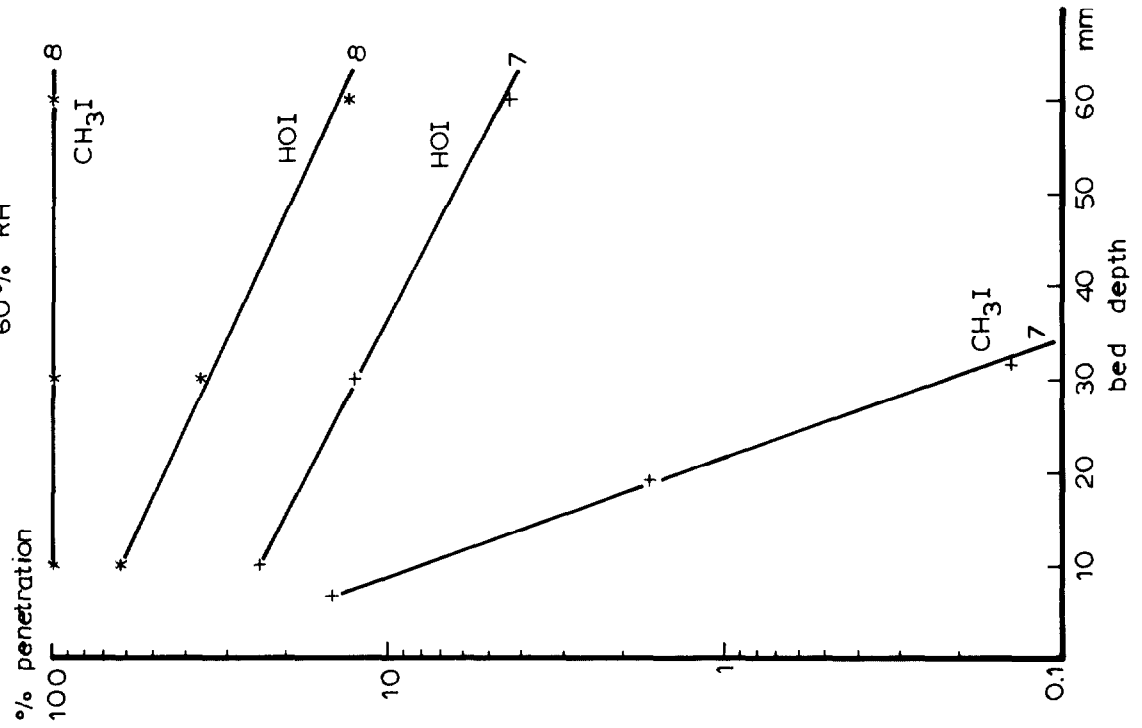
TABLE 4. Penetration Data for Bituminous and Petroleum Base, KI Impregnated Carbons

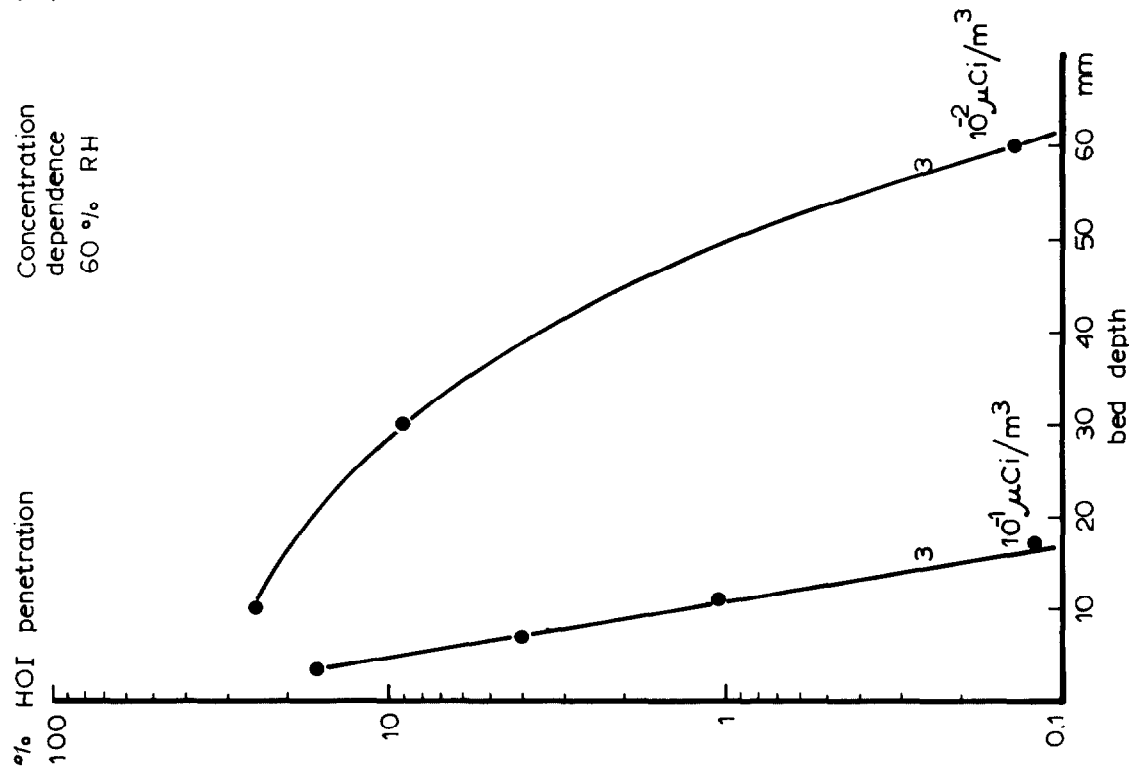| RUN	Base(1)	Bed Depth mm	Conc mg/m^3	TEST BED CONDITIONS Temp °C	RH %	Press. psia	Vel. m/min	Feed Period min	Elution Period min	Penetration %
Contaminant: $^{127}I_2 + ^{131}I_2$										
I 11-3	Bitumin, U.S. (A)	25.4	17.1	131	94.0	54.7	11.8	90	90	1.58
I 11-3	"	50.8	17.1	131	94.0	54.7	11.8	90	90	0.0283
I 11-4	"	25.4	15.8	132	94.4	54.7	12.8	90	90	1.61
I 11-4	"	50.8	15.8	132	94.4	54.7	12.8	90	90	0.0205
I 12-1	"	25.4	18.4	131	95.4	54.7	12.2	90	90	0.188
I 12-1	"	50.8	18.4	131	95.4	54.7	12.2	90	90	0.04
I 2-2	Petrol, U.S. (C)	50.8	17.5	130	92.0	55	12.6	60	120	21.6
I 2-3	"	50.8	17.5	130	92.5	55	12.7	60	120	20.7
Contaminant: $CH_3 {}^{127}I + CH_3 {}^{131}I$										
J 26-4	Bitumin, U.S. (A)	50.8	2.1	24.4	72.6	15.2	12.4	120	120	0.0237
J 26-5	"	"	1.85	24.4	72.6	15.2	12.4	120	120	3.04
J 26-6	"	"	2.04	23.8	70.8	15.2	12.4	120	120	0.019
J 27-3	"	"	2.2	132.2	92.1	54.7	12.4	90	90	0.18
J 27-4	"	"	1.93	131.7	93.2	54.7	12.3	90	90	0.26
J 27-5	"	"	1.84	132.7	92.1	54.7	12.6	90	90	0.15
J 28-1	"	"	1.56	36.7	70.5	15.0	12.6	120	120	0.054
J 28-2	"	"	1.5	38.9	77.3	15.0	12.6	120	120	0.065
J 28-3	"	"	1.54	37.2	72.3	15.0	12.5	120	120	0.053
J 25-4	"	"	1.9	87.2	70.0	15.2	12.5	60	120	0.08
J 32-7	Bitumin., Foreign (B)	"	~5	129.4	92.7	54.6	11.1	90	90	0.546
J 3-4	Petrol, U.S. (C)	"	13.4	130	92.2	54.7	12.9	60	240	15.9
J 3-8	"	"	19.9	25	82.4	15.0	11.3	60	120	0.8
J 32-6	"	"	8.1	132	90.5	54.5	11.6	90	90	1.14
J 35-1	Bitumin, U.S. (D)	50.8	1.2	41.1	90.2	14.9	12.9	120	120	0.064

(1) See section 5.0 for descriptions.

PERFORMANCE OF NON-COCONUT BASE
ADSORBERS IN REMOVAL
OF IODINE AND ORGANIC IODIDES

R.D. Rivers, Mohiuddin Pasha, Evans E. Fowler, and J.M. Goldsmith
American Air Filter Company, Inc.
Louisville, Kentucky

ABSTRACT

Systems for the removal of radioactive iodine and organic iodides have used impregnated coconut shell activated carbons almost exclusively. Coconut shell carbons have some disadvantages: their geographical origin determines their trace chemical content; pore structures and impregnant effectiveness are highly dependent on activation and impregnation techniques. The authors report laboratory performance of a group of iodine-organic iodide adsorbers using bases other than coconut shell carbon. These have been evaluated in conformity with USAEC Regulatory Guide 1.52 and RDT M16 1T. Performance with regard to $^{131}I_2$ and $CH_3^{131}I$ penetration and high temperature elution have equaled or exceeded both the requirements of Guide 1.52 and results on typical coconut-shell carbons. Some performance outside Guide 1.52 ranges is included. Experimental problems in simulated LOCA testing are discussed.

1.0 INTRODUCTION

Activated carbon derived from coconut shells can have high total surface area, and high pore volume which make it the medium of choice for adsorption of many gaseous contaminants. It has long been used in both impregnated and unimpregnated forms for removal of radioiodine and radioactive organic iodide contaminants. However, there are certain disadvantages in using coconut base activated carbons, such as (i) base material has to be imported, (ii) the place of origin of the coconut shell and growing conditions cause variations in the trace chemical content of the carbon and its physical properties, (iii) processing is expensive, and (iv) there have been recent shortages. Other bases for adsorption media could overcome some of these deficiencies. In the last year, we have investigated several alternate adsorbers, comparing their radioiodine/iodide removal efficiencies and other properties to impregnated coconut shell materials. The results of these tests show that non-coconut bases are every bit as effective as coconut bases for this service.

2.0 EVALUATION CRITERIA

We have used USAEC Regulatory Guide 1.52 [Ref 1] for the basic criteria for acceptability of these carbons in nuclear power plant service. Table 1 lists acceptable penetrations according to the Regulatory Guide, along with test conditions for which these penetrations are to be demonstrated. (The Guide does not define precisely the combination of temperature and humidity conditions for test; those listed are our interpretation of the term "DBA Temperature and Pressure" in Table 1 of the Guide. The listed values are believed to be worst-case conditions that would be faced by systems inside and outside containment following a DBA (Design Basis Accident).)

TABLE 1. Radioisotope Adsorber Test Conditions
USAEC Regulatory Guide 1.52

Test	Simulated Condition (DBA)	Contaminant	FEED CYCLE Concentration mg/m³	FEED CYCLE Duration min	FEED CYCLE Temp C	FEED CYCLE RH %	ELUTION CYCLE Duration min	ELUTION CYCLE Temp C	ELUTION CYCLE RH %	Bed Depth mm	Penetration for Acceptance %
Efficiency Tests:											
1.6.1 Primary Systems		I_2	15 - 20	90	130	95	90	130	95	25.4	0.1
1.6.2 Primary Systems		CH_3I	1.5 - 2.0	90	130	95	90	130	95	50.8	5.0
1.6.4 Secondary Systems		CH_3I	1.5 - 2.0	120	40	70	120	80	70	50.8	0.5
Retention Test:											
1.7	--	CH_3I	1.5 - 2.0	120	25	70	240	180	ambient	50.8	1.0

Primary Systems: in containment

Secondary Systems: outside containment

All tests are run at 12 ± 1 m/min

802

Some variation from the listed 'Retention Test' was made during the Loading/ Retention portion of this study. In that portion of the work we sought to demonstrate that some non-coconut shell adsorbers could hold more radioactive material than the amount specified by the Regulatory Guide Retention Test (about 5.7 mg per test, or 0.12 mg of methyl iodide per g of carbon), yet still pass the penetration criteria for the Retention test. Details of the conditions for that study are given in Section 4.2.

In addition to the above radioactive contaminant performance criteria, Regulatory Guide 1.52 lists physical parameters for acceptable material. Some of these can be applied rationally to an adsorber having any base: Particle size distribution, hardness, ignition temperature, impregnant leachout. These items define the ability of the material to be retained in practical filter cells; to operate at reasonable pressure drops; to resist abrasion and vibration; and to avoid ignition by radioactive decay heat. The remaining criteria - surface area, moisture content, ash content, bulk density, and impregnant content - appear to reflect norms for impregnated coconut shell carbons, and are not therefore necessary criteria for non-coconut bases.

3.0   TEST EQUIPMENT

The test equipment used is shown schematically in Figure 1. This conforms in its essentials to the equipment described in RDT M16 1T [Ref 2]. Within the pressure vessel it is possible to reproduce the atmosphere predicted to exist in a reactor containment under post DBA conditions. The maximum operating pressure is 689 kN/m^2 (100 lb/in^2). Any ratio of air to steam is possible, with temperatures up to 150 C.

Separate feed systems are provided for air, steam, and the two radioactive contaminants ($^{131}I_2$ and $CH_3^{131}I$). The radioactive contaminants are carried into the system as tagging molecules in supplies of I_2 and CH_3I gas; the actual percentage of ^{131}I atoms present is very small, and the activity is at the microcurie level.

In most tests, the specific gamma activity of the test contaminants is such that the carriers provide appropriate amounts of non-radioactive contaminant. However, on occasion it is desirable to feed additional non-radioactive material; the system is arranged to accomplish this.

The canisters for holding carbon are shown in Figure 2. Each canister holds a bed of carbon 25.4 mm deep and 50.0 mm in diameter, retained by perforated metal screens. These screens can be removed for emptying the carbon and cleaning and decontaminating the canister. A 3 mm wide baffle ring at each screen eliminates by-pass of the carbon bed along the canister walls. Up to fourteen of these canisters can be stacked together in our rig, to allow testing of deeper beds. Adjacent canisters are sealed together with O-rings, to eliminate leakage. Four tie-rods pass through the canister walls to provide clamping force.

The assembly of canisters to be tested is mounted inside the pressure vessel which is insulated and temperature controlled. Downstream of the test position lie the main condensers (to reduce test gas humidity before it reaches the backup beds) and the backup assemblies. These assemblies are essentially identical to the test canister assembly; their canisters, loaded with a carbon of known performance, can also be disassembled for gamma counting at the end of a test. Downstream of these beds is a safety filter, to capture any radioactivity which might
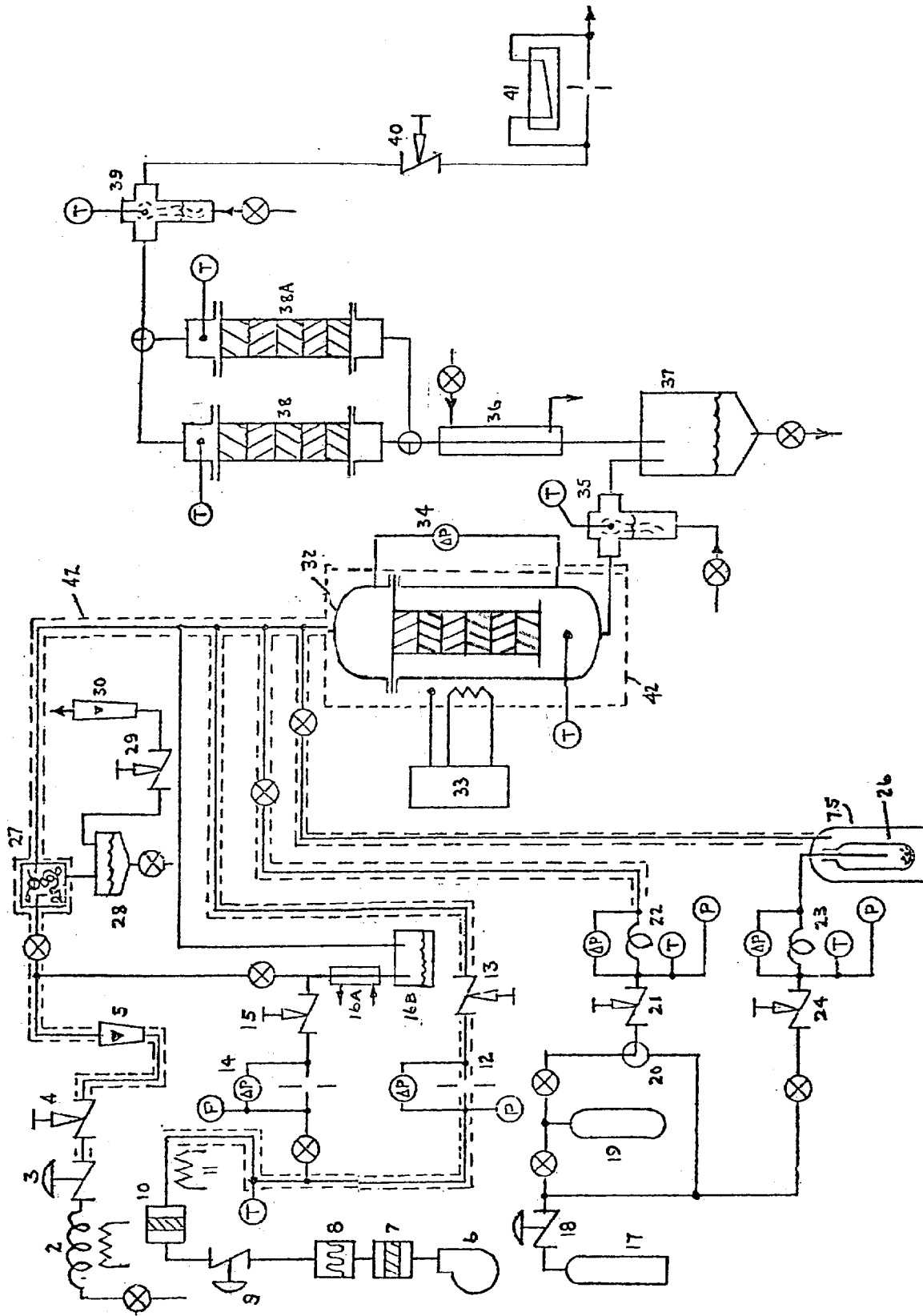
FIGURE 1.   Schematic of Radioisotope Efficiency/Retention Test Facility

LEGEND

Steam Supply (for high humidity conditions)

1. Water Feed Solenoid Valve
2. Boiler
3. Pressure Regulator
4. Flow Control Valve
5. Measurement (Rotometer)

Air Supply

6. Air Compressor
7. Dryer
8. HEPA Filter
9. Pressure Regulator
10. Gas Contaminant Adsorber
11. Air Preheater
12. Main Air Flowmeter (orifice meter)
13. Main Air Flow Control Valve

Humidifier (for low humidity conditions)

14. Saturator Air Flowmeter (orifice meter)
15. Saturator Air Flow Control Valve
16a. Saturator Condenser
16b. Saturator Demister/Sump

Contaminant Feed System

17. Nitrogen Carrier Gas Supply Tank
18. Pressure Regulator
19. Contaminant Storage Vessel (CH$_3$I)
20. Carrier Gas By-pass Valve
21. Feed Flow Control Valve
22. CH$_3$I Capillary Meter

23. I$_2$ Capillary Meter
24. I$_2$ Feed Control Valve
25. Pressure Vessel/Vial Crusher
26. I$_2$ Vial

Moisture Separator

27. Mesh-filled Separator
28. Sump
29. Separator Secondary Gas Flow Control Valve
30. Separator Secondary Gas Flow Rotometer

Sample Beds

31. Sample Bed Holders
32. Pressure Vessel
33. Temperature Regulator/Heater
34. Bed Pressure Differential Gage
35. Humidity Sensor (for low humidity conditions)(wet bulb thermometer with wick feed)

Main Flow Condenser

36. Condenser
37. Sump
38. Backup Beds
39. Humidity Sensor (wet bulb thermometer with wick feed)

Main Air Flow Measurement

40. Main Flow Control Valve
41. Orifice Meter
42. Heat Tracing and Insulation

pass even the backup canisters.

A moisture separator is in the entrance to the main stream to eliminate droplets from the flow at super-saturated conditions. This separator, with assistance from judiciously placed tape heaters, enables the system to produce conditions from essentially zero RH to saturation. Such precautions have eliminated test anomalies which appeared in earlier work.

Each test canister is individually counted for gamma activity before and after each test run. The canister count is taken to be the average of three counts, properly corrected for background and count-rate effects. Counting of activity is carried out by a NaI crystal-scintillometer, using the 0.364 MeV I-131 gamma line. The scintillometer consists of two 125 mm diameter crystals with flat faces opposing each other. The crystals are separated by 53 mm, a space adequate to allow insertion of an entire canister. The outputs of the photomultipliers joined to the two crystals are fed through preamplifiers to a single channel pulse height discriminator.

The crystal geometry approaches 4π configuration, but we were concerned whether various patterns of depth-loading of the canisters would significantly affect the measured gamma activity of the canisters. Runs were made on canisters labelled with equal amounts of radioiodine distributed in different ways in the filter media, and in water. Table 2 lists the results. The labelled water evidently provides some self-adsorption; otherwise, one would expect higher counting efficiency with so little mass in the surrounding container. The carbon beds were surrounded by the rather massive canister (Figure 2) which adsorbed some of the radiation. The activity was contained in 5 ml of water in cases 3 - 5. This was spread over the upper face of the media and allowed to trickle through the media. None of the water passed through the media beds; we assume it was distributed with maximum concentration at the surface. Case 5 was the same carbon and activity as case 4, stirred to distribute activity homogenously throughout the media. The tests indicate that distribution is relatively unimportant, but that each media used should be put through a calibration process to determine its effect on counting efficiency. Calculated penetrations based on counting of test beds and backup beds will otherwise be in some degree of error.

4.0   TEST PROCEDURES

4.1   Penetration Tests

In the penetration tests, there are slight operating differences depending on the temperature and humidity conditions. For the peak DBA temperature at high (95%) RH, it is necessary to bring the carbon to operating temperature (here $\approx$130 C) with ambient low humidity air, then slowly increase the steam flow until the proper RH is obtained at the test temperature. A slow increase is necessary to allow the carbon to adsorb water and come to equilibrium with the humid air stream, without being overheated by the carbon 'heat of adsorption'. This is called the 'equilibrium' period. At lower temperatures and humidities, humid air may be used from the start, but the equilibration process takes much longer - usually 16 to 24 hours, for example, at 25 C and 70% RH.

At the upper range of temperature used, the pressure at saturation is about four atmospheres and no reliable direct readout humidity or dewpoint sensors are available. It is necessary to weigh condensed moisture and account for any

TABLE 2   Scintillator Geometry Factors for Various Holders of Adsorption Media

Case	Media	Container	Interfering Mass g(1)	Counting Efficiency %	Notes
1	Point Source	12 mm dia Plexiglas Rod	<1.2 g plexiglas(2)	68.6	Mock iodine, buried in plastic
2	Water	100 ml plastic	100 g water + 21 g plastic	22.5	Plastic dish, 75 mm diam
3	Carbon	std. canister (Fig 2)	25 g carbon + 865 g SS	22.1	Activity dispersed in <5 ml water; trickled into bed
4	Carbon	light wall canister	25 g carbon + 161 g SS	22.8	"
5	Carbon, homogenized	light wall canister	25 g carbon + 865 g SS	22.5	"

(1) "Interfering Mass" is the mass of material lying between the radioactive material and the scintillation crystal, for at least some portion of the solid angle surrounding the radioactive material.

(2) Weight of first 12 mm of plexiglas canister rod. Source is mounted very near the tip of the rod.

All canisters were inside a plexiglass carrier having 1.3 mm thick walls when in the scintillometer. Weight of carrier: 49.0 g.

BED ID
50.4+0.6

25.4
+0.4

BAFFLE ID
44.4+0.6

DIMENSIONS MM
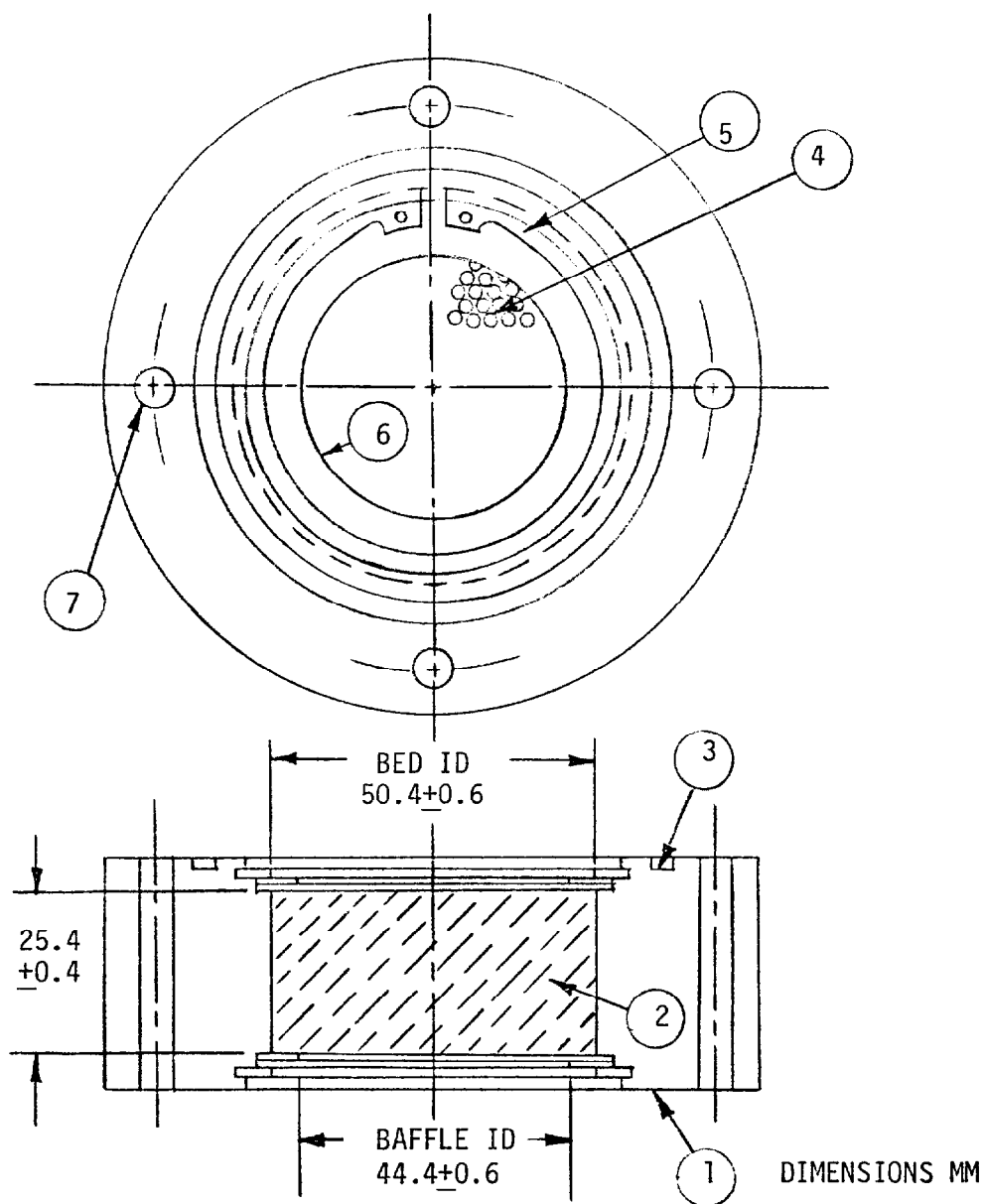
LEGEND

1. Bed Holder
2. Adsorption Media
3. O-ring Gland
4. Perforated Screen (both ends)
5. Retaining Snap Ring (both ends)
6. Baffle (both ends)
7. Holes for Assembly Tie-rods (4)

FIGURE 2. Adsorption Media Test Bed Holder

that is not condensed. The test system is arranged to allow these things to be accomplished without test interruption, as is necessary to the Loading/Retention tests.

The calculation of test flows and relative humidity from test parameters is straightforward for low-temperature, low humidity runs, but both complex and tedious for high-temperature, high humidity runs. It is not permissible to ignore such things as gas compressibilities when making these calculations. We have followed the relative humidity calculation concepts described in RDT M16 1T [Ref 2] It is not, however, clear from those references how one obtains gas compressiblities. AAF has set up a step-by-step procedure for doing this, along with algorithms for use in computer coding of the method. The routines of the calculation are sufficiently compact so that we have been able to automate them completely on a programmable desk calculator (Wang 600-6).

The system is considered in equilibrium when thermocouples both up and downstream of the test beds are within 1 C of each other. After equilibration is complete, feed of radioactive contaminant is started, and continues for the required feed period. At the end of the feed period, the flow of humid air is continued with the test conditions unchanged for the "Elution" period. The flow is then stopped, the system allowed to cool, and the beds disassembled for counting. Penetration is the ratio of count in the backup beds to the sum of counts in the test beds and backup beds; Efficiency is (in percent)(100%-Penetration). The condensed water is also counted, and any activity appearing in it is considered to have penetrated the test bed.

4.2   Loading/Retention Tests

Regulatory Guide 1.52 requires that a 'Retention Test' be run, as listed on line 1.7, Table 1 above. This is identical with 'Efficiency Tests' except that during the elution period, temperature is raised to 180 C, and steam flow is discontinued. The specified elution period for the Retention test is 240 min. This exposure is intended to simulate heating of the bed by radioactive decay heat. Two types of carbon were evaluated by this test. In addition, we made runs to determine how much additional contaminant could be fed to the media and still meet the 1% penetration criteria for Retention. This was accomplished by a two-step test: first, CH_3I was fed under the 38 C - 70% RH condition until the integrated penetration exceeded 0.5%. This could be done by a continuous run because the system includes two parallel backup beds which can be valved in and out of the flow alternately. After the CH_3I loading needed to reach 'breakthrough' had been determined, the test was repeated. About 70% of breakthrough loading was fed before switching to 'Elution': Flow temperature was then raised to 180 C and held for four hours, in the same manner as the Regulatory Guide test for Retention.

5.0   CHARACTERISTICS OF MEDIA TESTED

5.1   Descriptions

(A,D) Bituminous base, U.S. origin. An 8 x 16 USS mesh carbon, impregnated with KI only (<5%, by wt.)

(B)   Bituminous base, foreign origin, 8 x 16 USS mesh carbon, impregnated with KI only (<5%, by wt.)

(C)   Petroleum base, U.S. origin, 8 x 16 USS mesh carbon, spherical, impregnated with KI_3 (≈5%, by wt.)

Table 1. Surface Area of Base (Bituminous) Carbon (Type A) Inter-laboratory comparison

Laboratory	Test Type	Sample Size g	Outgassing Time hr	Outgassing Temp C	Surface m²/g
Particle Data Laboratories Ltd. Box 205 Elmhurst, Ill 60126	Multipoint Dynamic	0.149	5	100	1165
Coors Spectrochemical Laboratory Box 500 Golden, Colo. 80401	Multipoint Dynamic	?	~20	250-275	1068
American Instrument Co. 8030 Georgia Ave. Silver Spring, Md. 20910	Multipoint Static*	0.3804	3.5	325	960
Micromeritics Instrument Corp. 800 Goshen Springs Rd. Norcross, Ga. 30071	Single Point Dynamic	0.0709 0.1093	0.67 0.67	165 150	915 751

*This method is specified in Regulatory Guide 1.52, but is less frequently used today than the multipoint dynamic method. Regulatory Guide 1.52 does not specify out gassing time and temperature, which appear to have some significance.

5.2   BET Surface Areas

Regulatory Guide 1.52 and many other specifications for adsorbers, use the BET-nitrogen surface area of the material as a measure of 'activity'. This may well be a significant property of adsorbers for this application; however, it has been very difficult to correlate BET surface with penetration. In the course of this study, several media samples were subjected to BET surface measurements. The values were puzzling enough to us so that we decided to make an inter-laboratory comparison on a small sample of one base carbon (Type A). The results are listed in Table 3. There is every reason to believe that the laboratories are equally competent; the difference in results seems due to differences in the vigor of out-gassing prior to surface-area measurement; time is more important than temperature. We suggest further study of this matter, to reach an industry standard method by which surface area can be measured reliably.

6.0   TEST RESULTS

6.1   Penetration Tests: U.S. Bituminous-KI Impregnated Carbon, Petroleum-KI$_3$ Impregnated Carbon, and Foreign Bituminous-KI Impregnated Carbon

Table 4 lists the results of these tests. The penetrations obtained on bituminous base KI impregnated carbon were excellent, comparing with the best of results obtained on coconut base materials [Ref 3]. Petroleum base carbon gave lower performance. It should be noted, however, that a considerable time span separates tests I2-2, I2-3, J3-4 and J3-8 from test J32-6. The lower numbered series of tests were made on a production lot in 1970, while the J32-6 test is on a laboratory sample tested in 1974. It is likely that the difference in performance represents improved impregnation techniques.

6.2   Loading - Retention Tests

Retention tests were run according to Regulatory Guide 1.52 specifications on a coconut/KI$_3$ carbon and bituminous base /KI, with the results listed in Table 5. All carbons performed substantially better than the Regulatory Guide require-ment.

TABLE 5.   Retention Tests

Run	Carbon Tested	Total Feed mg/g	Feed Concentration mg/m^3	Feed Period min	Elution Period min	Penetration (Including Elution Per.)
J26-6	A	0.11	1.85	120	240	0.125
J26-7	A	0.13	2.24	120	240	0.25
J26-8	A	0.12	2.03	120	240	0.02
J33-5	D	0.08	1.2	120	240	0.03
J24-3	Coconut	0.07	1.18	120	240	0.026
J26-9	Coconut	0.12	2.06	120	240	0.100
J27-1	Coconut	0.12	2.03	120	240	0.047

Comparison runs were made with total feed of CH_3I increased considerably above the Regulatory Guide condition. The results are given in Table 6. In those runs which did not include elution, the holding capacity of the better bituminous (D) material is close to that for coconut, and would probably have equaled it if the run had been continued to the same penetration. When these runs were extended to include 240 min elution at 180 C, the better bituminous (D) was clearly superior to the coconut.

TABLE 6.   Loading/Retention Tests

Run	Carbon Tested	Loading mg/CH_3I/ g carbon	Elution Period min	Penetration %
(W I T H O U T E L U T I O N)				
J29-1	Coconut	11.9	--	0.5
J30-2	Bitumin A	2.0	--	0.5
J33-5	Bitumin D	8.4	--	.035
(W I T H E L U T I O N A T 1 8 0 C)				
J29-4	Coconut	7.1	240	2.4
J30-3	Bitumin A	1.6	240	0.767
J33-5	Bitumin D	8.4	240	0.038

It appears that some form of chemisorption is in operation on the bituminous base carbon surface. Confirmation of this was obtained by studies made with $CH_3{}^{127}I$ using a gas chromatograph. Under conditions which produced almost complete $CH_3{}^{127}I$ penetration (95%) through unimpregnated coconut base carbon ($\approx$1500 m^2/g BET nitrogen surface) the bituminous base carbon ($\approx$1000 m^2 BET nitrogen surface) used in this study (also unimpregnated) gave only 16.7% penetration.

7.0   ANALYSIS OF TEST RESULTS

It appears that one U.S. bituminous base carbon tested is at least equal in performance to coconut base impregnated carbons and superior to the petroleum base carbon tested. Comparison with foreign bituminous base KI impregnated carbons is not conclusive because of limited experimental data.

Our experimental studies indicate that base materials can influence I_2 and CH_3I adsorption, confirming Collins' findings. Further studies are being conducted to investigate base material influence.

**

The authors wish to express their appreciation to Mr. David K. O'Hara for his contributions to the experimental work in this study.

REFERENCES

[1]   USAEC Regulatory Guide 1.52: Design, Testing and Maintenance Criteria for Atmospheric Cleanup System - Air Filtration and Adsorption Units of Light-Water-Cooled Nuclear Power Plants (USAEC Directorate of Regulatory Standards, 1973)

[2]   RDT Standard M16 1T (October 1973): Gas Phase Adsorbents for Trapping Radioactive Iodine and Iodine Compounds (USAEC-DRT, 1973)

[3]   Rivers, R.D., Pasha, M., and Buckler, W.H.: Correlation of Radioiodine Efficiencies Resulting from a Standardized Test Program for Activated Carbons in Proc 12th USAEC Air Cleaning Conf. (USAEC-CONF-720823, 1972)

[4]   Collins, D.A., Taylor, L.R., and Taylor, R.: The Development of Impregnated Charcoals for Trapping Methyl Iodide at High Humidity. TRG Report 1300W (UKAEA) also in Proc 9th AEC Air Cleaning Conf (USAEC-CONF-660904, 1966)

DISCUSSION

DEITZ: In table 4, examples are given for petroleum charcoals where the I_2 penetration is greater than that for methyl iodide. I have been informed by many investigators that the reverse is generally the case and that the problem is to attain efficient methyl iodide trapping. Would you comment?

RIVERS: Table 4 refers to only four tests made on petroleum base material. We did not investigate this material thoroughly, but the material showed very poor results in the beginning. I believe there are some inequalities in humidity. The iodine tests were run at 130°C in about 93 percent R.H. One of the methyl tests was run at lower concentration. The last test in the list is certainly a nominal elution period of 120 to 90 min.

RIVERS:[*] This question is for Ronald Bellamy. All of us have been seeking conclusions to as "low as practical". The disturbing thing of this paper is that there isn't any problem,as the effluent concentration is near zero. We are told to have better and better efficiency. However, the concentration is listed in microcuries per milliliter and I cannot find after a very quick perusal of the paper any evidence of the mass concentration of the methyl iodide. It is presented in microcuries per milliliter; was it used as pure 131? Were there no other isotopes present?

BELLAMY: I started with pure iodine 131, yes.

RIVERS: Again to my question: I am pointing out that if this is true, which in your paper is within as "low as practical", the problem is solved because as the concentration goes down, efficiency goes up; therefore, do we have to worry about very low releases?

BELLAMY: I would like to make the point that when I started my research, I personally defined "low" as approaching 10^{-9} microcuries per milliliter, but since that time I have been convinced from the Commission's point of view that it is more like 10^{-11} to 10^{-13} microcuries per milliliter. Therefore, I was a factor of 10^4 higher than I would define as "low" today.

RIVERS: Is there any evidence that performance falls off when you go below the point where you quit testing?

BELLAMY: Not that I know of. I haven't seen any.

[*]Mr. Rivers is referring to Dr. Bellamy's paper, no. 8-2

ADSORPTION OF METHYL IODIDE ON IMPREGNATED ALUMINA[x]

I.J.Gal, A.Muk, M.Todorović, J.Rajnvajn,
D.Cvjetićanin and Lj.Vujisić

Boris Kidrič Institute and Faculty of Sciences,
University of Belgrade, Belgrade, Yugoslavia

Abstract

The kinetics of adsorption of gaseous methyl iodide on a commercial alumina impregnated with various metal nitrate salts has been investigated in a static gas-solid adsorption apparatus, in the range 50-150°C. Strong chemisorption of iodine has been noted with silver nitrate impregnation, and to a lesser degree with cadmium and lead nitrate. At 100°C lead and cadmium nitrate are nearly as efficient in binding iodine as silver nitrate. In the absence of humidity, silver oxide is a superior impregnation than silver nitrate. Mixed-salts impregnation as Ag + Cd are also promising. The decrease of the rate of methyl iodide adsorption with increasing vapor pressure of water has been recorded for some adsorbents.

Samples impregnated with silver nitrate (7.4 w.% Ag) have been also tested in a dynamic adsorption facility, under various conditions of humidity, flow-rate and temperature of the air stream, at high methyl iodide concentrations. The retention of methyl iodide decreases strongly with increasing humidity and face velocity of the

air stream, but increases with increasing temperature. An improved technique of impregnation might be helpful to overcome at least partly the adverse effect of humidity.

Introduction

Methyl iodide is one of several radioactive airborne iodine species which are presently removed from off-gas streams by impregnated carbon adsorbents. Certain disadvantages of carbons stimulated several research groups to investigate the possible use of inorganic adsorbents, particularly silver-exchanged zeolite[1-3], silver nitrate impregnated alumosilicate[4] and silicagel[5-6]. Although it is generally believed that silver nitrate is the best impregnation for inorganic adsorbents, other salts and silver compounds cannot be entirely excluded, not to mention the broad possibility of mixed-salt impregnation in which a silver salt is only one of the possible components.

The present paper is the first part of a study of the kinetics of methyl iodide adsorption on a commercial alumina adsorbent impregnated with the following metal nitrates: Ag, Cu, Pb, Cd, Zn, Ni, Co, Ce, Ag + Cu, Ag + Ce, Ag + Cd. The kinetics of adsorption has been studied isothermally at 2-3 temperatures in the range 50-150°C, under static conditions, in an atmosphere of pure methyl iodide and in some cases in the presence of water vapor. For the silver nitrate impregnated base material some retention values obtained under dynamic conditions, at various humidities, temperature and flow-rates of the air stream are also reported.

Experimental

Preparation of adsorbents. The base material is ALCOA H-151 activated alumina. Its chemical compositions is given in Table I.

Specification of the base adsorbent: Alcoa alumina H-151

Composition:

AL_2O_3	90.0 %
Na_2O	1.4 %
Fe_2O_3	0.1 %
SiO_2	1.7 %
Loss on ignition (1100°C)	6.0 %
Surface area	390 m^2/g
Bulk density, packed	53 lb/ft^3
Specific gravity	3.2
Particle size	0.34 cm and 0.12 cm

Table I. Specification of base alumina

TABLE 2

Metal salt content of impregnated H-151 alumina samples

Nr.	Salt(s) impregnated	millimoles per 100 g	wt % metal
1	$AgNO_3$	70.5	8.47
2	$AgNO_3$	42.0	4.53
3	$Cu(NO_3)_2$	80.3	5.10
4	$Cu(NO_3)_2$	41.0	2.60
5	$Pb(NO_3)_2$	60.0	12.43
6	$Pb(NO_3)_2$	39.0	8.08
7	$Ni(NO_3)_2$	70.1	4.57
8	$Ni(NO_3)_2$	42.0	2.46
9	$Co(NO_3)_2$	80.0	4.72
10	$Co(NO_3)_2$	42.0	2.48
11	$Cd(NO_3)_2$	68.0	7.64
12	$Cd(NO_3)_2$	43.0	4.83
13	$Zn(NO_3)_2$	76.0	4.96
14	$Zn(NO_3)_2$	50.0	3.26
15	$Ce(NO_3)_3$	50.0	7.00
16	$AgNO_3 + Cu(NO_3)_2$	41.0 + 41.0	4.42 + 2.60
17	$AgNO_3 + Ce(NO_3)_3$	38.0 + 24.0	4.09 + 3.36
18	$AgNO_3 + Cd(NO_3)_2$	10.0 + 17.1	1.08 + 1.92

Table II. Impregnations of alumina

The base material is impregnated with metal nitrates by pouring 42 ml of an aqueous metal nitrate solution over 100 g of dried alumina, in a beaker, under constant tumbling. The aqueous solution is completely taken up, yielding surface wet particles, which were dried at 170°C, dedusted and analyzed. A list of prepared adsorbents is given in Table II. For experiments under static conditions always the original base material of average particle size 0.34 cm (98% of the bulk within 5-8 mesh) was used. For tests under dynamic (flow) conditions the base material was crushed, sieved, then the fraction corresponding to particle size 0.08-0.16 cm was impregnated with silver nitrate (7.4 w.% Ag) and used after drying and dedusting.

Preparation of radioactive methyl iodide. The radioactive CH_3I labelled with I-131 has been prepared from $K^{131}I$ and dimethyl sulphate according to a standard procedure[7]. Yields between 80-85% have been obtained. The radioactive sample was diluted with inactive methyl iodide to obtain a specific activity suitable for measurements.

Static adsorption. The apparatus is shown in Fig. 1. The main part is the large recipient vessel 1 to which the small detachable sample tube 2 is connected. Both are placed in a cylindrical glass tube heated by external heating coils and a hot-air blower. This "oven" can be operated up to 150°C and thermostated within ± 1-2°C. Before starting an adsorption experiment, vessel 1 and tube 2 containing the adsorbent is heated and outgassed, then sample tube 2 via valve 13 is disconnected from the main vessel 1. In the recipient vessel a known amount of radioactive CH_3I (and in some runs also water vapor) is introduced, and after the required constant temperature is achieved, sample tube 2 is again connected to vessel 1. At that moment the adsorption of methyl iodide on the sample starts. The increase of radioactivity of the sample was measured with a gamma-scintillation counter placed in a collimated lead
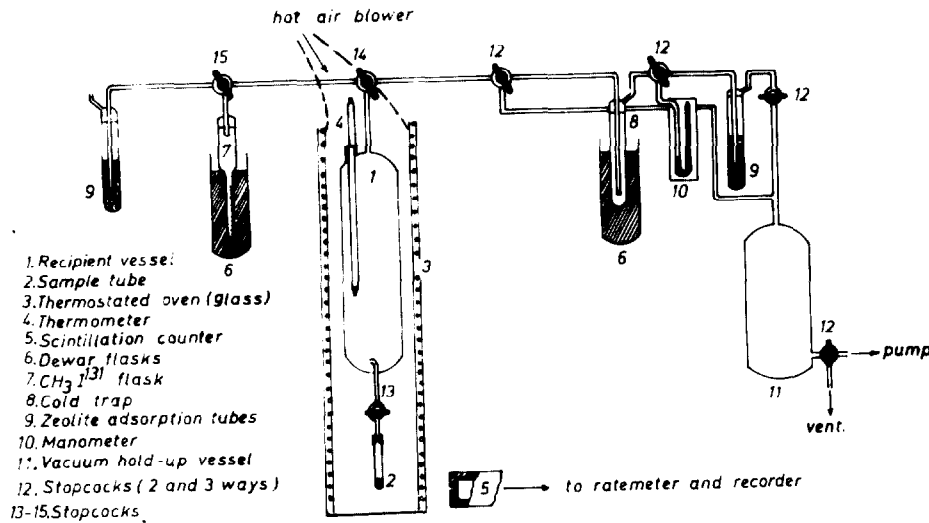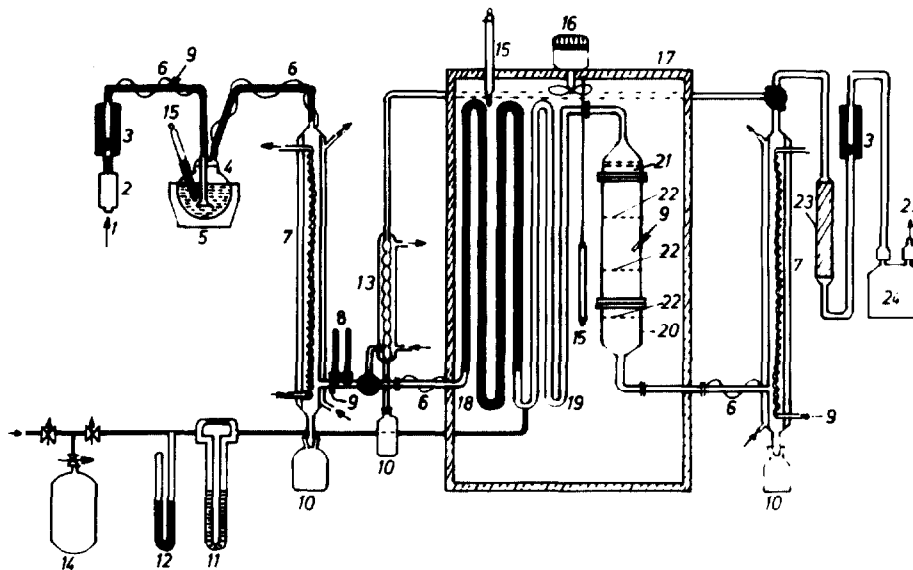
Figure 1.
Static gas-solid
adsorption appa-
ratus

1. Recipient vessel
2. Sample tube
3. Thermostated oven (glass)
4. Thermometer
5. Scintillation counter
6. Dewar flasks
7. $CH_3 I^{131}$ flask
8. Cold trap
9. Zeolite adsorption tubes
10. Manometer
11. Vacuum hold-up vessel
12. Stopcocks (2 and 3 ways)
13-15. Stopcocks

Figure 2.
Dynamic adsorpti-
on testing faci-
lity.

(1) air inlet, (2) filter, (3) flowmeter, (4) steam generator,
(5) heater, (6) heating tape, (7) Dew-point condenser, (8) wet-
and dry-bulb thermometer, (9) thermocouple, (10) condensate,
(11) flowmeter, (12) barometer, (13) by-pass condenser, (14) CH_3I
cylinder, (15) thermometer, (16) fan, (17) oven, (18) stainless-
-steel heat-exchanger, (19) mixing tube, (20) adsorption tube,
(21) HEPA filter, (22) adsorbent bed, (23) safety trap, (25) ex-
haust.

shield. The counter was connected to an amplifier, ratemeter and recorder, so that adsorption vs. time curves were obtained. After the adsorption was completed, vessel 1 and sample tube 2 were out-gassed up to $2 \cdot 10^{-4}$ atm., and the eventual desorption of iodine was also recorded. To calculate the absolute amount of adsorbed methyl iodide, a standard sample of adsorbent containing a known amount of radioactive methyl iodide was placed in tube 2, then measured and recorded. In most experiments the initial conditions in terms of partial pressures at $100^{\circ}C$ were 0.09 atm CH_3I and 0.05 atm air.

Dynamic adsorption. The facility is shown in Fig. 2. It is similar to that described by Wilhelm[5] except that the adsorption tube is not placed in a liquid bath but in a thermostated oven which can be operated up to $200^{\circ}C$ and thermostated within $\pm 0.5^{\circ}C$. All parts in contact with gaseous streams are made of glass, stainless steel or teflon. The adsorption column is a pyrex glass tube and the front door of the oven has large double glass-walls, so that every part of the facility can be visually inspected. With the steam generator and the dew-point condenser a desired constant humidity of the air stream can be obtained. The relative humidity of the air stream in the adsorption tube can be readily calculated from the temperature at the outlet of the dew-point condenser and the temperature inside the adsorption tube. To check the operation of the dew-point condenser, the wet- and dry-bulb thermometers placed near the condenser's air-outlet can be used. The flow-rate of the methyl iodide stream is negligible compared to the main wet air stream. Before entering the adsorption column, these two streams are mixed in a long glass tube inside the oven. At the top of the adsorption tube is a HEPA filter, then follows a bed of impregnated alumina adsorbent and two charcoal safety beds. After leaving the oven, the air-stream is cooled down to about $18^{\circ}C$ in a long condenser and then filtered through large charcoal safety beds before being discharged through the pump.

Static adsorption tests

Comparison of different impregnations. In Fig. 3. the kinetics of methyl iodide adsorption on seven differently impregnated base materials is compared under identical condition. In most cases, after 120 minutes of adsorption, the saturation capacity is not reached. The adsorption is expressed in terms of moles of CH_3I per mol of impregnated salt, which is more indicative of the adsorption efficiency than a weight per weight scale. After 120 minutes of adsorption (full line curves) the whole apparatus was outgassed to 0.1 mm Hg and the desorption (broken lines) recorded. Fig. 3. shows that only $AgNO_3$ impregnation does not release the adsorbed iodine after outgassing. Cadmium and lead nitrate impregnation release iodine partially, whereas copper, nickel and cobalt nearly completely. This indicates that only silver and to a lesser degree lead and cadmium show a strong irreversible chemisorption of methyl iodide, probably by formation of metal iodides. The effect of temperature upon adsorption is shown in Fig. 4 and 5. In most cases, the adsorption increases significantly with temperature up to 100^oC and then decreases again at higher temperature (see the 146^oC runs). At 146^oC, the highest temperature in our experiments, always a visible evolution of iodine vapors at the surface of the adsorbent has been noted. The moment of appearance of iodine vapors at the surface is shown on the curve by an arrow. It is interesting to note that at higher temperature the efficiency of methyl iodide adsorption is considerably increased in the case of cadmium and lead impregnation, and only a relatively small amount of iodine is released after outgassing. Thus, at 96^oC cadmium nitrate is nearly as efficient in binding methyl iodide as silver nitrate. However, these results are relevant only for a gaseous phase containing methyl iodide and dry air (initial conditions 0.09 atm CH_3I and 0.05 atm air), and they do not imply a similar behavior in the presence of water vapor.
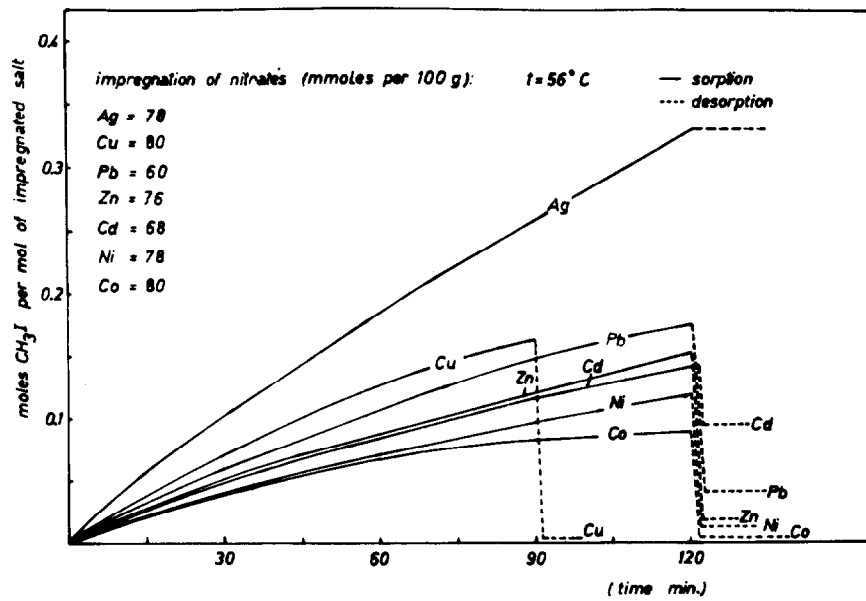
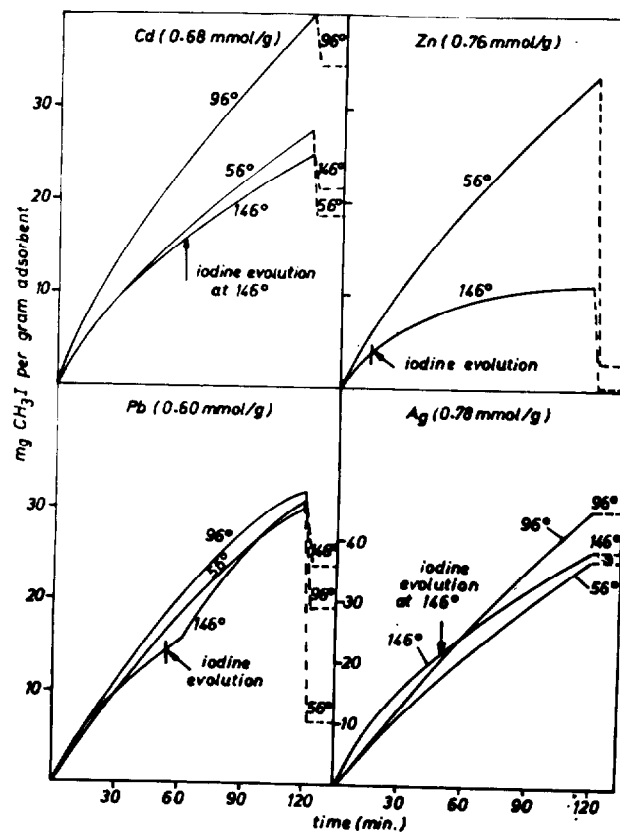**Figure 3. Dependence of CH₃I adsorption-desorption on the impregnation**

Figure 4. Adsorption on Cd, Zn, Pb and Ag impregnated alumina

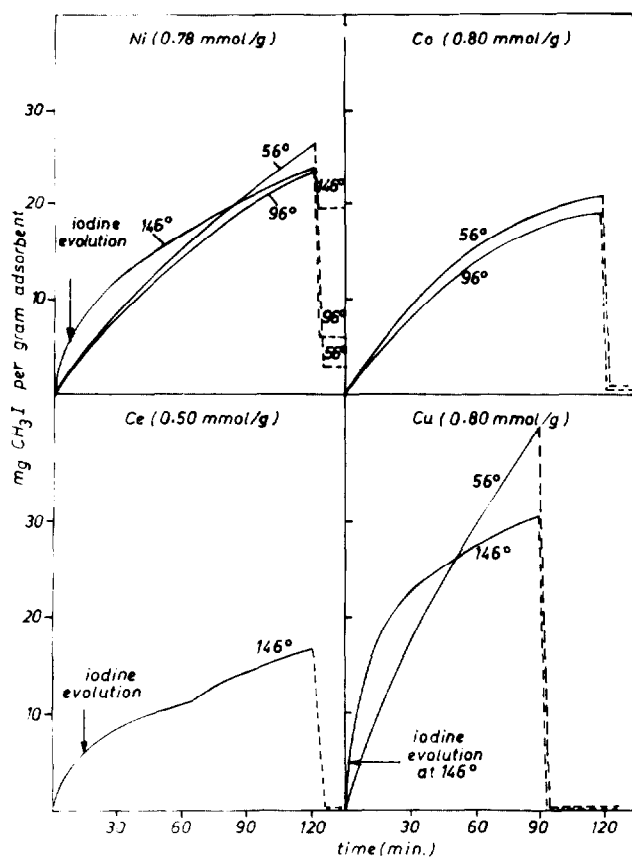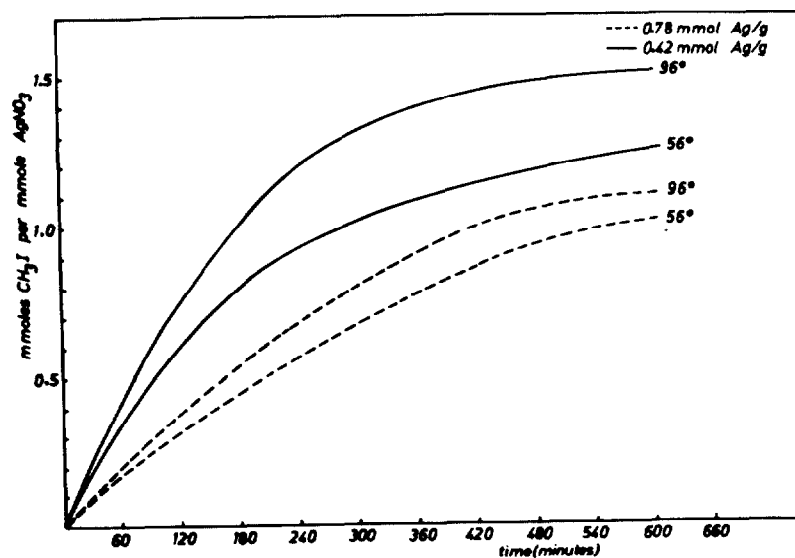**Figure 5.**

Adsorption on Ni, Co, Ce and Cu impregnated alumina

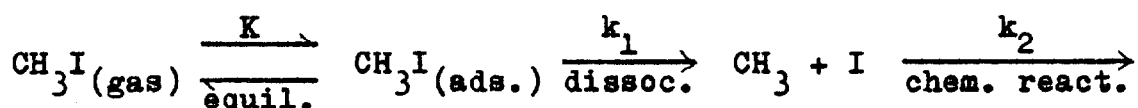**Figure 6. Influence of the amount of AgNO₃ impregnation. Adsorption expressed as millimoles of CH₃I per millimole AgNO₃**

The effect of the amount of impregnation. Fig. 6. shows the effect of the amount of impregnation on the adsorption kinetics. Although on a weight per weight basis the adsorption increases with the amount of silver nitrate, the true efficiently in binding methyl iodide, expressed in moles of CH_3I per mole of $AgNO_3$, is higher for the adsorbent containing less silver nitrate, as seen from Fig. 6. in the case of 0.42 and 0.78 millimole Ag per gram. The rate of adsorption expressed as mg CH_3I per gram adsorbent per minute is during the first 60 - 80 minutes equal for samples containing 0.42 and 0.78 millimole $AgNO_3$ per gram of adsorbent (Fig. 7.). A possible explanation for the adsorption curves in Fig. 6. and 7. might be the following one. The active outer surface of the particles (not necessarilly the inner pores) is in both cases, 0.42 and 0.78 mmole/g impregnation, always saturated with silver nitrate. There is, of course, a different concentration gradient from the surface toward the center of the particle in the two cases, but the outer surface, immediately accessible to CH_3I, might be saturated with silver nitrate and thus identical at low and high impregnation. In that case, the initial kinetic mechanism is also identical. Let us assume the following initial mechanism

$$CH_3I_{(gas)} \xrightarrow[\text{equil.}]{K} CH_3I_{(ads.)} \xrightarrow[\text{dissoc.}]{k_1} CH_3 + I \xrightarrow[\text{chem. react.}]{k_2}$$

in which the first step is a rapid surface equilibrium, the second step a slow dissociation of CH_3I (note iodine evolution, Fig. 4. and 5.) followed by rapid chemical reactions. In that case the following quasi first-order rate equation is obtained:

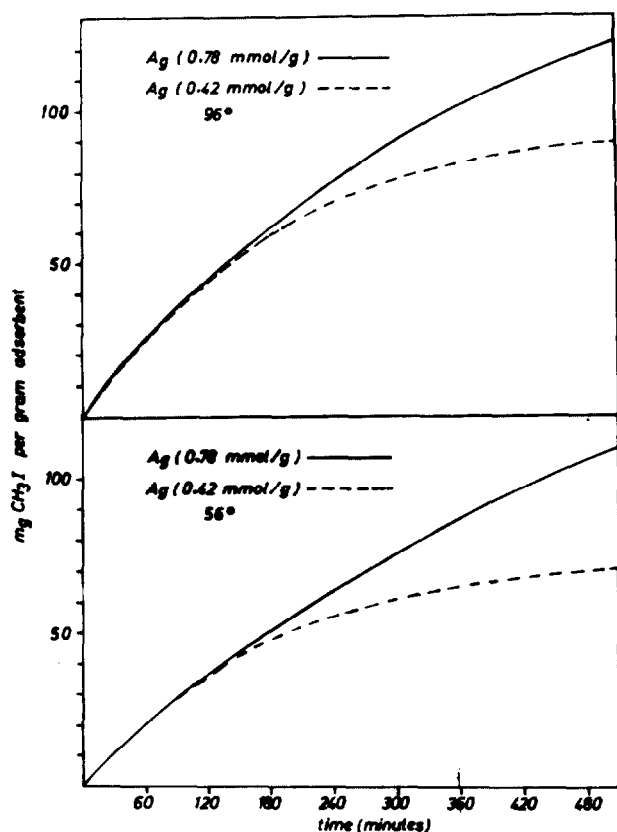$$\frac{dW}{dt} = k_1\frac{K}{V} (W_0 - W) = k (W_0 - W) \tag{1}$$

and after integration

Figure 7.

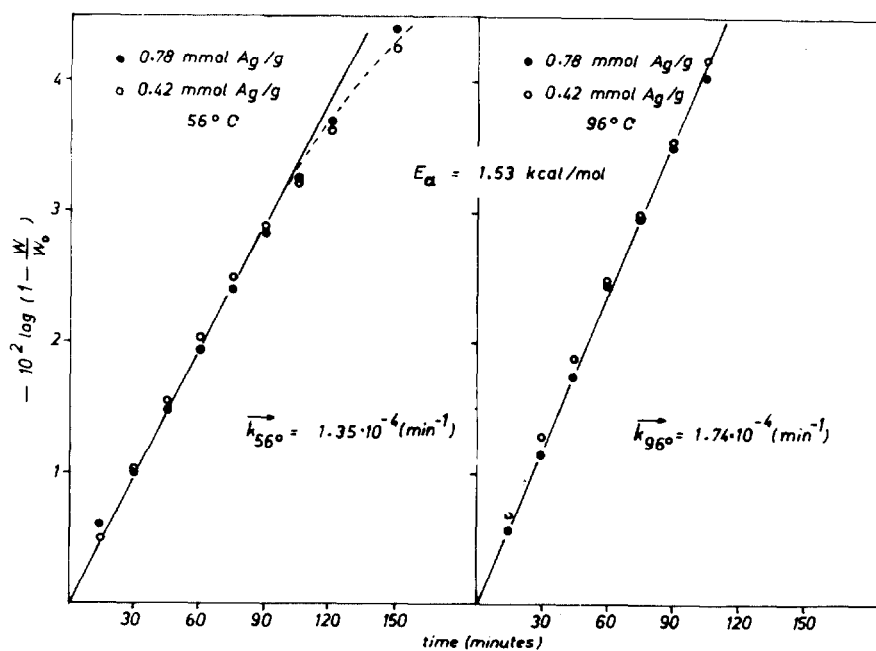Influence of the amount of $AgNO_3$ impregnation. Adsorption expressed as mg CH_3I per gram adsorbent

Figure 8. Kinetics of adsorption. Equation 2 applied to samples containing different amount of $AgNO_3$ impregnation (56° and $96^{\circ}C$)

$$- \ln (1 - \frac{W}{W_0}) = kt \tag{2}$$

In eq. 1 and 2 W is the amount of CH_3I adsorbed in time t, W_0 is the initial amount of CH_3I in the gaseous phase and V is the volume of the gaseous phase. Eq. 2 was tested at two temperatures as shown in Fig. 8. It can be seen that the agreement is fairly good for the fist 80 minutes of the adsorption process.

Silver oxide and mixed-salt impregnation. Thermodynamic calculations of standard free energy of metal iodide formation from methyl iodide indicate that silver compounds are indeed the best impregnation for binding iodine. The calculations also show that silver oxide (Ag_2O) might be a better choice than silver nitrate. Thermodynamic criteria are hardly applicable to a kinetic process; nevertheless, it seemed interesting to compare the kinetics of methyl iodide adsorption on samples impregnated with silver oxide and nitrate. The silver nitrate adsorbent was heated two hours in dry air at $650^{o}C$, then slowly cooled to ambient temperature. In that way most of silver nitrate is converted into silver oxide. In Fig. 9. the nitrate and oxide adsorbents are compared under identical conditions at $96^{o}C$. It can be seen that silver oxide is somewhat superior in terms of adsorption rate and saturation capacity. Silver oxide, in contrast to silver nitrate, is an insoluble impregnation, which is an advantage. However, later tests have shown that silver oxide is superior only in a dry atmosphere. In the presence of humidity silver nitrate is a much better impregnation.

Several mixed-salt impregnations have been tested in the static apparatus. Among them, the most promising seems to be a mixture of silver and cadmium nitrate. In Fig. 9. this mixed-salt impregnation is compared with pure silver nitrate at $96^{o}C$, in the absence of humidity. However, additional experiments under flow conditions and in the presence of humidity are necessary to evaluate the performan-
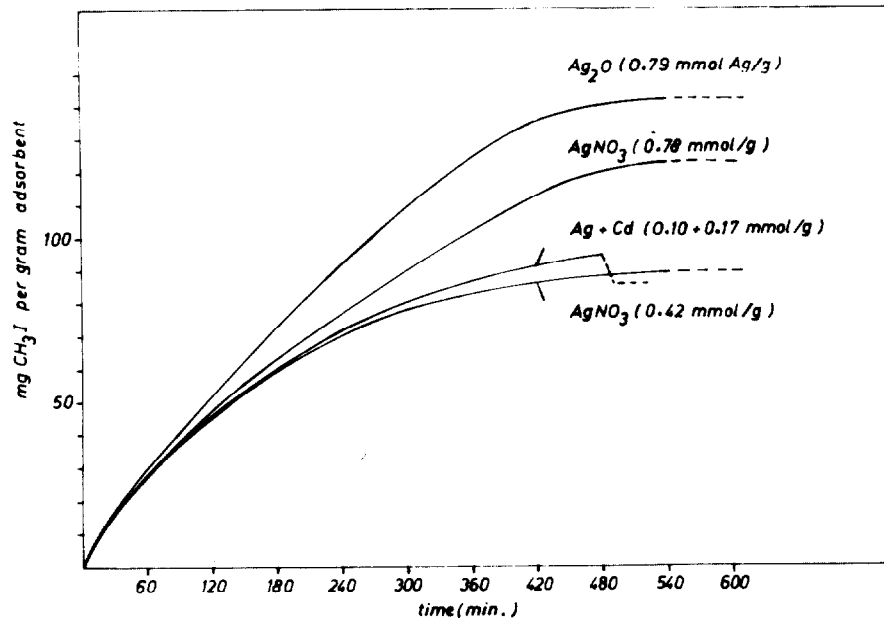
Figure 9. Comparison of Ag_2O and $AgNO_3$ impregnation and Ag + Cd and pure Ag impregnation (96°C)
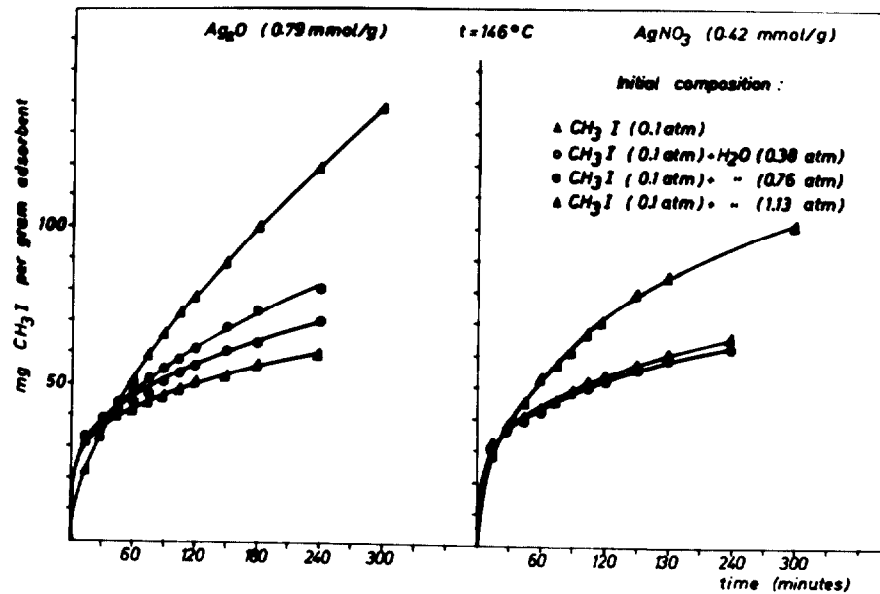

Figure 10. The influence of water vapor-pressure on CH_3I adsorption

ce of mixed-salt impregnations.

The effect of water vapor. Some adsorbents have been tested
in the static apparatus in the presence of water vapor. In all ca-
ses the adsorption of methyl iodide decreases sharply (Fig. 10.). As
dynamic (flow) adsorption experiments are more meaningful for tes-
ting adsorbents in humid air, further tests of that type have been
abandoned as soon as the dynamic facility was available.

Dynamic adsorption tests

The facility shown in Fig. 2. has been recently constructed
and only a small number of tests with a silver nitrate adsorbent
have been made. The most sensitive and important part of operation
in each test is the attainment of water saturation in the adsorbent
layer before starting the methyl iodide adsorption. At high humidity
it is often necessary to preequilibrate the adsorbent with wet air
for 10 - 15 hours. A sensitive method to check and record the water
saturation is the measuring of temperature changes in the bed. That
was done with a thermocouple and a microvoltmeter. True equilibrium
is reached when the temperature of the adsorbent is constant and
equal to the temperature of the oven. If the preequilibration time
is too short, usually higher but false retention values are obtai-
ned.

All tests were performed with an adsorbent bed of 5 cm dia.
and 5 cm deep. The activity of the adsorbent and all safety beds
(inside and outside the oven) as well as that of the condensate of
the second condenser was measured and the percent retention calcu-
lated. Each run was made according to the following procedure: pre-
equilibration 4 - 15 hours (depending on the humidity), methyl io-
dide adsorption 1.5 hours and purge time 2 hours. So far, only runs
at 36°, 50° and 90^oC at high methyl iodide concentration in the ga-
seous phase have been made. The results together with the relevant

Dinamic adsorption tests. AgNO$_3$ impreg-
nated alumina (7.4 w.% Ag), particle size 0.08 - 0.16 cm.
Adsorbent bed 5 cm ϕ x 5cm.

Temp. (°C)	face velocity (cm/sec)	relative humidity (%)	CH$_3$I conc in air (mg/m^3)	Average CH$_3$I loading (mg/g)	Retention (%)
50	8	27	220	1.9	99.9
		49	500	3.4	94.8
		78	780	5.1	75.3
	16	31	320	5.6	95.7
		51	120	1.7	72.0
		90	90	0.7	38.4
	25	32	110	2.2	86.0
		54	82	1.6	63.2
		87	278	2.2	26.7
36	20	38	2.4	0.05	92.5
		75	3.2	0.03	40.0
		90	2.2	0.02	28.6
90	20	30	0.9	0.02	93.0
		52	0.4	0.01	87.6
		87	6.1	0.13	88(?)

Table III. Dynamic adsorption tests

data are listed in Table III.

The data for 50°C refer to very high airborne methyl iodide concentrations (fourth column). They show that relatively high loadings can be achieved under favorable conditions, but the retention decreases sharply when humidity and face velocity is increased.

The two series of data for 36°C and 90°C refer to the same face velocity, but to lower airborne methyl iodide concentration. They show that the retention at higher humidities is much higher at 90°C, although the trend is somewhat obscured by the concentration effect. More systematic data are needed to evaluate the performance of the adsorbent, although Table III indicates that it is probably less efficient than some impregnated charcoals. However, the performance of this type of adsorbents depends on the impregnation technique, and in this respect it is believed that many improvements are possible. It might be also interesting to explore the possibility of

making the surface of the adsorbent water repellent and/or test other, less hygroscopic, base materials.

Further work is in progress.

References

1) W. J. Maeck, D. T. Pence and J. R. Keller, " A Highly Efficient Inorganic Adsorber for Airborne Iodine Species ", Proceedings of the 10th AEC Air Cleaning Conference, New York, 1968.

2) D. T. Pence, F. A. Duce and W. J. Maeck, " Metal Zeolites: Iodine Adsorption Studies ", TID - 4500, 1970.

3) D. T. Pence, F. A. Duce and W. J. Maeck, " Developments in the Removal of Airborne Iodine Species with Metal-substituted Zeolites ", Proceedings of the 12th AEC Air Cleaning Conference, Oak Ridge, 1972, (pp 417 - 433).

4) R. D. Ackley and R. J. Davis, " Effect of Extended Exposure to Simulated LMFBR Fuel Reprocessing Off-gas on Radioiodine Trapping Performance of Sorbents ", Proceedings of the 12th AEC Air Cleaning Conference, Oak Ridge, 1972, (pp 484 - 499).

5) J. G. Wilhelm, " Trapping of Fission Product Iodine with Silver Impregnated Molecular Sieves ", KFK - 1065, 1970.

6) J. G. Wilhelm and H. Schuettelkopf, " An Inorganic Material for Off-gas Cleaning in Fuel Reprocessing Plants", Proceedings of the 12th AEC Air Cleaning Conference, Oak Ridge, 1972, (pp 540 - - 550).

7) J. E. Mecca, " Charcoal Laboratory Test Procedure for Douglas United Nuclear, Inc., Facility ", HEHF - 17, 1972.

DISCUSSION

SHAPIRO: I was wondering whether the lower surface area of the alumina base material would be a significant factor in the low efficiency presented compared to what we can achieve with activated charcoal?

GAL: I think the humidity is more important. You see, we have very good results at low humidity; 99 and more percent retention on the same surface. I think the humidity is more critical.

WILHELM: Did you compare your results with results on silver impregnated silica?

GAL: We have only a few sets of dynamic data at very high concentrations. We shall run at lower concentrations and then I think these data can be compared. I haven't seen any data for silica at four or five hundred milligrams per cubic meter. I think we have too few data at low concentration to make comparisons. Besides, we think we can improve the impregnation.

WILHELM: If the silver nitrate is decomposed by high temperature, you will get silver oxide, but the removal efficiency at high temperature will still be the same in air of low relative humidity. For example, one can expect very low relative humidity in the high temperature atmosphere of an HTR containment after a depressurization accident. But, if the filter works first at a high temperature and then, after a certain cooling time, at low temperature, it loses some of its efficiency.

GAL: You mean silver oxide?

WILHELM: Yes.

GAL: Unfortunately, at low temperature, it's not as good as the nitrate.

DEITZ: Alumina and silica gels are very efficient catalytic cracking agents. Since the environment of the containment space includes hydrocarbons from several sources, the alumina base material could react with these at the higher temperatures and reduce surface area and produce inert carbon deposits, as in the commercial catalytic units of the petroleum industry. Therefore, the life time of the alumina support materials might be considered from this point of view for use under actual operating conditions of reactors.

IODINE SCRUBBING FROM OFF-GAS WITH CONCENTRATED NITRIC ACID*

O. O. Yarbro, J. C. Mailen, and W. S. Groenier

Oak Ridge National Laboratory
Oak Ridge, Tennessee 37830

Abstract

A new process, named Iodox, for effectively scrubbing all iodine forms from off-gas streams with concentrated (~ 20 M) nitric acid has been developed. This process removes all significant iodine species, both elemental and organic, from a gas stream by oxidizing them to the nonvolatile iodate form.

Advantages of the Iodox system for removing iodine from nuclear fuel reprocessing plant off-gas include:

1. It is capable of removing kilogram quantities of iodine while delivering a concentrated iodine waste stream for permanent disposal.

2. It is relatively insensitive to the contaminants normally found in a reprocessing plant off-gas stream and effectively removes all significant iodine forms.

3. Nitric acid is used in the process; thus no significant chemicals are introduced to the plant process or waste handling systems.

Laboratory-scale studies indicate that iodine retention factors in excess of 10^4 for methyl iodide can be obtained in a multistaged bubble-cap column. A small engineering-scale demonstration of the complete process, including the iodine scrubbing column, iodine waste concentration and solid I_2O_5 handling, and acid reconstitution and recycle, is in progress. The flowsheet being used for the engineering-scale system demonstration is typical of an application of the Iodox process to a fuel reprocessing plant.

I. Introduction

Iodine is present in spent nuclear power reactor fuels to the extent of about 350 g per ton of uranium. The ^{131}I activity may vary from 1.5 Ci/ton for conventional reactor fuel, decayed 180 days, to 1.3×10^5 Ci/ton for short-cooled Liquid Metal Fast Breeder Reactor (LMFBR) fuel. Iodine-129 is present to the extent of only 0.04 Ci/ton; however, because of its very long half-life (1.6×10^7 years), it must be removed from plant effluent streams in a form suitable for permanent storage.

The control and removal of iodine was one of the major problems to be solved in developing fuel reprocessing capability for the LMFBR program. An incentive exists to reduce the preprocessing decay time for LMFBR fuel, both to reduce the inventory charges on the valuable plutonium content of the stored fuel and to minimize the fuel cycle inventory and thus shorten the reactor cycle doubling time for plutonium. This incentive to reduce decay times, coupled with the trend toward minimizing the release of all noxious effluents to the environment, has necessitated the development of highly efficient removal systems for iodine as well as other fission products. The development of a liquid scrubber system for removal of iodine using hyperazeotropic nitric acid in the range of 20 M (called Iodox) is among the accomplishments of this development program. This paper summarizes the status, potential applications, and problems associated with the Iodox system.

II.   Flowsheet Application

The overall concept of a high-integrity effluent control system for an LMFBR fuel reprocessing plant handling 5 metric tons of fuel per day is illustrated in Figure 1. This flowsheet uses the Iodox scrubbing system for primary iodine removal from dissolver off-gas and for secondary iodine removal from vessel off-gas. Silver zeolite beds remove the final traces of iodine from the plant effluent gas prior to its discharge into the environment. A major fraction of the iodine (95 to 99%) present in the incoming fuel is evolved in the dissolution and feed preparation step and reports to the primary iodine removal system. The Iodox system is used here to remove approximately 2 kg of iodine per day with a decontamination factor (DF) of 10^5. The iodine that is not evolved from the dissolver solution passes into the downstream equipment, from which it eventually finds its way into the secondary Iodox system via the vessel off-gas. The mass of iodine reaching the secondary system is in the range of 20 to 100 g/day, but a large fraction of this total is made up of organic iodine species formed by contact with process organics. The Iodox system is particularly applicable for both the primary and secondary removal steps because of its capability for removing kilogram quantities of iodine while delivering a highly concentrated iodine waste stream for permanent disposal, and because of its high efficiency for removing organic as well as elemental species. The containment concept illustrated in Figure 1 is for a short-decay LMFBR fuel reprocessing plant where iodine retention factors approaching 10^9 may be needed, and includes a "sealed" process cell concept with very low air inleakage and internal recycle of process air and liquids. Application of the Iodox system to the removal of iodine from the off-gas of a conventional nuclear fuel reprocessing plant would be quite similar, with one or more Iodox scrubbers removing iodine from the vessel and the dissolver off-gas streams prior to their discharge to the environment.

III.   Chemistry of the Iodox System

The efficiency with which iodine is scrubbed from off-gas streams with hyperazeotropic nitric acid is dependent on the oxidizing power of the concentrated nitric acid which converts the volatile iodine species to the nonvolatile HI_3O_8 form. Results of laboratory studies of the kinetics and equilibria involved in these reactions and some physical property data of the process solutions are summarized here.

Oxidation of organic iodides, represented in this case by methyl iodide, proceeds first by the destruction of the organic iodide as shown by equation (1),
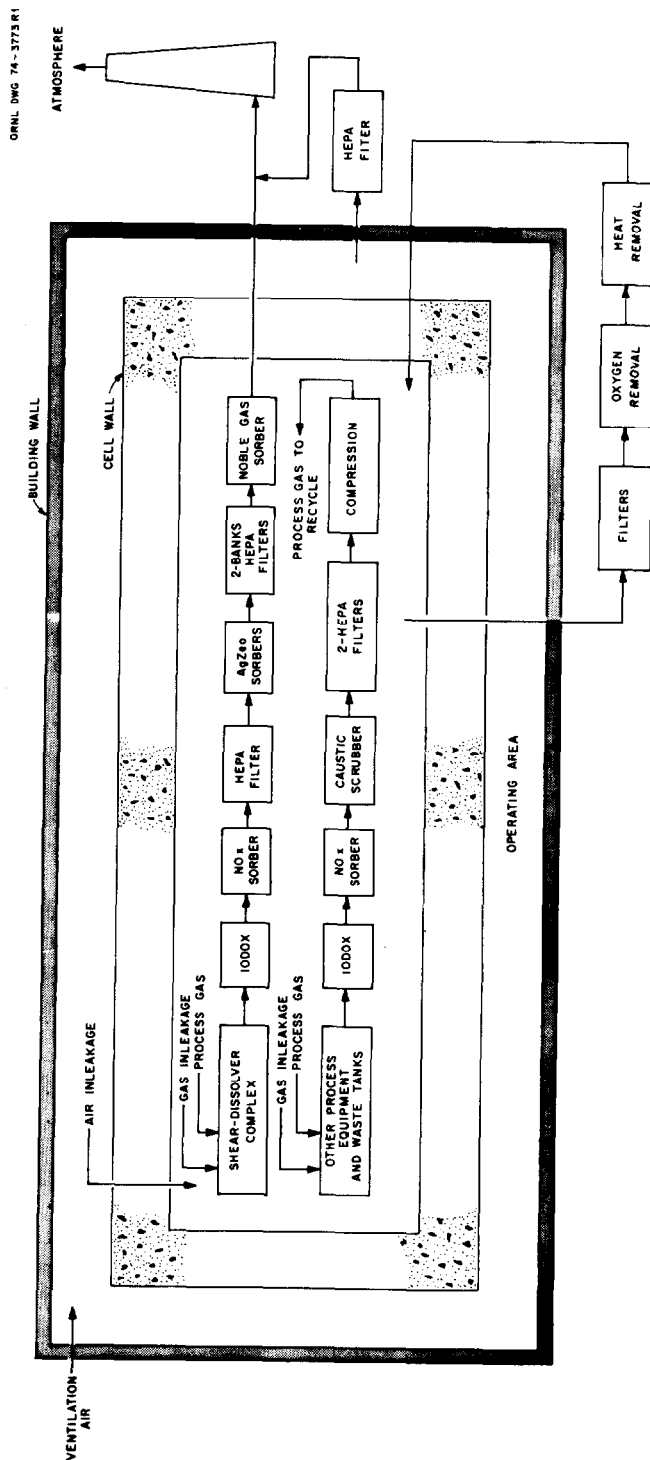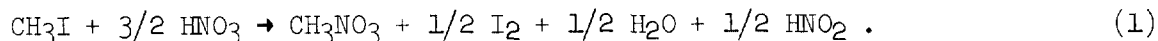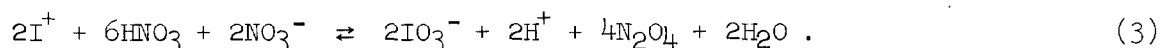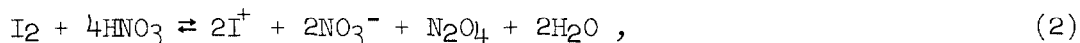
Figure 1. Off-gas flowsheet for 5-metric-ton/day LMFBR fuel reprocessing plant.

followed by the oxidation of the resulting elemental iodine as described below:

$$CH_3I + 3/2\ HNO_3 \rightarrow CH_3NO_3 + 1/2\ I_2 + 1/2\ H_2O + 1/2\ HNO_2 \ . \tag{1}$$

The oxidation of methyl iodide occurs in the liquid phase of the scrubber, and the reaction rate constant (k_5) varies as the 32.5 power of the nitric acid concentration, as shown in Figure 2[1]. Because of the strong dependence of reaction rate on acid concentration, concentrations above 19 M are required for effective removal of methyl iodide.

Kinetic and equilibrium studies[2,3] of the oxidation of elemental iodine indicate a two-step oxidation process fitting the relations given in equations (2) and (3):

$$I_2 + 4HNO_3 \rightleftharpoons 2I^+ + 2NO_3^- + N_2O_4 + 2H_2O \ , \tag{2}$$

$$2I^+ + 6HNO_3 + 2NO_3^- \rightleftharpoons 2IO_3^- + 2H^+ + 4N_2O_4 + 2H_2O \ . \tag{3}$$

Reaction (2) proceeds rapidly to produce a nonvolatile I^+ species, which is then slowly oxidized to HI_3O_8. Reaction rate constants for reactions (2) and (3) are shown in Figure 3 as k_1 and k_3, respectively. Equilibrium constants for reactions (2) and (3) have been determined at 25°C and are defined as:

$$K_{2A} = \frac{c_{I^+}^2\ c_{N_2O_4}\ a_{H_2O}^2\ a_{NO_3}^2}{c_{I_2}\ a_{HNO_3}^4} = 9.7 \times 10^{-16} \tag{4}$$

and

$$K_{3A} = \frac{c_{IO_3^-}\ c_{N_2O_4}^2\ a_H\ a_{H_2O}}{c_{I^+}\ a_{HNO_3}^3\ a_{NO_3}} = 2.8 \times 10^{-16} \ . \tag{5}$$

The presence of dissolved N_2O_4 or NO_2 tends to reverse the reactions given by equations (2) and (3) and thus reduces the removal efficiency of the scrubber. Also, the buildup of dissolved N_2O_4 in the iodine storage tanks will cause revolatilization of removed iodine.

Solubility of the HI_3O_8 in nitric acid sets limitations on the minimum liquid flow through the gas-liquid scrubbing column, as well as the extent to which the iodine waste stream can be concentrated for interim storage. The solubility of HI_3O_8 has been determined experimentally over the temperature range 25 to 100°C and the HNO_3 concentration range 12 to 20 M. The experimental data fit empirical equation (6) to within ±10%:

$$\ln S(g\ HI_3O_8\ per\ liter) = 13.28 - 0.4515\ c_{HNO_3}\ (M) - 1170/T\ (°K). \tag{6}$$

The solubility of HI_3O_8 in nitric acid at 25 and 100°C is plotted in Figure 4.

ORNL DWG. 74-6334
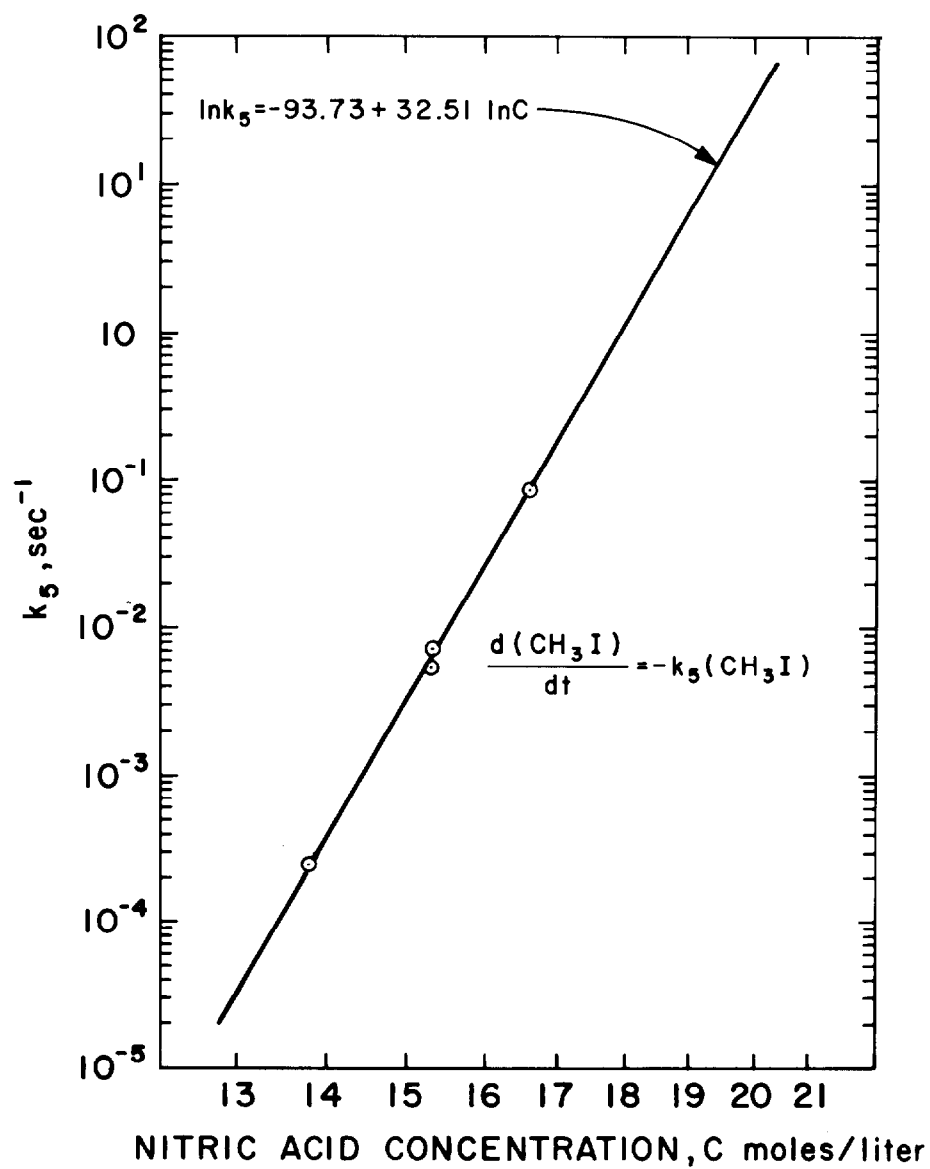
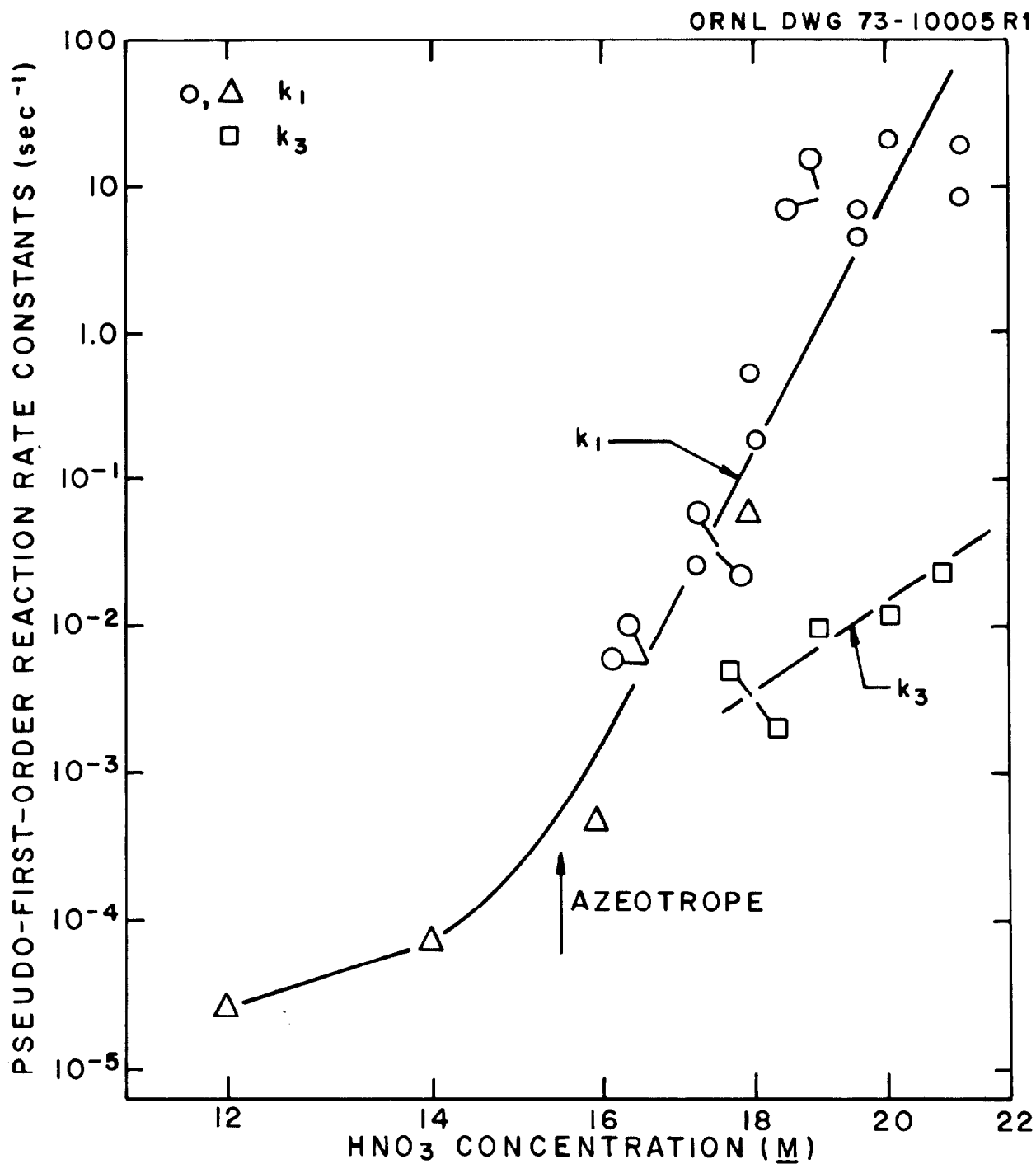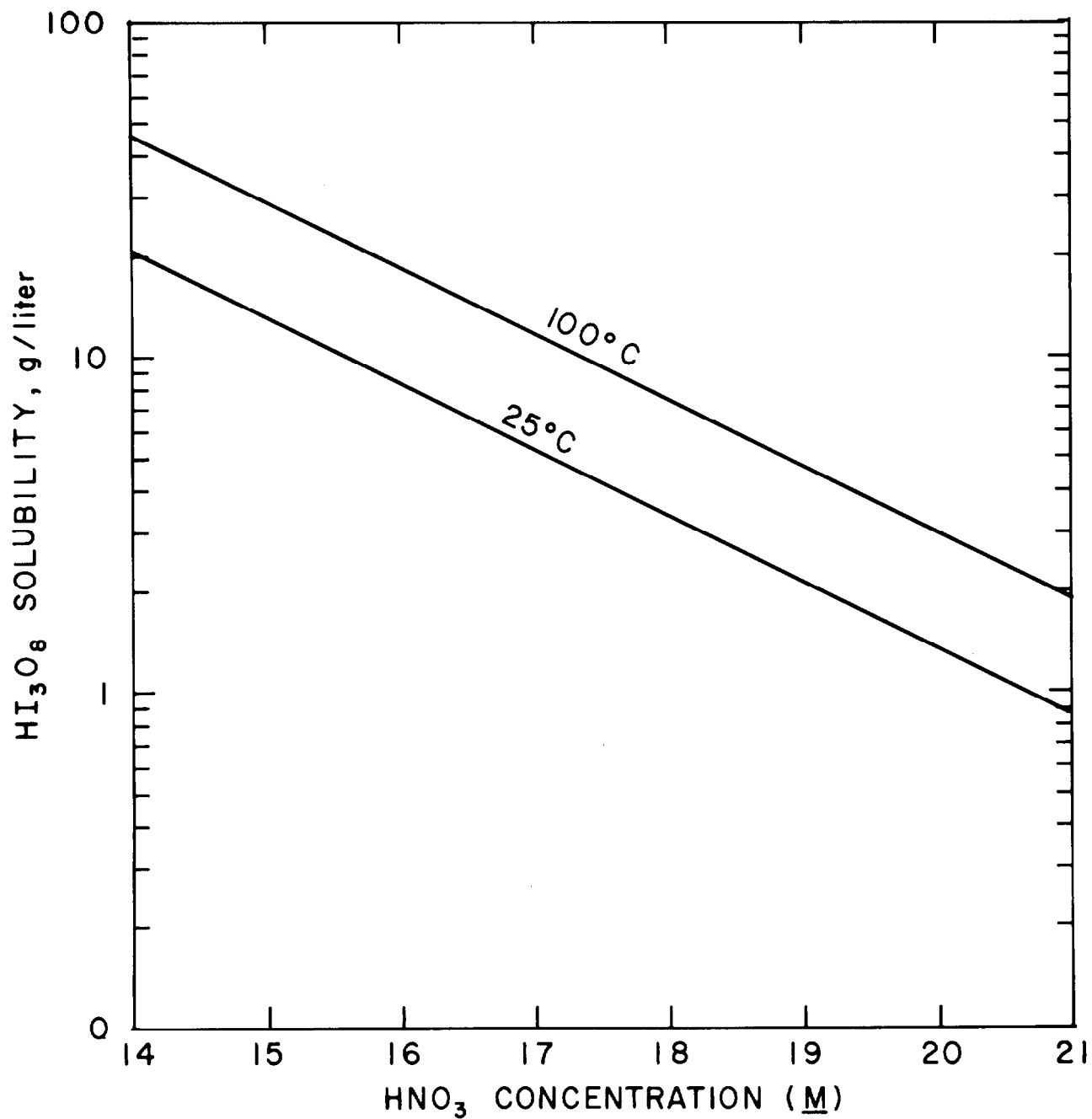Figure 2. Reaction rate constant for CH_3I oxidation by nitric acid.

ORNL DWG 73-10005 R1

Figure 3. Reaction rate constants for I_2 oxidation by HNO_3.

ORNL DWG 74-6335

Figure 4. Solubility of HI_3O_8 in nitric acid.

IV. Engineering Development

Over the past two years, studies have been carried out in small bubble-cap columns to optimize the operating parameters of the Iodox scrub column. Some of the more significant data are summarized here; in addition, a flowsheet for a complete Iodox system demonstration, which is in progress, is described.

Scoping experiments for the Iodox system were carried out in a 1-in.-diam, six-stage, bubble-cap column using ^{131}I-traced elemental or methyl iodide in the feed gas. Parameters investigated included the effects of acid concentration, temperature, gas and liquid flow rates, and iodine species on iodine decontamination factor (DF). The effect of nitric acid concentration on the stage DF for both elemental iodine and methyl iodide is summarized in Figure 5. As predicted from equilibrium and kinetic data, the DF for each of these iodine forms increases rapidly with increasing acid concentration, and acid concentrations above 19 M are needed for effective removal of iodine. Temperature has little effect on the elemental iodine DF over the range 25 to 75°C; however, a significant decrease in DF is observed at temperatures approaching 100°C. At acid concentrations above 18 M, methyl iodide DFs improve significantly as the temperature is reduced from 75 to 25°C. Figure 6 illustrates the effect of gas flow rate on elemental and methyl iodide stage DFs for 18 M acid in the 1-in.-diam column. Similar relationships hold for higher acid concentrations. Gas flow rates of 150 to 200 lb/hr · ft^2 and acid concentrations of 19 to 21 M appear to constitute the practical operating range.

Two 3-in.-diam columns[1,3] were tested to check the performance of the Iodox column on a larger scale. One column consisted of two plates with three metal bubble caps per plate and a 1-1/2-in. submergence. The second column had seven plates with a single glass bubble cap per plate and a 1-1/8-in. submergence. Performance data for both of these columns with 20 M HNO$_3$ at a gas flow rate of 150 to 200 lb/hr · ft^2 agreed with data from the 1-in. column, with CH$_3$I DFs in the range of 3 to 4 per stage. At low gas rates (50 lb/hr · ft^2) the two columns gave significantly different results, probably reflecting differences in gas-liquid contact efficiency at low flow rates. The experience to date indicates that stage DFs in the range of 3 to 4 for CH$_3$I and 6 to 7 for elemental iodine can be expected when operating a bubble-cap column at gas rates of 150 to 200 lb/hr · ft^2 with 20 M nitric acid on the plates.

In order to demonstrate the complete Iodox system on a small engineering scale, the equipment shown in flowsheet form in Figure 7 has been fabricated from zirconium and glass and is about ready for operation. Except for scale, this equipment is typical of an Iodox system applicable to a large fuel reprocessing plant. The Iodox scrubbing column is 3 in. in diameter with six bubble-cap plates located below and three above the 22 M acid addition point. The three top plates serve to recover acid and to reduce the acid content of the off-gas by scrubbing with a small water flow added to the top plate. The acid concentration below the feed plate will range from 20 to 21 M. The concentrated acid feed rate is set by the larger value determined by the iodine solubility on the bottom plate (~1 g/ liter) or by dilution of acid by the water content of the feed gas. Typical acid addition rates are 1 to 2 liters of 22 M acid per minute per 100 scfm of feed gas. The raffinate from the bottom of the Iodox column is concentrated to about 10 g/ liter in the iodine concentrator. The vapor from the concentrator, decontaminated from iodine by more than a factor of 1000, is routed to the acid concentration tower; the iodine concentrate is pumped to an iodine waste solidification can, where it is evaporated to dryness as HI$_3$O$_8$. After the ^{131}I has been allowed to decay, the iodine solids containing the ^{129}I can be sent to a waste repository

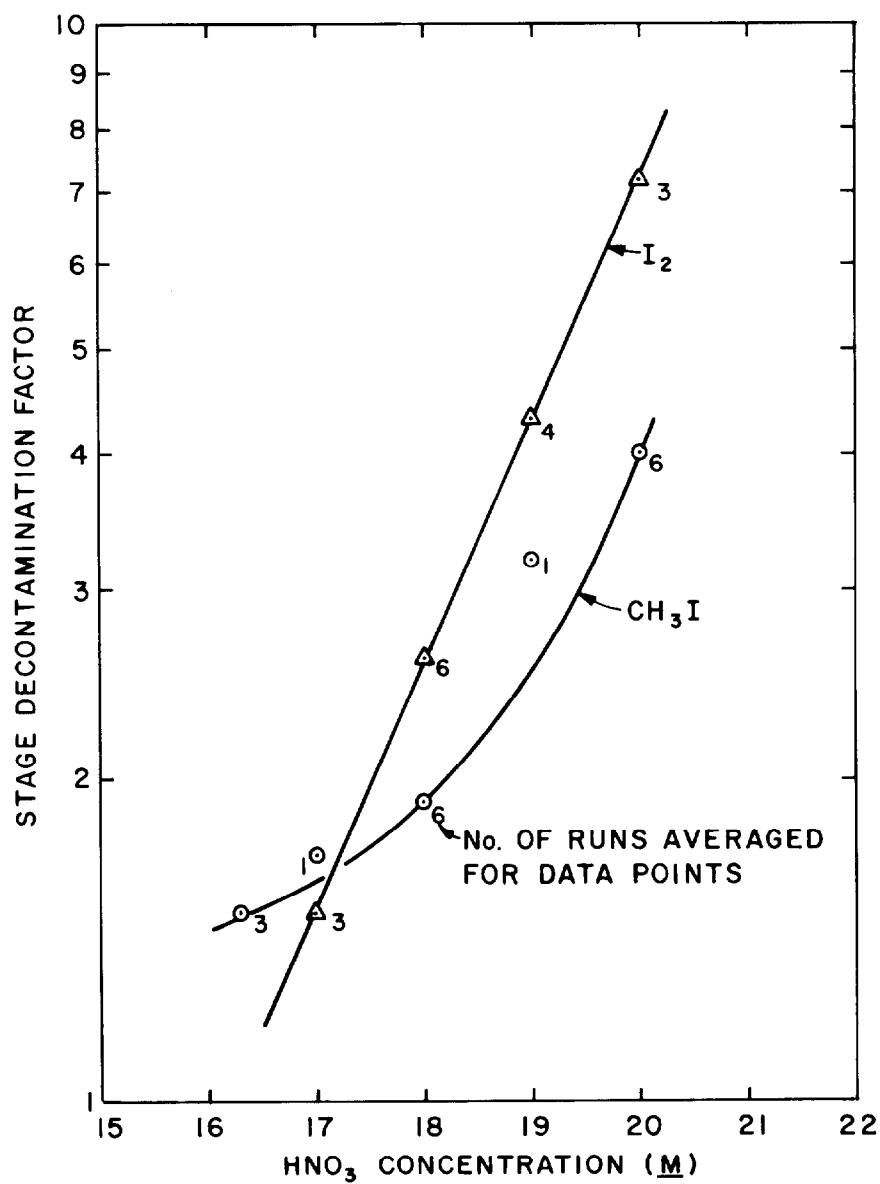ORNL DWG 74-6336

Figure 5. Effect of HNO_3 concentration on I_2 and CH_3I stage decontamination factors in 1-in.-diam bubble-cap column at a 140 lb/hr · ft^2 gas rate.
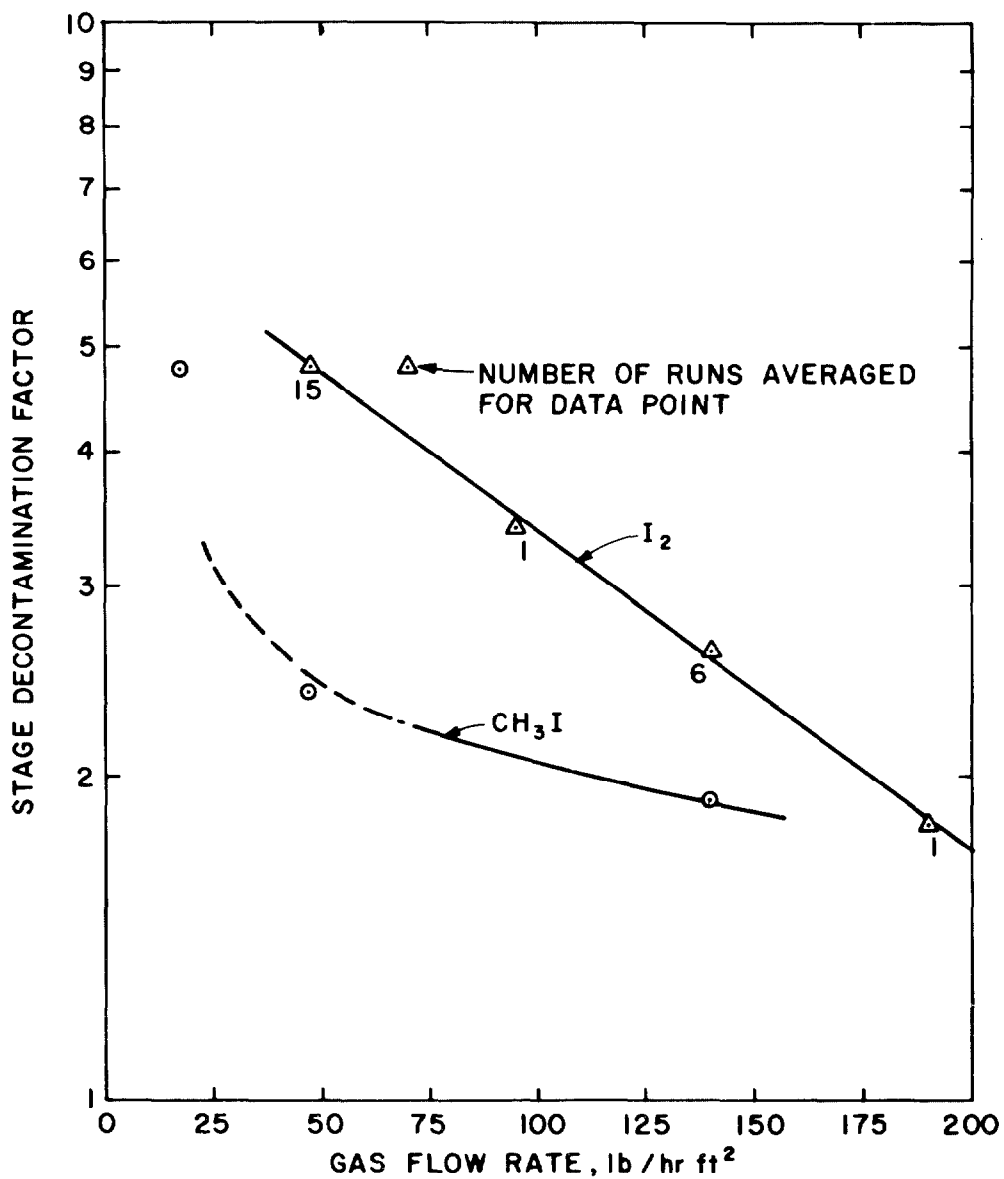
ORNL DWG 74-6337

Figure 6. Effect of gas flow rate on I_2 and CH_3I stage decontamination factors in 1-in.-diam column and 18 M nitric acid.
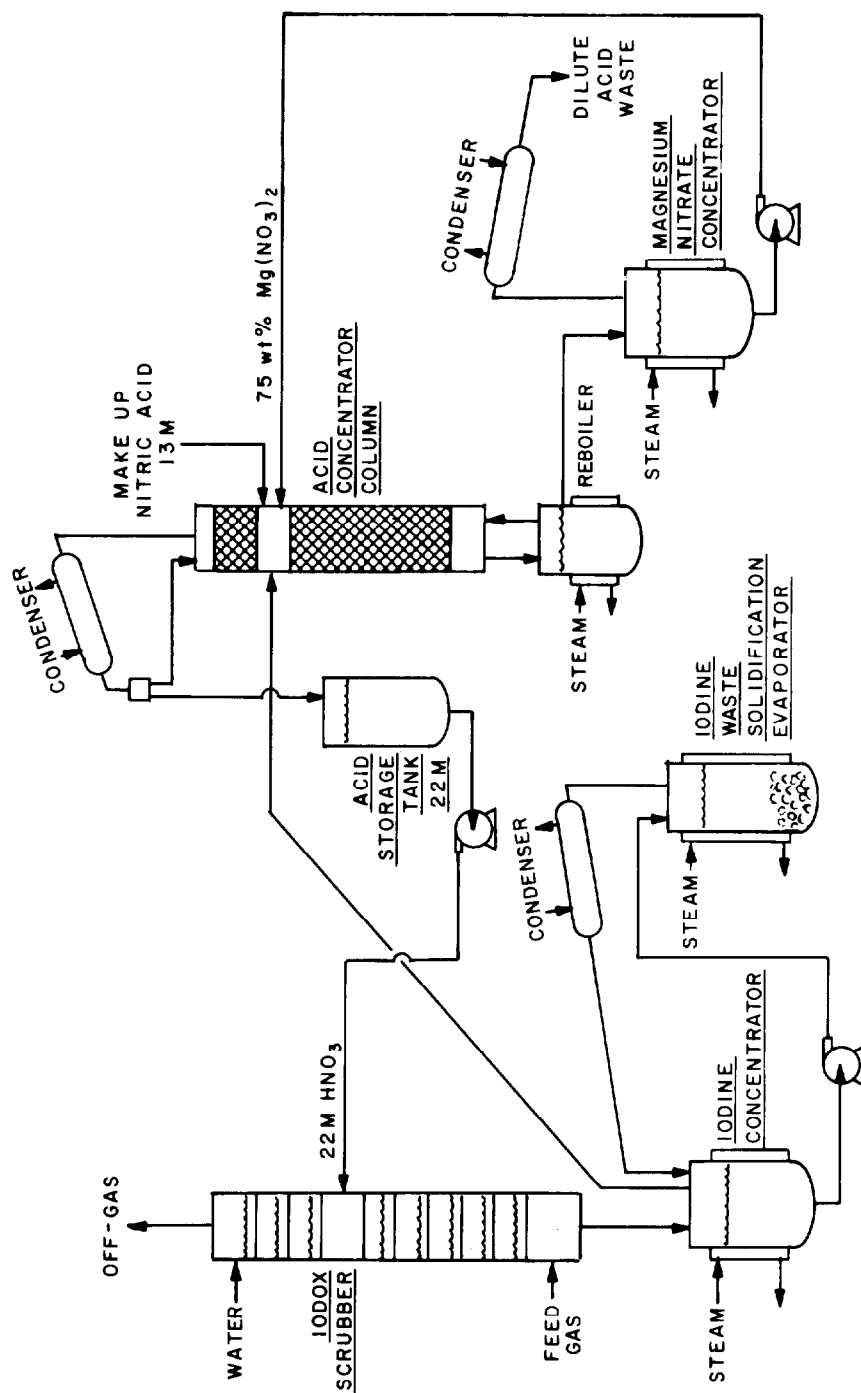
ORNL DWG 74-6338

Figure 7. Flowsheet for Iodox system demonstration.

for permanent disposal. Vapor from the iodine concentrator is reconcentrated to 22 M in an extractive distillation column using magnesium nitrate as a dehydrating agent. The diluted acid (18 to 19 M) is mixed with 75 wt % magnesium nitrate and fed to the distillation column. The upper section of the column serves to concentrate the acid to 22 M, while the lower section strips acid from the diluted magnesium nitrate. Excess water, picked up in the column by the magnesium nitrate, is evaporated in the magnesium nitrate concentrator, and the magnesium nitrate concentrate is recycled to the column. This acid concentration system is in common use in nitric acid manufacturing plants. The behavior of iodine in the system needs to be determined; also, other possible interface problems unique to the Iodox system need to be investigated and resolved. The overall Iodox flowsheet illustrated in Figure 7 will be used to further define operating parameters of the Iodox column and to demonstrate the long-term run capability of the entire Iodox system.

V. Conclusions

The Iodox system for scrubbing iodine species from nuclear fuel reprocessing plant off-gas streams has been developed to the point where an engineering-scale system could be designed for removing the kilogram quantities expected to be present in typical off-gas systems. Further studies are in progress to optimize column operating parameters and to demonstrate acid reconcentration and iodine solidification and disposal techniques. Materials of construction which can safely accommodate the combination of concentrated nitric acid and various iodine forms include zirconium, titanium, and tantalum. Zirconium appears to be the best choice when corrosion resistance, cost, and fabrication are considered.

References

1. W. E. Unger et al., Aqueous Fuel Reprocessing Quarterly Report for Period Ending December 31, 1973, ORNL-TM-4394 (June 1974), Sect. 10. (Available from the U. S. Atomic Energy Commission, Technical Information Center, P. O. Box 62, Oak Ridge, Tennessee 37830.)

2. J. C. Mailen, "Equilibrium in the oxidation of iodine by hyperazeotropic nitric acid," submitted to J. Inorg. Nucl. Chem.

3. W. E. Unger et al., Aqueous Fuel Reprocessing Quarterly Report for Period Ending March 31, 1974, ORNL-TM-4587 (in press), Sect. 10. (Available from the U. S. Atomic Energy Commission, Technical Information Center. P. O. Box 62, Oak Ridge, Tennessee 37830.)

DISCUSSION

FIRST: I was struck with the likelihood that you could lose considerable quantities of nitric oxide and nitrogen dioxide.

YARBRO: There's no really significant loss of nitric oxides from the system if you compare the concentration leaving this system to the concentration that you get out of the dissolver. The fact of the matter is, we have to remove nitric oxide from the feed gas because the nitrous oxide tends to reverse the reaction to form iodine. So we have to reduce NO_x inlet concentration down to a few percent by volume. NO_x production is not significant even at high radiation levels.

DEMPSEY: I was wondering if you have any plans to run the system hot, and also, have you considered where to place the radioactive isotope for the many years that it takes for it to decay?

YARBRO: We'll run this system with tracers. We hope to run it hot, but to do that, we need a source of iodine. Sooner or later we'll get around to it. I don't think it makes much difference how you remove it. One thing I should mention that I left out, you don't build this system out of stainless steel unless you want to be risky. Zirconium, titanium, or tantalum are options.

THE CALCULATION OF CHARCOAL HEATING IN AIR FILTRATION SYSTEMS

E. A. Bernard
Los Alamos Scientific Laboratory
Los Alamos, New Mexico

and

R. W. Zavadoski
U. S. Atomic Energy Commission
Washington, D. C.

Abstract

A computer program, TOOHOT, has been developed to be used in the calculation of temperature increases in a charcoal filter when iodine is adsorbed in the filter. It employs an implicit computational technique and has stability and convergence characteristics which make it suitable for calculating temperatures for days of real time without excessive amounts of computer time. Calculational results are compared with similar results obtained at ORNL and found to give lower temperatures. TOOHOT includes the effect of oxidation heating which is calculated to be minimal for air velocities in excess of 4 ft/min and depths of charcoal up to 8 inches. Ignition is calculated to occur in the instantaneous loading case at an air velocity of 4 ft/min.

I. Introduction

In 1971 Oak Ridge National Laboratory published a report on the effect of iodine decay heat on forced air cooled charcoal adsorbers (Reference (1)). Results therein are based in part on a general heat transfer computer code in which the heat source results from an instantaneous or gradual adsorption of a fraction of the iodine fission product inventory on the charcoal filter. The direct effect of iodine decay heat is used in the heat source term. However, the effect of oxidation heating is not included in the ORNL study.

CHART, the computer program used at ORNL to calculate the heating of charcoal filters, is a general heat transfer program and therefore its capabilities far exceed those required to solve the charcoal heating problem. The resulting complexity turns out to be a handicap in this application because computer time requirements are excessive except for the simplest problems and modifications are difficult to incorporate into the program.

A modified explicit technique is used in CHART to calculate temperature rises in the charcoal. In order to insure stability of the calculation an initial time increment of 0.02 min or less is required. This restriction limits the use of CHART in analyzing the long term heating of charcoal filters in the safety analysis of nuclear power plants.

In view of these problems with CHART, another program, TOOHOT, has been developed to calculate the temperature increase in charcoal filters when iodine adsorption occurs. The equations, boundary conditions and heat source terms are the same as those in use at ORNL. An implicit method is used, thereby removing the small time increment stability requirement. Every effort has been made to keep the program simple, thereby making it easy to follow, understand and, if necessary, modify. A variety of source terms and reduction mechanisms can be introduced so that the effectiveness of engineered safety features in reducing the maximum charcoal temperature can be determined.

II. Numerical Technique

Equations and Boundary Conditions

The one dimensional, time dependent partial differential equations which describe the heating of the charcoal filter and the air are :

$$\rho \, c_p \frac{\partial T(x,t)}{\partial t} = K \frac{\partial^2 T(x,t)}{\partial x^2} + Q(x,t) - H(T(x,t) - T'(x,t)) \tag{1}$$

and

$$\rho' c_p' v' \frac{\partial T'(x,t)}{\partial x} = H\big(T(x,t) - T'(x,t)\big) \tag{2}$$

where :

$T(x,t)$ = charcoal temperature

$T'(x,t)$ = air temperature

X = position variable

t = time variable

ρ = density of charcoal

ρ' = density of air

c_p = specific heat of charcoal

c_p' = specific heat of air

K = thermal conductivity of the charcoal

$Q(x,t)$ = heat source term

H = volumetric heat transfer coefficient, and

v' = air velocity

The constants are all specified or evaluated in Reference (1). The right hand side of Equation (1) includes the net heat diffusion (first term), a heat source (second term) and the heat transfer term between the charcoal and air (third term). The heat transfer term appears as the source for heating the air in Equation (2).

Boundary conditions are as follows :

$$T(x,0) = T'(x,0) = T_0 \qquad\qquad\qquad (3)$$

$$T' = (0,t) = T_0 \qquad\qquad\qquad (4)$$

$$\left.\frac{\partial T(0,t)}{\partial x}\right| = \left.\frac{\partial T(L,t)}{\partial x}\right| = 0 \qquad\qquad\qquad (5)$$

$$\left.\frac{\partial T'(L,t)}{\partial x}\right| = 0 \qquad\qquad\qquad (6)$$

Equations (3) and (4) state that both the charcoal and air are at the ambient temperature, T_0, initially and that the air inlet temperature remains constant at T_0. The fact that there is zero net diffusion of heat across the charcoal boundaries is expressed in equation (5). Equation (6) states that the air approaches its constant temperature outside the charcoal with a continuous spatial derivative.

Difference Equations in Implicit Form

The partial derivatives in Equations (1) and (2) are expressed in difference form, using a forward difference for the partial with respect to time, a central difference for the second partial with respect to position and a forward difference over a double spatial increment for the first partial with respect to position in Equation (2). The right hand side of Equation (1) and all of Equation (2) are weighted in time with weighting factors of W_1 and W_2 ($W_1 + W_2 = 1$) at the existing and subsequent time steps respectively. With j and k being the spatial and time indices, Equations (1) and (2) can be transformed so that the left hand sides contain the unknowns at t_{k+1} and the right hand sides are known.

The results are:

$$
T_{j-1}^{k+1}\left(\frac{-W_2 K}{\Delta x^2}\right) + T'_{j}{}^{k+1}\left(-W_2 H\right) + T_{j}^{k+1}\left(\frac{\rho c_p}{\Delta t} + W_2\left(\frac{2K}{\Delta x^2} + H\right)\right)
$$

$$
+ T_{j+1}^{k+1}\left(-\frac{W_2 K}{\Delta x^2}\right) = T_{j-1}^{k}\left(\frac{W_1 K}{\Delta x^2}\right) + T'_{j}{}^{k}\left(W_1 H\right) \tag{7}
$$

$$
+ T_{j}^{k}\left(\frac{\rho c_p}{\Delta t} - W_1\left(\frac{2K}{\Delta x^2} + H\right)\right) + T_{j+1}^{k}\left(\frac{W_1 K}{\Delta x^2}\right) + Q_{j}^{k}
$$

$$
T'_{j-1}{}^{k+1}\left(\frac{-W_2 \rho' c'_p v'}{2\Delta x}\right) + T'_{j}{}^{k+1}\left(W_2 H\right) + T_{j}^{k+1}\left(-W_2 H\right)
$$

$$
+ T'_{j+1}{}^{k+1}\left(\frac{W_2 \rho' c'_p v'}{2\Delta x}\right) = T'_{j-1}{}^{k}\left(\frac{W_1 \rho' c'_p v'}{2\Delta x}\right) \tag{8}
$$

$$
+ T'_{j}{}^{k}\left(-W_1 H\right) + T_{j}^{k}\left(W_1 H\right) + T'_{j+1}{}^{k}\left(\frac{-W_1 \rho' c'_p v'}{2\Delta x}\right)
$$

Equations (7) and (8) form a set of equations which can be written in matrix form

$$
AX = B
$$

where the column vector X is made up of the nodal temperatures :

$$X = \begin{bmatrix} T_1 \\ T'_1 \\ T_2 \\ T'_2 \\ \vdots \\ T_J \\ T'_J \end{bmatrix}$$

The elements of A and B are determined from constants of the charcoal-air system and the known temperatures at time t_k. Knowing the inverse of A, the temperatures at t_{k+1} can be obtained from the equation

$$X = A^{-1}B$$

where A^{-1} is the inverse of A. Use of this implicit scheme allows time increments on the order of minutes, thereby permitting long term calculations (days) with reasonable amounts of computer time (minutes).

Application of Boundary Conditions

At the first and last nodes (x = 0 and x = L) the boundary conditions are used to remove the reference to nodes outside the charcoal. For the charcoal equation at the first node (j=1) the diffusion term

$$\frac{K}{\Delta x^2} (T_0 - 2T_1 + T_2)$$

reduces to

$$\frac{2K}{\Delta x^2}(-T_1 + T_2)$$

and at the last node (j=J) to

$$\frac{2K}{\Delta x^2}(T_{J-1} - T_J)$$

due to the fact that the partial derivatives of the charcoal temperatures are zero at these points. The air temperature at the first node is constant so its equation is

$$T_1'^{k+1} = T_0$$

For j=2 the air equation is written as

$$\frac{\rho' c_p' v'}{\Delta x}(T_2' - T_1') = \frac{H}{2}\left((T_1 - T_1') + (T_2 - T_2')\right);$$

that is, the heating of the air in moving from node 1 to node 2 is based on the average of the charcoal-air temperature difference at the two nodes.

The air temperature at the last node has a continuous spatial derivative. From equation (2), it follows that

$$T_J' = T_J$$

These adjustments to Equations (7) and (8) for the respective nodes define the appropriate elements of the matrices A and B.

Heat Source Term and Ignition Criterion

The charcoal is heated by two mechanisms, iodine decay heat and oxidation. The iodine decay heat term is handled in the same way that it is handled in Reference (1). Oxidation is based on Reference (2) and for the oxidation calculations, the oxidation heating is given by

$$QX = 1.087 \times 10^9 \, \exp\left(-10.39\left(\frac{1000}{T_{ABS}}\right)\right)$$

where T_{ABS} is the absolute temperature in degrees Kelvin.

A number of experiments have been conducted at ORNL to study the ignition characteristics of various types of charcoal. Near ignition, all samples were observed to rise in temperature very rapidly. This being the case, it is difficult to define an "ignition temperature." Ignition occurs at roughly 600°F but a more practical definition of ignition is believed to be the heating rate of charcoal per unit mass. In all samples, ignition occurred at a heating rate of approximately 15 cal/min-gm of charcoal.

This criterion, 15 cal/min-gm of charcoal, is used in TOOHOT. to establish ignition conditions.

Stability and Convergence

TOOHOT is stable over a wide range of Δx and Δt. A number of different calculations have been made with

$$0.005 \text{ in} \leqslant \Delta x \leqslant 0.5 \text{ in.}$$

and

$$0.01 \text{ min} \leqslant \Delta t \leqslant 10.0 \text{ min.}$$

Evidence of instability has not been observed within these limits.

Convergence considerations cause limitations within the above established ranges of Δx and Δt. Using the parameters listed in Table I, the maximum charcoal temperatures given in Table II were computed. To limit the differences to less than 1% between the computed values for various increments, it is necessary that

$$\Delta x \leq 0.05 \text{ in.}$$

and

$$\Delta t \leq 5.0 \text{ min.}$$

Note the small requirements for CPU time in these calculations, all of which were run for 40 minutes of real time. These were run on the IBM 370/60 computer.

Table I

Parameters for stability and convergence computations

Depth of Charcoal	2 in
Air Velocity	4 ft/min
Ambient Temperature	100°F
Thermal Power	3077 MWt
Face Area of Charcoal	2800 sq ft
Delay Time (Instantaneous Loading)	10 min
Δx Increment	0.005 in $\leq \Delta x \leq$ 0.1 in
Δt Increment	0.05 min $\leq \Delta t \leq$ 10 min
Weighting Factor	0.5

Table II

Results of convergence calculations

Δx (in)	Δt (min)	T_{max} (°F)	Time @ T_{max} (min)	CPU (Sec)
0.005	0.05	430	34	165
0.01	0.05	429	34	85
0.05	0.05	432	34	18
0.10	0.05	481	36	10
0.005	0.5	430	35	17
0.01	0.5	428	35	9
0.05	0.5	431	35	6
0.10	0.5	481	35	2
0.05	1.0	430	35	2
0.05	5.0	433	35	1
0.05	10.0	450	35	1/2

<u>Input/Output</u>

The input data are read into a 50 element array and include ambient temperature, depth of charcoal, run time, Δx, and Δt, the constants appearing in Equations (7) and (8), the time weighting factor, heat source term parameters, reactor thermal power level, face area of charcoal, primary containment leak rate, ignition criterion, and a parameter to designate instantaneous or gradual loading.

At each designated time step, the temperature profiles for both the charcoal and the air are printed. For the nodes in the print-out, the iodine heating, oxidation heating and heat transfer between the charcoal and air are tabulated.

Included in these printouts is an energy balance check. During the computations the cumulative heat source is calculated and stored. At the designated printout time this is compared with the net source implied by the temperature changes at each node from the ambient temperature to the calculated value. An energy discrepancy percentage is printed out. For the various computations, this discrepancy varies up to 4%, with the larger discrepancies observed for the larger values of Δx and Δt.

Finally, there is a listing of the maximum charcoal temperature at various times. The frequency with which the maximum temperatures are found and stored is controlled with an input parameter. The calculation is terminated once the maximum for all times has been reached.

<div align="center">

III. Computations

</div>

<u>Comparison with ORNL Results</u>

Reference (1) (Figure 7) gives the results of the temperatures that were calculated for a 2 inch charcoal bed, 4 and 20 ft/min air velocity and an instantaneous iodine deposition model with a 10 minute delay time to deposition. The model used, CHART B, is more nearly equivalent to TOOHOT. Using the same input data, TOOHOT calculates maximum temperatures which are approximately 10% lower than those calculated with CHART B. Comparative results are shown in Table III. Potential causes for these differences have been investigated, namely,

(i)   application of boundary conditions

(ii)   implicit versus explicit method, and

(iii)   stability conditions.

It is believed that the latter two are the causes of the differences. In essence, the stability conditions in CHART B are such that a check is made throughout the calculations in an iterative manner to ascertain that stability exists for an incremental increase of the time increment used. If so, the time increment is increased and the

calculation proceeds. The criterion used to determine that the time increment is to be changed and the change itself are likely causes for the differences.

As seen in Table III the lower temperatures calculated in TOOHOT occur slightly earlier in time than the equivalent TOOHOT calculation. The difference in time is about 10% also.

<div align="center">

Table III

Comparison with ORNL temperature calculations
(2 inch charcoal depth)

</div>

Air Velocity	4 ft/min		20 ft/min	
	T_{max} (°F)	Time (min)	T_{max} (°F)	Time (min)
CHART B	385	36	190	8
TOOHOT	330	34	175	7
Difference	-55	-2	-15	-1
% Difference	-14	-6	-8	-12

Iodine Heating with Oxidation

The effect of various air flow rates with various depths of charcoal was investigated. At given depths (2, 4, and 8 inches) the air velocity was varied (20, 10, 8, 6, and 4 ft/min) to determine the conditions under which ignition might occur. Results are shown in Table IV. Input data is the same as that tabulated in Table I, and instantaneous loading of iodine is assumed. The difference between these and the previous calculations is that oxidation is now included in the heat source term.

In this case the effect of bed depth is the lowering of the maximum temperature with increasing depth. Times for these maximum temperatures change significantly, being almost proportional to the depth of charcoal. For the deeper depths, the energy discrepancy becomes smaller since the same charcoal heating source is spread over a greater length. Ignition takes place in the calculations for 2, 4, and 8 inch charcoal depths. The time of ignition was observed to increase with increasing depth of charcoal.

These results demonstrate two points. First, ignition is calculated to occur with an air flow of 4 ft/min. Second, with the assumed source loading (instantaneous) the increased depth of charcoal lowers the maximum temperature but ignition finally does occur.

Table IV

Results showing effect of oxidation

Air Velocity (ft/min)	T_{max} (°F)	Time @ T_{max} (min)	Energy Discrepancy (%)
	2 inch charcoal		
20	177	6	-2.3
10	246	14	-2.3
8	280	17	-2.3
6	334	23	-2.3
4	600 (Ignition)	37	-4.0
	4 inch charcoal		
20	176	10	-1.0
10	243	22	-1.0
8	275	28	-1.1
6	326	37	-1.1
4	600 (Ignition)	54	-1.2
	8 inch charcoal		
20	174	19	-0.6
10	237	38	-0.6
8	266	48	-0.6
6	313	64	-0.6
4	600 (Ignition)	90	-0.8

Gradual Loading

This set of calculations was performed with input data that are more realistic than those previously used. The latter are more representative of filter systems inside of the containment. For these cases, the calculations consider filter systems representative of an annulus ventilation system or a stand-by gas treatment system. In addition, a gradual loading, representative of a primary containment leak rate of 0.5% per day is used.

Input data are shown in Table V. Again, charcoal depths are specified at 2, 4, and 8 inches. Results are given in Table VI.

With the gradual loading used here, a small increase in temperature is calculated. With increasing depth of charcoal, however, the increase is not sufficient to cause ignition. At the lower realistic system limit of 4 ft/min air velocity, depth of charcoal has a very small effect on temperature up to 8 inches depth. Even at 2 ft/min, the differences are less than 1°F and do not lead to ignition.

Table V

Gradual loading data

Power Level	3600 MWt
Containment Leak Rate	0.5%/day
System Capacity	2000 CFM
Face Area of Charcoal	24 ft^2
Air Velocity	4 ft/min

Table VI

Gradual loading results
(2 ft/min air velocity)

Depth of Charcoal	T_{max} (°F)	Time @ T_{max} (days)	Energy Discrepancy (%)	CPU (min)
2	215.9	13.4	-2.3	1
4	216.4	13.4	-1.1	2
8	216.5	13.5	-0.6	4

IV. Summary

A new program, TOOHOT, has been developed specifically for the computation of temperature increases in charcoal filters caused by iodine adsorption. Its stability and convergence characteristics are such that long computation times are not required to run calculations for days of real time.

Calculations have been compared with similar calculations conducted at ORNL with the CHART program. It is seen that TOOHOT computes lower maximum temperatures which occur at earlier times. The differences are believed to be caused by the different computational techniques used in the two programs.

Under conditions of instantaneous iodine loading, the maximum temperature is calculated to decrease with increasing depth of charcoal. Ignition occurs at all depths with an air velocity of 4 ft/min but it takes longer for this to happen in the deeper filters.

In the more realistic case with gradual loading, calculations were performed at an air velocity as low as 2 ft/min. Up to 8 inches depth of charcoal, ignition is calculated not to occur. There is, however, a very small trend toward a higher maximum temperature for the greater depths of charcoal.

The authors wish to express their appreciation to R. A. Lorenz, ORNL, and R. B. Codell, AEC, for their advice and assistance in the development of TOOHOT.

References :

(1) ORNL - 4602,, The Effect of Iodine Decay Heat on Charcoal Adsorbers, April 1971.

(2) Letter, Lorenz, R. A., Oak Ridge National Laboratory, to Zavadoski, R. W., USAEC, dated July 24, 1973.

(3) Private communication, R. A. Lorenz, Oak Ridge National Laboratory.

DISCUSSION

SHAPIRO: A couple of questions. First, you seem to be using a one-dimensional slab model for your computer code. Have you tried to evaluate a two or three-dimensional case to model side effects off the slab?

BERNARD: No, I have not because the work done at Oak Ridge shows that three-dimensional effects are not significant except very near the edges. This is discussed in ORNL 4602.

SHAPIRO: Second question, have you addressed the complete loss of forced air flow and natural convection heat removal? The worst case is a situation not due to blockage, but a loss of the power to the fan or total loss of air flow.

BERNARD: I have not investigated this effect.

SHAPIRO: I was wondering, if your TOOHOT code can handle this kind of calculation or if you intend to address it in subsequent calculations.

BERNARD: No. The air velocity is an input parameter to the computation and does not change during the computation.

SHAPIRO: Do you consider it worthwhile to follow up? Is the Commission going to follow up on expanding the capabilities of the code to handle the natural convection situation?

BERNARD: I do not know. There are some things that need to be cleaned up in the code before it is released, but we have not considered this particular problem.

DEMPSEY: I am wondering if you checked out actual data obtained by Lorenz on your computer code and how they compared?

BERNARD: I have these data and intend to do the calculation and compare the calculated results with the experimental data.

FIELDING: I can't help but think of the consequences of 10,000 pounds of carbon in one bed catching fire. In addition to that, I am a member of a group at NRL that is occupied with putting out fires with nitrogen. I wondered if the matter of putting out fires in these carbon beds with liquid nitrogen, which is cheap and available, has been addressed?

KOVACH: This was covered in quite a bit of detail in a previous Air Cleaning Conference. Jack Murrow showed movies of how you put out fires.

WILHELM: I remember this movie that Mr. Kovach pointed
out was shown at the 11th Air Cleaning Conference. I can't make
up my mind if it is wise to put water on the charcoal. The char-
coal starts to ignite, we put water on it, and the charcoal may get
extinguished this way but you can't use it after you pour water on
it. You can't extinguish the fire without flooding the charcoal.
Additionally, it may generate hydrogen and by this means cause an
explosion. What is the sense of putting water on a burning char-
coal unit? The only thing I really see you could do is to shut
off the air flow. There would be no supply of oxygen anymore.
Nobody could rely on a filter which burned so the filter is lost
anyway. I would like to get some remarks because this fact is
creating some headaches in my country. We are thinking of changing
from charcoal to inorganic iodine sorption materials in special
cases because of the danger of losing off-gas filtration after an
accident, and having an iodine release to the environment in a
highly populated area.

MURROW: Perhaps I should make some comments on that as
long as I started it four years ago. The whole experiment started
with an effort to determine the ignition point of charcoal and had
very little to do with collection of iodine on charcoal. We
determined that it was difficult to extinguish a fire in charcoal
once it ignited. I have cautioned many times that this experiment
had two important parameters that may have been overlooked ever
since. One, the experiment was in a system where the air continued
to flow. Second, it was in a one inch convoluted type of charcoal
bed that is not extensively used today; at least not in the power
plant industry. On Thursday afternoon, there will be a discussion
of this subject. There has only been, as far as I know, one
large scale experiment to extinguish a charcoal fire after it
ignited and that was with the air shut off, and with a completely
different type of charcoal configuration. It is true that once
you apply water, the impregnant and perhaps the iodine will be
washed off, but that was not the point of the experiment when it
was conducted several years ago.

BURCHSTED: To address this matter of the carbon fire again:
Jack mentioned water washing out the iodine and impregnants. If
we ever get close to the ignition point of the carbon, we have lost
containment for radio-iodine. I think proper attention should be
given to maintaining temperature below the desorption temperature
of iodine rather than the ignition point. If we can keep the
temperature below the desorption point, fire and ignition will take
care of themselves.